Y3.N88:25/5129

MAY 21 1988

NUREG/CR-5129

Experimental Assessment of the Influence of Dynamic Loading on the Permeability of Wet and of Dried Cement Borehole Seals

Prepared by G. Adisoma, J.J.K. Daemen

Department of Mining and Geological Engineering
University of Arizona

Prepared for
U.S. Nuclear Regulatory Commission

COMPLETED

BEST COPY AVAILABLE

G.M.

ORIGINAL

NOTICE

This report was prepared as an account of work sponsored by an agency of the United States Government. Neither the United States Government nor any agency thereof, or any of their employees, makes any warranty, expressed or implied, or assumes any legal liability of responsibility for any third party's use, or the results of such use, of any information, apparatus, product or process disclosed in this report, or represents that its use by such third party would not infringe privately owned rights.

NOTICE

Availability of Reference Materials Cited in NRC Publications

Most documents cited in NRC publications will be available from one of the following sources:

1. The NRC Public Document Room, 1717 H Street, N.W.
   Washington, DC 20555
2. The Superintendent of Documents, U.S. Government Printing Office, Post Office Box 37082,
   Washington, DC 20013-7082
3. The National Technical Information Service, Springfield, VA 22161

Although the listing that follows represents the majority of documents cited in NRC publications, it is not intended to be exhaustive.

Referenced documents available for inspection and copying for a fee from the NRC Public Document Room include NRC correspondence and internal NRC memoranda; NRC Office of Inspection and Enforcement bulletins, circulars, information notices, inspection and investigation notices; Licensee Event Reports; vendor reports and correspondence; Commission papers; and applicant and licensee documents and correspondence.

The following documents in the NUREG series are available for purchase from the GPO Sales Program: formal NRC staff and contractor reports, NRC-sponsored conference proceedings, and NRC booklets and brochures. Also available are Regulatory Guides, NRC regulations in the *Code of Federal Regulations*, and *Nuclear Regulatory Commission Issuances*.

Documents available from the National Technical Information Service include NUREG-series reports and technical reports prepared by other federal agencies and reports prepared by the Atomic Energy Commission, forerunner agency to the Nuclear Regulatory Commission.

Documents available from public and special technical libraries include all open literature items, such as books, journal and periodical articles, and transactions. *Federal Register* notices, federal and state legislation, and congressional reports can usually be obtained from these libraries.

Documents such as theses, dissertations, foreign reports and translations, and non-NRC conference proceedings are available for purchase from the organization sponsoring the publication cited.

Single copies of NRC draft reports are available free, to the extent of supply, upon written request to the Division of Information Support Services, Distribution Section, U.S. Nuclear Regulatory Commission, Washington, DC 20555.

Copies of industry codes and standards used in a substantive manner in the NRC regulatory process are maintained at the NRC Library, 7920 Norfolk Avenue, Bethesda, Maryland, and are available there for reference use by the public. Codes and standards are usually copyrighted and may be purchased from the originating organization or, if they are American National Standards, from the American National Standards Institute, 1430 Broadway, New York, NY 10018.

BEST COPY AVAILABLE

NUREG/CR-5129
RW

Experimental Assessment of the Influence of Dynamic Loading on the Permeability of Wet and of Dried Cement Borehole Seals

Manuscript Completed: February 1988
Date Published: April 1988

Prepared by
G. Adisoma, J.J.K. Daemen

Department of Mining and Geological Engineering
University of Arizona
Tucson, Arizona 85721

Prepared for
Division of Engineering
Office of Nuclear Regulatory Research
U.S. Nuclear Regulatory Commission
Washington, DC 20555
NRC FIN B6627
Under Contract No. NRC-04-78-271

ABSTRACT

An experimental sealing performance assessment of cement borehole plugs that have been subjected to dynamic loading is provided. This includes a study of plugs that have dried, as well as of plugs that have remained wet throughout the testing period.

An introductory literature review indicates that deep underground structures in competent rock are safer than surface structures, openings at shallow depth, and openings in fractured rocks, when subjected to earthquakes and subsurface blasts.

Cement plugs are installed in 2.5 cm diameter coaxial holes in 15 cm diameter granite cylinders. Water is injected under pressure on top of the plugs and is collected below the plugs. Hydraulic conductivities are calculated from the measured flowrates. Once a long-term steady-state flow trend has been established, the samples are subjected to dynamic loading on a shaking table. Shaking is performed at accelerations up to 2 g and for durations up to 300 seconds.

Flow tests show that wet cement seals are less permeable than intact Charcoal granite. Sealing performance can degrade severely when cement seals are allowed to dry. Dye injection shows very limited and uniform penetration into wet plugs, but strongly preferential flow along the plug/rock interface of dried plugs. The permeability of wet and of rewetted previously dried cement seals does not change significantly after the application of dynamic loads.

Sealing in an unsaturated environment may affect the drying (curing, aging) conditions of cementitious seals, as well as the structure of earthen seals. An unsaturated environment will need to be integrated realistically into sealing performance tests and analyses.

BLANK PAGE

TABLE OF CONTENTS

	Page
ABSTRACT	iii
LIST OF FIGURES	viii
LIST OF TABLES	xiii
ACKNOWLEDGMENTS	xv
EXECUTIVE SUMMARY	1
CHAPTER ONE: INTRODUCTION	5
1.1 Objective	5
1.2 Scope and Limitations	8
1.3 Organization	9
1.4 Rock Mass Sealing Contract No. NRC-04-78-271 - Reports Issued	10
CHAPTER TWO: DYNAMIC LOADING AND ITS EFFECT ON UNDERGROUND EXCAVATIONS: A LITERATURE REVIEW	15
2.1 Observational Study from Case Histories	15
2.1.1 Effects of Earthquakes	15
2.1.2 Effects of Subsurface Blasts	19
2.2 Seismic Analysis of Underground Structures in Rock	22
2.2.1 Dynamic Response of Underground Openings	22
2.2.2 Analytical Methods	23
2.2.3 Empirical Methods	25
2.2.4 Numerical Methods	25
2.3 Seismic Hazard and Design Response Criteria for Nuclear Facilities	28
2.4 Implications for Repository Rock Mass Sealing	28
CHAPTER THREE: EXPERIMENTAL METHODS AND EQUIPMENT	32
3.1 Introduction	32
3.2 Specimens	32
3.2.1 Rock	32
3.2.2 Seal Material	33
3.3 General Overview of the Test System	36
3.4 Flow Test Apparatus	36
3.4.1 Pressure Intensifiers	36
3.4.2 Hydraulic Accumulators	39
3.4.3 Positive-Displacement Handpumps	39
3.4.4 Inflow Measurement	43
3.4.5 Outflow Measurement	43
3.4.6 Control Panel	45

TABLE OF CONTENTS--Continued

		Page
3.5	Dynamic Loading (Shaking) Apparatus	45
3.5.1	Shaking Table	45
3.5.2	Rock Cylinder Holder	45
3.5.3	Sinusoid G-Meter	45
3.5.4	Slotted Optical Limit Switch	50
3.6	Accessories	50
3.7	Test Procedures	53
3.7.1	Flow Test and Dye Injection Test	53
3.7.2	Dynamic Loading	55
3.7.3	Temperature, Humidity, and Evaporation Observations	55
CHAPTER FOUR:	EXPERIMENTAL RESULTS	57
4.1	Flow Tests	57
4.1.1	Flow Through Granite Rock Bridge	63
4.1.2	Flow Through Wet Cement Plugs	63
4.1.2.1	Specimen CG5309-08	63
4.1.2.2	Specimen CG5309-06	66
4.1.2.3	Specimen CG5309-31V	66
4.1.2.4	Specimen CG5309-10	73
4.1.3	Flow Through Dried-out Cement Plugs	73
4.1.3.1	Specimen CG5309-28	78
4.1.3.2	Specimen CG5309-01	78
4.1.3.3	Specimen CG5309-21	78
4.1.3.4	Specimen CG5309-31V	82
4.2	Dynamic Loading Tests	82
4.2.1	Wet Cement Plugs	82
4.2.1.1	Specimen CG5309-06	82
4.2.1.2	Specimen CG5309-31V	86
4.2.1.3	Specimen CG5309-08	86
4.2.2	Dried-out Cement Plugs	89
4.2.2.1	Specimen CG5309-28	89
4.2.2.2	Specimen CG5309-01	94
4.3	Dye Injection Tests	94
4.3.1	Wet Cement Plugs	94
4.3.1.1	Specimen CG5309-06	94
4.3.1.2	Specimen CG5309-31V	97
4.3.2	Dried-out Cement Plugs	97
4.3.2.1	Specimen CG5309-31V	97
4.3.2.2	Specimen CG5309-01	102
CHAPTER FIVE:	ANALYSIS AND DISCUSSION OF EXPERIMENTAL RESULTS	106
5.1	Hydraulic Conductivity Determination	106
5.1.1	Hydraulic Conductivity of Charcoal Granite	110
5.1.2	Hydraulic Conductivity of Wet Cement Plugs	110
5.1.3	Hydraulic Conductivity of Dried-out Cement Plugs	116

TABLE OF CONTENTS--Continued

		Page
	5.1.4 Summary of Hydraulic Conductivities	121
5.2	Comparison with Other Results	121
	5.2.1 Results in Granite	121
	5.2.2 Results in Wet Cement Plugs	125
	5.2.3 Results in Dried-out Cement Plugs	125
	5.2.4 A Comparison with Published Cement and Concrete Permeabilities	126
	5.2.5 The Effect of Plug vs. Host Rock Mass Permeabilities	140
5.3	The Effect of Cement Plug Drying on Its Hydraulic Conductivity	140
5.4	The Effect of Dynamic Loading on Plug Hydraulic Conductivity	142
5.5	Transition from Time-dependent to Steady-state Flow	143
CHAPTER SIX:	SUMMARY, CONCLUSIONS, AND RECOMMENDATIONS FOR FURTHER RESEARCH	157
6.1	Summary	157
6.2	Conclusions	157
6.3	Suggestions for Future Investigations	159
REFERENCES		163
APPENDIX A:	ANALYTICAL SOLUTION OF ONE-DIMENSIONAL TRANSIENT FLOW THROUGH POROUS MEDIA	189
APPENDIX B:	FINITE ELEMENT SOLUTION OF ONE-DIMENSIONAL FLOW THROUGH A CEMENT PLUG	193
APPENDIX C:	CEMENT MIXING PROCEDURE, COMPOSITION AND PROPERTIES, AND UNIAXIAL COMPRESSIVE STRENGTH	198
APPENDIX D:	LIST OF TEST EQUIPMENT	201
APPENDIX E:	TEMPERATURE, RELATIVE HUMIDITY, EVAPORATION RECORDS	205
APPENDIX F:	TEST RESULTS AND LABORATORY NOTES	215
APPENDIX G:	ROCK CYLINDER AND BOREHOLE PLUG DEFORMATION DURING BOREHOLE PRESSURIZATION	265

LIST OF FIGURES

Figure		Page
2.1	Principal types of deformation in a tunnel due to seismic motion	24
2.2	Seismic hazard map of the United States, showing contours of effective peak acceleration	29
3.1	Schematic diagram of flow test lay-out	37
3.2	Laboratory arrangement for flow test and dynamic loading of borehole seals	38
3.3	Schematic illustration of the gas-over-water pressure intensifier	40
3.4	Cutaway view of a hydraulic accumulator	41
3.5	Sectional view of the Ruska 2240 positive displacement handpump	42
3.6	Inflow and outflow measurement for flow tests	44
3.7	Flow test control panel	46
3.8	Eberbach 5900 shaking table with platform and utility carrier	47
3.9	A plugged specimen (CG5309-01), securely placed on top of the shaking table platform, ready for dynamic loading	48
3.10	The sinusoid g-meter in g-mode, indicating a peak acceleration of 2 g while shaking specimen CG5309-01	49
3.11	Monsanto MCT8 slotted optical limit switch used to sense the frequency input for the sinuosoid g-meter	51
3.12	A styrene infrared light breaker in the slot of the optical limit switch	52
4.1	Linear regression plot of outflow as a function of time for a wet cement plug	60
4.2	Linear regression plot of outflow as a function of time for a dried-out cement plug	61
4.3	An example of longitudinal outflow rate through a cement seal as a function of total (cumulative) time, specimen CG5309-31V, wet cement seal in Charcoal granite cylinder	62

LIST OF FIGURES--Continued

Figure		Page
4.4	Longitudinal flow rate through a Charcoal granite rock bridge as a function of total test time	64
4.5	Peripheral flow rate through granite around the rock bridge as a function of total test time, specimen CG5309-04	65
4.6	Longitudinal flow rate through a wet cement plug as a function of total test time. Specimen CG5309-08, plug length of 54 mm	67
4.7	Peripheral flow rate through the rock around the plug as a function of total test time, specimen CG5309-08 . . .	68
4.8	Inflow rates at various injection pressures as a function of elapsed total test time, specimen CG5309-08	69
4.9	Longitudinal flow rate through a wet cement plug as a function of total test time. specimen CG5309-06, plug length 31 mm	70
4.10	Peripheral flow rate through the rock around the plug as a function of total test time, specimen CG5309-06 . . .	71
4.11	Longitudinal flow rate through a wet cement plug as a function of total test time, specimen CG5309-031V	72
4.12	Peripheral flow rate through the rock around the plug as a function of total test time, specimen CG5309-31V . .	74
4.13	Mechanical packer used for flow testing of specimen CG5309-10	75
4.14	Longitudinal flow rate through a wet cement plug as a function of total test time, specimen CG5309-10, plug length of 59 mm	76
4.15	Peripheral flow rate through the rock around the plug as a function of total test time, specimen CG5309-10 . . .	77
4.16	Longitudinal flow rates through a dried-out cement seal (log scale) as a function of total test time for specimen CG5309-28, plug length of 88 mm	79
4.17	Peripheral flow rate through the rock around the plug as a function of total test time, specimen CG5309-28 . . .	80
4.18	Longitudinal flow rates through a dried-out cement seal (log scale) as a function of total test time for specimen CG5309-01, plug length of 86 mm	81

LIST OF FIGURES--Continued

Figure		Page
4.19	Longitudinal flow rates through a dried-out cement seal (log scale) as a function of total test time for specimen CG5309-21, plug length of 84 mm	83
4.20	Longitudinal flow rates through a dried-out cement seal (log scale) as a function of total test time for specimen CG5309-31V, plug length of 42 mm	84
4.21	Specimens CG5309-06 and -31V, placed in tandem for dynamic loading test on the shaking table	85
4.22	The effect of dynamic loading at an acceleration of 1 g on the longitudinal flow rate through a wet cement plug, specimen CG5309-06	87
4.23	The effect of dynamic loading at an acceleration of 1 g on the longitudinal flow rate through a wet cement plug, specimen CG5309-31V	88
4.24	The effect of dynamic loading at an acceleration of 2 g on the longitudinal flow rate through a wet cement plug, specimen CG5309-08	90
4.25	The effect of dynamic loading at an acceleration of 2 g on the peripheral flow rate through the rock around the plug, specimen CG5309-08	91
4.26	Inflow rate at various injection pressures as a function of time, specimen CG5309-08	92
4.27	The effect of dynamic loading at an acceleration of 1 g on the longitudinal flow rate through a dried-out cement plug, specimen CG5309-28	93
4.28	The effect of dynamic loading at an acceleration of 1 g on the peripheral flow rate through the rock around the plug, specimen CG5309-28	95
4.29	The effect of dynamic loading at an acceleration of 1 g on the longitudinal flow rate through a dried-out cement plug, specimen CG5309-01	96
4.30	Longitudinal flow rate through a wet cement plug prior to and during dye injection test, specimen CG5309-06	98
4.31	Section through a wet cement plug in Charcoal granite after dye injection	99
4.32	The observed longitudinal flow rate through a wet cement plug prior to and during dye injection tests, specimen CG5309-31V	100

LIST OF FIGURES--Continued

Figure		Page
4.33	Peripheral flow rate through the rock around the wet plug prior to and during dye injection tests, specimen CG5309-31V	101
4.34	Longitudinal flow rates through an oven-dried plug (log scale) observed during dye injection tests, specimen CG5309-31V	103
4.35	Inflow rate and longitudinal outflow rate through a dried-out cement plug during the dye injection test, specimen CG5309-01	104
4.36	Cross-section of a dried-out cement plug in Charcoal granite	105
5.1	Volumetric flow rate through a dried-out cement plug as a function of the injection pressure for specimen CG5309-01	109
5.2	Linear relationship of volumetric flow rate vs. pressure difference for specimen CG5309-31V with oven-dried cement plug	111
5.3	Hydraulic conductivity of Charcoal granite rock bridge as a function of time, specimen CG5309-04	112
5.4	Hydraulic conductivity of a wet cement plug in granite as a function of time, specimen CG5309-06	113
5.5	Hydraulic conductivity of a wet cement plug in granite as a function of time, specimen CG5309-08	114
5.6	Hydraulic conductivity of a wet cement plug in granite as a function of time, specimen CG5309-31V	115
5.7	Hydraulic conductivity of a wet cement plug in granite as a function of time, specimen CG5309-10	117
5.8	Hydraulic conductivity of a dried-out cement plug in granite as a function of time, specimen CG5309-01	118
5.9	Hydraulic conductivity of a dried-out cement plug in granite as a function of time, specimen CG5309-28	119
5.10	Dried-out cement plug permeability calculated using Darcy's law for flow through a porous medium	120
5.11	Hydraulic conductivity of a dried-out cement plug in granite as a function of time, specimen CG5309-21	122

LIST OF FIGURES--Continued

Figure		Page
5.12	Hydraulic conductivity of an oven-dried cement plug in granite as a function of time, specimen CG5309-31V	123
5.13	Permeabilities of Charcoal granite and of wet and dried-out cement plugs as a function of time	141
5.14	The effect of dynamic loading at a = 1 g on the hydraulic conductivity of a wet cement plug, specimen CG5309-06	144
5.15	The effect of dynamic loading at a = 1 g on the hydraulic conductivity of wet cement plug specimen CG5309-31V	145
5.16	The effect of dynamic loading at a = 2 g on the hydraulic conductivity of wet cement plug specimen CG5309-08	146
5.17	The effect of dynamic loading at a = 1 g on the hydraulic conductivity of dried-out cement plug specimen CG5309-28	147
5.18	The effect of dynamic loading at a = 2 g on the hydraulic conductivity of dried-out cement plug specimen CG5309-01	148
5.19	Discretization of cement plug into line elements for numerical transient flow analysis, specimen CG5309-31V, l = 10.4 cm	150
5.20	Hydraulic head at three locations in a 10.2 cm Charcoal granite rock bridge and in a 10.4 cm wet cement plug as a function of time, when injection pressure is increased from 2 to 4 MPa	152
5.21	Hydraulic head at each nodal point in the Charcoal granite rock bridge and in the wet cement plug for various time steps	153
5.22	Transition time as a function of plug legnth and head difference	154
5.23	Transition time for transient to steady-state flow as a function of K/S_s ratio (hydraulic diffusivity)	155

LIST OF TABLES

Table		Page
2.1	Possible Modes of Damage due to Shaking for Openings in Rock	17
3.1	Rock Cylinder Dimensions	34
4.1	Flow Test Record, Specimen CG5309-08, Wet Cement Seal	58
4.2	Flow Test Record, Specimen CG5309-01, Dried-out Cement Seal	59
5.1	Summary of Hydraulic Conductivities	124

ACKNOWLEDGMENTS

The research reported on has been performed by the University of Arizona, Department of Mining and Geological Engineering, for the U.S. Nuclear Regulatory Commission (NRC). Project monitor for the NRC is Mr. Jacob Philip. The project is under Dr. F.A. Constanzi, Chief, Waste Management Branch, Division of Engineering, Office of Nuclear Regulatory Research.

Dr. Jaak J.K. Daemen, Associate Professor, Department of Mining and Geological Engineering, University of Arizona, is the Principal Investigator. Dr. James G. McCray, Acting Director, Nuclear Fuel Cycle Research Program, Department of Nuclear and Energy Engineering, University of Arizona, has provided project management assistance. Gatut S. Adisoma has performed the experimental and theoretical work as part of his M.S. degree requirements. Experimental assistance, data handling and drafting have been provided by Robert Nordlund, Owowonta Ahanonu, Judy Bertuca, and Tim Sutter. Valuable discussions with Raoul Roko and Amitava Ghosh are gratefully acknowledged. Michael Porter has typed, assembled and produced the report.

We gratefully acknowledge the assistance of Dowell-Schlumberger, Tulsa, OK, for donating cements and additives, and in particular the technical help provided by Mr. Erik B. Nelson.

EXECUTIVE SUMMARY

An experimental sealing performance assessment is reported of cement borehole plugs that have been subjected to dynamic loading. This includes a study of plugs that have been dried and rewetted, as well as of plugs that have remained wet throughout the testing period.

An introductory literature review indicates that deep underground structures in competent rock are safer (i.e. more stable) than surface structures, than underground openings at shallow depth, or than openings in fractured rock, when they are subjected to earthquakes or to subsurface blasts. The major deformation mechanisms to which such openings are likely to be subjected during the impact of waves are summarized briefly. Such deformations will need to be accounted for in the design of plugs, e.g. with regard to the deformability of the materials. They have also served as an initial selection guide for the experimental work.

Cement plugs are installed in 2.5 cm diameter coaxial holes in 15 cm diameter 30 cm long granite cylinders. Type A Portland cement is mixed with 50% distilled water, and with an expansive agent and a dispersant, and poured on top of a stopper in the hole. After curing (for varying lengths of time, at room temperature, under water and atmospheric pressure), water is injected under pressure on top of the plugs and is collected below the plugs. Flow through the rock and through the plug is collected separately. Hydraulic conductivities are calculated from the measured flowrates. Once a long-term steady-state flow trend has been established, the cylinders are subjected to dynamic loading on a shaking table. Shaking is performed at accelerations of up to 2 g and for durations of up to 300 seconds. Flow testing is continued during and after the shaking.

Flow tests show that wet cement seals are somewhat less permeable than intact Charcoal granite. (The hydraulic conductivity of the latter is of the order of 10^{-11} to 10^{-12} cm/s.) Sealing performance can degrade severely when cement seals are allowed to dry. Drying induces shrinkage, initially resulting in the opening up of a gap along the plug-rock interface. Under more severe drying, e.g. at higher temperature or for longer duration, shrinkage cracks develop within the plug body and further enhance flow. Rewetting rapidly decreases the hydraulic conductivity of the seals, at least in part due to an apparent renewed expansion, although such results unavoidably are also affected by resaturation. The hydraulic conductivity does not decrease to the same orders of magnitude as that of plugs which have never been allowed to dry out. Dye injection shows very limited and uniform penetration into wet plugs, but strongly preferential flow along the plug/rock interface of dried plugs. The permeability of wet and of rewetted previously dried cement seals does not change significantly after the application of dynamic loads.

Sealing in an unsaturated environment may affect the drying (curing, aging) conditions of cementitious seals, as well as the structure of earthen seals. The influence of seal emplacement in an unsaturated environment, or of the thermally driven desaturation and possibly drying of the seal emplacement areas, will need to be integrated realistically into sealing performance tests, analyses, and allocations.

The basic approach in this study to evaluate the influence of shaking (dynamic loading) was to establish steady-state flow through a cement borehole plug in a rock cylinder, then subject the plugged cylinder to dynamic loading using a shaking table, and assess its influence on plug performance. The parameter determined in the flow testing prior to and after dynamic loading was the flow rate at various injection pressures, which was used to calculate the hydraulic conductivity of the cement plug. Distilled water has been used as a permeant. All flow tests have been conducted at relatively high pressure gradients, although a (small) variation in gradients has been used to obtain some information about the potential influence of the gradients on the hydraulic conductivity results. All experiments have been conducted on rock cylinders that are not loaded, except for the injection pressure and (unknown) cement swelling pressure, both of which induce a tensile tangential stress in the rock cylinder. It is postulated that this should impose a rather severe condition with regard to interface flow. Only at plug locations with exceedingly anisotropic in-situ stress-fields should a more disadvantageous sealing condition, with respect to the stress state, be encountered. All flow analyses (hydraulic conductivity calculations) assume that the plug, rock, and interface gap, if any, are saturated. In the dynamic loading phase, the tests were carried out with increasing duration (up to 5 minutes) and peak accel ration (up to 2 g). Shaking tests have been performed on rock cylinders with cement plugs that have been maintained wet throughout curing and testing, as well as on plugs that have been allowed to dry (room environment) or forced to dry (oven). However, the dynamic shaking was applied only after the dried-out plugs had been flow tested with water for several weeks (typically), during which time considerable resaturation and re-swelling of the cement plugs took place. Shaking was not performed on truly dry plugs, in which a pronounced shrinkage gap may exist between plug and borehole rock wall.

The introductory chapter of this report briefly summarizes the regulatory context of rock mass sealing requirements, quotes commentaries and viewpoints on rock mass sealing from the literature on HLW disposal, outlines the organization of this report, and lists related reports issued under this contract.

Chapter Two introduces the subject of the stability of underground openings affected by dynamic loading, particularly earthquakes. This chapter briefly reviews the extensive literature on the subject, which includes several relatively recent reviews on past experience, i.e. an empirical reference basis, as well as theoretical and numerical anlyses of the problem. It specifically identifies the major deformation patterns to which openings (e.g. shafts, drifts, boreholes) may be subjected, and hence for which seals may need to be assigned, when they are impacted by waves.

Chapter Three describes the materials tested (rock and cement grout), the experimental equipment and the test methods used to study the sealing performance (hydraulic conductivity, flow path identification) of cement plugs placed in boreholes in rock cylinders. Tests are performed on plugs that are allowed to dry out and on plugs kept wet throughout the test cycle. Dynamic loading is exerted by means of a shaking table.

Results of the experiments are presented in Chapter Four, and detailed analysis and discussion of the results in Chapter Five. Chapter Six includes a summary of the work performed, the conclusions drawn, and suggestions and recommendations for follow-up investigations.

Appendix A presents details of the analytical solution of one-dimensional transient flow testing which has been used for some plug testing. Appendix B gives a numerical (finite element) solution for the same problem. Cement grout composition, components and some properties are presented in Appendix C. Appendix D consists of a list of equipment and instrumentation used for the experimental program. Appendix E gives examples of temperature and of evaporation monitoring records taken during the testing period. A comprehensive set of experimental results is given in Appendix F. This includes laboratory comments and observations made in the course of the experiments.

BLANK PAGE

CHAPTER ONE

INTRODUCTION

1.1 Objective

The fundamental objective of this "Rock Mass Sealing" research project is to assess experimentally the performance of existing products and methods for sealing rock masses, in the current phase of the project to conduct an experimental evaluation of borehole plug performance. This work is aimed at determining the feasibility of sealing boreholes intersecting a repository rock mass to a level where it can reasonably be assured that the plugged boreholes will not become preferential radionuclide migration paths. This project studies experimentally the likelihood of preventing such migrations by sufficiently reducing the hydraulic conductivity of the plugged borehole (including the plug-rock interface). The work performed provides direct input to an assessment as to whether or not 10 CFR 60.134, Design of seals for shafts and boreholes (U.S. Nuclear Regulatory Commission, 1983, and, as amended, 1985, 1987) is likely to be satisfied by any particular proposed sealing methods. Some aspects of this study have broader implications, e.g. directly for 10 CRF.133 (d), and indirectly for 10 CFR.133 (a)(1),(2),(f) (U.S. Nuclear Regulatory Commission 1983a, and as amended, 1985, 1987), (h).

The study is conducted to establish a factual data basis on borehole sealing performance. Although some types of borehole sealing have been performed for many years, relatively little testing and sealing performance verification has been reported on.

Effective long-term isolation of high-level nuclear wastes in a deep underground repository relies on natural barriers (geologic, hydrologic, and geochemical environment of the site) and on engineered barriers (waste package, backfill materials). In the geologic media, hydrogeologic transport is the most important mechanism for potential transfer of radionuclides from the repository to the biosphere (Bredehoeft et al., 1978, p. 9; Boulton, 1978, p. 45; Committee on Radioactive Waste Management, 1978, p.2, ONWI, 1980, p. 6; Heckman and Minichino, 1982, p.1; Schneider and Platt, 1974, p. 4.88; Moody, 1982, p. 5). Therefore, one of the most important problems facing nuclear waste isolation, particularly with respect to possible contamination of groundwater, is long-term prediction of the movement of fluids in low-permeability rock surrounding the repositories (U.S. National Committee for Rock Mechanics, 1981, p. 22).

Groundwater migrates through the repository and eventually penetrates the waste canisters and dissolves or leaches the radioactive material. Current calculations suggest migration times of tens of thousands of years to hundreds of thousands of years to the surface water systems (Heckman and Minichino, 1982, p. 2). Nonetheless, one of the critical issues with respect to radionuclide migration remains

.... "the development of predictive hydrologic-flow models, which will include the near-field effects of repository construction (shafts, drill holes) and the superimposed thermal gradients caused by the waste" (Moody, 1982, p. 7).

The presence of manmade penetrations such as an open borehole intersecting a repository rock mass clearly compromises the integrity of the surrounding rock in slowing down the water migration. All associated penetrations must therefore be sealed reliably in order to prevent rapid migration of radionuclide-contaminated water to the biosphere. This is important especially if disposal strategies are adopted which do not emphasize the waste form and canister as a long-term barrier to release of radioactivity from the repository (South et al., 1981).

Concern about boreholes and their potential influence on the isolation performance of the rock mass surrounding repositories has been expressed in a number of basic reviews on underground HLW (High level radioactive waste) disposal (e.g. Atomic Energy of Canada Limited, 1978, p. 72; Bredehoeft et al., 1978, p. 8; Committee on Radioactive Waste Management, 1978, pp. 5,10; Heineman et al., 1978, p. 4; Boulton, 1978, p. 72; U.S. Department of Energy, 1979, p. 3.1.328; Arnett et al., 1980, p. 139; Barbreau et al., 1980, p. 528; Burkholder, 1980, p. 15; Irish, 1980, p. 42; OECD, 1980, Foreword; Pedersen and Lindstrom-Jensen, 1980, p. 195; U.S. Department of Energy, 1982, p. 29; Deju, 1983, p. 4; Kocher et al., 1983, p. 54; National Research Council, 1983, p. 8-9, 21, 63; U.S. Department of Energy, 1983, p. 25; Pigford, 1983, p. 10). Historically, attempts to seal manmade penetrations, particularly boreholes, started with the advent of drilling in the search for oil and gas. Although borehole plugging has been performed for decades, few measured data are available regarding its effectiveness (Christensen, 1980). Sealing requirements for a nuclear waste repository in deeply buried geologic media parallel, but are quite distinct from, the conventional borehole sealing technology which has evolved to date. For the first time, there is concern with extraordinary long-term durability in the order of thousands of years and longer. The seal must remain tight even if subjected to earthquakes and extensive differential surface erosion or subsidence (Roy et al., 1979, p. 1).

A repository of multiple barriers, engineered and natural, is expected to provide the desired waste containment and isolation. The system must also be designed to limit the release of radionuclides in case of an unlikely - but disruptive - event such as an earthquake (Wahi and Trent, 1982, p. 625), or other types of dynamic loading such as large scale nearby blasting. If a high-level waste repository is to be located near an underground nuclear weapons testing facility, such as the Nevada Test Site, ground motion generated by the blasts must be considered (e.g. Vortman, 1986). Seismic evaluations of critical structures such as nuclear waste repositories are required regardless of the degree of seismic hazard. Unfortunately, the state of the art in seismic design technology in rock is still poorly developed (Owen and Scholl, 1981, pp. xi, 162, 180-184).

Sealing materials that have been considered include cement and bentonite. These materials can have a low permeability. The plug/rock interface, and the potential interactions between plug and rock, may play a major role in the longer-term behavior of the borehole plug (Roy et al., 1979, p. 7; Gulick et al., 1980, p. 5; McDaniel, 1980, Abstract; Burns et al., 1982). Swelling of the sealing materials therefore is desirable in order to sufficiently reduce the hydraulic conductivity of the plug/rock interface, so that it will not become the preferential path for radionuclide migration. However, as pointed out by the advent of expansive cement for demolition purposes (Ishii et al., 1982; Sumitomo Cement, 1983), the importance to prevent excessive expansion of borehole, shaft, or drift seals cannot be overlooked. Conversely, if the volume expansion needs to be maintained over a prolonged period of time, reasonable assurance will need to be provided that this is feasible, e.g. that no or only acceptable shrinkage will develop, for example in an unsaturated environment exposure over many centuries.

Some years ago it was widely considered desirable, if not necessary, that sealing be performed such that the plug be at least as impermeable as the rock it replaces (e.g. Carlsson, 1982; Fernandez and Freshley, 1984, p. 43). Such a requirement was incorporated in the Proposed Rule 10 CFR Part 60 (U.S. Nuclear Regulatory Commission, 1981, §60.133), but has been relaxed in the Final Rule (U.S. Nuclear Regulatory Commission, 1983a, § 134(a)), for reasons discussed at some length in Staff Analysis of Public Comments (U.S. Nuclear Regulatory Commssion, 1983b, pp. 72-72, 422-430). The need for borehole plugging, and particularly for very high performance (e.g. very low hydraulic conductivity), is no longer universally accepted, nor obvious, and certainly might be a somewhat site dependent requirement, as shown by consequence assessments (e.g. Pedersen and Lindstrom-Jensen, 1980, p. 195; Klingsberg and Duguid, 1980, p. 43; Intera Environmental Consultants, Inc., 1981). These authors do recognize that borehole seals will provide "... an important redundant barrier ..." or "... will satisfy the concept of multiple barriers ...". A panel of experts convened by the Commission of the European Communities and the OECD Nuclear Energy Agency simultaneously considers backfilling and sealing (OECD, 1984, Section III.4) and, after stressing the host rock specificity of backfill and sealing functions, states that "they (i.e. seals) would be designed so as not to present any preferential flow paths ... there is confidence that they (i.e. the functional requirements) can be met by a number of different materials." That the controversy about sealing requirements is far from resolved is particularly well illustrated by the recently published disagreements among the ONWI Exploratory Shaft Peer Review Group (Kalia, 1986, p. 14). Site-specific analyses are most likely to provide information needed to finalize specific performance and design requirements (e.g. Stormont, 1984; Freshley et al., 1985; Seitz et al., 1987).

General guidelines for the separation of radioactive waste from the physical environment, and in particular for the acceptable radionuclide releases following repository closure, have been finalized by EPA (U.S. Environmental Protection Agency, 1986; 40 CRF 191). Detailed implement-

ation of the requirements is governed by 10 CFR 60 (U.S. Nuclear Regulatory Commission, 1983a, 1985). The research performed as part of this ongoing contract addresses specifically some of the remaining uncertainties associated with the sealing requirements in 10 CFR 60, including §60.51,(a)(4); §60.102,b(2),e(1),(2); §60.113; §60.133,(h), §60.142,(c), but particularly §60.134, Design of seals for shafts and boreholes.

Further guidance on implementation of NRC Rule 10 CFR 60 with respect to borehole and shaft sealing is provided in a Generic Technical Position (GTP) (U.S. Nuclear Regulatory Commission, 1986). The GTP identifies the information needs to be satisfied before construction authorization can be granted. It also states the need for including borehole and shaft seals in performance analyses. The work reported on here is in direct support of providing NRC with independent information and assessment tools for reviewing the corresponding parts of an eventual license application.

This research project addresses primarily the sealing of boreholes, as a form of manmade penetrations, using cement plugs. The objective is to assess the performance of model cement borehole plugs in granite, and their plugging effectiveness, under laboratory simulated dynamic loading conditions. The testing is performed for "ideal" (wet/saturated) cement plugs, and for cement plugs that have been allowed to dry out, the latter being plug conditions in locations above the groundwater table, in locations where the heat from the emplaced waste drives water away during the initial period of disposal, or in locations where repository drainage (e.g. during construction) results in temporary desaturation. The two represent good and poor cement/borehole interfacial conditions.

1.2 Scope and Limitations

The basic approach in this study was to establish steady state flow through a cement borehole plug in a rock cylinder, then subject the plugged cylinder to dynamic loading using a shaking table, and assess its influence on plug performance. The parameter determined in the flow testing prior to and after dynamic loading was the flow rate at various injection pressures, which was used to calculate the hydraulic conductivity of the cement plug. Only distilled water has been used as a permeant. All flow tests have been conducted at relatively high pressure gradients, although a (small) variation in gradients has been used to obtain some information about the potential influence of the gradients on the hydraulic conductivity results. All experiments have been conducted on rock cylinders that are not loaded, except for the injection pressure and (unknown) cement swelling pressure, both of which induce a tensile tangential stress in the rock cylinder. It is postulated that this should impose a rather severe condition with regard to interface flow. Only at plug locations with exceedingly anisotropic in-situ stressfields should a more disadvantageous sealing condition, with respect to the stress state, be encountered. All flow analyses (hydraulic conductivity calculations) assume that the plug, rock, and interface gap, if any, are saturated. In the dynamic loading phase, the tests were carried out with increasing duration (up to 5

minutes) and peak acceleration (up to 2 g). Shaking tests have been performed on rock cylinders with cement plugs that have been maintained wet throughout curing and testing, as well as on plugs that have been allowed to dry (room environment) or forced to dry (oven). However, the dynamic shaking was applied only after the dried-out plugs had been flow tested for several weeks (typically), during which time considerable resaturation and re-swelling of the cement plugs took place. Shaking was not performed on truly dry plugs, in which a pronounced shrinkage gap may exist between plug and borehole rock wall.

1.3 Organization

This introductory chapter briefly summarizes the regulatory context of rock mass sealing requirements, quotes commentaries and viewpoints on rock mass sealing from the literature on HLW disposal, outlines the organization of this report, and lists related reports issued under this contract.

Chapter Two introduces the subject of the stability of underground openings affected by dynamic loading, particularly earthquakes. This chapter briefly reviews the extensive literature on the subject, which includes several relatively recent reviews on past experience, i.e. an empirical reference basis, as well as theoretical and numerical anlyses of the problem.

Chapter Three describes the materials tested (rock and cement grout), the experimental equipment and the test methods used to study the sealing performance (hydraulic conductivity, flow path identification) of cement plugs placed in boreholes in rock cylinders. Tests are performed on plugs that are allowed to dry out and on plugs kept wet throughout the test cycle. Dynamic loading is exerted by means of a shaking table.

Results of the experiments are presented in Chapter Four, and detailed analysis and discussion of the results in Chapter Five.

Chapter Six includes a summary of the work performed, the conclusions drawn, and suggestions and recommendations for follow-up investigations.

Appendix A presents details of the analytical solution of one-dimensional transient flow testing which has been used for some plug testing. Appendix B gives a numerical (finite element) solution for the same problem.

Cement grout composition, components and some properties are presented in Appendix C.

Appendix D consists of a list of equipment and instrumentation used for the experimental program.

Appendix E gives examples of temperature and of evaporation monitoring records taken during the testing period.

A comprehensive set of experimental results is given in Appendix F. This includes laboratory comments and observations made in the course of the experiments.

1.4 Rock Mass Sealing Contract No. NRC-04-78-271 - Reports Issued

This Technical Report is the latest in a series of reports issued for the subject contract. A complete list of reports issued (to be issued for Schaffer and Daemen, 1987) is given below, to facilitate a general overview of work performed to date and of the overall context of ongoing work.

The first four reports, as well as the seventh, are literature surveys.

The fifth report is primarily a description of planning, experimental design and some preliminary tests.

The topical report by Jeffrey (1980) gives a comprehensive theoretical (analytical) discussion of transverse plug-rock interaction, based on elastic and viscoelastic calculations. This is complemented by the axial interaction discussed in Stormont and Daemen (1983), a report which is primarily experimentally oriented, but includes extensive analytical discussions.

The topical reports by Mathis and Daemen (1982) and by Fuenkajorn and Daemen (1986) present a detailed experimental assessment of drilling damage in granites and in basalts.

Experimental flow studies under polyaxial stress conditions are described in Cobb and Daemen (1982), under radially symmetric external loading in South and Daemen (1986), and on unloaded samples in Akgun and Daemen (1986). Additional data on plug performance under stressed and unstressed conditions are included in virtually all other reports.

Schaffer and Daemen (1987) describe experiments on rock fracture grouting, emphasizing the considerable lack of detailed knowledge and need for further research in this area.

Kimbrell et al. (1987) investigate the field performance of cement and of bentonite plugs installed in boreholes in granites.

Sawyer and Daemen (1987) describe some conventional soil mechanics characterization tests on bentonite, as well as flow tests on bentonite borehole plugs.

Williams and Daemen (1987) report flow tests on borehole plugs constructed of mixtures of crushed rock (basalt) and bentonite.

All annual reports subsequent to (5) include a combination of experiments, results, conclusions, and plans for future work, similar to the present annual report.

Quarterly progress reports are not listed as all information contained therein also is included in the annual reports.

1. South, D.L., R.G. Jeffrey, L.W. Klejbuk, and J.J.K. Daemen, 1979, "Rock Mass Sealing - Annual Report, October 1, 1978 - September 30, 1979," prepared for the U.S. Nuclear Regulatory Commission, SAFER Division, for Contract NRC-04-78-271, by the Department of Mining and Geological Engineering, University of Arizona, Tucson.

2. Daemen, J.J.K., 1979, "Rock Mass Sealing (Research in Europe)," 48 pp., Foreign Travel Trip Report to the U.S. Nuclear Regulatory Commission, SAFER Division, for Contract NRC-04-78-271, by the Department of Mining and Geological Engineering, University of Arizona, Tucson.

3. South, D.L., 1979, "Well Cementing," 75 + vii pp., Topical Report to the U.S. Nuclear Regulatory Commission, SAFER Division, for Contract NRC-04-78-271, by the Department of Mining and Geological Engineering, University of Arizona, Tucson.

4. Sultan, H.A., "Chemical Grouting for Rock Mass Sealing - a Literature Review," 45 + iv pp., Topical Report to the U.S. Nuclear Regulatory Commission, SAFER Division, for Contract NRC-04-78-271, by the Department of Mining and Geological Engineering, University of Arizona, Tucson.

5. South, D.L., R.G. Jeffrey, S.L. Cobb, S.P. Mathis, and J.J.K. Daemen, 1979, "Rock Mass Sealing - Annual Report, October 1, 1979 - September 30, 1980," prepared for the U.S. Nuclear Regulatory Commission, SAFER Division, for Contract NRC-04-78-271, by the Department of Mining and Geological Engineering, University of Arizona, Tucson.

6. Jeffrey, R.G., 1980, "Shaft or Borehole Plug-Rock Mechanical Interaction," 145 + xi pp., Topical Report to the U.S. Nuclear Regulatory Commission, SAFER Division, for Contract NRC-04-78-271, by the Department of Mining and Geological Engineering, University of Arizona, Tucson.

7. South, D.L., 1980, "Borehole Sealing with Clay (Part A). Considerations in Clay Mineral Stability (Part B)," 50 + iv pp.; 25 + ii pp., Topical Report to the U.S. Nuclear Regulatory Commission, SAFER Division, for Contract NRC-04-78-271, by the Department of Mining and Geological Engineering, University of Arizona, Tucson.

8. Cobb, S.L., W.B. Greer, R.G. Jeffrey, S.P. Mathis, D.L. South, and J.J.K. Daemen, 1981, "Rock Mass Sealing - Annual Report, September 1, 1980 - May 31, 1981," prepared for the U.S. Nuclear Regulatory Commission, SAFER Division, for Contract NRC-04-78-271, by the Department of Mining and Geological Engineering, University of Arizona, Tucson.

9. South, D.L., W.B. Greer, N.I. Colburn, S.L. Cobb, B. Kousari, S.P. Mathis, R.G. Jeffrey, C.A. Wakely, and J.J.K. Daemen, 1982, "Rock Mass Sealing - Annual Report, June 1, 1981 - May

31, 1982," prepared for the U.S. Nuclear Regulatory Commission, SAFER Division, for Contract NRC-04-78-271, by the Department of Mining and Geological Engineering, University of Arizona, Tucson.

10. Mathis, S.P. and J.J.K. Daemen, 1982, "Borehole Wall Damage Induced by Drilling: An Assessment of Diamond and Percussion Drilling Effects," 171 + xii pp., Topical Report to the U.S. Nuclear Regulatory Commission, SAFER Division, for Contract NRC-04-78-271, by the Department of Mining and Geological Engineering, University of Arizona, Tucson.

11. Cobb, S.L. and J.J.K. Daemen, 1982, "Polyaxial Testing of Borehole Plug Performance," 180 + xi pp., Topical Report to the U.S. Nuclear Regulatory Commission, SAFER Division, for Contract NRC-04-78-271, by the Department of Mining and Geological Engineering, University of Arizona, Tucson.

12. Daemen, J.J.K., D.L. South, W.B. Greer, J.C. Stormont, S.A. Dischler, G.S. Adisoma, N.I. Colburn, K. Fuenkajorn, D.E. Miles, B. Kousari, and J. Bertuca, 1983, "Rock Mass Sealing - Annual Report, June 1, 1982 - May 31, 1983," NUREG/CR-3473, prepared for the U.S. Nuclear Regulatory Commission, Division of Health, Siting and Waste Management, for Contract NRC-04-78-271, by the Department of Mining and Geological Engineering, University of Arizona, Tucson.

13. Stormont, J.C. and J J.K. Daemen, 1983, "Axial Strength of Cement Borehole Plugs in Granite and Basalt, NUREG/CR-3594, Topical Report to the U.S. Nuclear Regulatory Commission, Division of Health, Siting and Waste Management, for Contract NRC-04-78-271, by the Department of Mining and Geological Engineering, University of Arizona, Tucson.

14. Daemen, J.J.K., W.B. Greer, G.S. Adisoma, K. Fuenkajorn, W.D. Sawyer, Jr., A. Yazdandoost, H. Akgun, and B. Kousari, 1985, "Rock Mass Sealing - Annual Report, June 1983 - May 1984," NUREG/CR-4174, prepared for the U.S. Nuclear Regulatory Commission, Division of Radiation Programs and Earth Sciences, Office of Nuclear Regulatory Research, Contract No. NRC-04-78-271, by the Department of Mining and Geological Engineering, University of Arizona, Tucson.

15. Fuenkajorn, K. and J.J.K. Daemen, 1986, "Experimental Assessment of Borehole Wall Drilling Damage in Basaltic Rocks," NUREG/CR-4641, Technical Report to the U.S. Nuclear Regulatory Commission, Division of Radiation Programs and Earth Sciences, Office of Nuclear Regulatory Research, Contract No. NRC-04-78-271, by the Department of Mining and Geological Engineering, University of Arizona, Tucson.

16. Daemen, J.J.K., W.B. Greer, K. Fuenkajorn, A. Yazdandoost, H. Akgun, A. Schaffer, A.F. Kimbrell, T.S. Avery, J.R. Williams, B. Kousari, and R.O. Roko, 1986, "Rock Mass Sealing - Annual

Report, June 1984 - May 1985," NUREG/CR-4642, prepared for the U.S. Nuclear Regulatory Commission, Division of Radiation Programs and Earth Sciences, Office of Nuclear Regulatory Research, Contract No. NRC-04-78-271, by the Department of Mining and Geological Engineering, University of Arizona, Tucson.

17. Akgun, H., and J.J.K. Daemen, 1986, "Size Influence on the Sealing Performance of Cementitious Borehole Plugs," NUREG/CR-4738, Technical Report to the U.S. Nuclear Regulatory Commission, Division of Engineering Safety, Office of Nuclear Regulatory Research, Contract No. NRC-04-78-271, by the Department of Mining and Geological Engineering, University of Arizona, Tucson.

18. South, D.L. and J.J.K. Daemen, 1986, "Permeameter Studies of Water Flow through Cement and Clay Borehole Seals in Granite, Basalt and Tuff," NUREG/CR-4748, Technical Report to the U.S. Nuclear Regulatory Commission, Division of Engineering Safety, Office of Nuclear Regulatory Research, Contract No. NRC-04-78-271, by the Department of Mining and Geological Engineering, University of Arizona, Tucson.

19. Schaffer, A., and J.J.K. Daemen, 1987, "Experimental Assessment of the Sealing Effectiveness of Rock Fracture Grouting", NUREG/CR-4541, Technical Report to the U.S. Nuclear Regulatory Commission, Division of Engineering Safety, Office of Nuclear Regulatory Research, Contract No. NRC-04-78-271, by the Department of Mining and Geological Engineering, University of Arizona, Tucson.

19. Kimbrell, A.F., T.S. Avery, and J.J.K. Daemen, 1987, "Field Testing of Bentonite and Cement Borehole Plugs in Granite," NUREG/CR-4919, Technical Report to the U.S. Nuclear Regulatory Commission, Division of Engineering Safety, Office of Nuclear Regulatory Research, Contract No. NRC-04-78-271, by the Department of Mining and Geological Engineering, University of Arizona, Tucson.

20. Sawyer, W.D., II, and J.J.K. Daemen, 1987, "Experimental Assessment of the Sealing Performance of Bentonite Borehole Plugs," NUREG/CR-4995, Technical Report to the U.S. Nuclear Regulatory Commission, Division of Engineering, Office of Nuclear Regulatory Research, Contract No. NRC-04-78-271, by the Department of Mining and Geological Engineering, University of Arizona, Tucson.

21. Williams, J.R. and J.J.K. Daemen, 1987, "The Sealing Performance of Bentonite/Crushed Basalt Borehole Plugs," NUREG/CR-4983, Technical Report to the U.S. Nuclear Regulatory Commission, Division of Engineering Safety, Office of Nuclear Regulatory Research, Contract No. NRC-04-78-271, by the Department of Mining and Geological Engineering, University of Arizona, Tucson.

7. Gaudette, M.V., and J.J.K. Daemen, 1988, "Bentonite Borehole Plug Flow Testing with Five Water Types," Technical Report to the U.S. Nuclear Regulatory Commission, Division of Engineering, Office of Nuclear Regulatory Research, Contract No. NRC-04-76-271, by the Department of Mining and Geological Engineering, University of Arizona, Tucson. (In preparation)

CHAPTER TWO

DYNAMIC LOADING AND ITS EFFECT ON UNDERGROUND EXCAVATIONS: A LITERATURE REVIEW

2.1 Observational Study from Case Histories

2.1.1 Effects of Earthquakes

In order to have a better understanding of what effect dynamic loading might have on seals for underground nuclear waste repositories, a review of the effects of earthquakes and subsurface blasts on underground structures is appropriate. Case study surveys have been made of the effects of earthquakes on wells, tunnels, mines, and other underground structures. The results for 127 cases have been summarized in several reports (Stevens, 1977; Dowding, 1977; Dowding and Rozen, 1978; Owen and Scholl, 1981).

Most directly relevant for borehole plugging, Nazarian (1973) states that "published reports describing the conditions of numerous water wells during and after major earthquakes indicate very little damage to wells." Marine et al. (1981) and Pratt et al. (1979a) summarize several reports that include investigations of water and oil well damage induced by earthquakes. They conclude that water well damage is caused primarily by sanding and silting, and appears to be a near-surface phenomenon with little effect below 100 m, except where wells cross faults. "Major damage results from bending, crushing, or shearing of the casing as a result of differential movement of the surrounding rock." Eckel (1970), as referenced by Pratt et al. (1979a), states that no damage was reported to oil and gas wells after the 1964 Alaskan earthquake, one of the largest earthquakes that occurred in this century, and which induced extreme surface damage. Conversely, earthquakes have significantly affected flow regimes from wells, e.g. "earthquakes have caused wells to dry up, springs to increase or decrease their flow rates, and alterations of groundwater flow in mines" (Owen et al., 1980, p. 21). A more recent review by Summers (1984), as summarized by Isenberg and Taylor (1984), identified approximately 23 damaged wells as a result of the May 2, 1983, Coalinga, CA, earthquake. "Among these, damage to pumps was prevalent. For example, pump head misalignment was especially common. These pumps are at depths of 600 ft and greater. Instances of collapsed casings, diminished yield and damaged column assembly were also cited."

The surveys indicate that underground structures in general are less severely affected by earthquakes than surface structures at the same geographic location. A surface structure responds as a resonating cantilevered beam and, therefore, amplifies the ground motion, while an underground structure responds with the ground. Ground motion caused by earthquakes is less severely felt in bedrock than on the surface. Peak acceleration due to shaking is greater on the surface than at depth because shaking effects of seismic waves generally attenuate

with depth, although records exist of increasing amplitude of motion with depth (Iwasaki et al., 1977, as quoted by Owen et al., 1980, p. 25; Iwasaki et al., 1981). Theoretical analyses confirm that displacements induced by earthquake fault-slip can either decrease or increase with depth, depending on fault geometry and type (Pratt et al., 1979, pp. 34-38), at least within the near-field. Severe damage is often associated with structures in soil and poor rock, whereas damage to structures in competent rock is usually, but not always, minor (Pratt et al., 1979; Yanev and Owen, 1978; Bach, 1977; Manolis and Beskos, 1981).

Seismic damage to underground structures may be attributed to three factors, namely fault slip, ground failure, or shaking. Damage due to sudden fault slip has been reported in tunnels where the opening passes through a fault zone. Ground failures, such as rock slides, landslides, squeezing, soil liquefaction, and soil subsidence, have damaged portals and shallow structures (Owen and Scholl, 1981, p. 14). Seismic damage due to these two factors can be minimized or avoided with careful siting, especially for a deep underground nuclear waste repository. The effects of shaking could be the most seismically damaging to an underground repository. Table 2.1 lists possible modes of damage due to shaking and their possible consequences. It is clear from Table 2.1 that damage in the ordinary sense of the word will be of importance during the operational phase of the repository. Greater interest in the long term will be the seismic damage that creates or enhances fractures and cracks in the plug-rock system near the repository, which in turn will increase its permeability.

To evaluate damage due to earthquake shaking, information about the underground structures and about the earthquake is needed, in particular: shape and size of the opening, depth below ground surface, type, strength, and deformability of rock or soil, support and lining systems, and shaking severity.

The ground shaking at the site can be characterized by peak ground motion parameters, duration, frequency content, and intensity. Information on ground motion at the depth of the opening would be the most appropriate. This is not generally available since data are usually measured only for ground motion at the surface. Attempts have been made to correlate surface data and data at depth at the Nevada Test Site, and the empirical relationship generated can be used to predict the ground motion parameters at depth from surface data in the absence of the former (Vortman and Long, 1982a; Vortman and Long, 1982b; Owen and Scholl, 1981; Vortman, 1986). Still, no definitive statement can be made regarding the attenuation of seismic motions with depth due to the complexity of their nature. Observations in Japan (Iwasaki et al., 1981) found that in alluvial sites peak horizontal accelerations at depth fall between one-half and one-quarter of the values at the surface. On the other hand, peak accelerations in fairly uniform rock sites are not, in general, significantly reduced at depth as compared with peak accelerations at the surface. The study was conducted to a depth of 127 m. These results are confirmed by a parametric study of depth dependence using the 1966 Parkfield earthquake time-history (Owen and Scholl, 1981, p. 103-105).

Table 2.1 Possible Modes of Damage due to Shaking for Openings in Rock (after Owen and Scholl, 1981, p. 15)

Possible Modes of Damage	Possible Consequences
Rock fall	Injure personnel Block transportation/ ventilation Disrupt water management and other services Damage shaft wall/equipment
Rock slabbing	Same as for rock fall
Opening up of existing rock seams and fractures, shifting of rock blocks	Increase permeability along the opening Weaken rock structure
Cracking of concrete liners	Increase permeability Weaken liner
Spalling of shotcrete or other surfacing material	Lead to rock fall if extensive
Unraveling of rock bolted system	Same as for rock fall
Steel set collapse	Same as for rock fall

"The available data on the effects of earthquakes on underground structures are not sufficient to determine the relative importance of various parameters for predicting damage or lack of damage. Many of the documents do not provide details on all the parameters during and after the earthquake, and a great number of events occurred many years ago so that it is no longer possible to obtain complete information on all the relevant factors. The empirical relations between various ground motion parameters and the extent of damage are approximate and tentative. A more detailed definition of the relationship requires more comprehensive studies than are currently available." (Owen and Scholl, 1981, p. xii)

Nevertheless, the observations suggest that peak ground motion parameters, such as acceleration and particle velocity, seem to correlate with the extent of damage. It is not entirely clear whether damage should be correlated with peak acceleration or with peak particle velocity. Intuition suggests that correlation with peak acceleration is better for massive concrete structures in soil and that correlation with peak particle velocity is better for hard rock openings (Owen and Scholl, 1981, p. 177). However, since most damaging earthquakes normally have a low frequency range, i.e. 0.1 to 15.0 Hz (Owen and Scholl, 1981, p. 113), it is common to use a single value of acceleration as a criterion for intensity and damage potential (Oriard, 1972, p. 209). Duration of the earthquake shaking also influences the extent of damage (Oriard, 1982a, p. 87; Oriard, 1972, p. 210). Longer duration is expected to correlate with greater damage, particularly for buried concrete structures (Owen and Scholl, 1981, p. 177). Frequency content of the vibration may also be important because some researchers suspect that damage to openings in rock is associated with wavelength on the order of twice the cavity dimensions (Owen and Scholl, 1981, p. 178). Structural support and in-situ stresses are other important parameters that affect the stability of underground structures.

Three damage levels due to shaking have been identified. The classification 'no damage' means no new cracks or rock falls, 'minor damage' includes new cracking and minor rock falls, and 'damage' includes severe cracking, major rock falls, and closure. The following conclusions can be drawn from the review of the effects of earthquakes on underground structures (Dowding and Rozen, 1978; Owen and Scholl, 1981, pp. 35-37):

1. No damage was found in lined or unlined tunnels at ground surface accelerations below 0.19g.* There were few cases of minor damage for surface accelerations between 0.19g and 0.4g, which corresponds to surface peak particle velocities between 20 and 75 cm/s (8 and 30 in/s) at frequencies between 0.8 to 1.5 Hz.

2. Severe damage and collapse of rock tunnels from earthquake shaking occurred only under extreme conditions, such as ground surface

---

*g represents acceleration of gravity, 981 cm/s^2 (32.2 ft/s^2).

accelerations exceeding 0.5g, marginal construction, and poor rock. Complete tunnel closure was not due to shaking alone but appeared to be associated with movement of an intersecting fault or other major ground movement.

3. Tunnels were much safer than aboveground structures for a given intensity of shaking, and tunnels in deep rock were safer than shallow tunnels, although data for the latter were incomplete.

4. Duration of strong seismic motion appeared to be an important factor contributing to the severity of damage to underground structures.

Dowding and Rozen (1978), as well as Owen and Scholl (1981), correlate damage to both acceleration and peak particle velocity, at least in part because the former is the common practice in earthquake engineering, the latter in blasting. McGarr (1983), on the other hand, argues rather forcefully that peak acceleration is an inappropriate predictor of damage potential, an argument based in part on tunnel observations detailed in McGarr et al. (1981). Owen et al. (1980, Ch. 6, especially pp. 26-28) recognize the merits of peak ground motion parameters for simplified design, but stress that only very limited information about the complex ground motions can be provided by such simplified descriptors.

2.1.2 Effects of Subsurface Blasts

The most common source of explosion-induced ground vibrations on underground openings is conventional blasting, as used in mining and other underground excavations. Other sources are underground nuclear explosions and high explosives used in connection with defense studies. The ground motions from these sources differ from earthquake ground motions in frequency content, duration, and values of peak ground motion parameters at equal distances from the source. Most blasting vibrations are characterized by relatively high frequencies compared to earthquakes. A large bench blast typically will have a dominant-frequency range of 2 to 50 Hz, sometimes up to 100 Hz for construction blasting (Siskind et al, 1980, p. 6). Typical tunnel blasting frequency ranges are from 100 to 200 Hz (Oriard, 1982a, p. 1595). The cycle duration is shorter, just as the wavelengths are shorter, thus providing less opportunity for displacements to occur (Oriard, 1982b, p. 64).

As damage is caused by strain in the material (Jaeger and Cook, 1979, p. 535), the ground motion parameter associated with blasting operations commonly used for damage criteria is peak particle velocity (Oriard, 1982a, p. 1595, Owen and Scholl, 1981, p. 23, Holmberg, 1982, p. 1586). A high-amplitude, low-frequency motion has a greater damage potential than a high-frequency motion that produces a similar velocity or acceleration level, and the disparity is greatest when using acceleration values. For an equivalent strain, the higher the frequency of vibration, the greater the acceleration that can be tolerated because acceleration is proportional to frequency for a given amplitude (Jaeger and Cook, 1979, p. 534). Therefore, particle velocity rather than acceleration is preferred as a criterion for damage potential because

it appears to have the best correlation in the frequency range encompassed by most blasting vibrations. Nevertheless, the degree of conservatism may change with frequency.

Studies have been made to relate particle velocity and damage, mostly to surface structures. Some values are given for underground structures as well as for surface structures. A peak particle velocity of 5 to 10 cm/s (2 to 4 in/s) results in occasional falling of loose rock on slopes, 12.5 to 37.5 cm/s (5 to 15 in/s) causes falling of partly loosened sections of rock in underground and aboveground slopes, and 62.5 cm/s (25 in/s) or higher creates some damage in the relatively unsound rock types (Oriard, 1982a, p. 1600). Holmberg et al. (1984, p. 173) give critical values of peak particle velocity that cause tensile damage in different rock mass types. A peak particle velocity of 100 cm/s (40 in/s) or higher creates damage in hard rocks with strong joints, 70 to 80 cm/s (28 to 32 in/s) causes damage in medium hard rocks with no weak joints, and 40 cm/s (16 in/s) or lower results in damage for soft rocks with weak joints. Another study by Holmberg (1982) shows that at a peak particle velocity of 70 to 100 cm/s (28 to 40 in/s) cracks are induced or enlarged in a granite rock mass. The same values are also used as damage criteria in rock by Hoek and Brown (1980, p. 371) and by Holmberg and Maki (1982, p. 777), the latter in a study to determine the damage zone in pit slopes due to large-scale production blasting. An earlier study (Bauer and Calder, 1971, p. 94) suggests that a peak particle velocity less than 25 cm/s (10 in/s) causes no fracturing of intact rock, 25 to 63 cm/s (10 to 25 in/s) creates minor tensile slabbing, 63 to 251 cm/s (25 to 100 in/s) gives strong tensile cracking and some radial cracking, and a velocity over 251 cm/s (100 in/s) results in complete break-up of the rock mass. According to the third edition of The Modern Technique of Rock Blasting, a peak particle velocity of 30 cm/s (12 in/s) causes rock fall in galleries and unlined tunnels. No value is given for particle velocity threshold for crack initiation in rock (Langefors and Kihlstrom, p. 1978, p. 288). Owen and Scholl (1981, p. 23), quoting from the first edition of the aforementioned reference, suggest that the particle velocity threshold for the formation of new cracks in rock is 60 cm/s (24 in/s). However, this value does not appear to be listed in the original reference (Langefors and Kihlstrom, 1963, p. 288).

In general, these criteria from several independent studies correlate broadly with the peak particle velocity thresholds for earthquakes suggested by Dowding and Rozen, 1978 (see Section 2.1.1). The latter also review an experiment to investigate cracking of shotcrete liners caused by blasting vibrations. The tunnels are rock bolted and lined with 5 to 28 cm (2 to 11 in) of shotcrete. Formation of hairline cracks in the shotcrete liner occurs at a peak particle velocity of 90 cm/s (36 in/s), and shearing of existing cracks at 120 cm/s (48 in/s). A study of engineered concrete structures also shows that a particle velocity of 50 to 75 cm/s (20 to 30 in/s) in the frequency range of 20 to 100 Hz does not result in damage (Oriard, 1982a, p. 1600).

Underground explosion tests in rock tunnels conducted for the US Army Corps of Engineers produce similar results (Owen and Scholl, 1981, p. 23-27, adapted from the Engineering Research Associates' Report of

April 1953; also Labreche, 1983). The tests are conducted in unlined tunnels in granite, sandstone, and limestone using TNT explosives. Tunnel diameters vary from 1.8 to 9.15 m (6 to 30 ft), and the charge varies from 144 to 144,300 kg (320 to 320,000 lb). Damage to the tunnels is classified in four categories, from very heavy damage with tight closure of the tunnel in Zone 1 to intermittent spalling of rock in Zone 4, with no damage beyond Zone 4. The particle velocity associated with the the outer limit of Zone 4 is found to be 90 to 181 cm/s (36 to 72 in/s) and that of Zone 3, which represents continuous damage in the tunnel surface to intermittent spalling, is 392 cm/s (156 in/s). Further investigation of Zone 4 data shows that, of the 14 tests conducted, the lowest peak particle velocity value is 45 cm/s (18 in/s) and the average is 120 cm/s (48 in/s).

The effects of underground nuclear explosions on tunnel damage have been studied in connection with Project Hard Hat (Owen and Scholl, 1981, pp. 27-35, adapted from Holmes et al., 1963). The test is conducted in the Climax Granite at the U.S. Department of Energy's Nevada Test Site, and various tunnel cross-sections, liners, and backpacking are used. The charge yield of the Hard Hat device is 5.9 kiloton. Based on the free-field data obtained from stations along the access tunnel, experimentally determined relationships are plotted for peak acceleration, particle velocity, strain, and stress parallel to the direction of the shock wave. Values of these quantities for various zones of damage are determined from these plots. The peak particle velocity thresholds for Zone 4 and Zone 3 damage are 181 and 331 cm/s (72 and 132 in/s), respectively, the same order of magnitude as obtained from the underground explosion tests conducted for the US Army Corps of Engineers. However, peak accelerations for this test (20g at the outer limit of Zone 4 and 100g at the outer limit of Zone 3) exceed peak accelerations for earthquakes by more than an order of magnitude.

The above observations suggest that the large scale subsurface blasts of the Underground Explosion Test program and the Underground Nuclear Explosion tests create ground motions far more severe at closer distances than those from earthquakes. Nevertheless, these extreme situations provide insight into the dynamic behavior of tunnels useful in understanding earthquake performance of underground structures. The review of the effects of subsurface blasts on underground structures can be summarized in several important observations:

1. Conventional mine blasting in unlined rock tunnels creates minor damage at a peak particle velocity threshold of 30 cm/s (12 in/s), which correlates well with the threshold of 20 cm/s (8 in/s) found for earthquakes (conventional blasting typically produces much higher frequencies than earthquakes).

2. Large scale subsurface blasts, such as large conventional and nuclear underground explosion tests, give some indications that minor damage to unlined rock tunnels may be effectively prevented by thin concrete lining or by rock bolts and wire mesh.

3. The underground nuclear explosion test shows that thick concrete liners cast against the rock did not perform as well as thick concrete liners with backpacking, indicating that backpacking protects the liner during shock loading. Thick and rigid liners also suffer more damage than thinner - and more flexible - liners (Okamoto, 1984, p. 532).

4. The underground nuclear explosion test also shows that tunnels in highly fractured rock were more severely damaged than tunnels in more competent rock. A similar comparison of damage is to be expected from the much less severe ground motion of an earthquake.

2.2 Seismic Analysis of Underground Structures in Rock

The seismic behavior of rock sites is still poorly understood (U.S. National Committee for Rock Mechanics, 1981). Hence, the technologies for analyzing the seismic stability of an opening in rock and for determining hardening procedures are still poorly developed (Owen and Scholl, 1981, pp. 162, 180, 184). There are many reasons for this. Firstly, there is the somewhat unfortunate perception that openings in rock are not vulnerable to earthquake motion. (It needs to be recognized that others, e.g. Marine et al., 1981, probably would argue that this perception is correct, rather than unfortunate.) There are very few reports of major damage to openings in rock from earthquakes, and therefore designers tend to ignore this potential failure mode. Secondly, many of the simplifying assumptions employed in modeling the dynamic behavior of structures in soil cannot be used for structures in rock. Competent rock permits larger opening spans than soil, and the support may consist of rock bolts and/or a thin layer of shotcrete. The lining, if it exists, is so flexible that it cannot be viewed as an elastic beam embedded in an elastic medium, as is the case for many structures in soil. Thirdly, the development of sophisticated dynamic design methods in rock is not encouraged because of the lack of compatibility with prevalent static design methods, which is largely dominated by empirical procedures. However, this situation may be changing due to the progress in studies evaluating static ground-liner interaction and design procedures. Lastly, and perhaps the most significant reason, is that the state of the art in static design of underground structures in rock is itself still in its infancy.

It is therefore necessary to look at the static design methods in reviewing the seismic design methods of underground structures in rock. Current static and seismic analyses take different approaches depending upon whether the rock mass is assumed to be homogeneous and elastic or is assumed to be nonhomogeneous and inelastic. Based on the assumptions invoked, three methods of analysis are available: analytical methods, empirical methods, and numerical methods.

2.2.1 Dynamic Response of Underground Openings

Underground structures in rock differ from surface structures (buildings) in that the geologic medium is a major component of the structure. In cases where the rock does not require support or reinforcement, the geologic medium <u>is</u> the structure. The response of underground structures such as tunnels (lined or unlined) to seismic

motion may be understood in terms of three principal types of deformation: axial, curvature, and hoop. Axial and curvature deformations develop when waves propagate parallel or obliquely past a tunnel. Axial deformation induces alternating regions of compressive and tensile strain that travel as a wave train along the tunnel axis (Figure 2.1a). Curvature deformation creates alternate regions of negative and positive curvature propagating along the tunnel (Figure 2.1b). Hoop deformation results when waves propagate normal or nearly normal to the tunnel axis. Two effects of hoop deformation might be observed. One is a distortion of the cross-sectional shape (Figure 2.1c) that creates concentrations in the hoop stresses. The other effect is that of "ringing" or the entrapment and circulation of seismic wave energy around the tunnel. The latter occurs when the wavelengths are less than the tunnel radius.

Axial or curvature deformation created by the passage of seismic waves results in cycles of alternating compressive and tensile stresses in the tunnel wall. These dynamic stresses are superimposed upon the existing static state of stress in the rock and in the tunnel liner if it is present. Several failure modes may result. Seismic compressive stresses add to the static compressive stresses and may cause spalling along the tunnel perimeter due to local buckling. Seismic tensile stresses subtract from the static compressive stresses, and the resulting stresses may be tensile. This implies that joints or other discontinuities will open, permitting a momentary loosening of rock blocks and a potential fall of rock from the tunnel roof and walls. The response of the medium and liner for axial and curvature deformations is most appropriately analyzed by three-dimensional numerical methods. Similarly, hoop deformation due to the seismic motion creates seismic stresses around the tunnel, and the stability of the tunnel can be evaluated by comparing the rock strength with the sum of static and seismic stresses. The response of an underground opening to hoop deformation can be calculated by analytical methods for a simplified case, or computed by numerical methods for both idealized and more realistic rock conditions.

2.2.2 Analytical Methods

If the rock is assumed to be homogeneous and elastic, compatible procedures exist for the analysis of both static and seismic hoop stresses. For static analysis, the Kirsch solution can be used to determine the stresses around circular openings due to the in situ stress field (Timoshenko and Goodier, 1970, p. 91; Jaeger and Cook, 1979, p. 251; Hoek and Brown, 1980, p. 104). This general solution is used by Terzaghi and Richart (1952) to compute the distribution of stresses around a circular tunnel. Solutions for elliptical tunnels and spheroidal cavities are also presented.

The dynamic stress-concentration factors for the circumferential stress in homogeneous, elastic rock around a circular tunnel due to steady-state harmonic waves have been determined by Pao and Mow (1973). In an analysis for earthquake motion, this factor is used to estimate the maximum seismic stress around the opening by multiplying it by the peak seismic stress in the free field determined from the peak particle

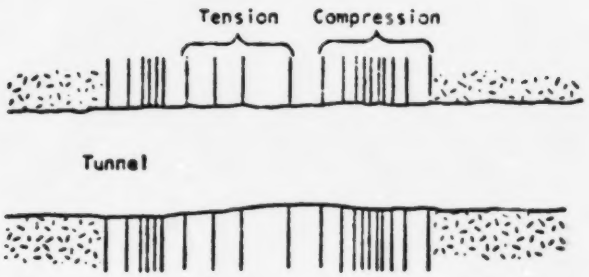

(a) Axial deformation along tunnel.

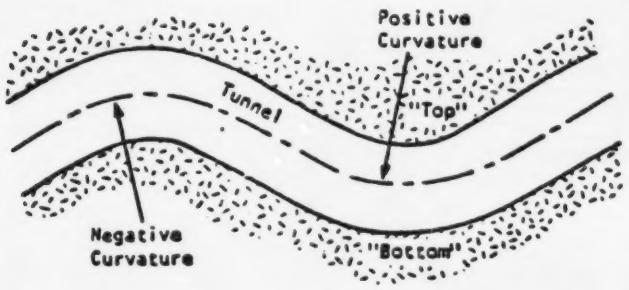

(b) Curvature deformation along tunnel.

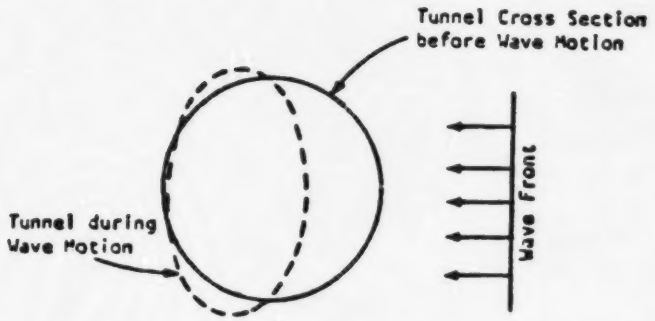

(c) Hoop deformation of cross section.

Figure 2.1 Principal types of deformation in a tunnel due to seismic motion (after Owen and Scholl, 1981, p. 50).

BEST COPY AVAILABLE

velocity of the earthquake. Thus, for circular tunnels in homogeneous elastic rock, the methods for the analysis of static and seismic stresses are quite compatible and the design can be evaluated by comparing the sum of the static and seismic stresses to the rock strength.

The analytical method of solution becomes extremely difficult - far beyond the present state of knowledge - for underground structures of arbitrary shape, not to mention for real (i.e. nonhomogeneous and inelastic) geologic media (Manolis and Beskos, 1981, p. 295, Kobayashi and Nishimura, 1982, p. 177). However, for static design of circular tunnels in nonhomogeneous and inelastic media, a simplified analytical method has been developed (Einstein and Schwartz, 1979). This method uses limited quantitative geological data in conjunction with a simple but rational analytical model to determine support requirements. Conceptually, this simplified analysis falls between the empirical and numerical methods. No exact solution is known for seismic design in nonhomogeneous and inelastic media.

2.2.3 Empirical Methods

Static design of tunnels in real rock masses continues to be dominated by empirical methods in spite of the increase in sophistication of numerical methods. The application of numerical methods requires accurate and detailed information on the geology and the development of appropriate constitutive models, whereas the application of empirical methods, which are based on actual observations of prototype openings, does not require such detailed quantification of the geologic information. Since information on the geology is usually very limited prior to excavation, empirical methods are favored in the design of an underground opening. During construction, although information about the geology has greatly increased, decisions regarding the initial support must be made rather quickly, again favoring the empirical over numerical methods.

A number of empirical methods are available for static design, one of the earlier ones being the Terzaghi rock load approach (Terzaghi, 1946). Others include the semi-analytical new Austrian tunneling method (Rabcewicz, 1973), and the methods by Wickham et al. (1974), Barton et al. (1974), and Bieniawski (1976), which use a number of parameters to quantify the rock mass behavior. The empirical methods have been reviewed in detail by Einstein et al. (1979) and by Hoek and Brown (1980, Chs. 2,8). A seismic design method for openings in real rock conditions compatible with the empirical method for static design is proposed by Owen et al. (1979). This method is based upon a qualitative assessment of rock-support interaction and upon the empirical relationship between damage to rock tunnels and peak ground motion parameters of earthquakes.

2.2.4 Numerical Methods

With the advance of computers, the application of numerical modeling for the analyis of static and dynamic behavior of underground structures becomes increasingly more common practice. It is used to

determine the static stability of structures, as well as their dynamic stability when subjected to earthquakes or large vibrations induced by explosions. With the development of more realistic and sophisticated material models, seismic damage such as the introduction or enhancement of cracks can be studied. This is certainly a subject of great interest in a nuclear waste repository performance predictions, since fractures and cracks could facilitate groundwater or air circulation around, into and out of the repository.

There are two fundamentally different methods of viewing a geologic material. Both recognize geologic material as being discontinuous due to the presence of faults, joints, bedding planes, and fractures. The more popular approach treats the rock mass as a continuum intersected by a number of discontinuities, while the other views the rock mass as a discontinuum or an assembly of independent particles. Finite element and finite difference analysis are the most widely used differential methods basically belonging to the continuum model, although they have been extended to allow limited discontinuum modeling. Discrete or distinct element modeling is the most powerful discontinuum method, and is rapidly gaining widespread acceptance. The great potential value of its application for purposes discussed here is particularly well illustrated by examples of the analysis of disturbed zones around underground excavations (e.g. Barton et al., 1987; Lorig and Brady, 1984; Voegele et al., 1977; Dowding et al., 1983). The applicability and realism of such approaches is enhanced further by the possibility to include realistic support and reinforcement modeling (e.g. Lorig, 1985). In the differential methods, the entire region of interest is approximated (discretized), either physically or mathematically. In recent years, another type of continuum model is regaining popularity, namely the integral methods. Integral or boundary element methods differ fundamentally from the differential methods in that discretization is necessary only along interior or exterior boundaries.

Static stresses around an opening of arbitrary shape can be computed by the above mentioned approaches. For an elastic medium, simple two-dimensional finite element formulations given in Desai and Abel (1972) and Desai (1979), or boundary element procedures outlined in Hoek and Brown (1980), Crouch and Starfield (1983), and Brebbia et al. (1984) can be used. Compatible methods exist for computing the seismic hoop stresses, for instance using the integral methods proposed by Niwa et al. (1976), Manolis and Beskos (1981), and Kobayashi and Nishimura (1982).

A numerical study of cavity response in an elastic half-space using the integral equation method shows that seismic response of a cavity is a function of depth. The seismic motion of a shallow cavity strongly interacts with the free surface, particularly in stiff soils or soft rocks. Conversely, the seismic motion of a deep cavity, especially in hard rock sites, will not interact with the free surface so that cavity response is essentially the same as the incident field response at that depth (Owen and Scholl, 1981, pp. 105-121). This is a common assumption for buried pipeline studies (e.g. O'Rourke and Wang, 1978; Wang, 1979; O'Rourke et al., 1979; Datta and Shah, 1982), although more generalized solutions have been developed (e.g. Ariman and Muleski, 1979). A

similar study confirms that the depth of embedment of buried pipelines or lined tunnels influences their dynamic response greatly (Datta and Shah, 1982).

For nonhomogeneous inelastic rocks, more elaborate computer programs are available for the evaluation of static stresses around an opening (Bathe et al., 1974; Hofman, 1976; Bathe, 1978; DeSalvo and Swanson, 1979). They include advanced constitutive models that represent many important rock mass properties, such as joint behavior, strain softening, dilatancy, tensile cracking, and plasticity. These and some other general purpose programs are also applicable for the dynamic analysis of underground openings, including the analysis for axial and curvature deformations. A numerical evaluation of stresses due to axial and curvature deformations requires a three-dimensional model and hence the high cost is a limiting factor.

Two examples of numerical studies of the dynamic response of underground openings are worth summarizing. The first example is the prediction of damage in underground structures due to ground motion using a simplified approach based on the calculation of maximum seismic stresses and strains in the free field, i.e. away from the opening. A two-dimensional finite element stress analysis is used in a comparative study of three candidate host formations for a nuclear waste repository at the Nevada Test Site, namely shale, granite, and tuff (Yanev and Owen, 1978; Owen et al., 1979). The earthquake time histories used include peak ground accelerations of 0.3 g to 1.0 g. This simplified approach does not account for the presence of the underground structure, and the results can be useful only in the qualitative evaluation of the stability of an opening in different types of rock.

The results of stress analysis show that for any of the specified ground accelerations, seismic stresses are much smaller than the strength of granite and tuff rock mass, both in tension and in compression. For shale, however, the calculated stresses indicate that crushing may occur at peak ground accelerations of 0.7 g and above, and tensile fracturing might be expected at peak ground accelerations of 0.5 g and above. The study indicates that openings in homogeneous rock have a fairly high degree of safety against earthquakes, but the nature and extent of jointing has a significant effect on dynamic stability.

The second example is a study by Wahi et al (1980) using an explicit finite difference code to simulate earthquake propagation through a two-dimensional mesh. Material models are developed for the non-linear behavior of three different host rocks, i.e. salt, granite, and shale. These include an isotropic plastic model, a joint-slip model, and a tensile-cracking model (see also Wahi and Trent, 1982; Marine et al., 1982; Ross-Brown et al., 1981).

The purpose of this study is to determine the conditions under which seismic waves generated by an earthquake might cause instability to an idealized, 8 x 8 m square opening located 600 m below the ground, or cause fracturing or joint movements that would lead to an increase in permeability of the rock mass. This study shows that in salt and granite, moderate earthquakes (up to 0.41 g) do not cause major

fracturing or tunnel instability. However, an artificial rock-burst tremor with high acceleration (up to 0.95 g) and high frequencies (or short wavelengths) is amplified around the opening, and fracturing may occur as a result of this seismic loading. In shale, even moderate loading results in tunnel collapse. High horizontal stresses are also shown to be undesirable for dynamic stability of underground openings in jointed media, at least with the joint geometry analyzed here. This investigation seems to be the first reported wave propagation study of an underground opening with two-component motion, one component being P-wave motion and the other SV-wave motion.

2.3 Seismic Hazard and Design Response Criteria for Nuclear Facilities

Seismic hazard is defined as any physical phenomenon associated with an earthquake (for example: ground shaking, ground failure) which may produce adverse effects on human activities (Algermissen, 1980, p.1, based on the definition suggested by the Seismic Risk Committee of the Earthquake Engineering Research Institute). By studying regional seismicity, the comparative seismic hazard for various locations can be determined. Seismic hazard can be expressed in the form of the odds that an earthquake that produces peak ground acceleration exceeding a given value within a given period of time will occur at a certain site. Such a probabilistic expression of seismic hazard is used to prepare the seismic hazard map of the United States shown in Figure 2.2. This map indicates the effective peak acceleration (EPA) that might be expected to be exceeded during a 50-year period with a 10% probability (Applied Technology Council, 1978). It is important to note, however, that the map is based solely upon seismic history, and the distribution of active faults has not been considered.

Information such as the seismic hazard map is important for siting and designing nuclear facilities. For a given site, the expected maximum ground motion is determined based on the historic earthquake record. This motion, together with the design response spectra specified for the facility, is used to prescribe the motion for which the facility must be designed.

The Nuclear Regulatory Commission has specified the design response spectra for nuclear reactors (Nuclear Regulatory Commission, 1973a,b). However, for nuclear waste storage facilities the design response criteria are yet to be established (Vortman, 1982, p. 5). It is important that seismic design response criteria be developed and incorporated into the design of facilities for any site under consideration for nuclear waste disposal (Algermissen, 1980, p. 1). While a separate risk analysis will have to be done for a repository, the procedures specified for reactors can be expected to be used, even though the applied criteria may be different.

2.4 Implications for Repository Rock Mass Sealing

The foregoing review shows that data of the effect of seismic loading on the hydraulic conductivity of rock and seals are virtually non-existent. Seismic design criteria for the rock and sealing material are not available. The effects of earthquake and large-scale

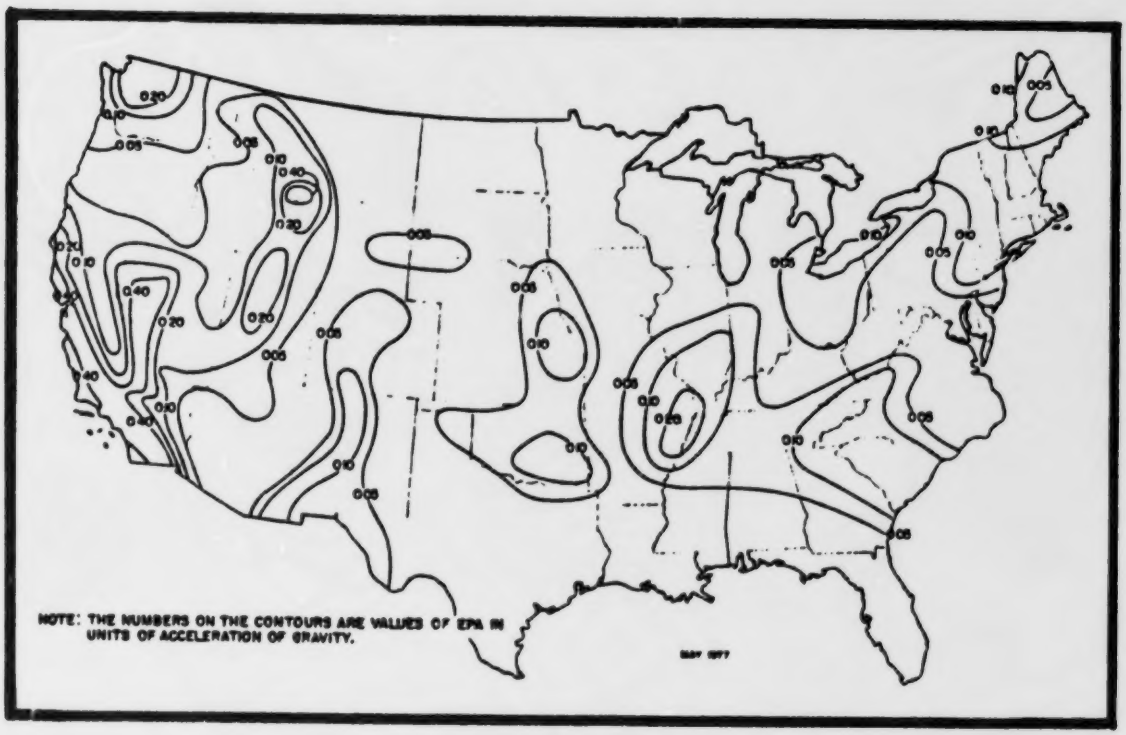

Figure 2.2 Seismic hazard map of the United States, showing contours of effective peak acceleration (after Applied Technology Council, 1978)

BEST COPY AVAILABLE

subsurface blasts on tunnels and other underground openings, however, are moderately well documented, at least qualitatively, and have been analyzed in considerable detail. This information can provide considerable guidance about the likely response of sealed openings and of seals to dynamic loading.

Studies have shown that underground structures, similar to those intended for nuclear waste repositories, are less severely affected by earthquakes and large-scale subsurface blasts than surface structures. Evidence, incomplete as it may be, also supports the contention that deep tunnels are safer than shallow tunnels when subjected to earthquakes. Damage in competent rock is less than that in highly fractured rock. In addition, it has been shown that minor damage to unlined tunnels in rock can be prevented by thin, flexible concrete (shotcrete) linings. If deep underground repositories are located in competent rock rather than in fractured rock, and if they are not affected directly by intersecting faults, the effects of dynamic loading should be minimal on the overall repository stability, especially if the openings are backfilled.

A number of questions remain with respect to the performance of repository seals, as can be deduced from the preceding overview of the current state of knowledge about the reaction of underground openings in response to earthquake shaking. An evaluation of the potential impacts needs to consider probable material response, and for this purpose it is appropriate to consider the two most likely sealing options to be pursued, relatively rigid cementitious seals (concrete shaft and drift plugs, borehole and fracture cement grout) and relatively soft earthen (bentonite, bentonite/crushed rock) seals.

The most likely effects to be experienced by repository seals are seismic motions, as potential repository seal locations are sufficiently close to seismic regions to be affected thereby (Figure 2.2), while sufficiently far so as not to experience major discontinuous (rock fall, slippage, and/or breakage) effects. Figure 2.1 illustrates the most likely influences to be experienced by seals, and hence can serve as a guideline for the design of an experimental program aimed at identifying uncertainties and potential problem areas associated with seal performance under dynamic loading. It seems probable that analyses of these deformation patterns, when considering plug inclusions, could benefit greatly from procedures developed for buried pipelines, several of which have been reviewed by Ariman and Muleski (1979) and by O'Rourke and Wang (1978), and from wave impact analyses (e.g. Pao and Mow, 1973, Ch. III; Miklowitz, 1978, Section 8.3).

Axial deformation parallel to the openings (longitudinal strain) is likely to induce differential longitudinal (axial) strain between emplacement hole or opening wall and the seal. The most obvious test configuration to simulate such differential strain loading would appear to be push-out and pull-out testing. This could include cyclic loading at a range of frequencies and amplitudes corresponding to likely upper limits for in-situ differential strains. Push-out tests could be performed with a rigid cylinder loading the plug, while the cylinder in

which the plug is emplaced is fixed, or could be performed with a pulsating liquid or gas pressure applied on one side of the plug. The latter procedure would facilitate concurrent application of the dynamic load with fluid flow (permeability) testing, but could be performed only in compression.

Curvature effects (Figure 2.1b) are unlikely to be significant for shaft or drift plugs, given the short length (relative to opening diameter and especially to wave lengths) such plugs are likely to have. For borehole studies they could be investigated most readily by subjecting sealed boreholes to cyclic bending, and, preferably, run flow tests on the plugs prior to, during, and after the dynamic loading.

The transverse relative deformation (Figure 2.1c) may well be the most severe loading for rigid plugs, as it will result in direct tension across some parts of the plug-rock interface, while compressive stresses are induced in a perpendicular direction. This combination would seem to be an open invitation to inducing tensile fractures across rigid plugs. Experimental simulation of this configuration may be most feasible by cyclic line loading of plugged cylinders.

Most of these seismically induced deformations are likely to remain within the elastic strain range of the ground, unless the initiating event is exceedingly large and close to the underground openings (Monsees and Merritt, 1984). Wahi et al. (1980), Wahi and Trent (1982), Marine et al. (1981) and Ross-Brown et al. (1981), illustrate cases, however, especially in jointed rock at considerable depth, where the combined effects of high in-situ stresses, thermal (waste-induced) stress, and earthquake-induced dynamic stress can cause substantial discontinuous failure. Rigid plugs should significantly reduce differential stresses around sealed openings, and hence should reduce the risk of failures. Conversely, under extreme loading conditions they might become subject to excessive stresses themselves. Relatively soft backfill (e.g. crushed rock/bentonite mixtures) may be less effective in reducing small rock displacements, but may accomodate larger deformations without excessively detrimental effects on its sealing capacity.

The experimental work performed here is based on the assumption that external shaking of a plugged rock cylinder will adequately simulate some aspects of dynamic waves impacting a sealed opening. The longitudinal wave impacts normal to the hole, i.e. the plugged cylinders are shaking transversely.

CHAPTER THREE

EXPERIMENTAL METHODS AND EQUIPMENT

3.1 Introduction

The purpose of the experiments was to assess the influence of dynamic loading on the plugging effectiveness of cement borehole seals in granite cylinders. Two types of experiments were conducted: flow tests through the rock and through cement borehole seals and tests to assess the influence of dynamic shaking on seal performance in terms of the change, if any, in the hydraulic conductivities.

Two cement seal conditions were tested. The first one was "wet" cement plugs, a good environmental sealing condition, in which cement plugs are never allowed to dry out. The second one was dried-out* cement plugs, which represent a less than ideal environmental sealing condition. To identify the distinct flow patterns in wet and in dried-out cement plugs, dye injection tests were performed. In these flow tests a dye marker is added to the injection fluid.

3.2 Specimens

3.2.1 Rock

Cylindrical Charcoal Granite specimens, approximately 150 mm (6 in) in diameter and 300 mm (12 in) long, had a 25 mm (1 in) nominal diameter hole drilled coaxially from both ends. A centering jig was made for this purpose. In the center of the hole either a rock bridge was left or a cement plug installed to seal the borehole.

The Charcoal Granite is Precambrian in age, and is obtained from the Charcoal Black Quarry of the Cold Spring Granite Company, St. Cloud, Minnesota. The Cold Spring Granite Company describes the rock as petrographically a quartz monzonite, with 68% feldspar, 18% quartz, 6% biotite, and 6% hornblende. Petrographic examination by South and Daemen (1986, p. 63) corroborated this data. It indicated that the rock comprises 66-67% feldspar up to 3 mm, 18% quartz up to 2.5 mm, 5% biotite 0.3-3 mm, 5% hornblende 0.3-3 mm, 1% pyroxene 0.3-3 mm, 2% opaque minerals 0.1-2 mm, and less than 1% apatite 0.1-0.2 mm. They also tested its physical properties, and obtained a Young's Modulus of

---

*No former (e.g. gravimetric) determination of the moisture conditions, moisture content or saturation of the plugs nor of the containing rock cylinder was performed. Throughout this report the term "wet plug" refers to a condition in which a plug was continuously kept covered with water, while "dried out" indicates that such was not the case, and indicates only that, i.e. it is not implied that all water of a certain type has been removed from such plugs.

56530 ± 6070 MPa, a Poisson's Ratio of 0.19 ± 0.05, an unconfined compressive strength of 123 ± 44 MPa, and a density of 2.70 ± 0.01 g/cm^3. The elastic moduli were measured for stresses of up to only 24 MPa.

Eight Charcoal Granite specimens were used. One specimen (CG5309-4) was flow tested with two different rock bridge lengths to check the effect of bridge length on hydraulic conductivity. Three specimens (CG5309-21, -28, and -01) had dried-out cement plugs. The four remaining specimens (CG5309-31V, -06, -08, and -10) were sealed with cement plugs that were maintained wet all the time. Specimen 31V was also flow tested at two different plug lengths. It was subsequently oven-dried and flow tested again to observe any change in plug conductivity due to drying at high temperature. Specimen dimensions are shown in Table 3.1.

3.2.2 Seal Material

Cement system 1, provided by Dowell, was used as sealing material. It is composed of Ideal Type A Portland Cement (Tijeras Canyon, N. M.), 50% distilled water, 10% D53 as an expansive agent, and 1% D65, a dispersant. All percentages are weight percent with respect to cement. The mixing was performed according to the American Petroleum Institute Specifications, API Standards No. RP-10B (American Petroleum Institute, 1977). Procedures for cement mixing are given in Appendix C. The cement mix was poured to the desired length into the specimen borehole, which had been plugged previously with a rubber stopper to hold the mix in place. The cement was cured under water for at least eight days. After the cement hardened, the rubber stopper was removed and a flat ended diamond bit was used to grind off the laitance forming the upper one eighth of the plugs. The milky colored laitance is very porous and soft, and removing it maintains the homogeneity of the cement plugs. Previous investigators (e.g. Cobb and Daemen, 1982, p. 113, 116) had experienced some problems in comparing the permeabilities of the cement plugs and the rock due to the presence of laitance zone in the plugs. Parker (1968, p. 12; see also Mehta, 1986, p. 115; Neville and Brooks, 1987, p. 82) describes this laitance as a weak and porous layer which disintegrates readily and permits water to pass through under slight pressure.

Three of the cement plugs were later allowed to dry at ambient room temperature for different periods of time. Four plugs were kept underwater until the testing program was started. Upon completion of the test, one of these wet plugs (CG5309-31V) was oven-dried. The dried-out plug represents poor sealing condition due to cracking in the plug and debonding of cement/rock interface. This condition is likely to occur in cement plugs located above the groundwater table or in a high temperature location close to waste emplacement. The wet cement plug represents a good environmental sealing condition.

The physical properties of cement system 1 were tested by South and Daemen (1986, p. 70), giving a Young's Modulus of 7627 ± 1454 MPa, a Poisson's Ratio of 0.14 ± 0.04, and an unconfined compressive strength of 30 ± 16 MPa for the three samples tested after 7 to 10 days of

Table 3.1 Rock Cylinder Dimensions (mm)

	Specimen Numbers				
	CG5309-04		CG5309-21	CG5309-28	CG5309-01
Specimen length (L)	312.9	312.9	310.6	312.2	308.9
Top hole length (L_t)	99.3	109.7	142.5	132.8	139.7
Bottom hole length (L_b)	101.6	101.6	83.8	91.9	82.9
Rock bridge length (L_r)	112.0	101.6	--	--	--
Plug length (L_p)	--	--	84.3	87.5	86.3
Inside (hole) diameter (D_i)	26.7	26.7	25.6	25.7	25.9
Outside (specimen) diameter (D_o)	157.0	157.0	157.2	157.0	157.7

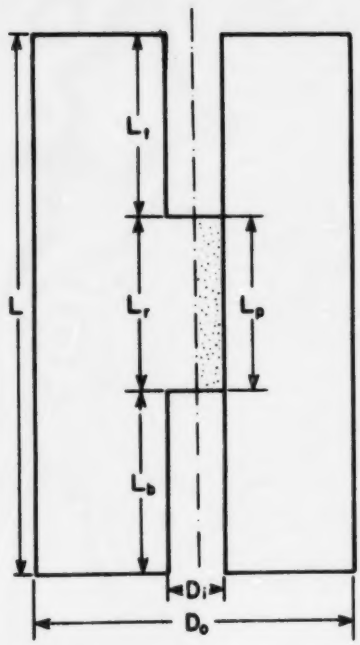

Table 3.1 Rock Cylinder Dimensions (mm)--Continued

	CG5309-31V		CG5309-06	CG5309-08	CG5309-10
Specimen length (L)	308.9	308.9	308.8	309.6	311.2
Top hole length (L_t)	101.3	101.3	146.0	128.6	150.8
Bottom hole length (L_b)	103.9	165.6	131.8	127.0	101.6
Rock bridge length (L_r)	--	--	--	--	--
Plug length (L_p)	103.7	42.0	31.0	54.0	58.8
Inside (hole) diameter (D_i)	26.2	26.2	27.8	27.0	27.0
Outside (specimen) diameter (D_o)	157.0	157.0	158.0	157.2	157.2

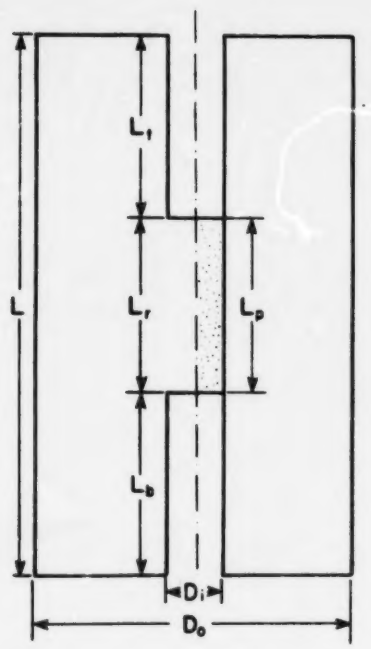

curing. The Young's Modulus and Poisson's Ratio are secant values at peak strength. In addition, data from cement system 1 cylinders tested at five different diameters (from 15.1 to 101.6 mm) were obtained for this testing program. The resulting unconfined compressive strength for these samples was 42 $\pm$ 9 MPa, and the density was 1.69 $\pm$ 0.05 g/cm^3, albeit after fairly complex curing (Section C.3 of Appendix C).

3.3 General Overview of the Test System

A schematic diagram of the flow test system is shown in Figure 3.1. The flow test is performed by injecting distilled water, at a constant pressure, into the top of the axial borehole in a cylindrical granite specimen with a rock bridge in the middle or into a granite cylinder plugged with cement. The selection of distilled water as the permeant is based on the desirability of having a readily available and consistently reproducible test liquid. The potential agressiveness, and hence enhanced permeability, of distilled water is recognized (e.g. Graham and Backstrom, 1975). It is postulated that chemical degradation (leaching) should not be excessively severe over the testing periods envisioned (e.g. Mehta, 1986, p. 132; Neville and Brooks, 1987, p. 272). It is recognized that the test conditions may not necessarily be limiting, i.e. establish the most severe degradation conditions, with regard to the environments at possible repository seal locations, based on broad classes of likely groundwater compositions (e.g. Freeze and Cherry, 1979, pp. 276, 281). Conversely, it is assumed that cementitious seals will not be emplaced in severely acidic environments.

High pressure, nitrogen-driven, gas-over-water pressure intensifiers (injection pumps) are used, as well as hydraulic accumulators, to maintain the constant injection pressure. A variety of injection pressures have been applied during the course of the tests. The outflow from the plug is collected in two pipettes, one for the longitudinal flow through the plug and the other for the peripheral flow through the rock around the plug and into the bottom hole. The radial flow to the sides of the specimen is not collected. The laboratory set-up of the flow test and dynamic loading test system is shown in Figure 3.2. A shaking table is used to generate the dynamic loads, with the specimen secured on its top. Dynamic loads have been applied to the specimens during flow tests in order to determine the effect of shaking on the hydraulic conductivity of the cement plug and/or the rock.

3.4 Flow Test Apparatus

3.4.1 Pressure Intensifiers

Two gas-over-water pressure intensifiers are used to inject water into the specimens at a constant pressure. The pressure intensifiers provide an effective means for maintaining a constant injection pressure while requiring minimal operator attention. They have been built at the University of Arizona's Instrument Shop based on the design presented in Cobb and Daemen (1982). The main components are two cylinders with different diameters. The larger diameter one is the

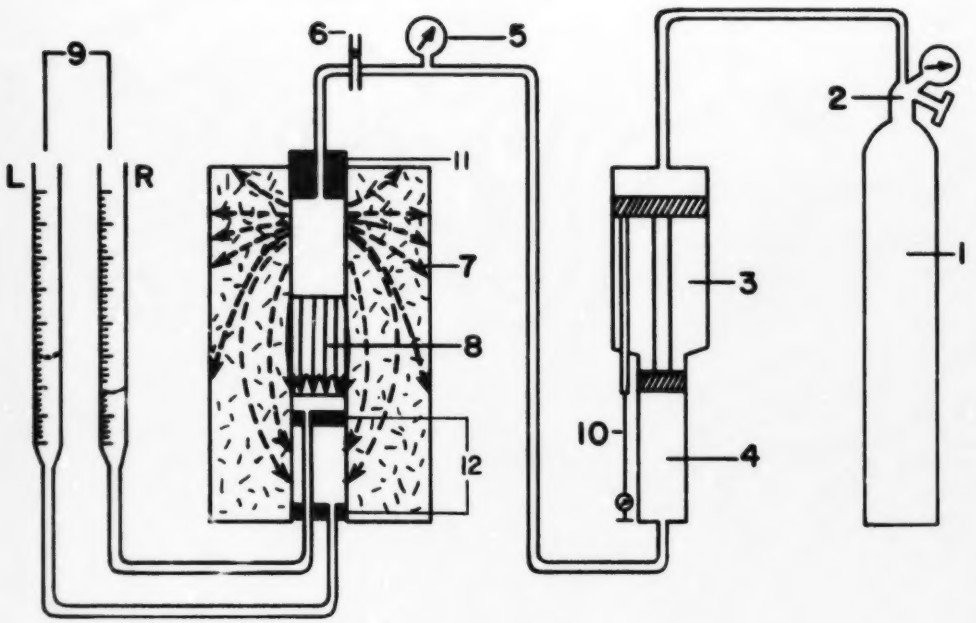

1. Nitrogen gas tank.
2. Pressure regulator.
3. Low pressure(gas) cylinder of pressure intensifier.
4. High pressure(water) cylinder of pressure intensifier
5. Water injection pressure gauge.
6. Rotameter (flowmeter).
7. Rock sample.
8. Borehole plug.
9. Measuring pipettes for outflow collection.
10. Dial gauge for piston displacement measurement.
11. Stainless steel connector.
12. Rubber stopper.

Figure 3.1 Schematic diagram of flow test lay-out. Using two Permatex-sealed rubber stoppers, the longitudinal flow through the plug and the peripheral flow through the rock around the plug are collected separately in the R and L pipettes, respectively. Broken arrows in the rock specimen are qualitative indications of possible flow paths.

BEST COPY AVAILABLE

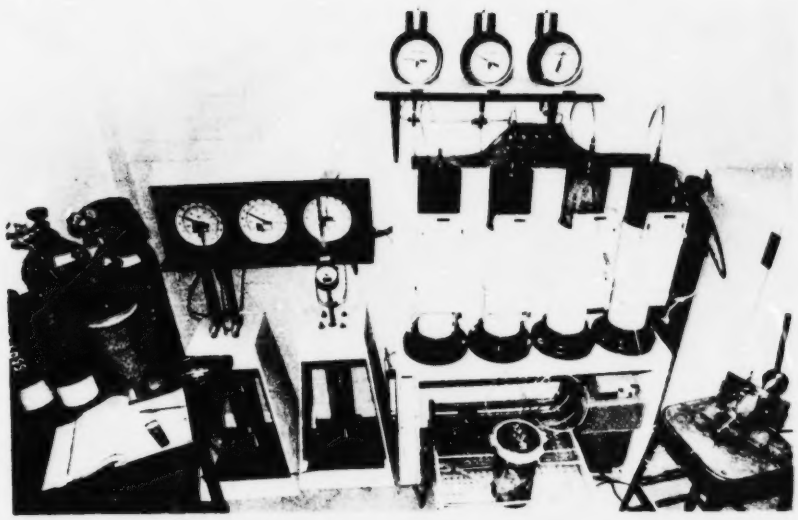

Figure 3.2 Laboratory arrangement for flow test and dynamic loading of borehole seals. Two pressure intensifiers, bottom left, and three hydraulic accumulators, top, can provide independent constant injection pressures for five specimens. One of the specimens is mounted on the shaking table, bottom. A positive-displacement handpump, bottom right, is shown during refilling of one of the testing stations with distilled water.

BEST COPY AVAILABLE

low pressure cylinder pressurized by nitrogen. The smaller diameter high pressure cylinder delivers pressurized water (Figure 3.3). The pressure ratio between the cylinders is 36 to 1. Their water injection capacity is approximately 32 cc. The amount of water dispensed can be measured from the displacement of a rod attached to the piston, monitored with a dial gage.

During the early stages of the flow tests, a problem was encountered with the rubber O-ring of the piston, which led to O-ring replacement twice in a three-week period. A slight design change allowed installation of a plastic back-up ring to the O-ring. No O-ring replacement was necessary during subsequent tests. The stick-slip of the piston inside the cylinders has been minimized by positioning the pressure intensifiers vertically.

3.4.2 Hydraulic Accumulators

Hydraulic accumulators have been used in place of pressure intensifiers to provide constant injection pressures during some flow tests. Figure 3.4 shows a cutaway diagram of an accumulator. A bladder inside the accumulator can be pre-charged with nitrogen gas through a charging valve. The accumulator is filled with distilled water through the hydraulic port with a handpump. The hydraulic accumulators are of the "Kwik-Kap" type, (EMG Accumulators, Inc., 1982). They have a capacity of approximately 473 cc (1 pint) and a maximum pressure of about 20 MPa (3000 psi) at 200°F.

The accumulators perform satisfactorily for the purpose of maintaining a constant pressure when the flow rate into a specimen is low. This is true for flow tests conducted in granite and wet cement plugs, which have extremely low permeability. At higher flow rates, such as during flow tests on dried-out cement plugs, the pressure decreases more rapidly. To maintain a constant pressure, they have to be refilled more often. They are lightweight and portable, readily available, and much less expensive than a pressure intensifier. Overall, the hydraulic accumulators have proven to be a worthwile addition to the system.

3.4.3 Positive-Displacement Handpumps

Prior to each flow test the pressure intensifiers and the hydraulic accumulators must be filled with distilled water using the handpump. The positive displacement handpump works by volume displacement. A plunger of uniform diameter is screwed into the water-filled cylinder by a spindle. The spindle is equipped with a turnstile that can advance or withdraw the plunger into or out of the cylinder. During the early tests, a Ruska model 2240 handpump was used (Figure 3.5). This high precision positive-displacement pump, with a capacity of 500 cm^3 delivers a maximum pressure of about 53 MPa (8000 psi) (Ruska Instrument Corp., 1980). Since the purpose of the pump is to refill the pressure intensifiers and hydraulic accumulators, the high precision is not required. A custom made positive displacement handpump, built by the University of Arizona's Instrument Shop, has replaced the Ruska pump.

BLANK PAGE

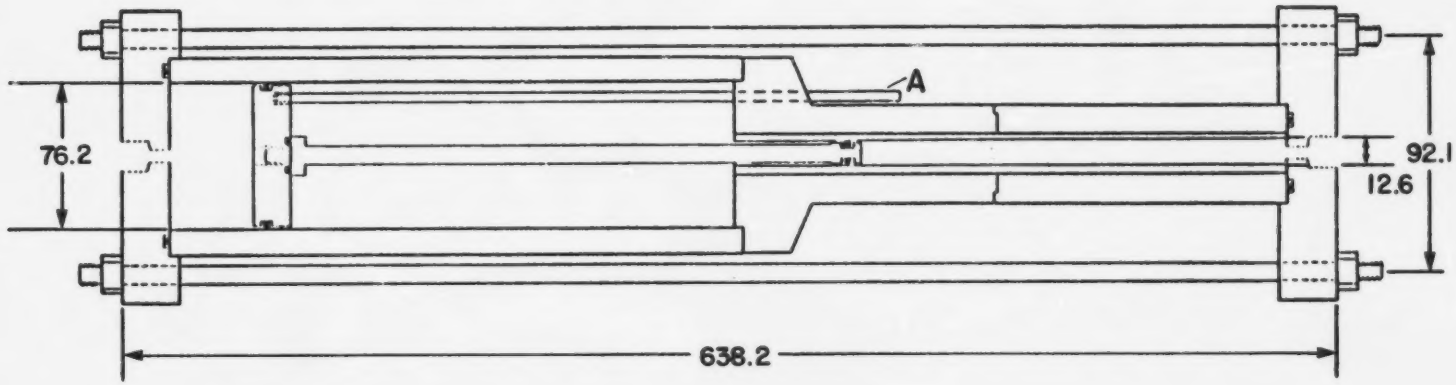

All dimensions in mm.

Figure 3.3 Schematic illustration of the gas-over-water pressure intensifier. The volume of water pumped is determined by measuring the displacement of the rod A attached to the piston. Made from 304 stainless steel except for the inner section of the high pressure cylinder, which is 316 stainless steel.

BEST COPY AVAILABLE

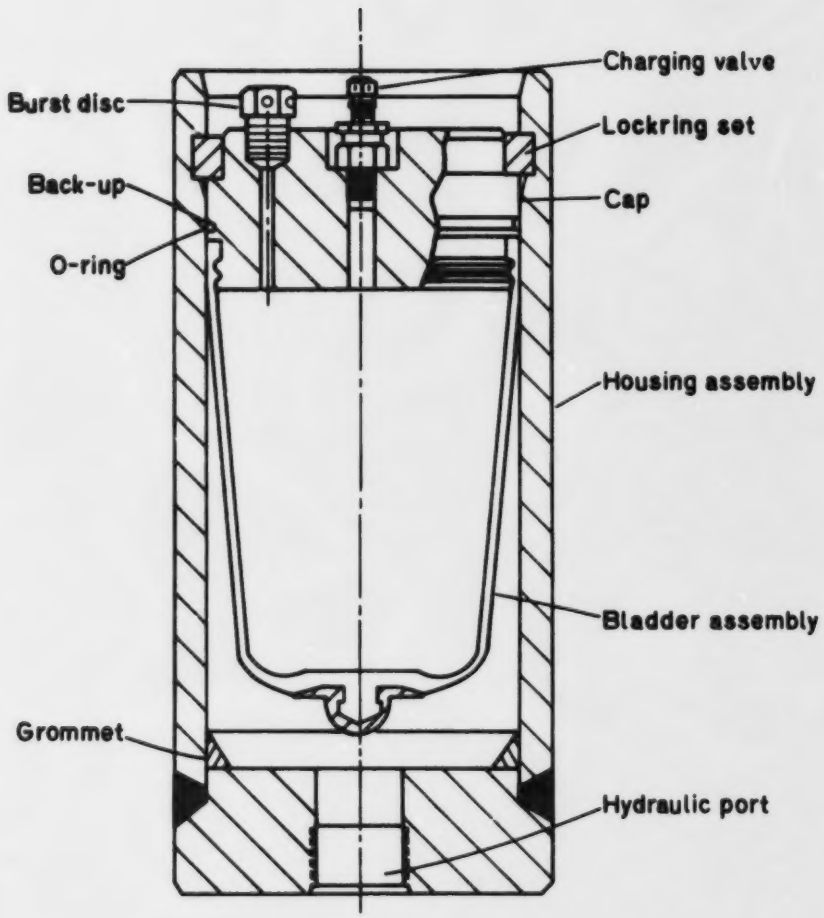

Figure 3.4 Cutaway view of a hydraulic accumulator.

BEST COPY AVAILABLE

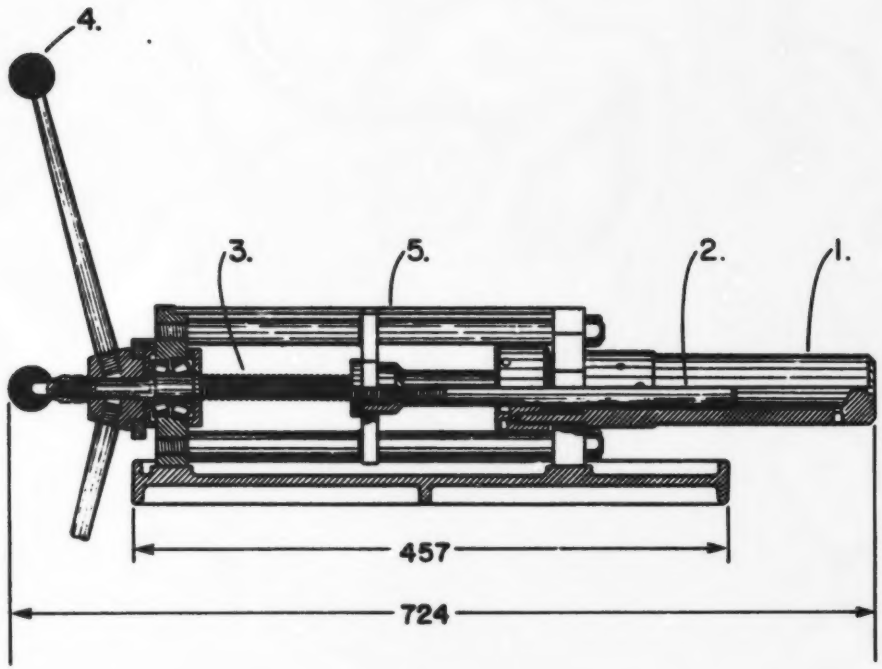

1. Cylinder
2. Hollow plunger
3. Spindle
4. Turnstile
5. Volumetric scale

(Approximate dimensions in mm)

Figure 3.5 Sectional view of the Ruska 2240 positive displacement handpump, showing the cylinder (1), plunger (2), spindle (3), turnstile (4), and volumetric scale (5).

BEST COPY AVAILABLE

42

3.4.4 Inflow Measurement

The flow into the specimens has been measured with two methods. In the indirect method, the displacement of the pressure intensifier piston is measured with a Starret 10 inch (25.4 cm) displacement dial gage, positioned so that it is always in contact with the steel rod attached to the piston. Since the diameter of the water cylinder of the pressure intensifier is known, the volume of water injected into the specimen per unit time can be calculated. The second method is the direct measurement using a flowmeter. Four rotameter-type flowmeters have been used. Three are Gilmont No. 10 compact, shielded type, with a maximum operating pressure of 4 MPa (600 psi) and a flow range of 0.002 to 1.1 cm^3/min (Figure 3.6). The fourth one is a Matheson No. 610 rotameter, with an operating pressure of up to 1.7 MPa (250 psi).

The rotameter is a simple and relatively precise means of indicating flow rate in fluid systems. The design of the instrument is based on the variable area principle. The three basic elements in a rotameter are: a uniformly tapered transparent tube, a float - usually spherical in shape, and a measurement scale. The tube is connected vertically in a fluid system with the smallest diameter end at the bottom, the fluid inlet. The float, located inside the tube, is engineered so that the diameter is nearly identical to the tube's inlet diameter. When fluid is introduced into the tube, the float is lifted from its initial position at the inlet. Fluid passes between it and the tube wall. As the float rises, the area between the float and the wall increases as the tapered tube's inside diameter increases. A point is reached when this flow area, called the annular passage, is large enough to allow the total volume of fluid to flow past the float. The float is now stationary within the tube, with its weight supported by the fluid flow forces that cause it to rise. Reading the corresponding point on the tube's scale permits a determination of the fluid flow rate directly or by means of a calibration chart for the fluid (Matheson Catalog, 1981).

3.4.5 Outflow Measurement

The outflow collection subsystem comprises two rubber stoppers in the bottom hole of the specimen, one just below the plug, the other one at the bottom of the hole (Figure 3.1). 1/4 inch (6 mm) copper tubing is inserted into each rubber stopper, and is connected to a 1 cm^3 measuring pipette (with 1/100 cm^3 increment) by transparent Tygon tubing. Larger pipettes, up to 24 cm^3, are used when testing dried-out cement plugs. The two measuring pipettes separately collect the longitudinal flow through the cement plug or through the rock bridge from the top rubber stopper, and the peripheral flow through the rock surrounding the plug from the bottom rubber stopper. To prevent leakage, Permatex non-hardening gasket sealant, a 3M product, is used in all connections between the rubber stopper, the rock, and the copper tubing Dow Corning silicon lubricant is used for the same purpose in pipette, Tygon tubing, and copper tubing connections. Figure 3.6 shows inflow and outflow measurement subsystem for the flow test.

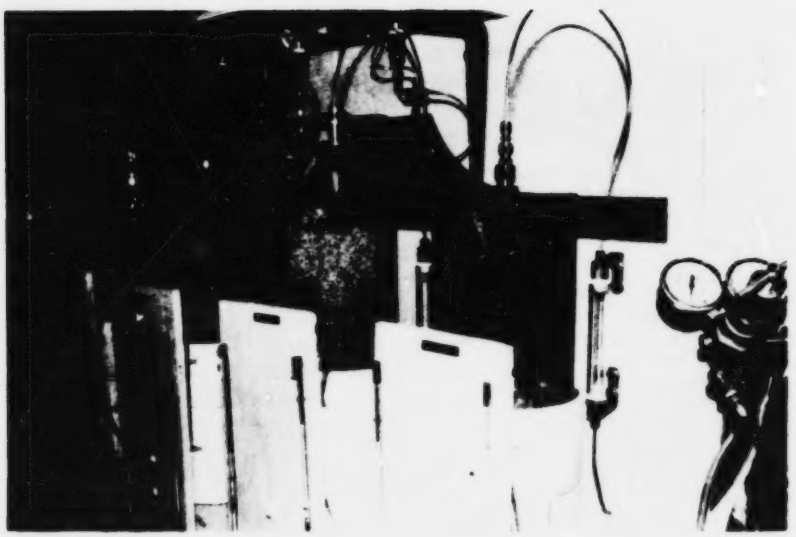

Figure 3.6 Inflow and outflow measurement for flow tests. Inflow rate is measured by Gilmont No. 10 flowmeters located behind each specimen. Two 1 cm^3 pipettes in front of each specimen are used to measure the outflow. The right pipette measures longitudinal flow through the plug and the left pipette measures peripheral flow through the rock around the plug.

BEST COPY AVAILABLE

3.4.6 Control Panel

The control panel for the flow test consists of five independent control systems for five testing stations, enabling five specimens to be tested simultaneously. Each set of controls has a pressure gage, a quick connect and a cap for water recharge, and two needle valves. One valve controls the flow to the injection source, the other one controls the flow to the specimen. Each testing station is served by a water injection source (a pressure intensifier or a hydraulic accumulator). The control panel is shown in Figure 3.7.

3.5 Dynamic Loading (Shaking) Apparatus

3.5.1 Shaking Table

A model 5900 shaking table (Eberbach Corp., 1974) shakes the specimens. It generates a reciprocating horizontal motion in one direction (Figure 3.8). Its maximum load capacity is 50 lbs (23 kg). The shaker power unit has a continuously variable speed from 60 to 240 excursions per minute (a frequency of 1 to 4 Hz), and an adjustable stroke (amplitude) of 1.9 cm, 2.9 cm, and 3.8 cm (0.75 in, 1.125 in, and 1.5 in). The wide range of frequency and amplitude settings enables it to produce a wide range of peak particle velocities (12 cm/s to 96 cm/s) and peak accelerations (0.1 g to 2.5 g).

3.5.2 Rock Cylinder Holder

The shaking table is equipped with a platform and a utility carrier bolted onto the moving part of the table. Two crosswise bar clamps are attached to the utility carrier to hold the sides of the rock cylinder. These are standard features of the shaking table. Two rock cylinders can be mounted on top of the platform and tested simultaneously. Each specimen sits on a specimen seat which is bolted to the platform. Clamps hold the top of the specimen. Four cables, each with a turn-buckle to tighten the cable, extend from the top clamp to the corners of the platform (Figure 3.9). The seats and top clamps, built by the University of Arizona Instrument Shop, are made of lightweight aluminum.

3.5.3 Sinusoid G-Meter

To measure the acceleration of the shaking table, a sinusoid g-meter (Figure 3.10) has been designed and built by the University of Arizona Instrument Shop (Central Electronics Laboratory, 1983). It indicates the acceleration generated along the horizontal axis due to a sinusoidal velocity. The shaking table generates a simple harmonic motion, hence the velocity amplitude, V, and the acceleration amplitude, A, can be defined as (e.g. Oriard, 1982b, p. 56):

$$V = 2\pi fD \tag{3.1}$$

$$A = (2\pi f)^2 D \tag{3.2}$$

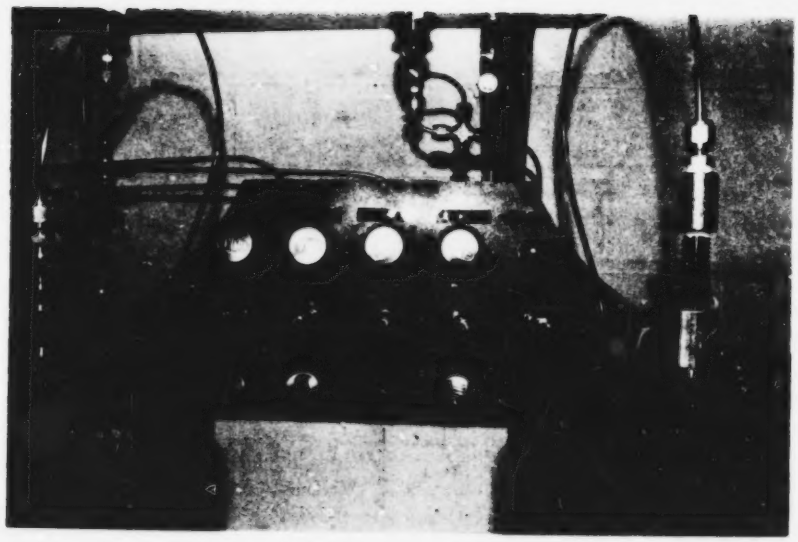

Figure 3.7 Flow test control panel.

BEST COPY AVAILABLE

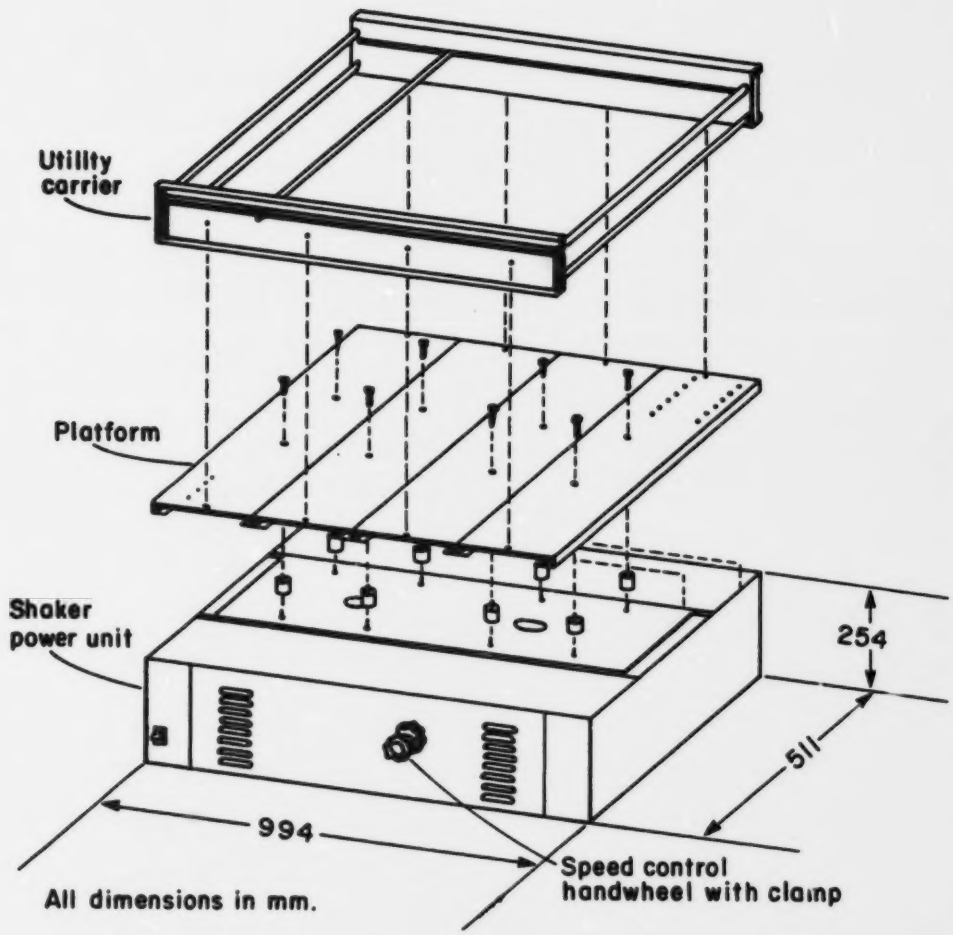

Figure 3.8 Eberbach 5900 shaking table with platform and utility carrier.

BEST COPY AVAILABLE

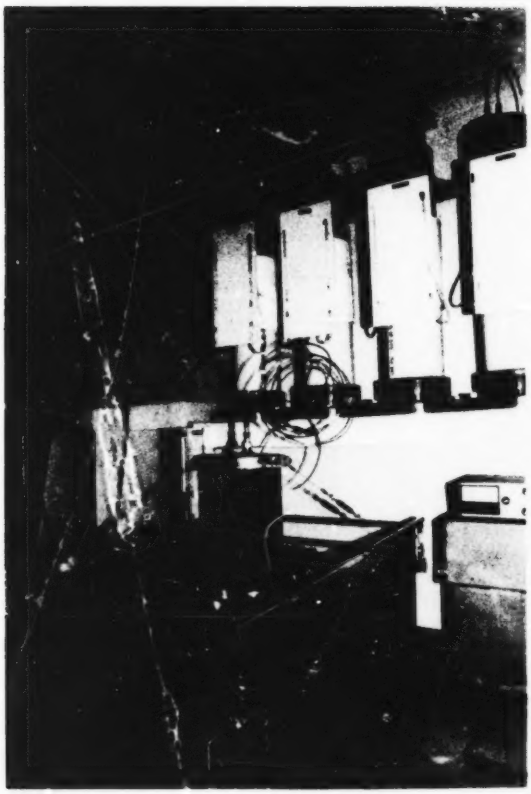

Figure 3.9 A plugged specimen (CG5309-01), securely placed on top of the shaking table platform, is ready for dynamic loading. The top of the specimen is fastened with clamps and a set of four tensioned cables. On the right is the sinusoid g-meter which measures the acceleration of the shaking table.

BEST COPY AVAILABLE

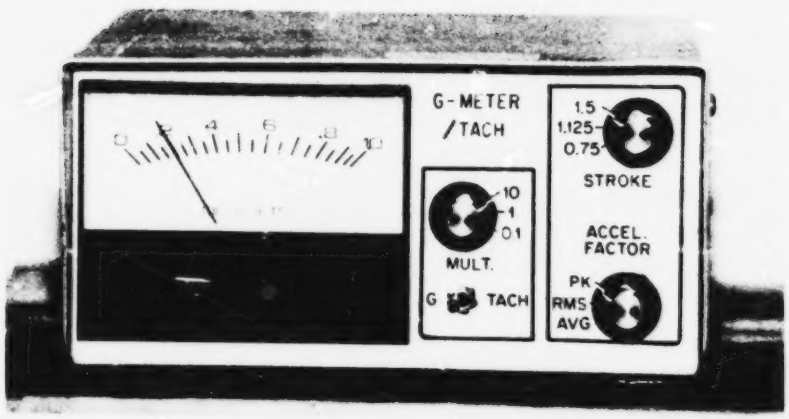

Figure 3.10 The sinusoid g-meter in g-mode, indicating a peak acceleration of 2 g in testing specimen CG5309-01. A multiplication factor of 10 is used in reading the scale for this test. The stroke setting of 1.5 inches (3.8 cm) is used to match the stroke length of the shaking table.

BEST COPY AVAILABLE

where f and D are frequency and displacement amplitude (stroke length) of the shaking table, respectively. The stroke length is set prior to the test and shown in the stroke setting of the sinusoid g-meter (0.75 in, 1.125 in, or 1.5 in). It also has a setting for peak, root mean square, and average acceleration, which in essence is a multiplication factor of 1.0, 0.707, and 0.636, respectively, for the acceleration equation. Since the acceleration is measured in g, Equation (3.2) is divided by the acceleration of gravity to obtain the g-meter reading.

The unit can also operate in the tach-mode. The g-mode gives the acceleration in g. The tach-mode indicates the number of excursions per minute or motion frequency. It is capable of detecting a frequency from 0 to 5 Hz. The acceleration range is from 0 to 5 g.

3.5.4 Slotted Optical Limit Switch

The sinusoid g-meter uses the frequency as a basic measured input parameter. This is achieved using a Monsanto MCT8 slotted optical limit switch (Figure 3.11), which emits infrared light accross its air gap. The frequency input is sensed by the optical limit switch from the break in the infrared light transmission due to the movement of a piece of styrene in the air gap. The styrene is connected to the moving part of the shaking table (Figure 3.12) so that one interruption occurs for each linear excursion. Once the infrared light breaker is connected to the shaking table, its movement can be adjusted using the speed control handwheel to obtain the desired acceleration level for the dynamic loading test.

3.6 Accessories

Various accessories are used during the tests, mostly in support of the flow tests. Three nitrogen tanks and pressure regulators are utilized to pressurize the system, one for each of the two pressure intensifiers and one for the three hydraulic accumulators. The gas line comprises 1/4 inch (6 mm) copper tubing, valves and brass unions. A tire chuck is used to recharge the accumulator.

The water line consists of 1/8 inch (3 mm) stainless steel tubing, tee-and cross-joints, male/female connector, bulkhead unions, and reducers of various sizes. Needle valves, quick-connects and caps stop the flow when needed. The male connector is glued to the top hole of the specimen using epoxy (Scotch Weld structural adhesive 2216). A 1-inch (2.51 cm) diameter compression packer is used inside the top hole as an alternative for one specimen. Five pressure gages indicate water pressure, one for each testing station. A large plastic container is used for distilled water reservoir.

Room temperature is recorded using a continuous recorder. It is also read daily along with the relative humidity on a temperature/humidity indicator. Evaporation is observed using measuring pipettes identical to those used for outflow collection in the flow tests. A detailed list of apparatus used in the testing program is given in Appendix D.

BLANK PAGE

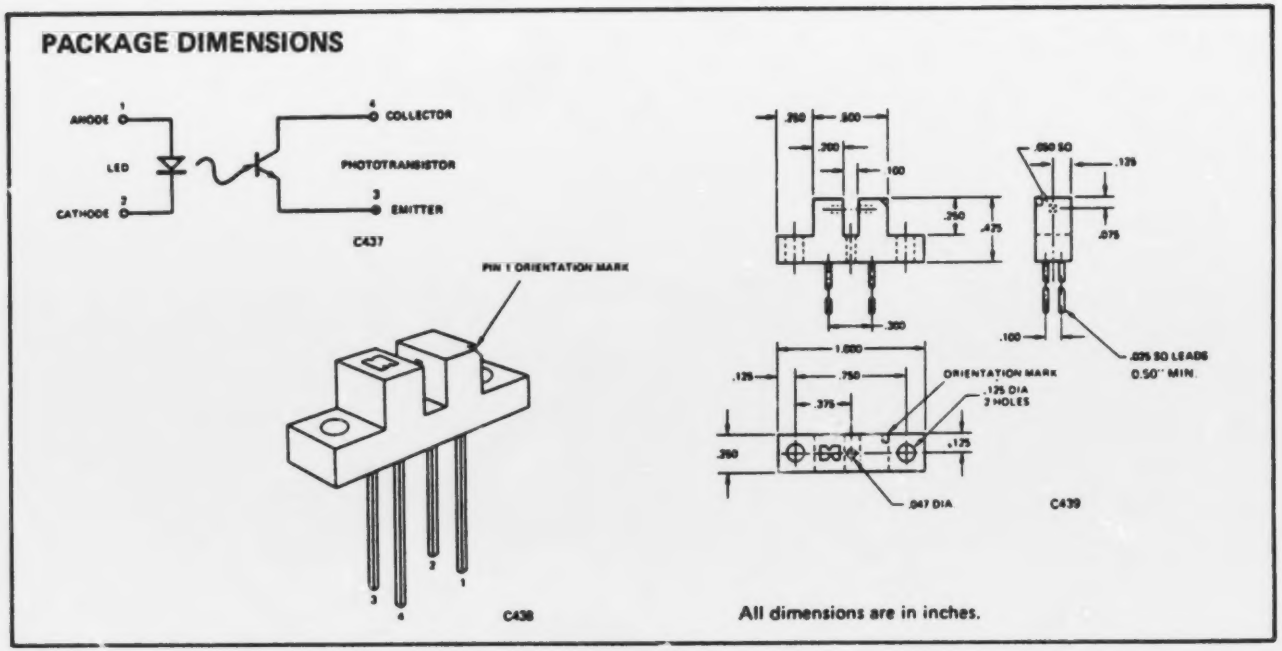

Figure 3.11 Monsanto MCT8 slotted optical limit switch used to sense the frequency input for the sinusoid g-meter. An infrared light is emitted from a GaAs infrared light-emitting diode onto a silicon phototransistor across the air gap in the slot. An object in the air gap is sensed by its interruption of the light transmission.

BEST COPY AVAILABLE

51

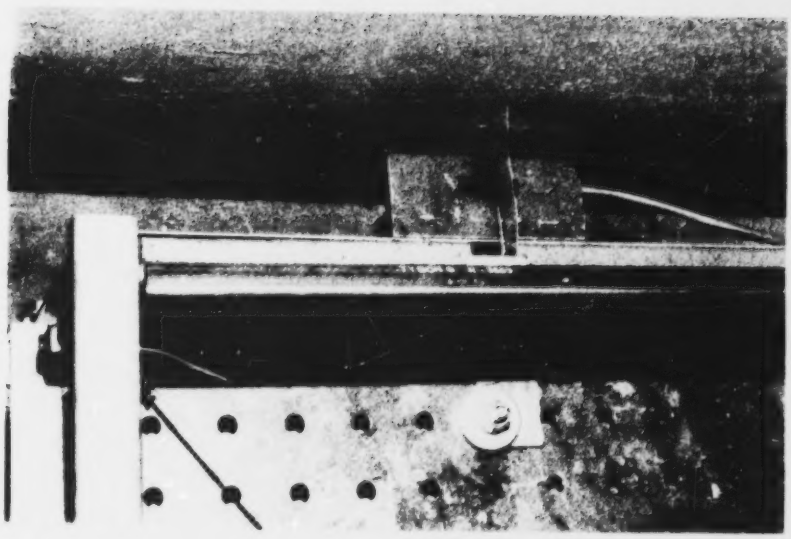

Figure 3.12 A styrene infrared light breaker in the slot of the optical limit switch. The styrene is secured to the platform of the shaking table.

BEST COPY AVAILABLE

3.7 Test Procedures

3.7.1 Flow and Dye Injection Tests

Prior to the test, the pressure intensifier or the hydraulic accumulator is filled with distilled water using the positive-displacement handpump. The handpump is always de-aired prior to usage by connecting it to a vacuum pump in order to minimize air bubbles in the water injection system (top hole of the specimen, water line, pressure source).

The water collection system in the bottom hole of the specimen is filled with water and de-aired before it is coupled to the two measuring pipettes. Two catheter-equipped syringes are used simultaneously for this purpose. Air is withdrawn from the bottom hole with one syringe through one of the copper tubes, while water is injected with the other syringe into the same hole through the second tubing. It is very important to eliminate air bubbles as much as possible, as they may affect the accuracy of the test. The pipettes are covered with tape and plastic caps during the test to minimize the effect of evaporation.

Flow test procedures using a pressure intensifier are as follows:

(1) Fill the pressure intensifier with water using the handpump.
   (a) Check the nitrogen gas tank valve; it should be open (tank pressure is indicated on the high-pressure gage of the pressure regulator).
   (b) Turn the pressure regulator adjusting screw counterclockwise to release the adjusting spring pressure.
   (c) Open the valve in the gas line. The low pressure gage of the pressure regulator should point to zero.
   (d) Close the valve in the water line that leads to the specimen.
   (e) Engage the quick-connect of the handpump to the inlet nipple and open the inlet valve that leads to the pressure intensifier.
   (f) Turn the turnstile of the handpump clockwise to fill the pressure intensifier. Water will push the piston of the pressure intensifier, which drives the remaining gas out of the gas cylinder through the open release valve in the gas line.
   (g) After the water cylinder of the pressure intensifier is full, close the inlet water line valve and disconnect the handpump. Open the same valve slightly to release the water pressure and to let some water, and posibbly air bubbles, out.

(2) Run the flow test.
   (a) Close the release valve in the gas line.
   (b) Turn the pressure regulator adjusting screw slowly clockwise until the desired water injection pressure is attained; this is indicated on the water pressure gage.
   (c) Check the water position in both measuring pipettes; use a catheter-equipped syringe to add water or remove water as needed to obtain the desired initial level.

(d) Clean water droplets from the inner wall of the measuring pipettes so that they do not affect the reading.

(e) Open the valve in the water line to pressurize the specimen.

(f) Record the time, water position (outflow) in both collection pipettes, water injection pressure, and flowmeter or displacement dial gage reading. This should be repeated at a time interval depending upon the injection pressure and the plug condition (wet or dried-out). Observations such as change in injection pressure, water seepage and leakage, failure in system components, etc., are also recorded.

If a hydraulic accumulator is used in the flow test, the bladder must first be precharged with nitrogen to 90% of the working pressure. Then proceed with filling the accumulator with water until a pressure slightly higher than the desired injection pressure is obtained. Next open the water inlet valve slightly to release some water, and possibly air bubbles, until the desired injection pressure is reached. These are steps (1.d) to (1.g) with slight modifications. To run the flow test, steps (2.c) to (2.f) are followed.

The flow tests are essentially steady-state constant head tests, with an initial transient condition when injection pressure is applied or changed. A test is repeated using different injection pressures. Generally injection pressures of 1 MPa, 2 MPa, and 4 MPa are used for each specimen. Once the flow rate has become constant, a dynamic loading test can be performed. The duration of a flow test depends on the plug condition. An initial flow test conducted on a dried-out cement plug may last only for one minute, due to the open plug/rock interface, which acts as a preferential flow path. Subsequent flow tests on the same specimen have increasingly longer durations, as the cement plug expands with increasing saturation. On the other hand, a single flow test conducted on a wet (saturated) cement plug may last for one or two days, depending on the injection pressure. To obtain a good picture of the hydraulic conductivity of the plug as a function of time, the flow tests are repeated many times. A specimen may be tested for as long as nine months.

Because steady-state constant head flow tests take a long time, operator patience is required. Constant attention is needed to read the flow regularly, as well as to maintain the pressure, to refill the water, and to take care of other aspects. For this reason, five specimens were ultimately tested simultaneously, compared to only one specimen at a time in the beginning of the experiments.

To carry out a dye injection test, liquid concentrate dye marker is injected with water in the top hole of the specimen. The flow test procedures are then followed. A dye injection test is conducted following the completion of flow tests and dynamic loading tests on a specimen. The test is repeated at different injection pressures, for at least a month, to make sure that the dye marker leaves traces in the plug. The specimen is then sectioned in half along its length using a diamond-blade saw. Visual inspection is carried out on the cross-section of the rock and the cement plug, and photographs are taken. Dye injection has been performed on three specimens, to allow

observation of the flow paths in wet and in dried-out cement seals. The dye traces in the cement plug and in the rock indicate the flow pattern.

3.7.2 Dynamic Loading

The specimen is securely fastened on the shaking table platform before dynamic loads are applied. For this purpose, an aluminum sample seat is secured to the platform by four bolts. The top of the specimen is clamped and stabilized by tensioned cables that extend to the corners of the platform. Two crosswise bar clamps (attached to the utility carrier) on both sides of the specimen further reduce the possibility of specimen movement relative to the shaking table during the test. To prevent the shaking table from the tendency to "walk" on the floor at high frequency and long shaking strokes, the rubber suction cup feet of the shaking table are fixed to the floor using contact cement.

Prior to applying dynamic loads, the movement of the table is calibrated for the desired acceleration. A standard rock specimen with very nearly the same weight as the specimen to be tested is placed on the platform. The small speed control handwheel is adjusted during the shaking motion until the desired acceleration, indicated by the sinusoid g-meter, is achieved. The speed adjustment can be made only when the table is in motion. The large handwheel is then tightened to clamp the setting.

The acceleration and the duration are recorded during the test, as well as the stroke setting (length of motion) and the tach reading (frequency of motion). The latter data are used to calculate the peak particle velocity. Dynamic loads with moderate to high accelerations (0.5 g, 1.0 g, and 2.0 g) are applied. Each specimen is subjected to a single acceleration, but the duration varies, increasing from 20 to 300 seconds, typically in five increments. A dynamic load test is conducted during ongoing flow tests so that flow rates before and after dynamic load has been applied can be compared directly. After a dynamic load is applied, several flow tests are conducted consecutively before dynamic load is applied again with a longer duration. The final dynamic load is followed by several flow tests. Enough flow rate data are obtained to make it possible to conclude whether or not a change in hydraulic conductivity results from the shaking.

3.7.3 Temperature, Humidity, and Evaporation Observations

Room temperature is continually recorded. A new weekly temperature chart is inserted every Monday. The average room temperature during the testing period was 24° $\pm$ 2°C (75° $\pm$ 3.5°F). Temperature is also recorded twice a day, together with relative humidity, by a dual thermometer/hygrometer. The relative humidity reaches 60% in the summer and gradually decreases to 35% in the spring.

Evaporation is observed daily by reading the water level in the evaporation control pipettes. These are identical to the pipettes used for outflow collection in the flow test, namely 24 cc to 1 cc pipettes. The amount of water lost (evaporated) is plotted against time using a

linear regression fit. The coefficient of correlation is 1.0 for all plots, showing a good fit. Evaporation ranges from 1.66×10^{-5} cm^3/min for the 24 cm^3 pipette to 2.78×10^{-6} cm^3/min for the 1 cc pipette.

A scheme to prevent evaporation tried without success was to cover the water surface in the pipettes with oil. This proved too cumbersome. Oil smeared the inner wall of the pipettes following the rise and fall of the water level. Eventually plastic caps were used to cover the top of the pipettes to minimize evaporation. Appendix E contains records of temperature, relative humidity, and evaporation.

CHAPTER FOUR

EXPERIMENTAL RESULTS

4.1 Flow Tests

Flow tests are conducted by injecting water into the plugged center hole of cylindrical rock specimens. The data are recorded and tabulated as in Table 4.1 (for a wet cement plug) and Table 4.2 (for a dried-out plug). These two tables (and the accompanying Figures 4.1 and 4.2) show the contrast between the low rate of flow through a wet cement plug and the high rate of flow through a dried out cement plug. Pressure is maintained constant during a flow test. Small variations that occur are assumed to average out. The duration of each test (in minutes) is calculated from the recorded time.

The longitudinal and peripheral outflows are plotted as a function of time to obtain the flow rates through the plug and through the rock around the plug, respectively. Each individual flow test lasts for a relatively short time (typically a minute to a day, see Chapter 3). Therefore, the flow rate during a flow test is assumed constant. The flow rate is defined as the slope of the straight line fit between the volume of outflow and time, as shown in the Figures 4.1 and 4.2. These figures illustrate the result of a single test, i.e. the flow rate measured for a particular specimen on a particular day. The straight line equation is given by:

$$V = a + bT \qquad (4.1)$$

where V = outflow volume, cm^3
T = time, minutes
a,b = intercept and slope, respectively, of the regression line

Linear regression provides the best fit for the data, as compared to power, exponential, or logarithmic fits. It gives the highest coefficient of determination, r^2, typically equal to or close to one.

The calculated flow rates for a single specimen can be plotted as a function of total test time, i.e. the time (in days) since testing on that specimen first started. An example of a flow rate vs. total time plot is shown in Figure 4.3.

The inflow rate, i.e. the rate at which water is injected into the specimen, is determined directly using a flowmeter, or indirectly by means of a displacement dial gage that measures the piston displacement of the injection pump (pressure intensifier). The inflow rate is usually several orders of magnitude larger than the flow rate through the wet cement plug or through the rock bridge. This is because the radial outflow to the circumference of the specimen, which constitutes the major portion of the flow, is not collected. For the dried-out

Table 4.1 Flow Test Record, Specimen CG5309-08, Wet Cement Seal

Date	Time	Outflow (cm^3) Left Pipette (Peripheral Flow)	Outflow (cm^3) Right Pipette (Plug Flow)	Inflow Piston Displacement (in)	Injection Pressure (MPa)	Notes
2/20/84	8:40 am	0.300	0.300	0.3610	3.96	Start
	9:31	0.303	0.301	1.3350	3.90	
	10:10	0.309	0.311	1.9950	3.98	
	10:51	0.309	0.320	2.8090	4.01	
	11:19	0.310	0.330	3.3100	4.00	
	12:58 pm	0.323	0.349	5.1450	4.13	decrease pressure
	13:46	0.340	0.359	6.0580	4.10	
	14:56	0.350	0.375	7.3460	4.20	decrease pressure
	15:33	0.352	0.381	7.9907	4.02	
	16:49	0.363	0.400	9.4160	4.15	decrease pressure
	17:13	0.369	0.406	9.8605	4.03	stop

NOTE: Linear regression gives flow rates of 1.25×10^{-4} cm^3/min in the left pipette (peripheral flow through the rock) and 1.99×10^{-4} cm^3/min in the right pipette (longitudinal flow through the seal). Inflow rate is determined using linear regression as 5.83×10^{-2} cm^3/min (2.54 cm (1 in) of piston displacement corresponds to a 3.1537 cm^3 volume).

58

Table 4.2 Flow Test Record, Specimen CG5309-01, Dried-out Cement Seal

Date	Time	Outflow (cm^3) Left Pipette (Peripheral Flow)	Outflow (cm^3) Right Pipette (Plug Flow)	Inflow Piston Displacement (in)	Injection Pressure (MPa)	Notes
1/27/84	9:59 am	0.800	0.00	-	1.51	Start
	10:00	0.800	0.07	0.050	1.51	
	10:02	0.800	0.19	0.050	1.51	
	10:04	0.800	0.30	0.050	1.51	
	10:06	0.800	0.41	0.050	1.51	
	10:08	0.800	0.53	0.050	1.51	
	10:10	0.800	0.66	0.050	1.51	
	10:12	0.800	0.76	0.050	1.51	
	10:14	0.800	0.87	0.050	1.51	
	10:16	0.800	0.99	0.050	1.51	
	10:18	0.800	1.09	0.050	1.51	
	10:20	0.800	1.20	0.050	1.51	
	10:22	0.800	1.31	0.050	1.51	
	10:24	0.800	1:43	0.050	1.51	
	10:26	0.800	1.54	0.050	1.51	Stop

NOTE: Linear regression gives flow rate in the right pipette (longitudinal flow through the dried seal) of 5.75×10^{-2} cm^3/min (see Figure 4.2). No peripheral flow is observed in the left pipette. Inflow rate is read directly from the flow meter (5.0×10^{-2} cm^3/min).

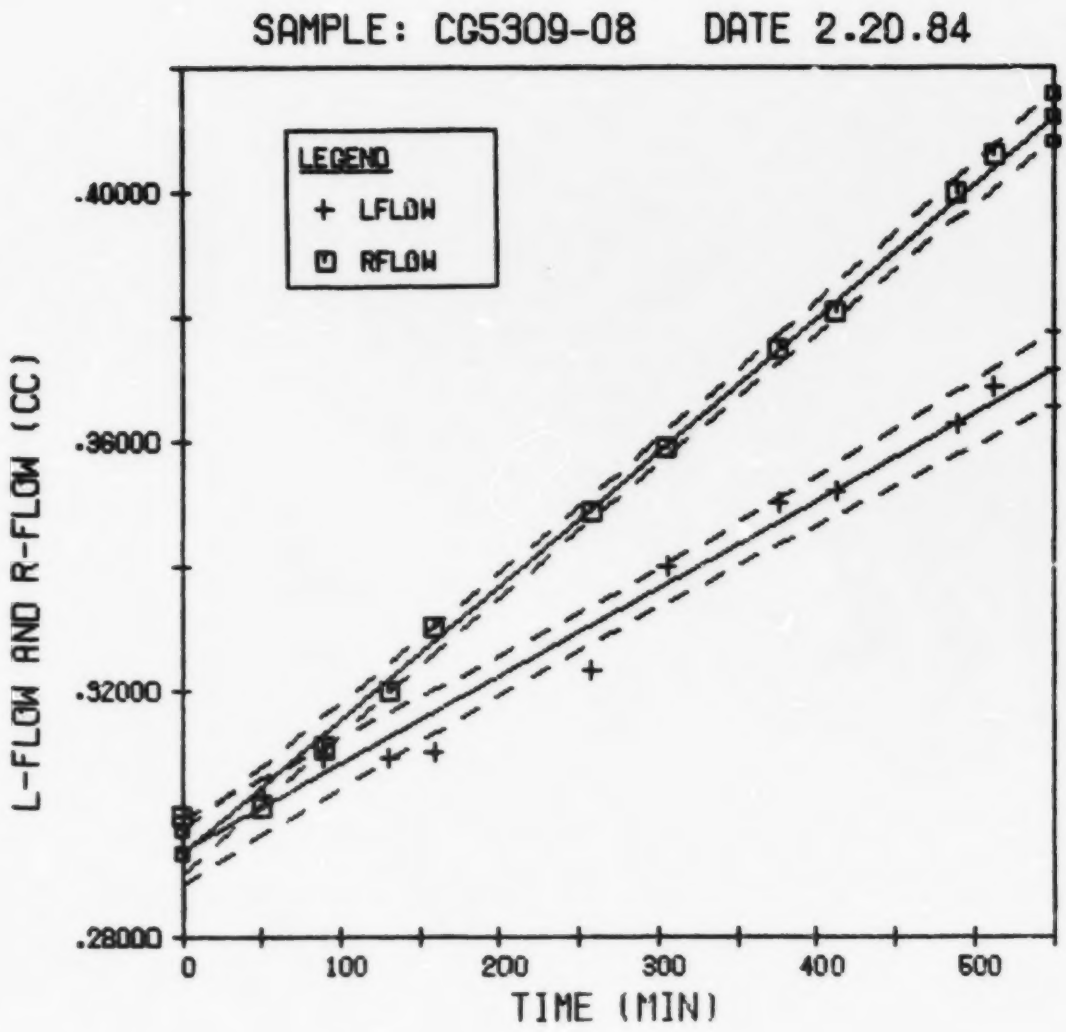

Figure 4.1 Linear regression plot of outflow as a function of time for a wet cement plug (Table 4.1). For the injection pressure used here (4 MPa), the longitudinal flow rate through the plug (R-flow) was 1.99×10^{-4} cm^3/min, with $r^2 = 0.99$. The peripheral flow through the rock around the plug (L-flow) was 1.25×10^{-4} cm^3/min. A 95% confidence band is shown around each regression line.

BEST COPY AVAILABLE

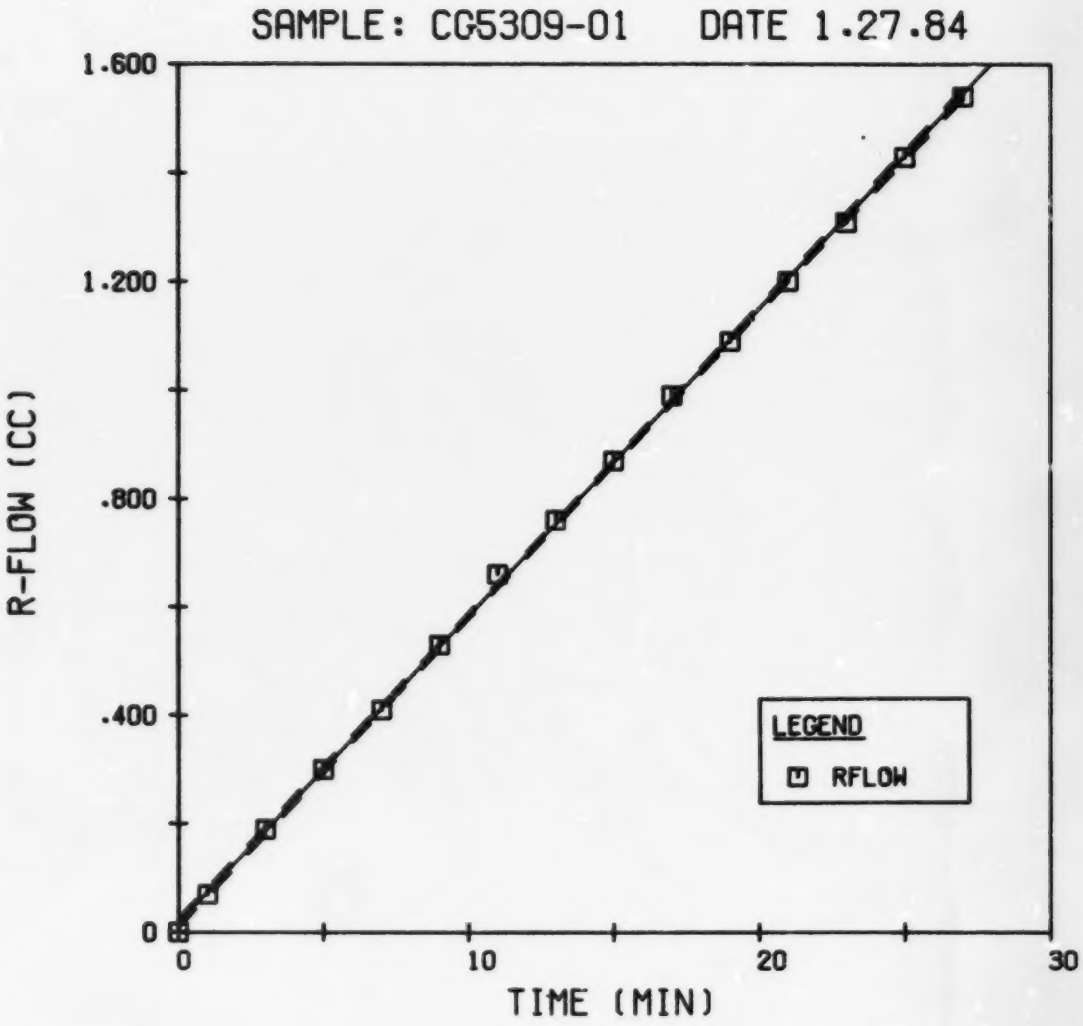

Figure 4.2 Linear regression plot of outflow as a function of time for a dried-out cement plug (Table 4.2). The longitudinal (plug) flow rate is 5.75×10^{-2} cm^3/min for the injection pressure of 1.5 MPa, with $r^2 = 1.00$. Broken lines around line of best fit and virtually coincident with it represent a 95% confidence band.

BEST COPY AVAILABLE

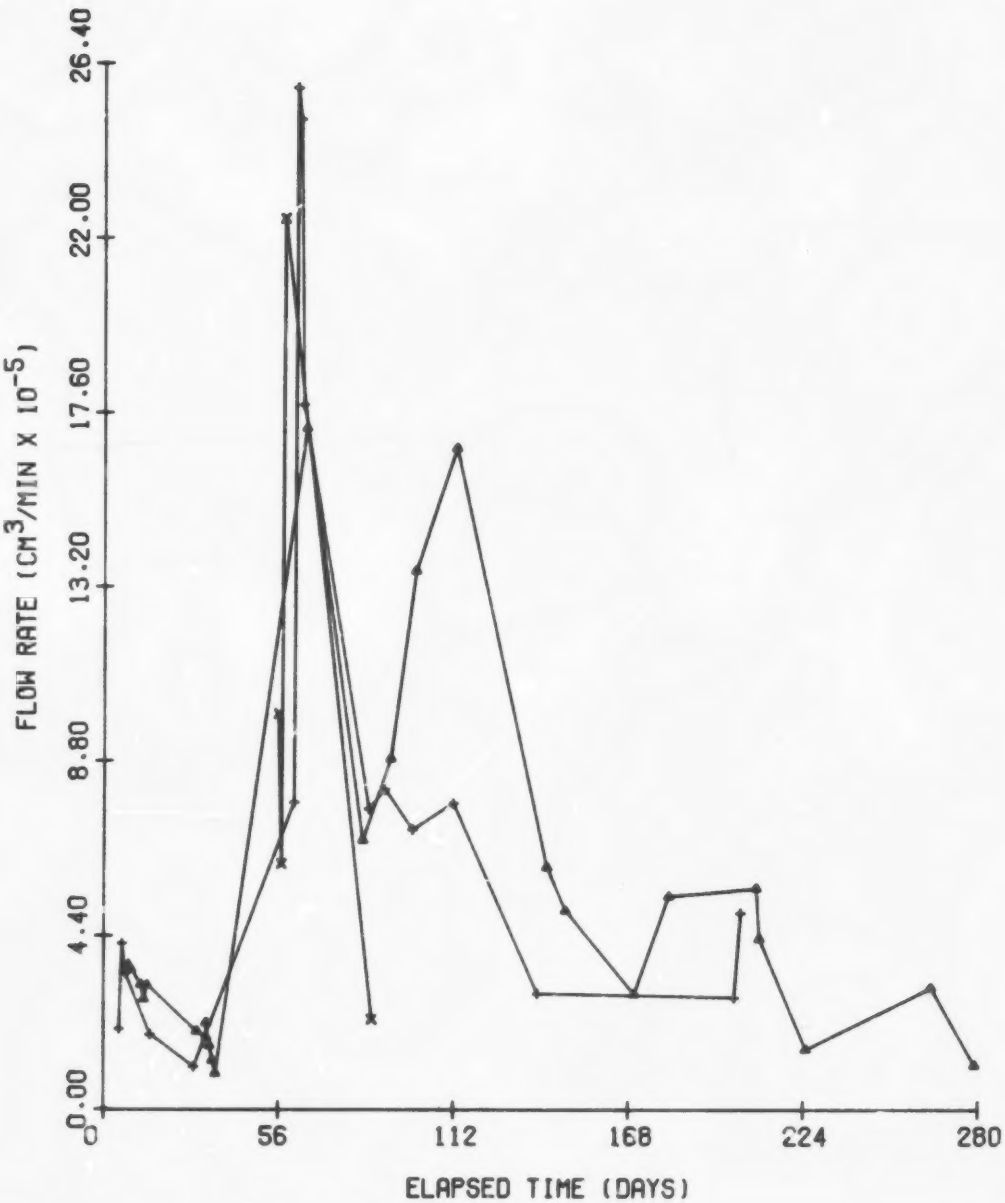

Figure 4.3 An example of longitudinal outflow rate through a cement seal as a function of total (cumulative) time, Specimen CG5309-31V, wet cement seal in Charcoal granite cylinder.

▲ - ▲ : injection pressure = 4 MPa
\+ - + : injection pressure = 2 MPa
x - x : injection pressure = 1 MPa

cement plug, inflow and outflow rates are about the same (see Tables 4.1 and 4.2).

4.1.1 Flow Through Granite Rock Bridge

To provide a reference point for measuring plugging effectiveness, flow rate through the Charcoal granite was determined first. For this purpose, a granite rock cylinder (specimen CG5309-04) was drilled from both ends, leaving a rock bridge in the middle. This Charcoal granite rock bridge was flow tested at two different lengths to check the effect of bridge length on the measured hydraulic conductivity.

The first series of flow tests was conducted for 19 days on a nominal rock bridge length of 112 mm. During the following seven months no flow test was conducted on this specimen. The rock bridge was then partially drilled out and shortened to 102 mm. The flow tests were resumed and continued for 38 days until the epoxy bond that glued the steel connector (injection insert) to the rock specimen failed.

Figure 4.4 shows the longitudinal flow rate through the Charcoal granite rock bridge as a function of time. Figure 4.5 gives the peripheral flow rate through the granite around the rock bridge. They are of the same order of magnitude, although the peripheral flow has a slightly lower rate. The slight reduction in rock bridge length (roughly 9% of the initial length) has little effect on the flow rates.

Inflow measurements were taken during the second series of flow tests (i.e. for the shorter rock bridge) using a flowmeter. Several inflow readings gave values beyond the flowmeter range (1.0 cm^3/min). This is attributed to oil (possibly from the pressure intensifier) that covered the float and made the reading inaccurate. Complete test results are given in Table F-1 of Appendix F.

4.1.2 Flow Through Wet Cement Plugs

The "wet" cement plugs denote cement seals that are kept immersed in water and are never allowed to dry out (see Sections 3.1 and 3.2.2). Four Charcoal granite specimens (CG5309-08, -31V, -06, and -10) had wet cement seals of various lengths. Specimen 31V was flow tested at two different plug lengths (Table 3.1).

4.1.2.1 Specimen CG5309-08. The plug was installed by pouring cement into the center hole. Flow testing started a month later. The laitance in the top portion of the plug was ground off just prior to testing, leaving a plug length of 54 mm (see Table 3.1 for specimen dimensions). After eight days of testing, excessive leakage occurred along the epoxy bond that glued the stainless steel connector of the injection line to the top hole of the specimen. The test had to be stopped. Flow tests were resumed after the epoxy bond was replaced.

Extensive flow rate data has been obtained for this specimen (see Table F-2 of Appendix F) during eight months of testing. The longitudinal flow through the cement plug shows a distinct pattern at injection pressures of 1, 2, and 4 MPa when plotted as a function of time (Figure

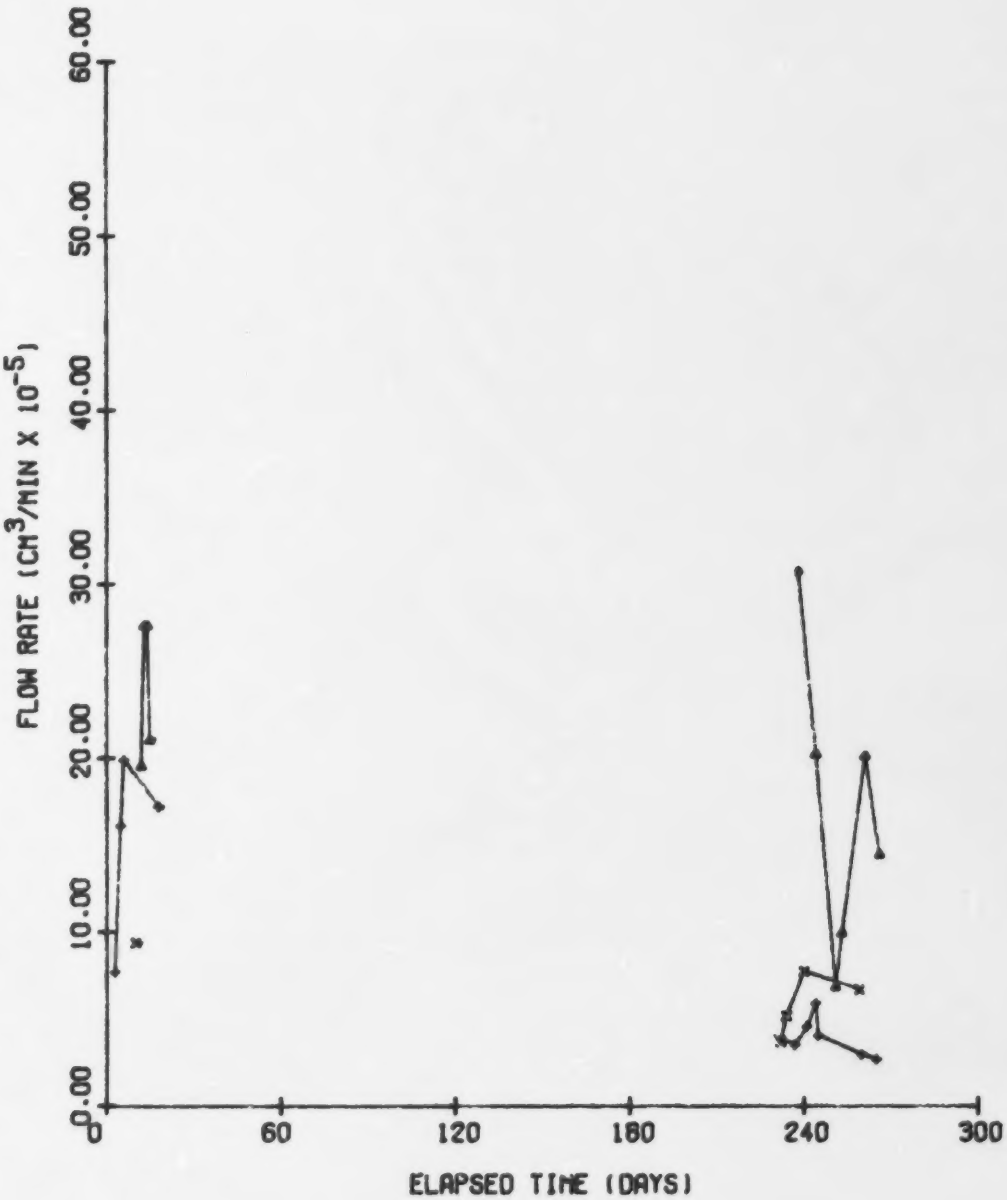

Figure 4.4 Longitudinal flow rate through a Charcoal granite rock bridge as a function of total test time. Rock bridge was 112 mm long for the first 19 days of the test and was cut to 102 mm for the last 38 days; specimen CG5309-04.

▲ - ▲ : injection pressure = 4 MPa
\+ - + : injection pressure = 2 MPa
x - x : injection pressure = 1 MPa

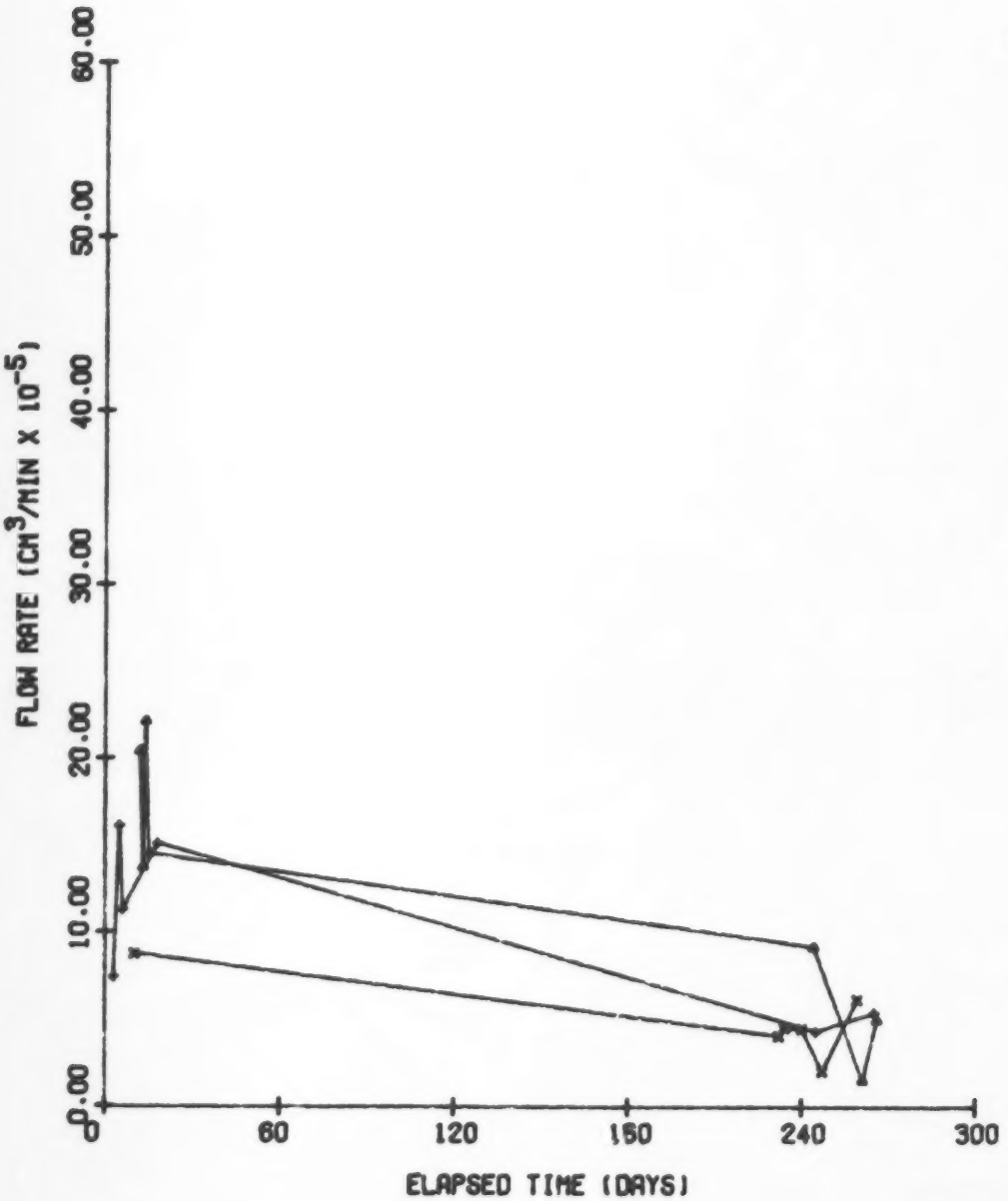

Figure 4.5 Peripheral flow rate through granite around the rock bridge as a function of total test time, specimen CG5309-04.

▲ - ▲ : injection pressure = 4 MPa
\+ - + : injection pressure = 2 MPa
x - x : injection pressure = 1 MPa

4.6). The peripheral flow rates through the rock around the plug (Figure 4.7) are slightly higher than the longitudinal flow rates through the cement plug. They also show a more irregular pattern and depend less on the injection pressure. The inflow rate, calculated from piston displacement of the pressure intensifier, is plotted against time in Figure 4.8. Inflow rates obtained in this manner have proven to be more precise than those obtained with a flowmeter, especially for low flow rates.

4.1.2.2 Specimen CG5309-06. The cement plug was installed at the same time as specimen CG5309-08. Flow tests commenced after a curing period of 22 days. Before the test started, laitance was ground off the top portion of the plug, leaving a plug length of 31 mm.

Flow rate data collected during the seven months of testing is given in Table F-3 of Appendix F. Figure 4.9 shows the longitudinal flow rate through the cement seal. Especially during the early part of the test, no flow could be recorded at 1 MPa injection pressure, except for one reading. Distinct flow patterns at different injection pressures can also be observed. Figure 4.10 shows the peripheral flow rate through the rock around the plug. Different injection pressures yielded roughly similar peripheral flow rates. The bypass flow rate is lower than the longitudinal (plug) flow rate.

Inflow rate calculated from measured piston displacements varied from 9 x 10^{-5} to 2 x 10^{-3} cm^3/min at injection pressures of 1 to 4 MPa (Table F-3 of Appendix F). Higher values were observed due to leakage along the epoxy bond during the early part of the test. Inflow rate measured from flowmeter reading is generally higher and much more variable. The flow tests were interrupted by an early failure of the epoxy bond that connects the stainless steel injection line to the specimen. This problem was corrected and the test resumed. During the last 41 days of the flow testing, a dye marker was injected (see Section 4.3).

4.1.2.3 Specimen CG5309-31V. Flow testing started after the laitance was ground off the plug, leaving a cement plug 104 mm long. At this time, the plug had been cured underwater for almost a month. Early tests yielded very low flow rates through the plug, in the lower range of 10^{-5} cm^3/min (Figure 4.11). This posed considerable difficulties in reading the outflow pipettes. The test was interrupted for 16 days because the epoxy bond that glued the water injection line to the specimen failed. This period was used to reduce the plug length to 42 mm to increase the flow rate, and thus allowing a more reliable pipette reading. The flow test was continued for nine months, making this the longest testing time for any plug.

Figure 4.11 is a plot of the longitudinal flow rate through the plug as a function of time. An increase in flow rate is observed after the plug was shortened (day 60). The flow rate tends to decrease with time thereafter, and on many occasions no flow can be observed at 1 MPa, at 2 MPa, or sometimes even at 4 MPa injection pressure.

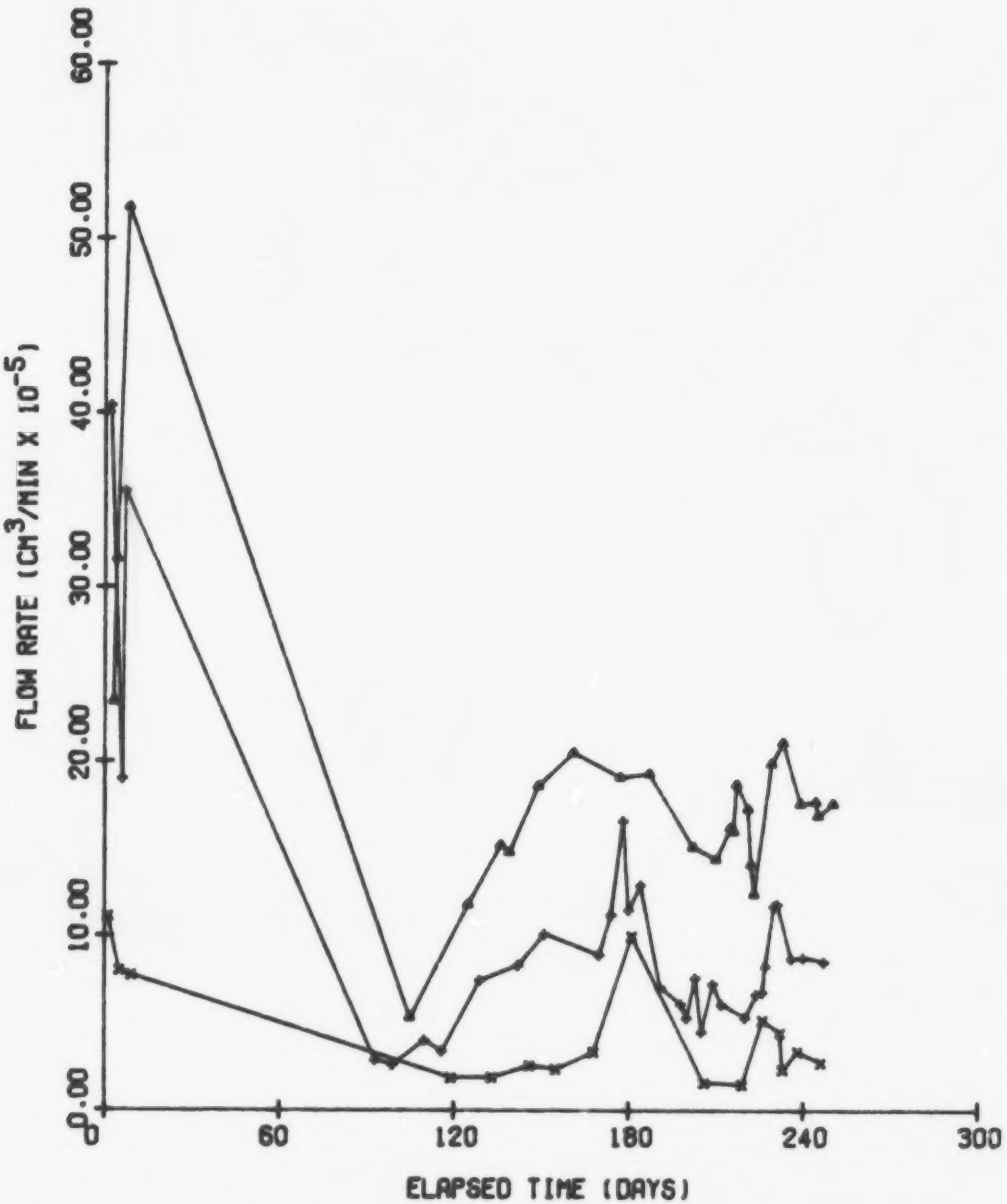

Figure 4.6 Longitudinal flow rate through a wet cement plug as a function of total test time. Specimen CG5309-08, plug length of 54 mm.

▲ - ▲ : injection pressure = 4 MPa
\+ - + : injection pressure = 2 MPa
x - x : injection pressure = 1 MPa

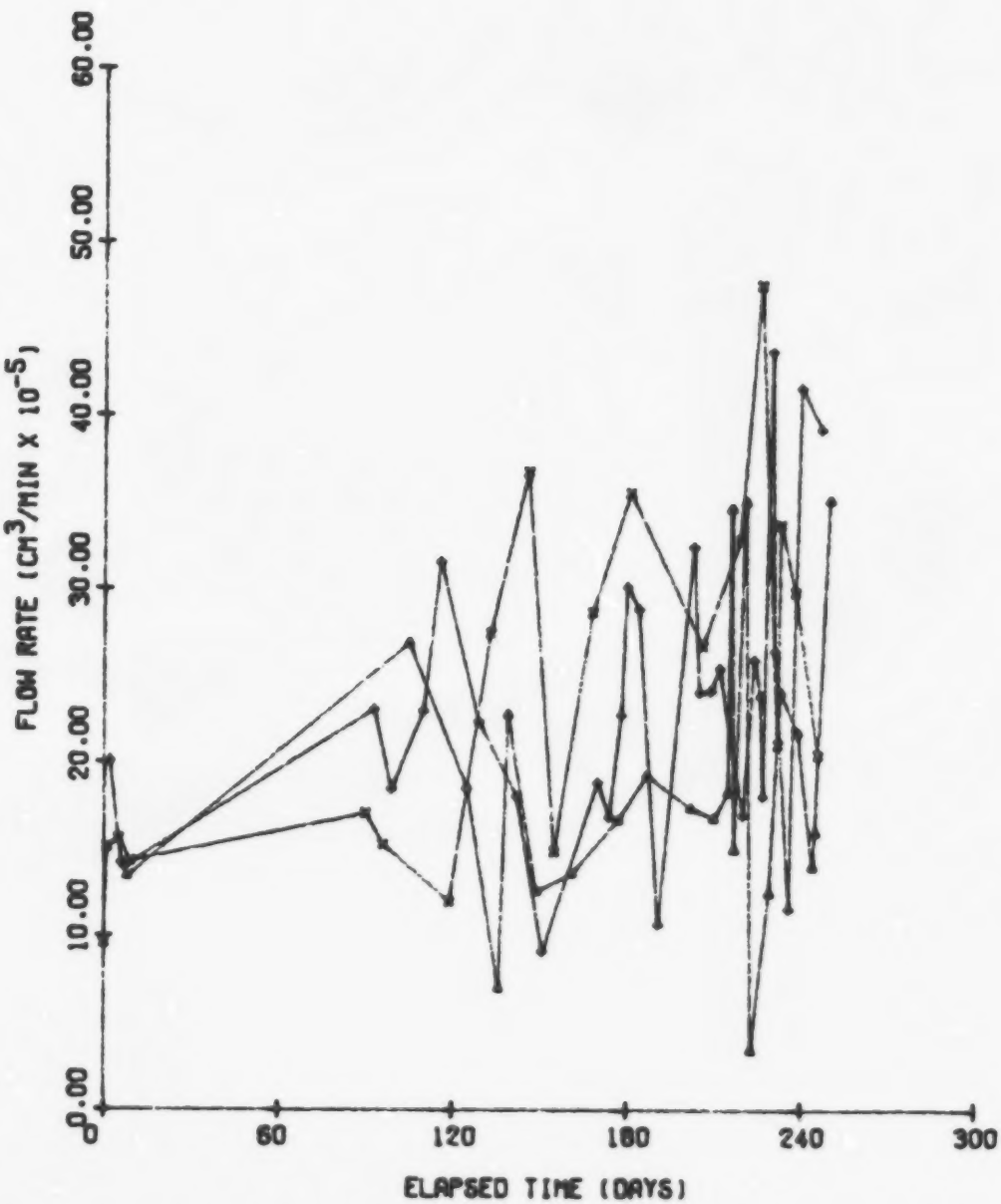

Figure 4.7 Peripheral flow rate through the rock around the plug as a function of total test time, specimen CG5309-08. Note the lack of correlation between injection pressure and flow rate.

▲ - ▲ : injection pressure = 4 MPa
\+ - + : injection pressure = 2 MPa
x - x : injection pressure = 1 MPa

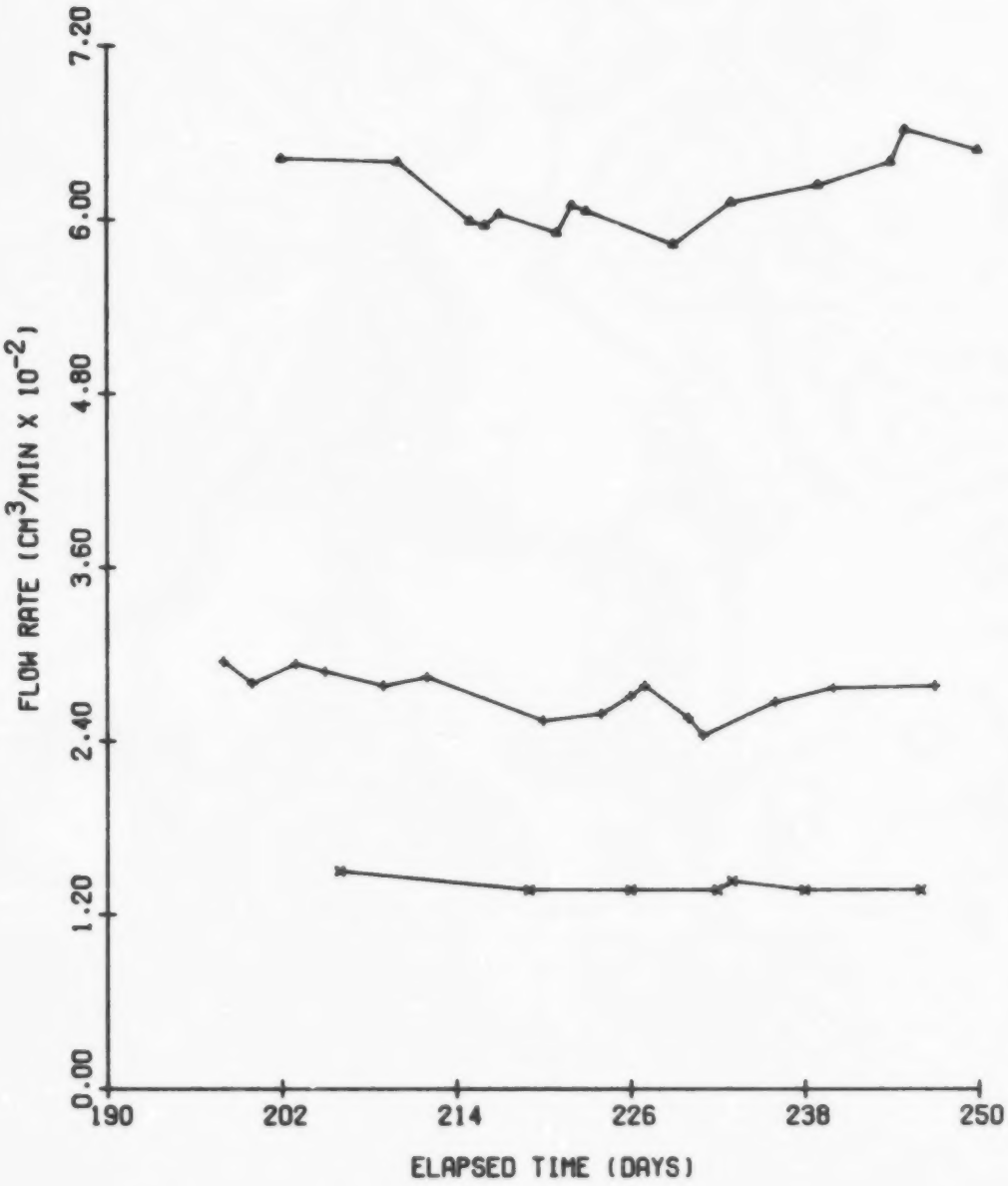

Figure 4.8 Inflow rates at various injection pressures as a function of total test time, specimen CG5309-08.

▲ - ▲ : injection pressure = 4 MPa
+ - + : injection pressure = 2 MPa
x - x : injection pressure = 1 MPa

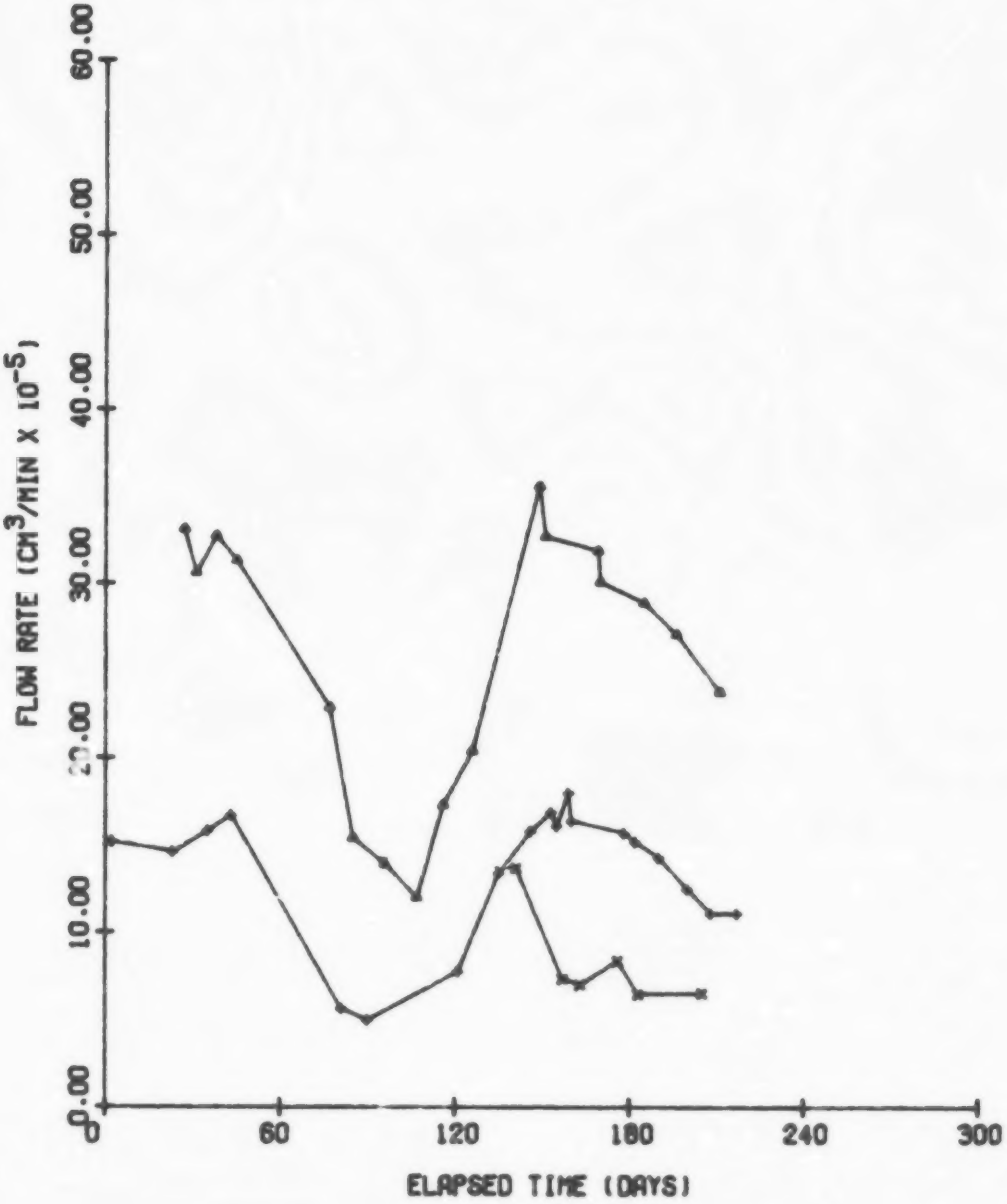

Figure 4.9 Longitudinal flow rate through a wet cement plug as a function of total test time. Specimen CG5309-06, plug length 31 mm.

▲ - ▲ : injection pressure = 4 MPa
\+ - + : injection pressure = 2 MPa
x - x : injection pressure = 1 MPa

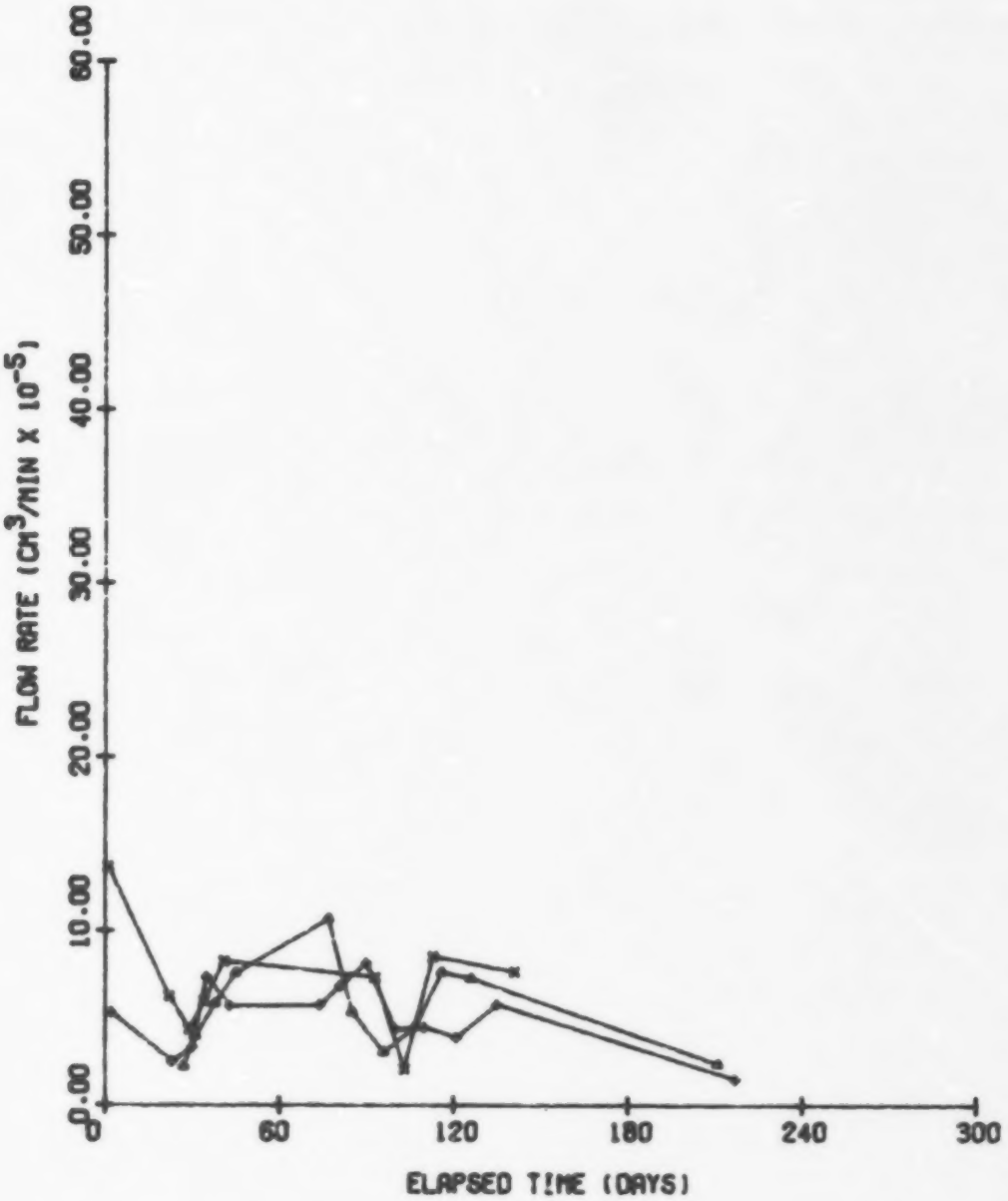

Figure 4.10 Peripheral flow rate through the rock around the plug as a function of total test time, specimen CG5309-06.

▲ - ▲ : injection pressure = 4 MPa
\+ - + : injection pressure = 2 MPa
x - x : injection pressure = 1 MPa

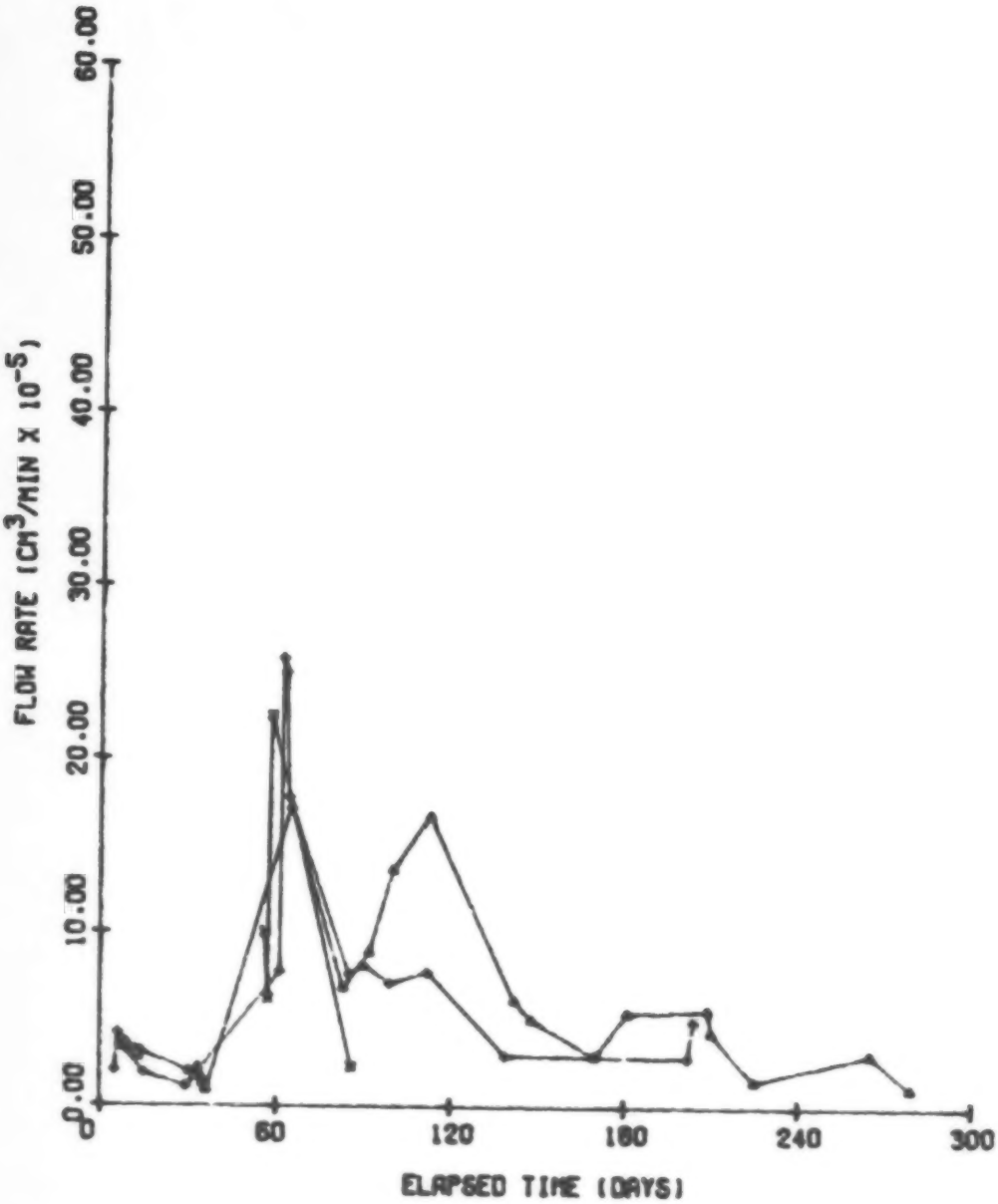

Figure 4.11 Longitudinal flow rate through a wet cement plug as a function of total test time, specimen CG5309-031V. Plug length was 104 mm for the first 40 days of testing, and was reduced to 42 mm thereafter.

▲ - ▲ : injection pressure = 4 MPa
\+ - + : injection pressure = 2 MPa
x - x : injection pressure = 1 MPa

Figure 4.12 shows the peripheral flow rate through the rock as a function of time. A decreasing flow rate with time is observed here also. In general, the peripheral flow rate (Figure 4.12) is of the same order of magnitude as the longitudinal seal flow rate (Figure 4.11).

Inflow rate measurements using a flowmeter gave inconsistent results. After several tests the flowmeter tended to give high readings. Oil accumulated and coated the surface of the float, creating a larger surface area, thus causing the float to rise higher inside the flowmeter. Inflow rate observations using piston displacement measurements have proven more accurate. The inflow rates measured in this way consistently range from 2×10^{-3} cm^3/min (at 1 MPa), 4×10^{-3} cm^3/min (at 2 MPa), and 1×10^{-2} cm^3/min (at 4 MPa). Complete test results for this specimen are given in Table F-4 of Appendix F.

During the final month of the flow test, a dye marker was injected (see Section 4.3). At the end of the test, this specimen was oven-dried for five days and then was flow tested again (Section 4.1.3).

4.1.2.4 Specimen CG5309-10. Flow testing started after a curing period of almost two months. Prior to the test, laitance was ground off until the plug length was 59 mm.

An expandable mechanical packer (Figure 4.13) was used in the top hole instead of a steel connector (injection insert) epoxy glued in the hole. Its purpose was to minimize radial flow to the sides of the specimen. The packer worked satisfactorily after its original multi-layered rubber sleeve had been replaced by a thicker, single-layer sleeve. Prior to that, it tended to slide up at high injection pressures.

The rock cylinder failed as the nut of the packer was tightened during a flow test. The injection pressure used in that test was 4 MPa. Failure is possibly due to overtightening the packer, combined with injection water pressure, creating excessive tensile stress in the rock cylinder. Over a little more than two months, fifteen flow tests had been conducted. No flow could be observed at the 1 MPa injection pressure. At 2 MPa, measurable flow occurred only on one occasion. Even at 4 MPa, no flow could be observed on two occasions (Table F-5 of Appendix F). The longitudinal and peripheral flow rates are given in Figures 4.14 and 4.15 respectively. In both figures, a tendency of decreasing flow rate with time can be observed.

4.1.3 Flow Through Dried-out Cement Plugs

The dried-out cement plugs denote cement seals which, after curing at least eight days under water, are allowed to dry for different periods of time (see Sections 3.1 and 3.2.2). Cement borehole seals installed in three granite cylinders (CG5309-28, -01, -21) were dried at room temperature. Specimen CG5309-31V was oven dried.

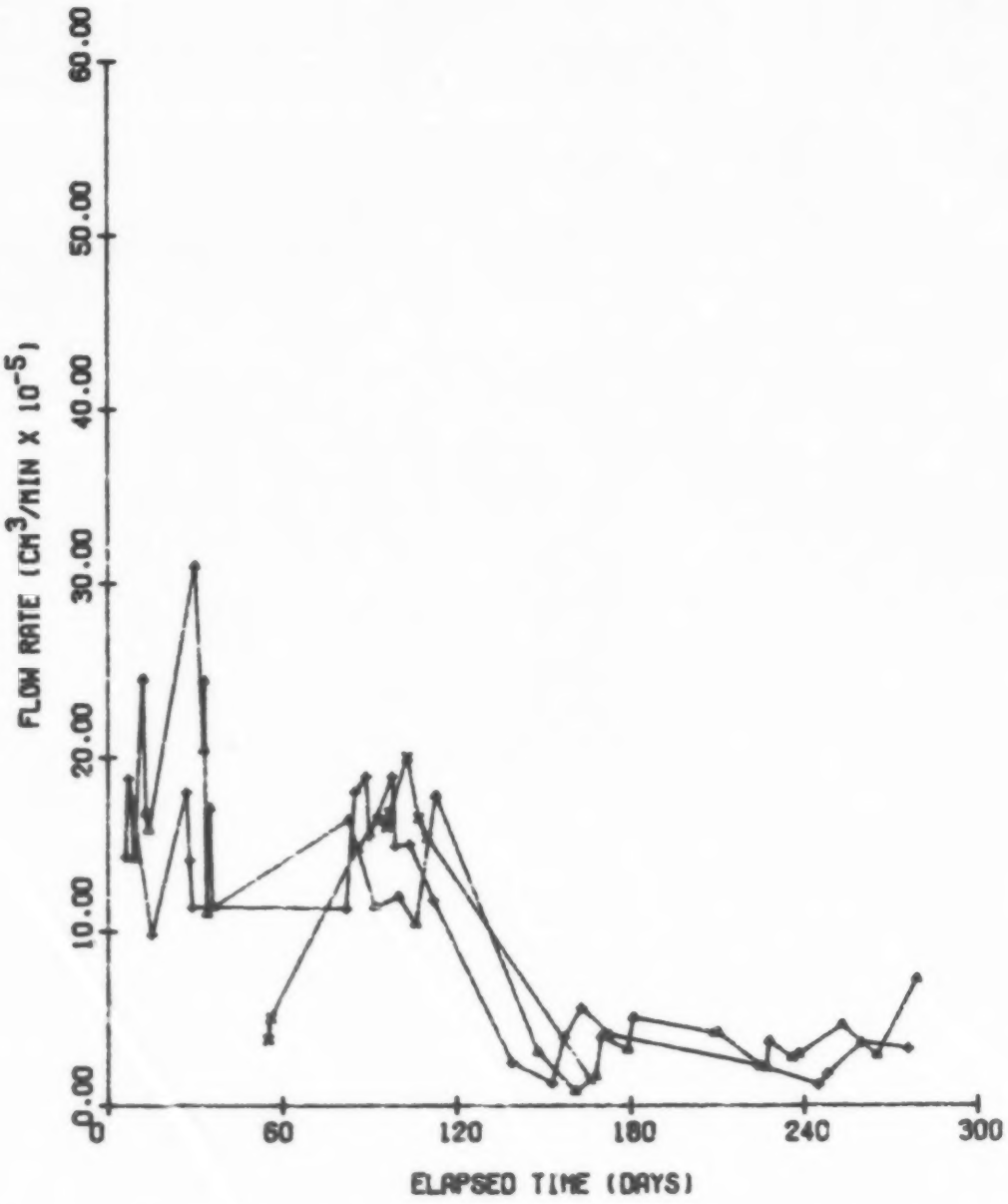

Figure 4.12 Peripheral flow rate through the rock around the plug as a function of total test time, specimen CG5309-31V.

▲ - ▲ : injection pressure = 4 MPa
+ - + : injection pressure = 2 MPa
x - x : injection pressure = 1 MPa

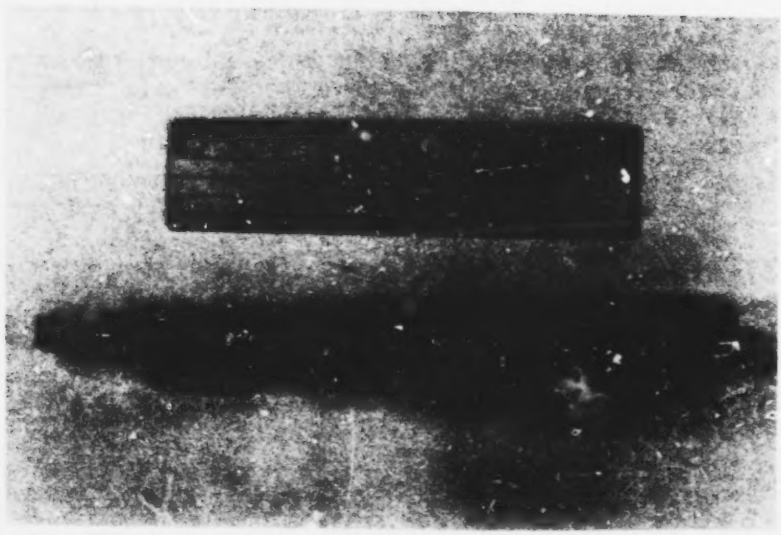

Figure 4.13 Mechanical packer used for flow testing of specimen CG5309-10. The packer is inserted in the top hole of the rock cylinder. As the nut is tightened, the rubber sleeve expands against the borehole wall. Water is injected through a hole along the center of the packer.

BEST COPY AVAILABLE

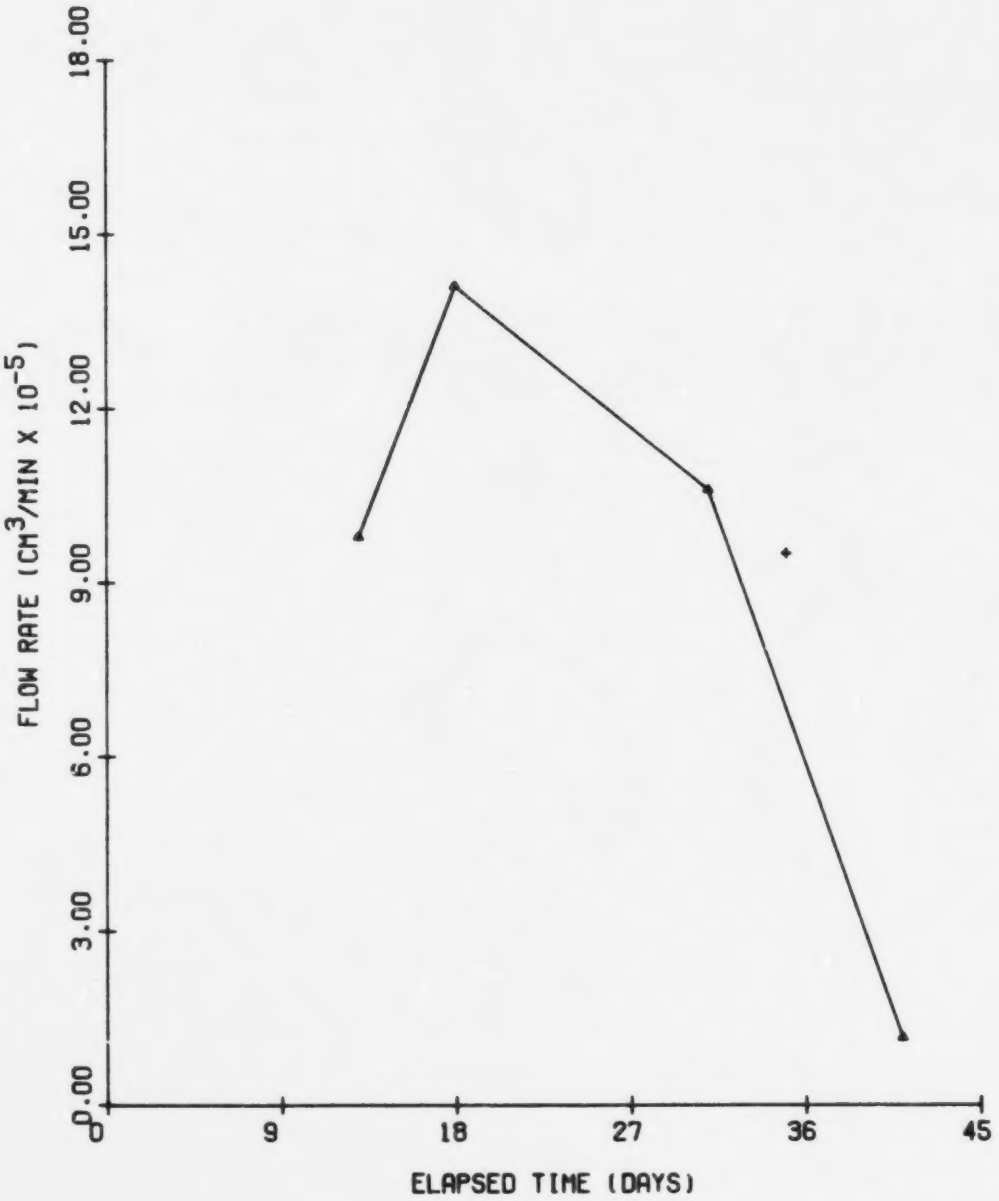

Figure 4.14 Longitudinal flow rate through a wet cement plug as a function of total test time, specimen CG5309-10, plug length of 59 mm.

▲ - ▲ : injection pressure = 4 MPa
\+ : injection pressure = 2 MPa

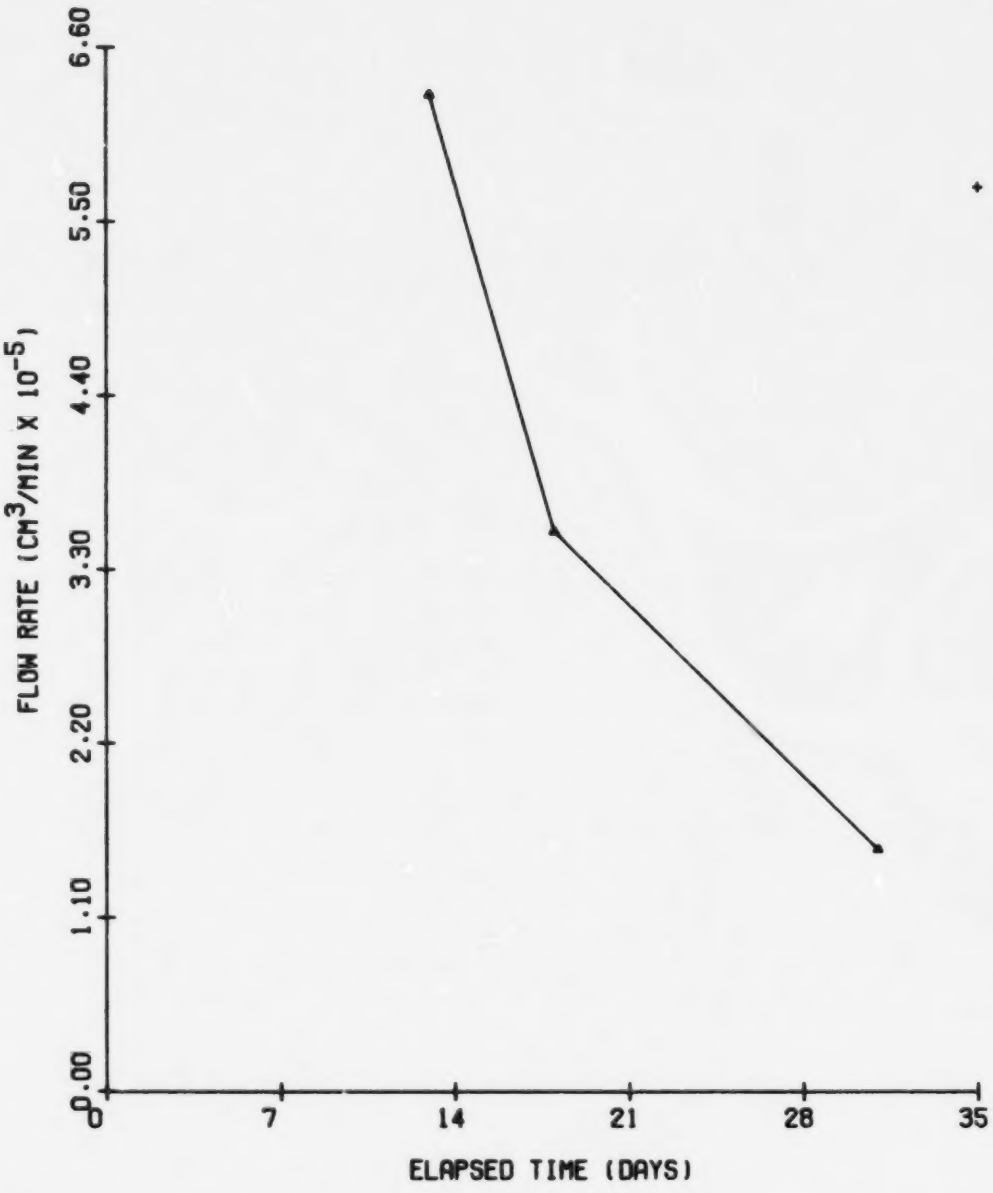

Figure 4.15 Peripheral flow rate through the rock around the plug as a function of total test time, specimen CG5309-10.

▲ - ▲ : injection pressure = 4 MPa
\+ : injection pressure = 2 MPa

4.1.3.1 Specimen CG5309-28. The cement mix was poured and after eight days of curing under water, the upper soft zone of laitance was ground away, resulting in an 88 mm long borehole seal. This plug was then left to dry out for three months at room temperature.

Figure 4.16 shows flow rate through the dried seal. The flow rates had to be plotted on a log scale due to their large range (up to three orders of magnitude). Two observations can be made. First, the initial flow rate is exceedingly high, greater than 0.1 cc/min. Drying caused cement plug shrinkage and opening up of a preferential flow path along the plug/rock interface. This is confirmed by the dye injection test described in Section 4.3.2. Second, the flow rate decreases rapidly (by up to two orders of magnitude) during the first two months of flow testing. This indicates that shrinkage reverses once the flow test starts. The flow rate levels off thereafter, but still at values much higher than those of wet cement seals for comparable length.

Figure 4.17 shows the peripheral flow rates through the rock around the plug. They are in the order of 10^{-5} to 10^{-4} cm^3/min. This is similar to the results for the wet cement plugs (Section 4.1.2). Complete test results are given in Table F-6 of Appendix F.

4.1.3.2 Specimen CG5309-01. The cement seal was installed at the same time as that of specimen CG5309-28. After curing for eight days, the soft laitance on the top of the plug was removed. The resulting net plug length was 86 mm. This specimen was left for seven months, while its cement seal dried at ambient temperature.

The same observations as for specimen CG5309-28 can be made here. The longitudinal flow rate through the plug is even higher in this specimen. Initial flow rate was 28.5 cc/min. The first flow test, at an injection pressure of 1.5 MPa, lasted less than a minute. This injection pressure was then used throughout the test sequence. During the first two months, the flow rate rapidly decreased by two orders of magnitude (Figure 4.18). Thereafter, it decreased at a much slower rate. After eight months, the flow rate (at 0.1 cc/min) is still two orders of magnitude higher than that of specimen CG5309-28, and four orders of magnitude higher than that of wet cement plugs.

Figure 4.18 also shows the inflow rates observed in the flowmeter. They are in the same range as the flow rates through the dried plug, but almost consistently higher, probably due to the flowmeter problem discussed in the previous Section. No peripheral flow can be observed because of the strongly preferential longitudinal flow along the plug/rock interface, and the short duration of each test. During the last 39 days of the test, dye marker was injected (Section 4.3.2). Table F-7 of Appendix F gives complete results for this specimen.

4.1.3.3 Specimen CG5309-21. The cement seal of this specimen was installed together with that of specimen -28. Net plug length, after grinding off the laitance, was 84 mm. Flow testing started after the plug was left to dry for three months at ambient room temperature. The

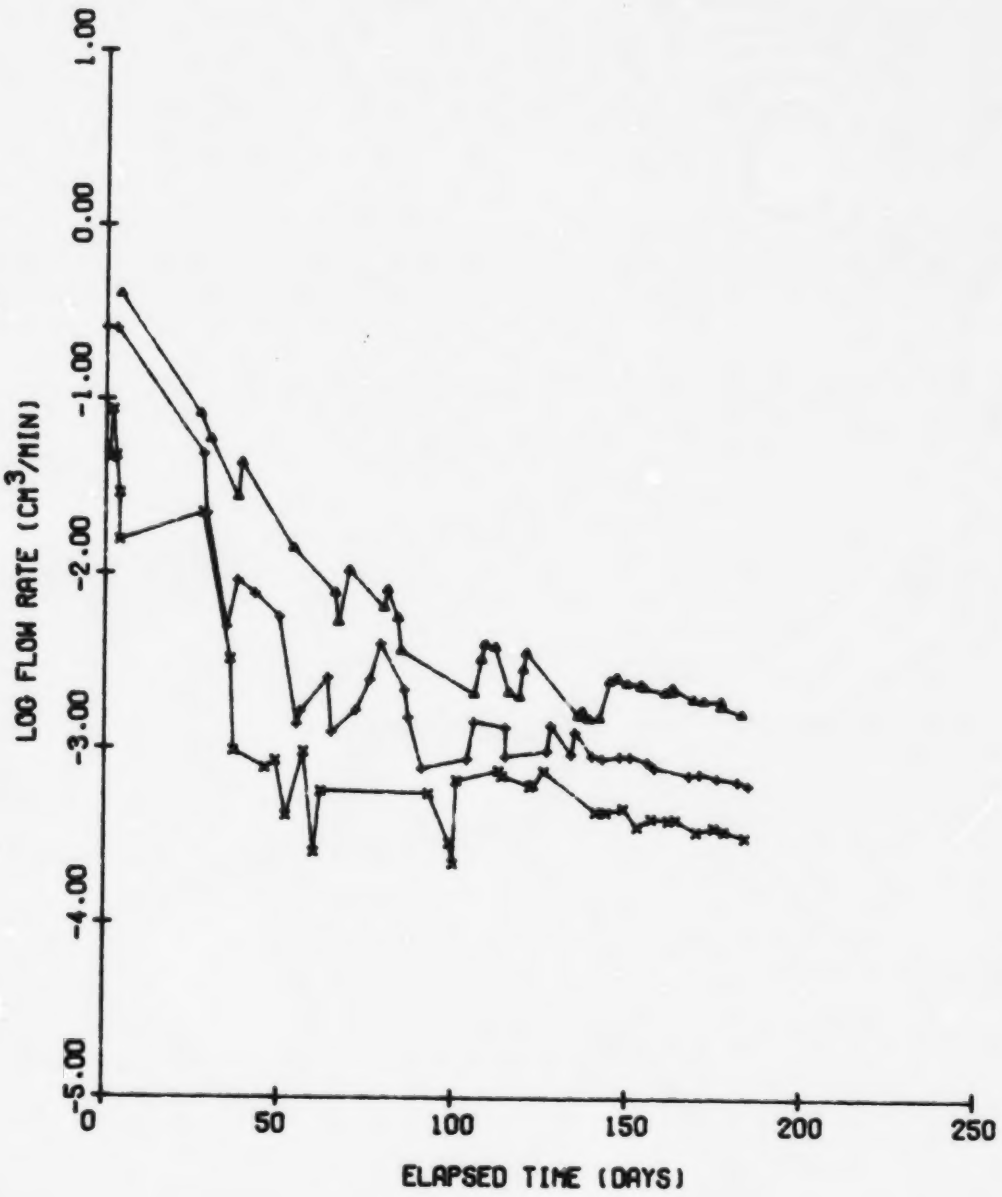

Figure 4.16 Longitudinal flow rates through a dried-out cement seal (log scale) as a function of total test time for specimen CG5309-28, plug length of 88 mm. Flow rates decrease rapidly in the beginning and level off with total test time.

▲ - ▲ : injection pressure = 4 MPa
\+ - + : injection pressure = 2 MPa
x - x : injection pressure = 1 MPa

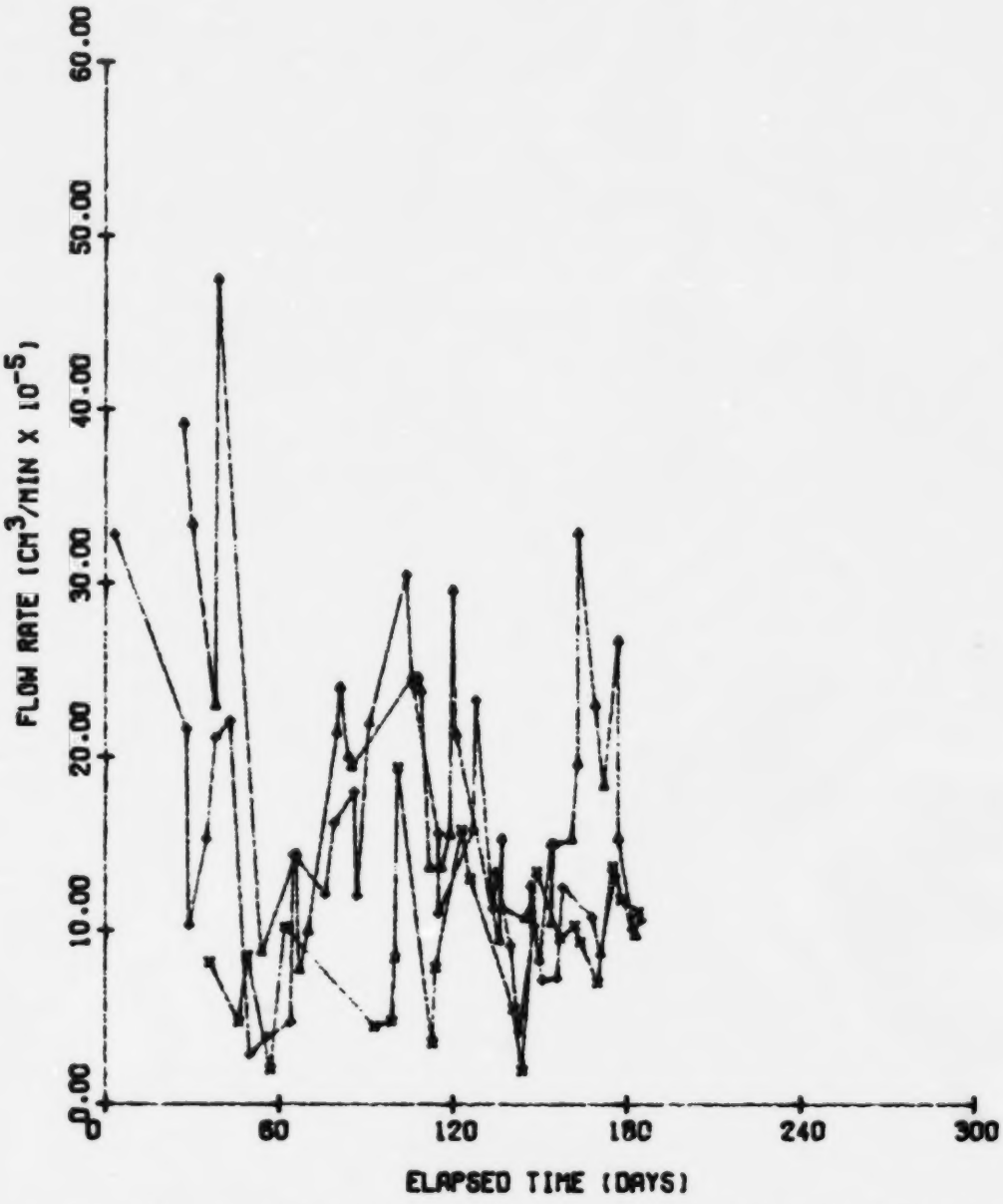

Figure 4.17 Peripheral flow rate through the rock around the plug as a function of total test time, specimen CG5309-28.

▲ - ▲ : injection pressure = 4 MPa
\+ - + : injection pressure = 2 MPa
x - x : injection pressure = 1 MPa

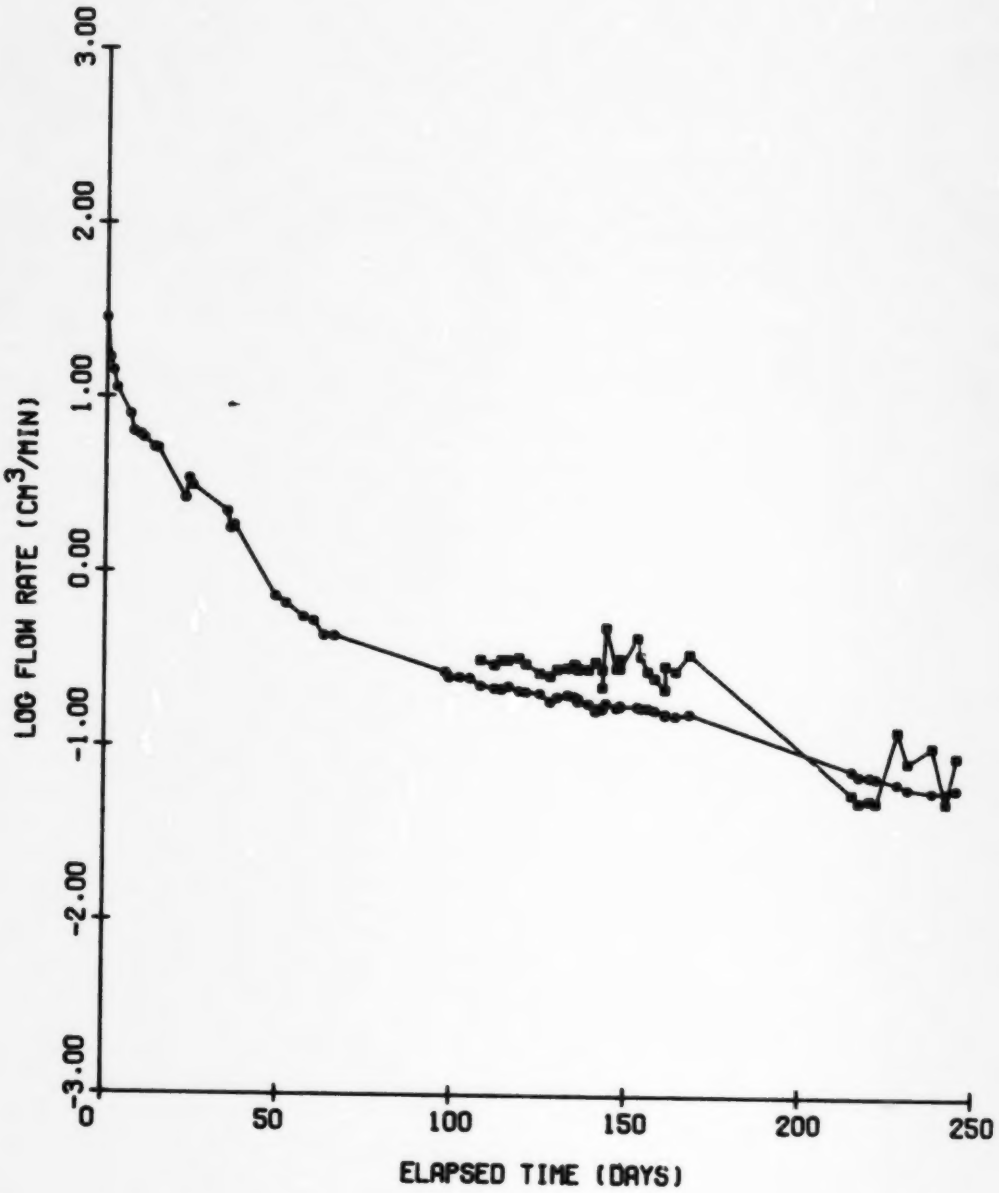

Figure 4.18 Longitudinal flow rate through a dried-out cement seal (log scale) as a function of total test time, specimen CG5309-01, plug length of 86 mm. The flow rate decreased rapidly as resaturation took place and leveled off with time thereafter.

■ - ■ : inflow rate at 1.5 Mpa
● - ● : outflow rate at 1.5 MPa

specimen hydraulically fractured at 7 MPa injection pressure, after only 21 days of testing.

A wide range of injection pressures was used during the short period of the test, from 0.2 MPa to 7 MPa (Table F-8 of Appendix F). Flow test results (Figure 4.19) indicate a high initial flow rate, followed by a rapid decrease with time, similar to other specimens with dried cement plugs. Flow rates are in the same range as for specimen 28, which has similar plug length and drying conditions.

4.1.3.4 Specimen CG5309-31V. This specimen with a wet cement seal had been flow tested previously (Section 4.1.2.3). It was dried in an oven for five days at an average temperature of 90°C (195°F). Flow testing resumed immediately afterwards. Excessive leakage occurred along the epoxy bond. Apparently, the epoxy dried and cracked during heating and it was necessary to replace it. Subsequent flow testing was carried out using an expandable mechanical packer (Figure 4.13).

Table F-9 in Appendix F gives the flow test results for the oven dried specimen. Figure 4.20 shows flow rate through the plug as a function of time since initiation of post-drying testing. The high initial flow rate followed by its rapid decrease with time is observed here also. This indicates the similarity of drying effects at both ambient and higher temperatures. This experiment allows a direct comparison of a very low flow rate through a wet cement seal and its dramatic increase, by three orders of magnitude, once the seal is dried.

4.2 Dynamic Loading Tests

Specimens with both wet and dried-out cement seals have been subjected to dynamic loads during ongoing flow tests. Therefore, flow rates before and after the application of a dynamic load can be compared directly. The plugged specimens were subjected to dynamic loads near the end of their flow test program, when the flow rates had become more or less constant with time. This is especially critical for the dried plugs, where the effect of dynamic loading must be distinguished from the effect of plug resaturation during the early part of the flow test, i.e. when the flow rate is still rapidly decreasing with time.

The flow rates obtained in the previous section, therefore, have incorporated the effect of dynamic loading. This applies for specimens CG5309-06, -31V, and -08 (wet cement plugs) and specimens -28 and -01 (dried-out cement plugs). In this section results for these specimens are presented, with dynamic loading details included in the plots.

4.2.1 Wet Cement Plugs

4.2.1.1 Specimen CG5309-06. This specimen has been subjected to dynamic loading together with specimen 31V. Both specimens were placed in tandem on the shaking table platform (Figure 4.21). Dynamic loading was carried out on the two specimens at an acceleration of 1 g.

The stroke length of the shaking table was set at 3.8 cm (1.5 in). Using Equation (3.1) and dividing by the gravity acceleration of 9.81

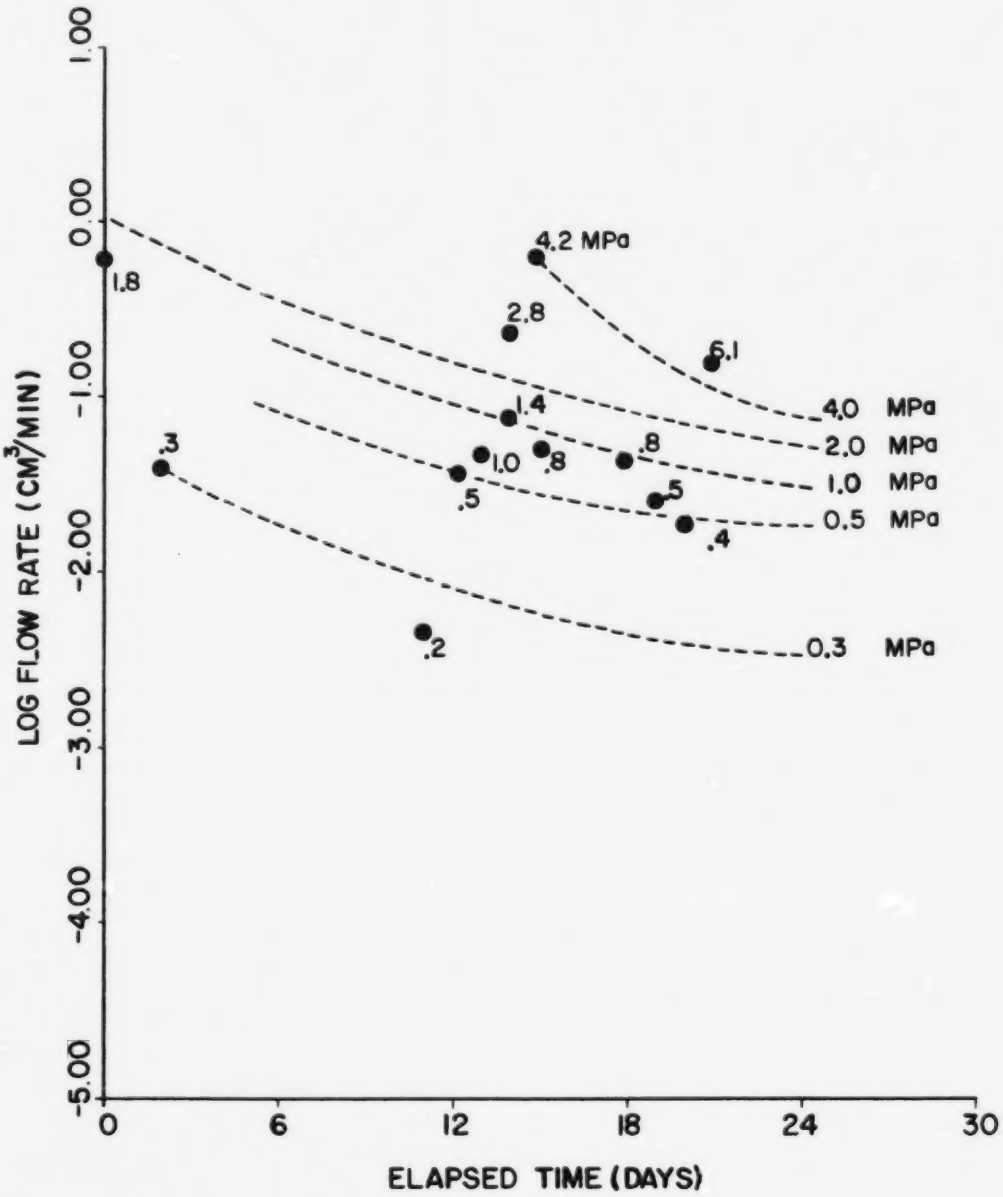

Figure 4.19 Longitudinal flow rate through a dried-out cement seal (log scale) as a function of total test time, specimen CG5309-21, plug length of 84 mm. Injection pressures used are indicated in the plot. Note the decrease of flow rates with time.

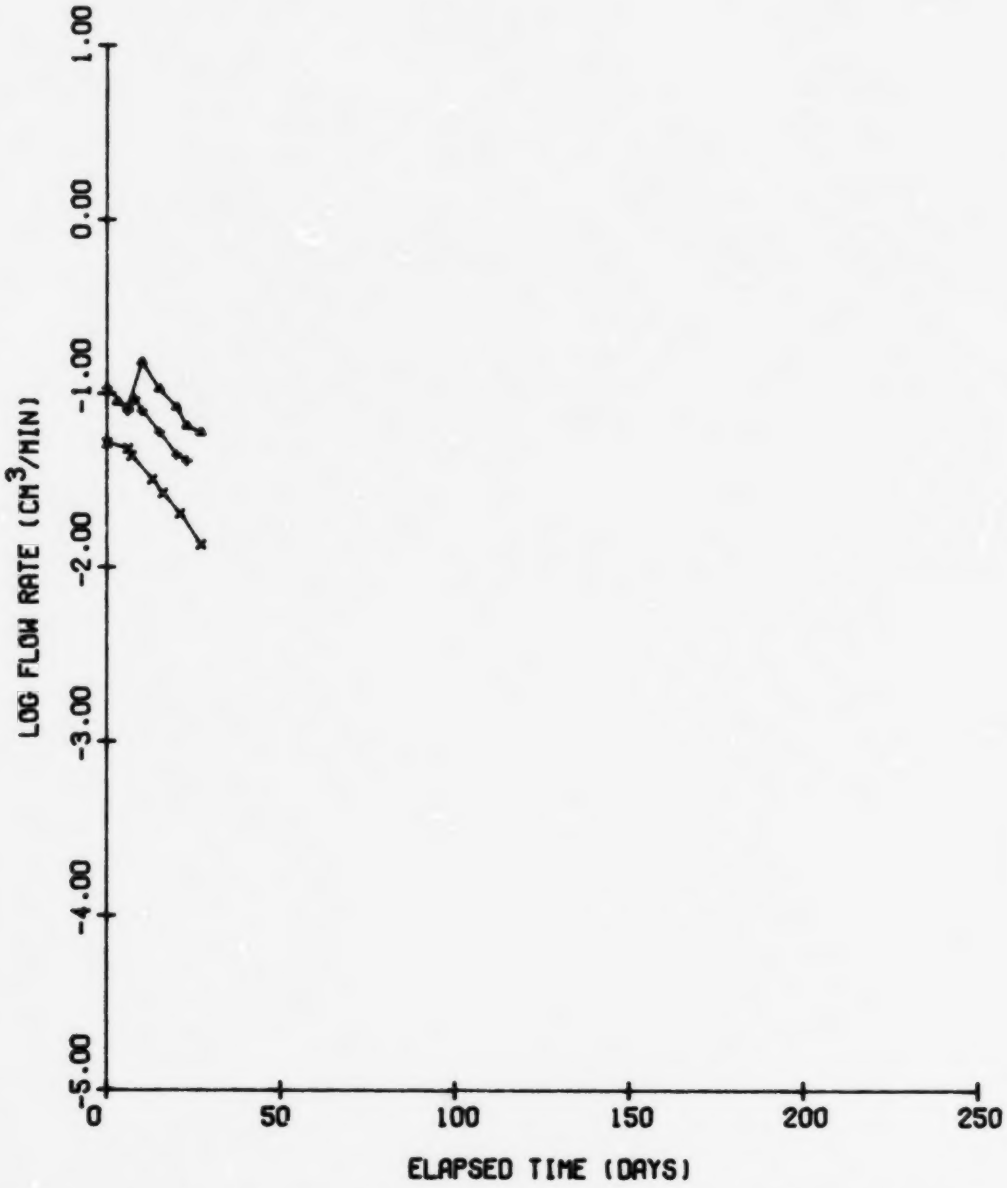

Figure 4.20 Longitudinal flow rate through a dried-out cement seal (log scale) as a function of total test time, specimen CG5309-31V (oven dried), plug length of 42 mm. Flow rates decrease rapidly with time.

▲ - ▲ : injection pressure = 4 MPa
\+ - + : injection pressure = 2 MPa
x - x : injection pressure = 1 MPa

Figure 4.21 Specimens CG5309-06 and -31V, placed in tandem for dynamic loading test on the shaking table.

BEST COPY AVAILABLE

m/s^2 (32.2 ft/s^2), the motion frequency was calculated at 2.6 Hz, which agrees with the tach reading of the sinusoid-g-meter. The corresponding peak particle velocity was 7.32 m/s (24 ft/s). Shaking was performed four times, for 40, 80, 160, and 320 seconds, respectively.

Dynamic loads were applied during a three week period after this sample had undergone flow tests for five months. Figure 4.22 indicates no effect of dynamic loading on the longitudinal flow rate through the plug. On day 150 a dynamic load was applied for 40 seconds during a flow test at 4 MPa. It was followed by a slight flow decrease. On day 154 a second dynamic load was applied during a flow test at 2 MPa. Its duration was 80 seconds. It was followed by a slight flow decrease. The dynamic load applied on day 159, with a duration of 160 seconds and at a 2 MPa injection pressure, also yielded a slight flow decrease. The last dynamic load, applied on day 169 at 4 MPa for 320 seconds, was followed by a slight flow decrease. Flow rate changes due to the dynamic loads are within the normal flow variation during the flow test before the dynamic loads are applied.

Virtually no peripheral flow through the rock could be observed during the last seven weeks of the flow tests, during which period the dynamic loading was applied (Figure 4.10). Hence, it is safe to conclude that the applied dynamic loads did not significantly enhance the peripheral flow through the rock around the plug.

4.2.1.2 Specimen CG5309-31V. Details of the shaking of this specimen are the same as for specimen CG5309-06. Shaking was conducted on days 219, 223, 228, and 238 of the flow tests. All dynamic loads except one were introduced during ongoing flow tests at 4 MPa. On day 223, the injection pressure was 2 MPa.

Figure 4.23 gives the longitudinal flow through the plug. No change could be detected in the flow through the plug, since no flow could be observed either immediately prior to or after the shaking. The flow was below the lowest limit of resolution of the flow test apparatus. (The no-flow points immediately preceding and following the shaking are not included on the graph.)

The effect of dynamic loads on the peripheral flow through the rock around the plug was also negligible. From Figure 4.12, it is obvious that there was not much change in the peripheral flow rate between day 219 and day 238, days on which the dynamic loads were applied.

Shaking for up to 320 seconds at an acceleration of 1 g, corresponding to a motion frequency of 2.6 Hz, motion amplitude of 3.81 cm (1.5 in), and peak particle velocity of 7.32 m/s (24 ft/s), does not degrade the performance of this cement plug.

4.2.1.3 Specimen CG5309-08. Dynamic loading tests have been performed on this specimen during the last five weeks of flow testing. A peak acceleration of 2 g was used throughout the tests. At a stroke length setting of 3.81 cm (1.5 in) and motion frequency of 3.6 Hz, this

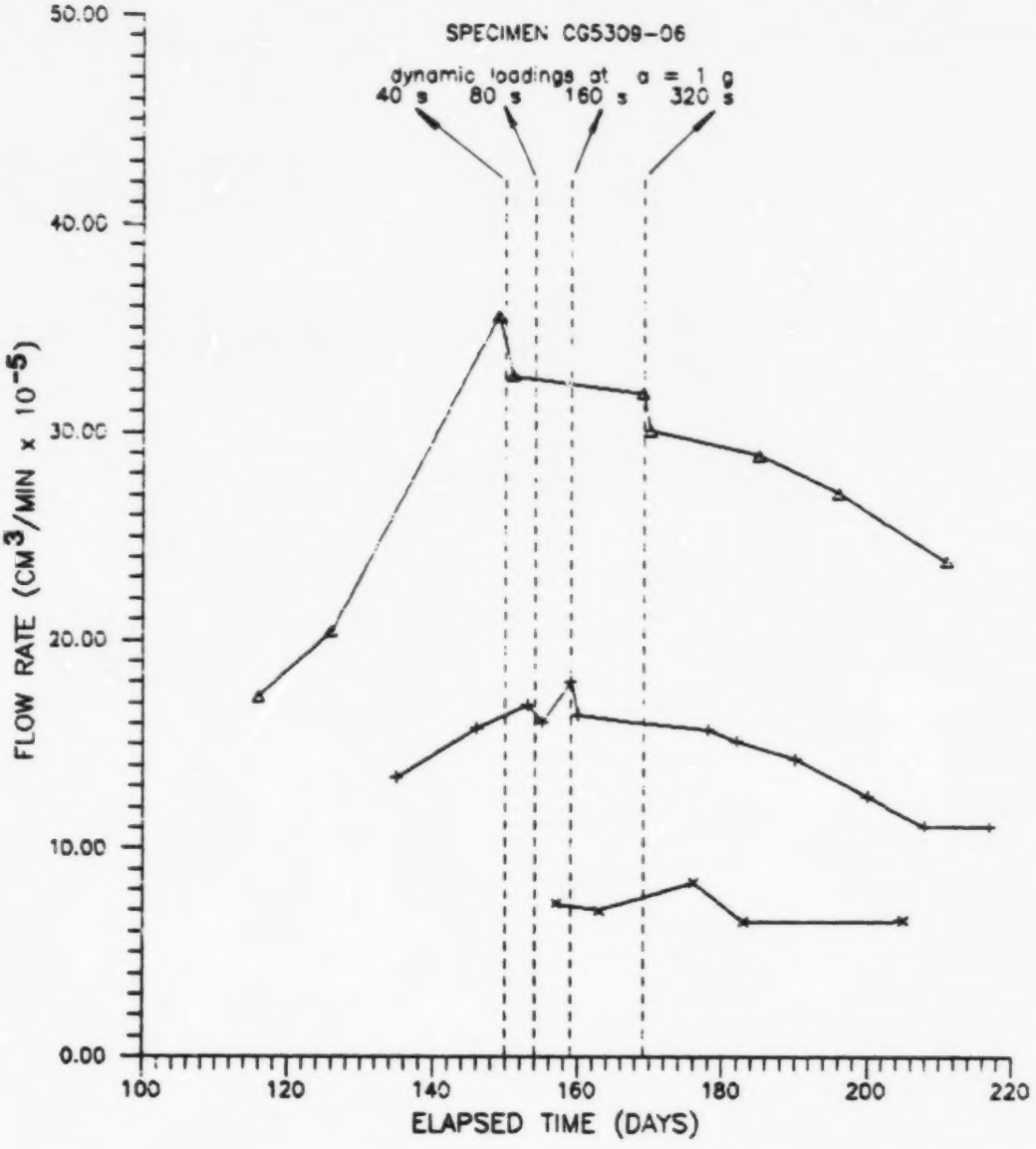

Figure 4.22 The effect of dynamic loading at an acceleration of 1 g on the longitudinal flow rate through a wet cement plug, specimen CG5309-06. No significant flow rate change can be observed as a result of the application of dynamic loads at durations of up to 320 s. Dashed lines indicate the time and duration of shaking.

Δ - Δ : injection pressure = 4 MPa
\+ - + : injection pressure = 2 MPa
x - x : injection pressure = 1 MPa

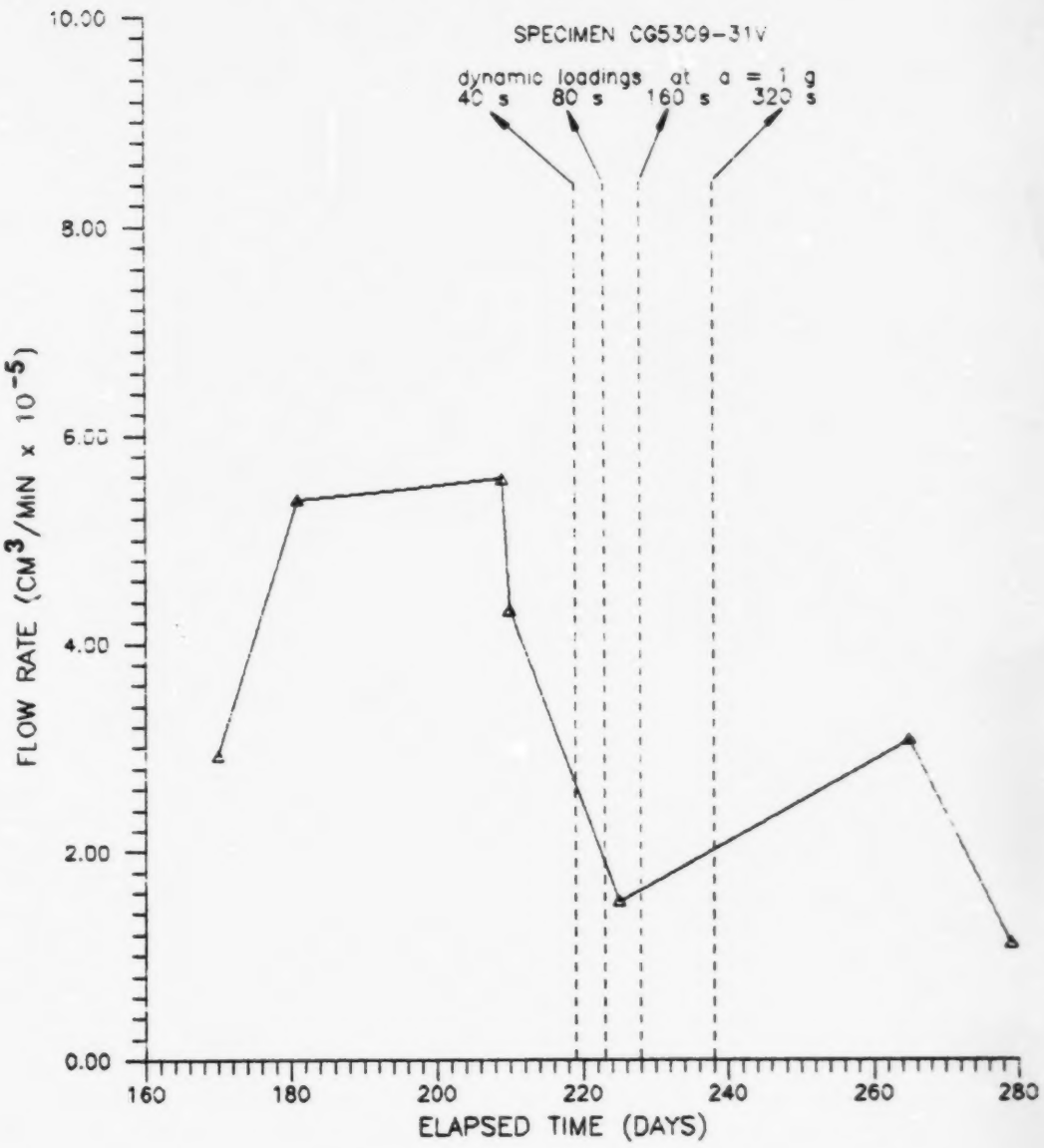

Figure 4.23 The effect of dynamic loading at an acceleration of 1 g on the longitudinal flow rate through a wet cement plug, specimen CG5309-31V. No flow could be observed before or after the dynamic loading tests were performed. (Points corresponding to no-flow measurements, immediately before and after shaking, are not included on this graph.)

Δ - Δ : injection pressure = 4 MPa
\+ - + : injection pressure = 2 MPa

corresponds to a peak particle velocity of 10.36 m/s (34 ft/s). Dynamic loads were applied five times during the test. Their durations were 20, 40, 80, 160, and 300 seconds, respectively.

Figure 4.24 shows the effects of the dynamic loads on the longitudinal flow through the plug. The first dynamic load, on day 216 of the flow test at 4 MPa, is followed by a slight flow rate increase. The second one, on day 221 and during injection at 4 MPa, is followed by a slight flow decrease. The third, on day 226 and at 2 MPa, is followed by a slight flow increase. The fourth, on day 232 and at 1 MPa, is followed by a slight flow decrease. The fifth dynamic load, applied for 300 seconds on day 244, during flow testing at 4 MPa, is followed by a slight flow decrease. Again, flow rate variation subsequent to the dynamic loads is smaller than the overall flow rate variation in the flow tests. Therefore, this variation is most likely caused by problems in measuring very low flow rates (at the lowest limit of resolution of flow test instrumentation) rather than by the dynamic loads.

Figure 4.25 shows the effect of dynamic loads on the peripheral flow through the rock around the plug. The flow varies slightly more after the dynamic loads have been applied. This includes flow decrease as well as flow increase. The overall flow rate remains unchanged.

Figure 4.26 indicates that dynamic loads also have no effect on the inflow rate into the specimen. This figure shows that flow variation due to the dynamic loads is negligible and is similar to the flow variation without dynamic loading.

It can be safely concluded that dynamic loading for up to 300 seconds and at an acceleration of 2 g, corresponding to motion frequency of 3.6 Hz, motion amplitude of 3.81 cm (1.5 in), and peak particle velocity of 10.36 m/s (34 ft/s), did not impair the sealing performance of the cement plug in this specimen.

4.2.2 Dried-Out Cement Plugs

4.2.2.1 Specimen CG5309-28. Dynamic loads have been applied five times to this specimen during the last seven weeks of the flow testing. An acceleration of 1 g was used for all the shaking applications. Their durations were 20, 45, 86, 166, and 326 seconds, respectively. The stroke length of the shaking table was set at 2.86 cm (1.125 in), giving a nominal frequency of 3 Hz and a peak particle velocity of 6.37 m/s (20.9 ft/s).

Figure 4.27 gives the longitudinal flow rate through the plug and plug/rock interface as a function of time, before and after the application of dynamic loads. The first dynamic load, applied on day 137 of the flow testing, while the injection pressure was 3 MPa, was followed by a slight flow rate increase. The next dynamic load, on day 147 and at 4 MPa injection pressure testing, is followed by a slight flow decrease, as was the third, on day 154, at 4 MPa injection pressure. The fourth shaking, on day 163 and at 4 MPa, was followed by a slight flow increase. Finally, a dynamic load applied for 326

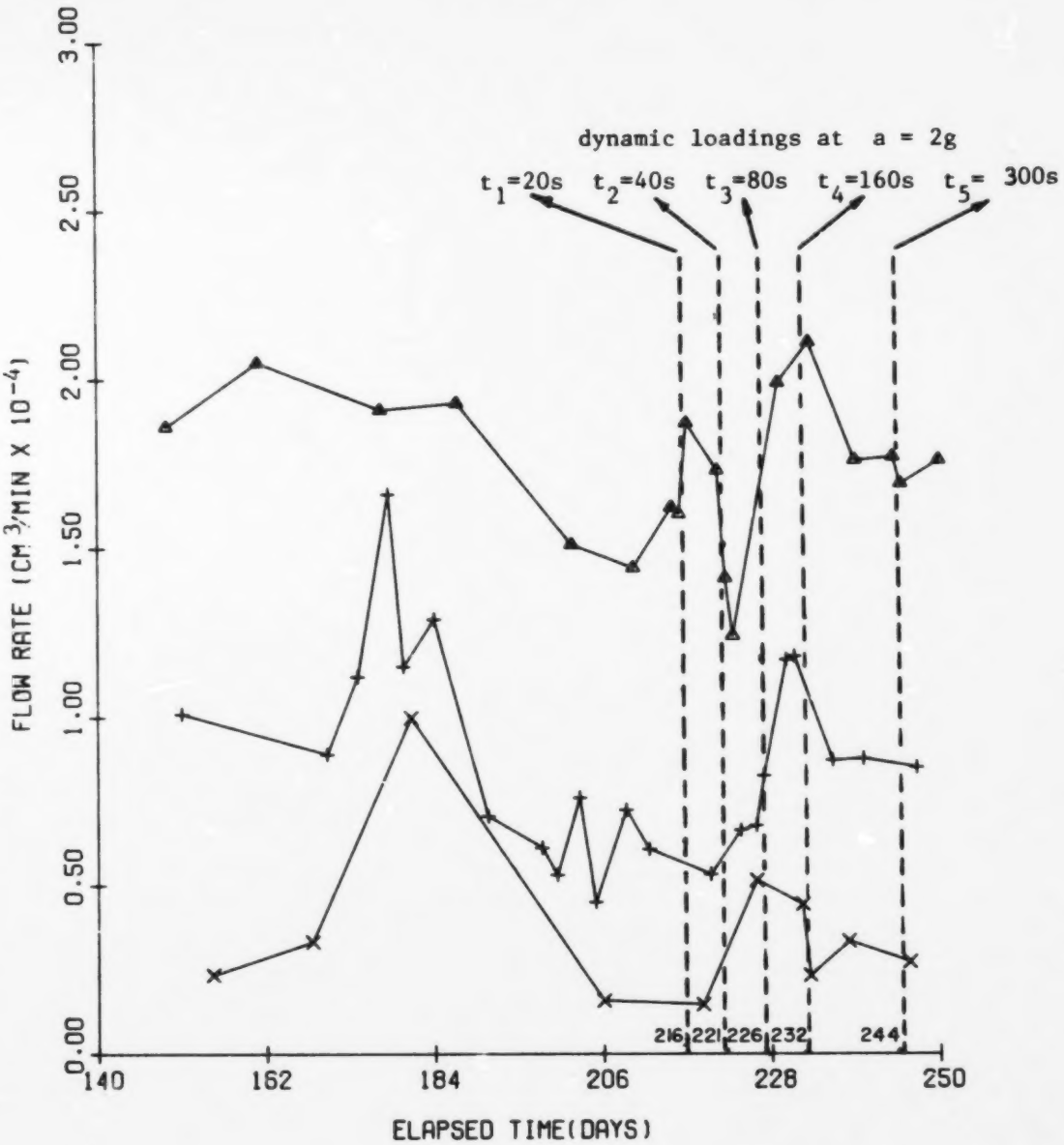

Figure 4.24 The effect of dynamic loading at an acceleration of 2g on the longitudinal flow rate through a wet cement plug, specimen CG5309-08. Dynamic loads at durations up to 300 sec do not change the flow rate significantly.

Δ - Δ : injection pressure = 4 MPa
\+ - + : injection pressure = 2 MPa
x - x : injection pressure = 1 MPa

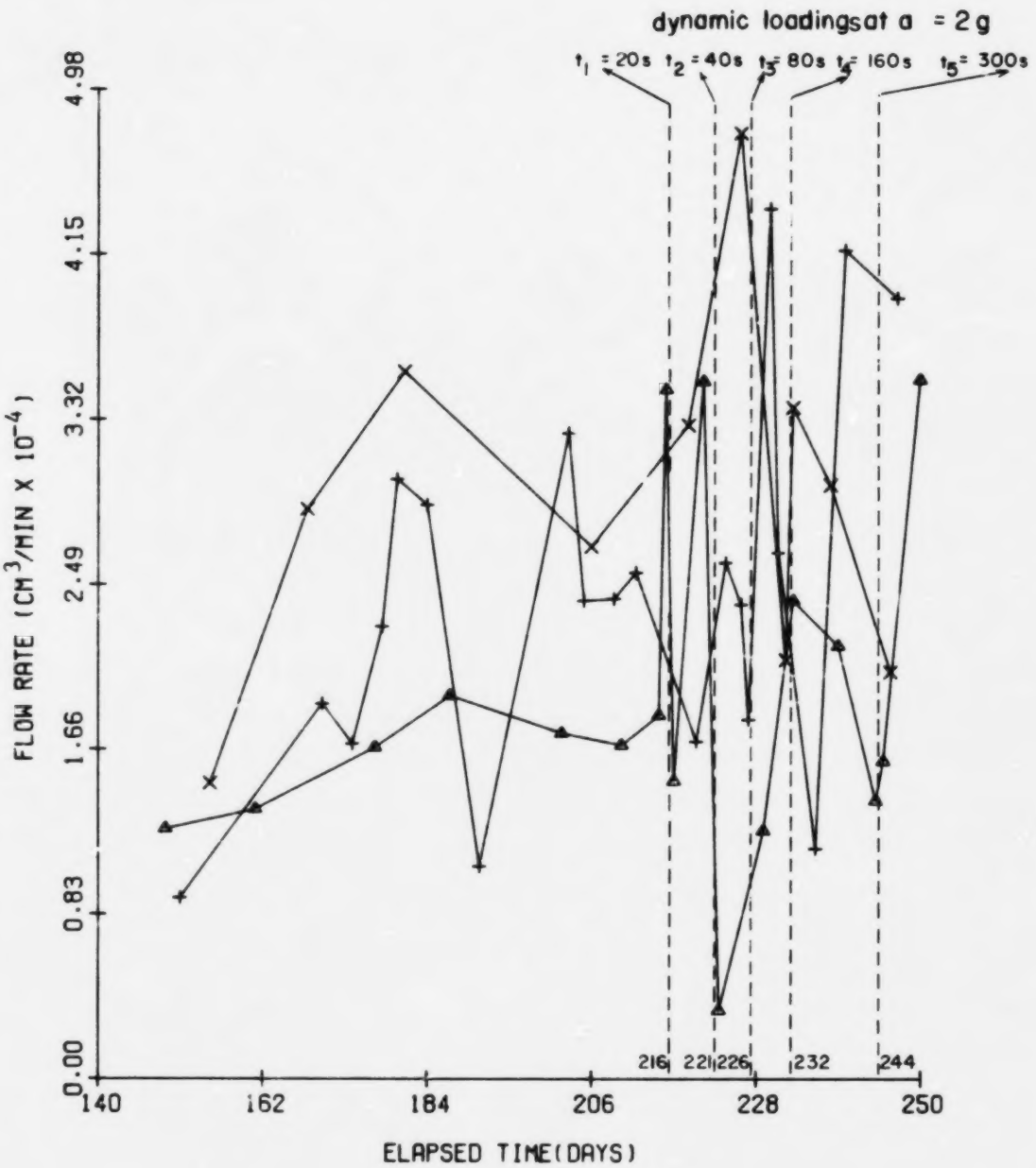

Figure 4.25 The effect of dynamic loading at an acceleration of 2g on the peripheral flow rate through the rock around the plug, specimen CG5309-08. Dynamic loads cause the flow rates to vary, but overall flow rate remains constant.

Δ - Δ : injection pressure = 4 MPa
\+ - + : injection pressure = 2 MPa
x - x : injection pressure = 1 MPa

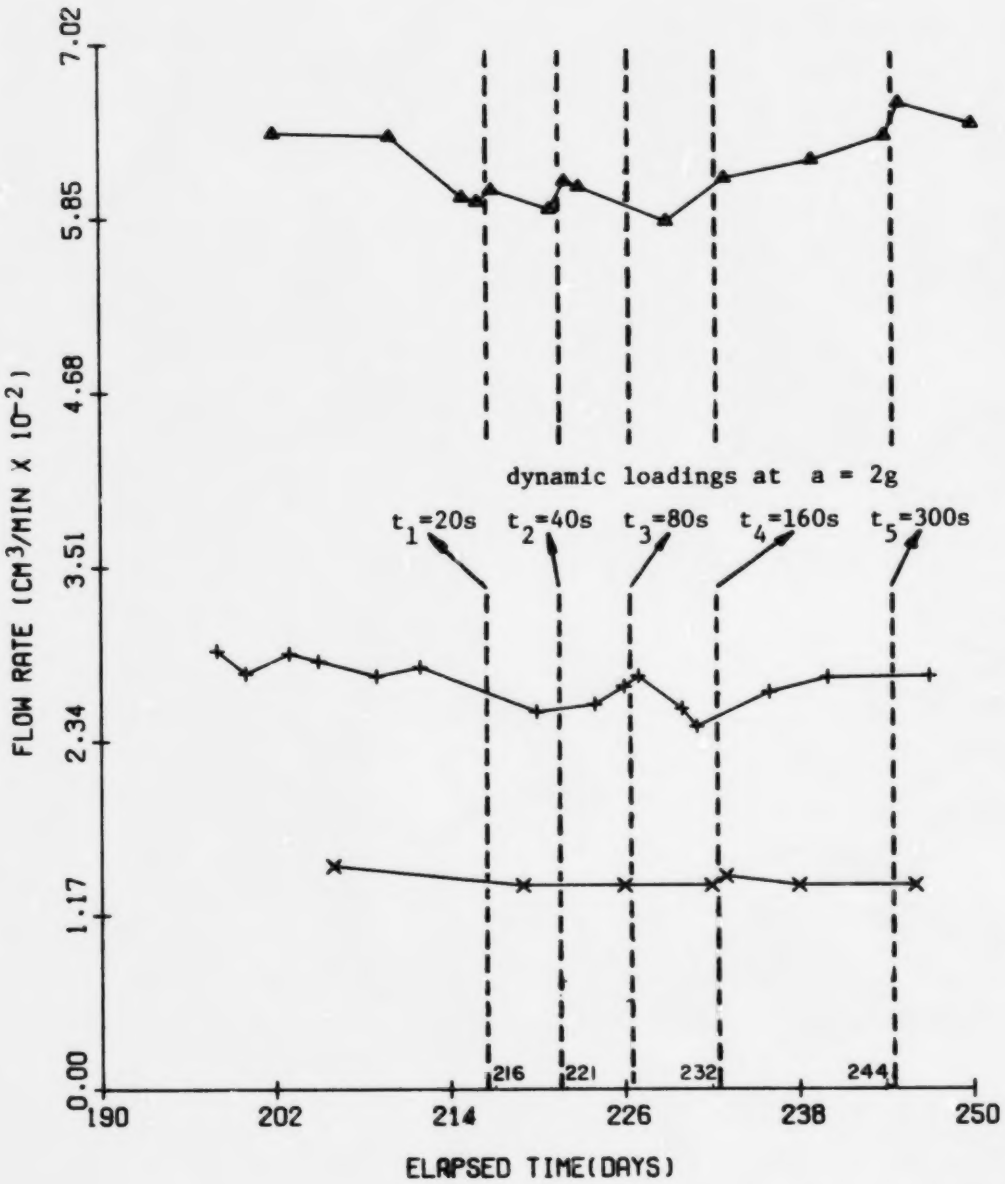

Figure 4.26 Inflow rate at various injection pressures as a function of time, specimen CG5309-08. Flow rate variation due to shaking remains well within the overall flow rate variation.

Δ - Δ : injection pressure = 4 MPa
\+ - + : injection pressure = 2 MPa
x - x : injection pressure = 1 MPa

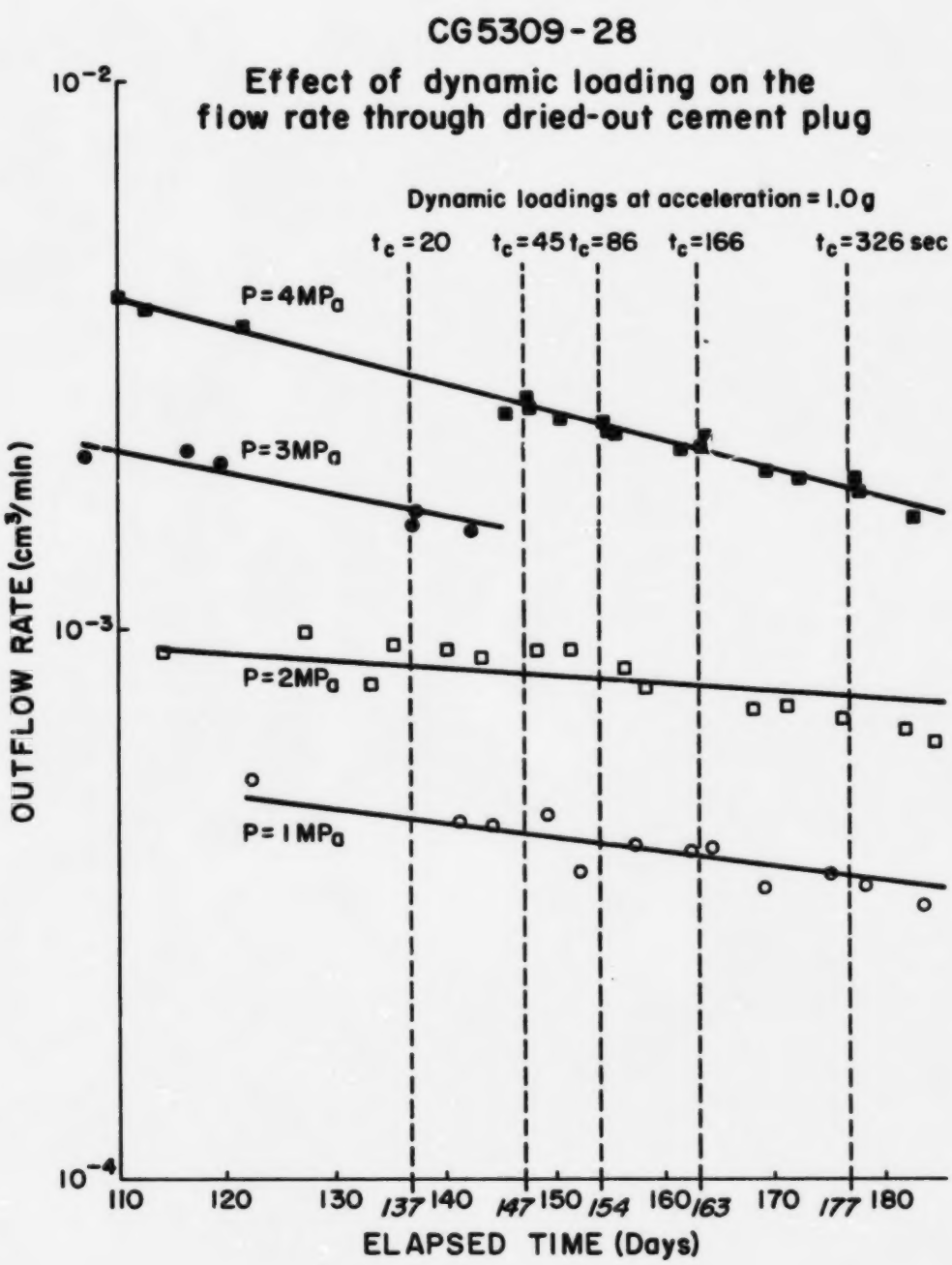

Figure 4.27 The effect of dynamic loading at an acceleration of 1 g on the longitudinal flow rate through a dried-out cement plug, specimen CG5309-28. The applied dynamic loading at durations up to 326 seconds does not change the flow rate significantly.

seconds on day 177 of the flow testing, during injection at 4 MPa, again yielded a slight flow decrease.

Figure 4.27 shows that until the sixth month of testing, a dried-out cement plug still exhibits a trend of slightly decreasing longitudinal flow rate with time. It is important to note that this trend is obviously stronger than the effect of dynamic loads at 1 g.

Figure 4.28 plots the rate of peripheral flow through the rock prior to and after the application of dynamic loads. Flow variation due to dynamic loads is in the same range as flow variation without them. Overall, the rate of peripheral flow through the rock before and after dynamic loads were introduced remains constant.

4.2.2.2 Specimen CG5309-01. Dynamic loads were applied five times. Their durations varied from 40 to 300 seconds. A 2 g acceleration was used throughout. At a stroke setting of 3.81 cm (1.5 in), the frequency was 3.6 Hz and the peak particle velocity 10.36 m/s (34 ft/s).

The effect of applied dynamic loads on the longitudinal flow rate through the plug/rock interface is shown in Figure 4.29. All dynamic loads were introduced during ongoing flow tests at 1.5 MPa injection pressure. All were followed by a slight flow decrease immediately after application. Flow variation with dynamic loads is much smaller than the overall flow variation without dynamic loads. The trend of slowly decreasing flow rate with time exhibited by this dried-out plug clearly is stronger than the effect of dynamic loading on flow rate. The same figure also shows that inflow rate variation as a result of dynamic loading is small compared to the overall inflow rate variation.

The results show that shaking of a dried-out cement plug for up to 300 seconds, at 2 g, which corresponds to a frequency of 3.6 Hz, motion amplitude of 3.81 cm (1.5 in), and peak particle velocity of 10.36 m/s (34 ft/s), did not affect its sealing performance.

4.3 Dye Injection Test

The dye injection test was carried out after the dynamic loading tests and the subsequent post-shaking flow tests were completed.

The test has been performed on two specimens with wet cement plugs (CG5309-06 and -31V), one specimen with a dried-out cement plug (01), and an oven-dried specimen of the former (31V). Specimens 06 and 01 were sawed in half after dye test had been completed. This allowed visual observation of the flow pattern in both wet and dried-out plugs, as well as verification of results obtained from the flow tests.

4.3.1 Wet Cement Plugs

4.3.1.1 Specimen CG5309-06. A red liquid concentrate dye marker, manufactured by Formulab, was injected on day 177 of the flow test. The test continued for 41 days at injection pressures of 2 and 4 MPa.

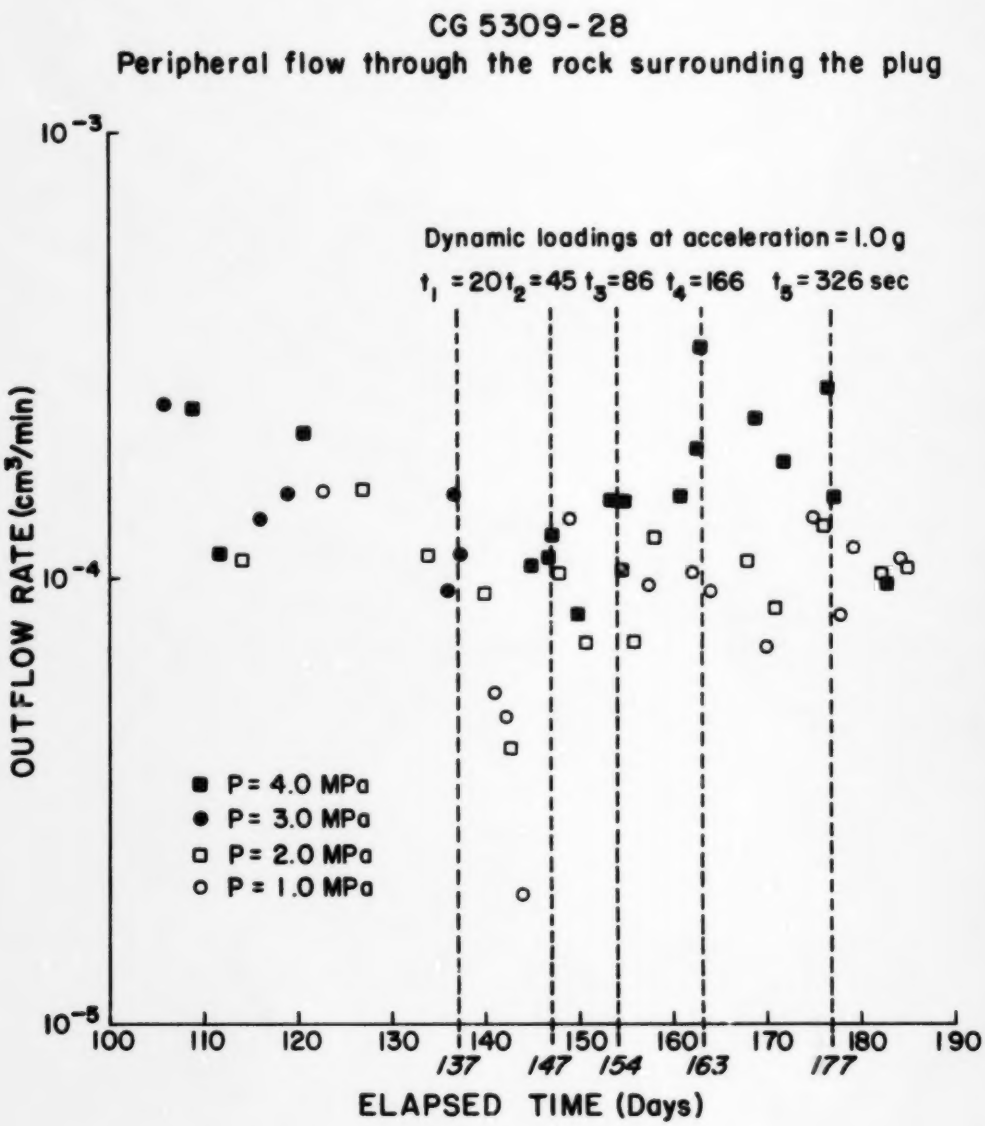

Figure 4.28 The effect of dynamic loading at an acceleration of 1 g on the peripheral flow rate through the rock around the dried-out plug, specimen CG5309-28. No significant change in flow rates attributable to the dynamic loads can be observed.

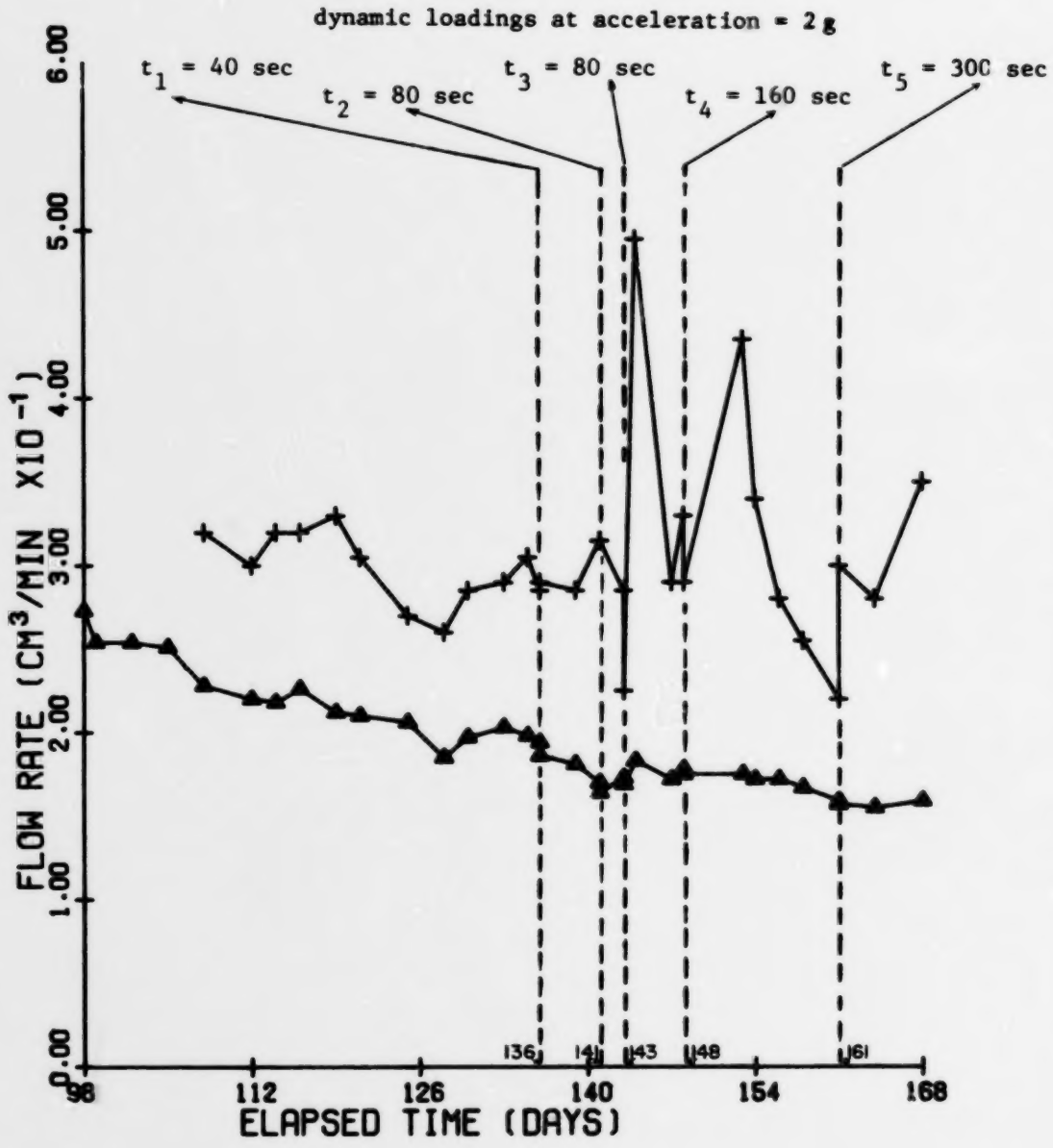

Figure 4.29 The effect of dynamic loading at an acceleration of 2 g on the longitudinal flow rate through a dried-out cement plug, specimen CG5309-01. The outflow plot shows no effect of dynamic loading at durations up to 300 seconds on the rate of longitudinal flow through the dried-out plug. Injection pressure was 1.5 MPa. Inflow may indicate some enhanced flow shortly after the last three dynamic load applications, but more likely is affected by monitoring problems (Sections 4.1.2.3, 4.1.3.2).

+ - + : inflow rate observed in the flowmeter
Δ - Δ : outflow rate through the plug-rock interface

The flow rates obtained during this period were consistent with previous values, as shown in Figure 4.30.

A week after the test ended, the specimen was sawed in half along its length. A large oil-cooled saw was used to cut it along a diameter. The excess oil was removed using Magnaflux cleaner/remover (SKC-NF/ZC-7). Pictures of the plug/rock cross-section were taken repeatedly at 12 hour intervals. Figure 4.31 shows a sawed half cross-section of specimen CG5309-06. The red dye penetrates the cement seal body uniformly. No traces of preferential flow path exist along the plug/rock interface. Visual inspection confirmed that the interface was tightly closed. The plug body remained intact, no visible cracks could be observed.

The uniformly penetrated cement plug body and the absence of a preferential flow path appear to be the typical flow pattern in wet cement borehole seals. It confirms the very low flow rate through the plug observed during the flow test. This shows that a cement seal is capable of preventing flow, with a sealing performance equal to or better than Charcoal granite, if it is maintained wet all the time.

4.3.1.2 Specimen CG5309-31V. The dye injection test was started on day 247 of the flow test and lasted 34 days. Formulabs' yellow/green liquid concentrate dye marker was used. Injection pressures during the test were 2 and 4 MPa. As in the previous tests, flow rates were very low. In many instances no flow could be observed. The observed flow rates during the dye injection test were consistent with the previous flow test results (Figures 4.32 and 4.33).

On the eleventh day of the dye injection test, the yellow color appeared in the longitudinal outflow collection pipette. On the 16th day, the same color showed up in the peripheral outflow pipette. However, the color was very much lighter than the original color of the dye solution. This reduction in color intensity was not observed for samples in which a clear preferential flowpath (shrinkage gap between plug and rock cylinder) was observed. This strongly suggests that considerable dye adsorption has taken place, and is an indication of the uniform, or at least widespread, flow penetration through the plug. The probable absence of a preferential flow path is confirmed by the low flow rates.

4.3.2 Dried-Out Cement Plugs

4.3.2.1 Specimen CG5309-31V. This is the same specimen which had previously undergone dye injection for 34 days (Section 4.3.1.2). At the end of the test, this specimen was oven-dried and then flow tested again using the same dye solution (see Section 4.1.3 for details of oven drying).

Two facts emerged from the subsequent dye injection/flow testing of this oven dried specimen. First, the yellow/green dye solution injected into the top hole appeared immediately in the longitudinal outflow collection pipette, in full color. Second, the (previously very low) longitudinal flow rate through the plug (Figure 4.32) increased dramatically, by four orders of magnitude, after drying

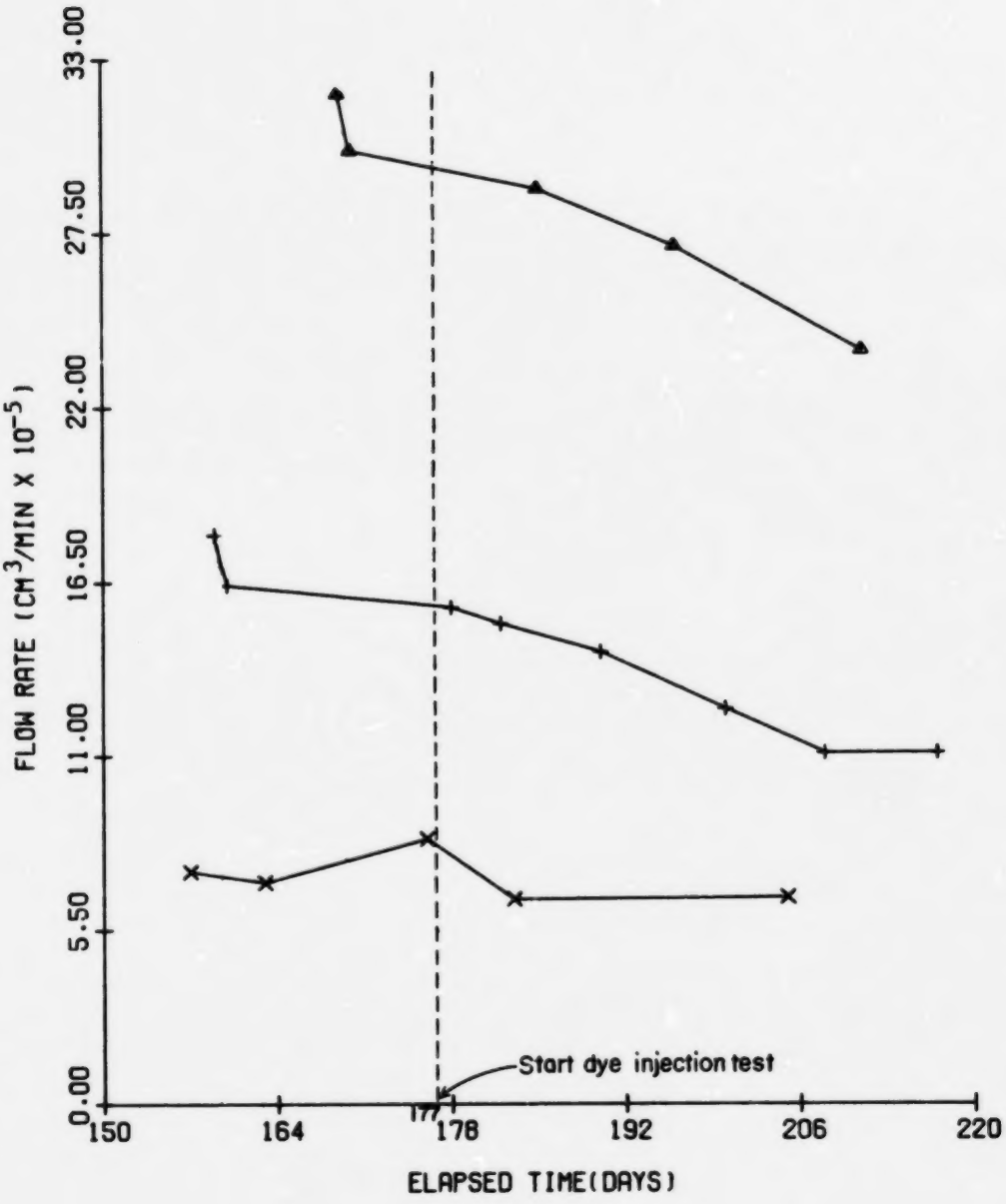

Figure 4.30 Longitudinal flow rate through a wet cement plug prior to and during dye injection test, specimen CG5309-06.

Δ - Δ : injection pressure = 4 MPa
\+ - + : injection pressure = 2 MPa
x - x : injection pressure = 1 MPa

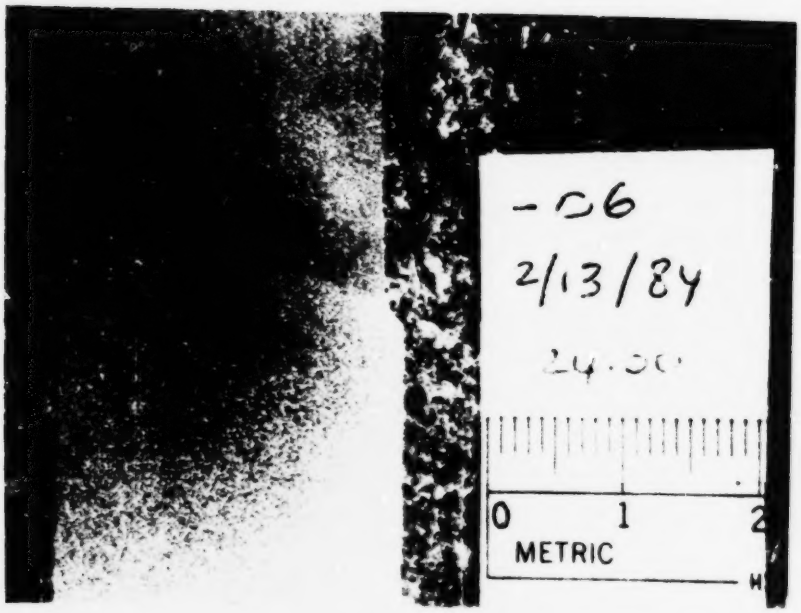

Figure 4.31 Section through a wet cement plug in Charcoal granite after dye injection. Uniform dye penetration of the plug. No obvious interfacial preferential flowpath. Specimen CG5309-06. Offset of hole is due to misalignment during drilling (performed from both ends in order to leave a rock brige for initial reference flow testing).

BEST COPY AVAILABLE

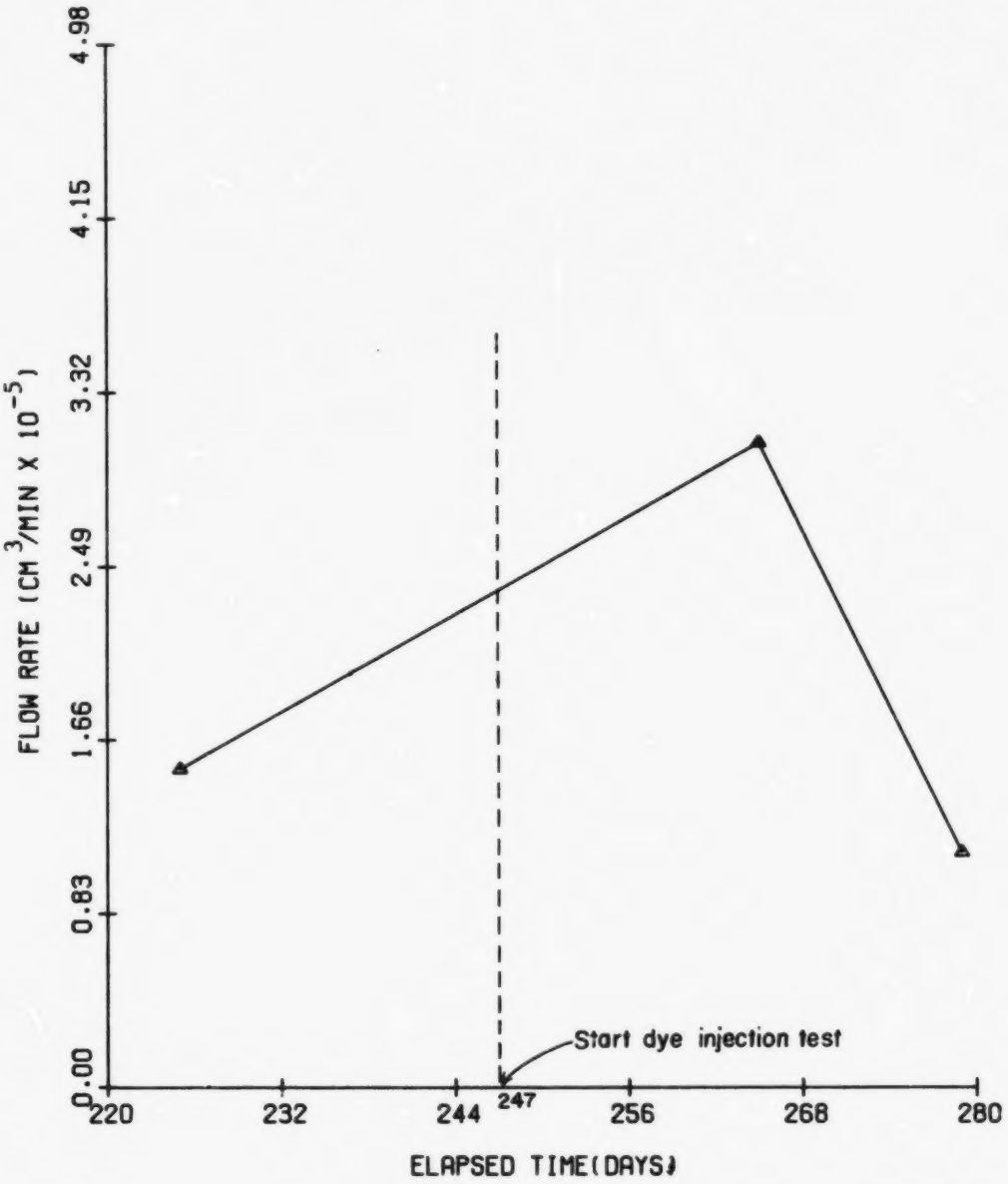

Figure 4.32 The observed longitudinal flow rate through a wet cement plug prior to and during dye injection tests, specimen CG5309-31V. No flow could be observed in many instances, especially at injection pressures of 1 and 2 MPa.

Δ - Δ : injection pressure = 4 MPa

BEST COPY AVAILABLE

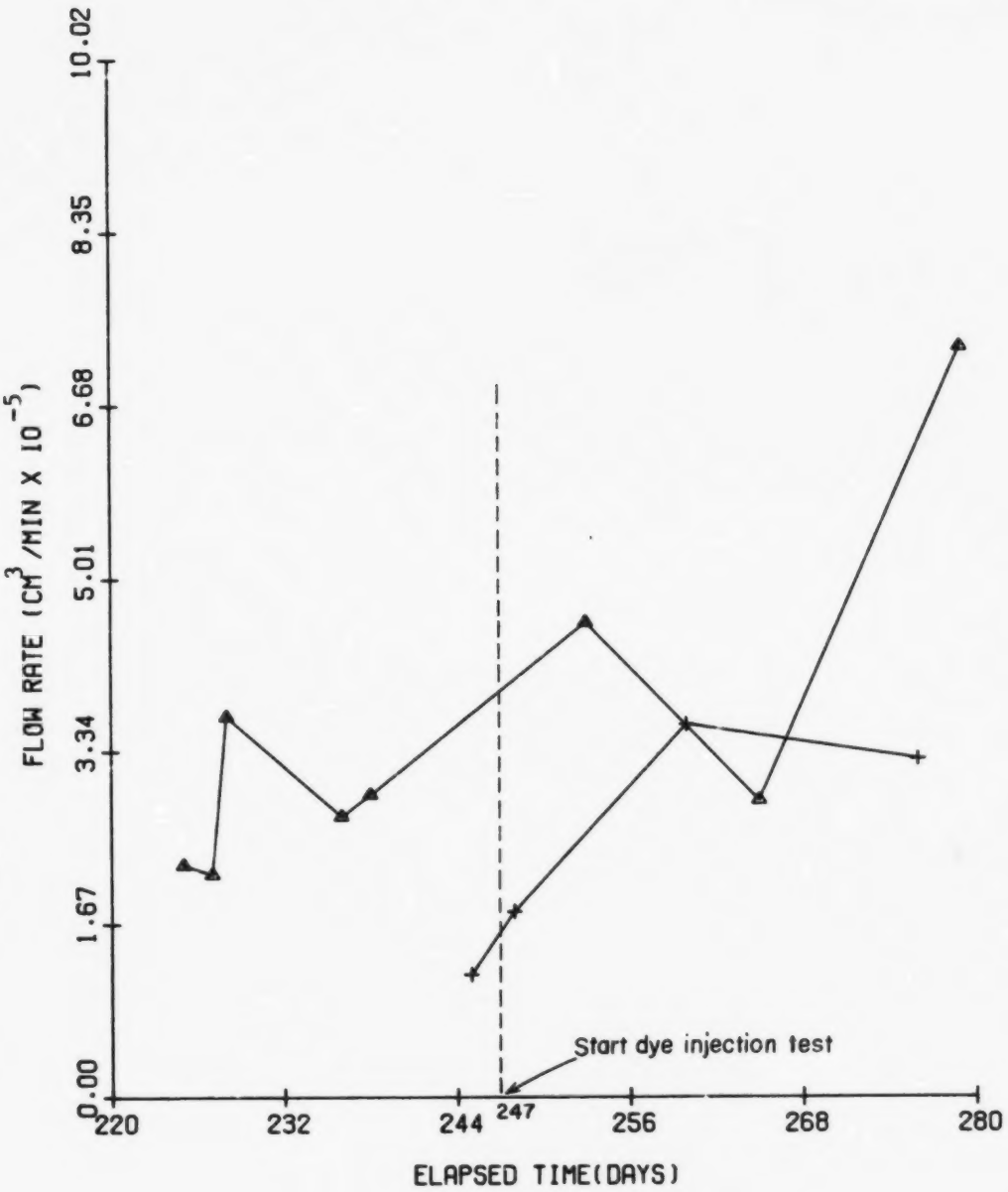

Figure 4.33 Peripheral flow rate through the rock around the wet plug prior to and during dye injection tests, specimen CG5309-31V.

Δ - Δ : injection pressure = 4 MPa
\+ - + : injection pressure = 2 MPa

BEST COPY AVAILABLE

(Figure 4.34). These two facts indicate that a preferential flow path opened up, most likely along the plug/rock interface, due to plug drying.

4.3.2.2 Specimen CG5309-01. Dye injection proceeded on day 206 of the flow test. Formulabs' red liquid concentrate dye marker was used in the test, which lasted for 39 days. Injection pressures of 1 and 2 MPa were used until until day 214. A constant injection pressure of 1.5 MPa was used throughout the remainder of the test.

Flow rates observed during the dye injection test at 1.5 MPa are shown in Figure 4.35. They are consistent with previous flow test results shown in Figure 4.18. The slow decrease in flow rate with time can still be observed after eight months of flow testing.

The specimen was sectioned in half using a large oil-cooled saw a week after dye injection tests were completed. After the excess oil was cleaned, photographs of the specimen were taken. Figure 4.36 is a picture of a sawed half, and clearly shows traces of red dye along the plug/rock interface. A dye-penetrated crack accross the plug body is also visible, extending from the left to the right interface. The crack and the interfacial fissures appear to be preferential flowpaths. None of the dye marker penetrated the main body of the plug. The presence of preferential flow paths appears to be typical in the dried-out plugs. They explain the high flow rates observed during the flow tests.

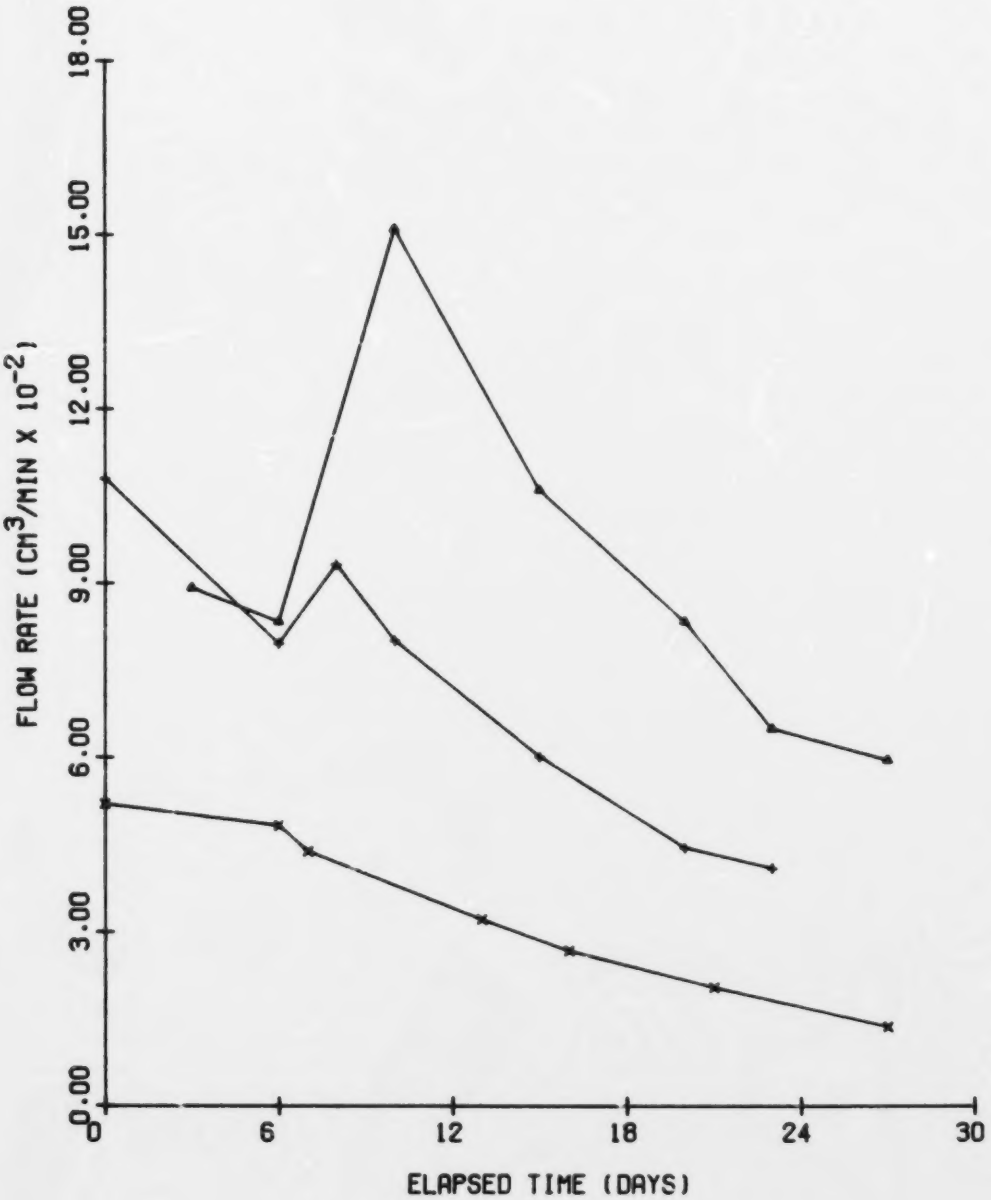

Figure 4.34 Longitudinal flow rates through an oven-dried plug (log scale) observed during dye injection tests, specimen CG5309-31V. Note initial flow rates as high as 10^{-1} cm^3/min.

▲ - ▲ : injection pressure = 4 MPa
\+ - + : injection pressure = 2 MPa
x - x : injection pressure = 1 MPa

BEST COPY AVAILABLE

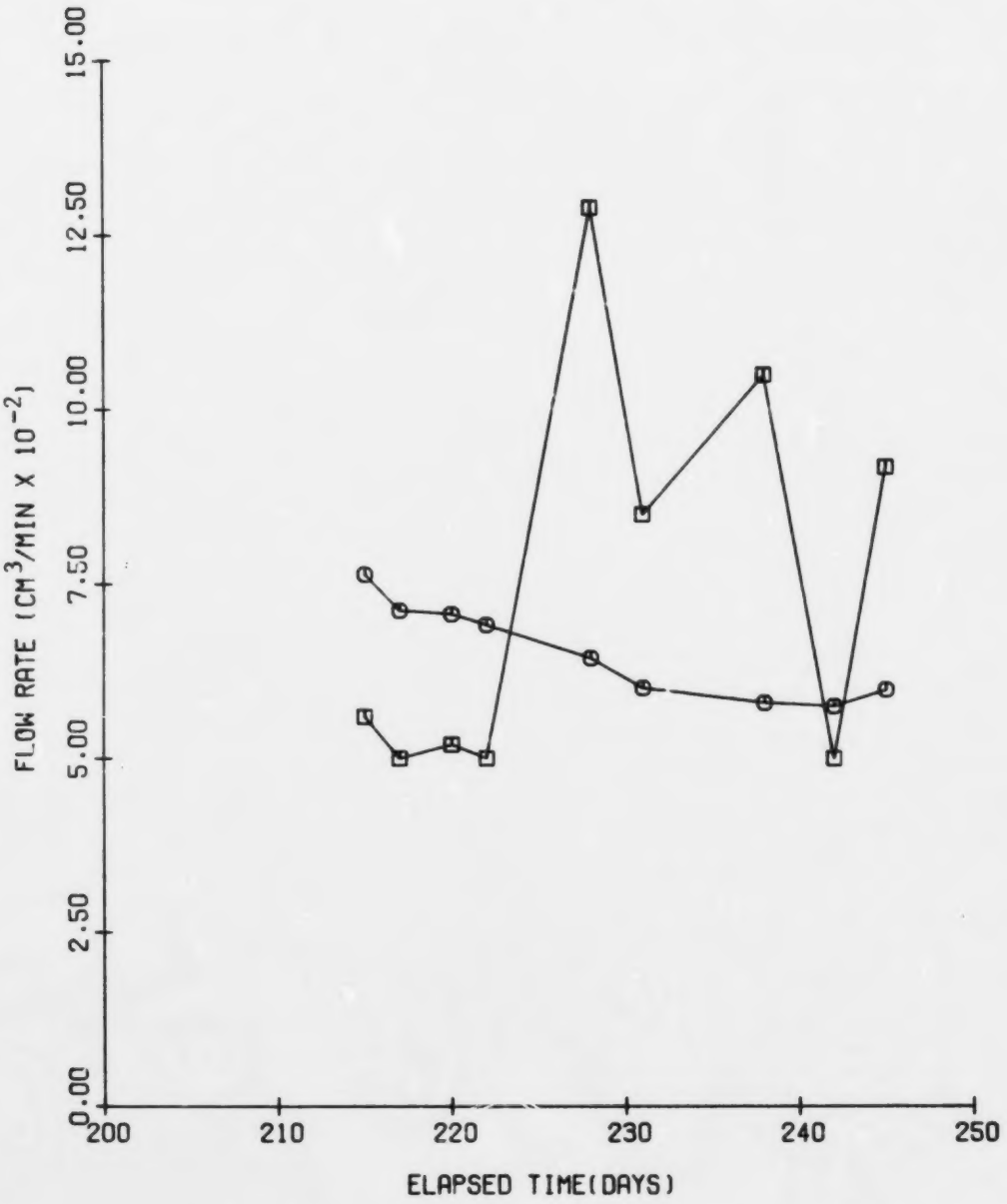

Figure 4.35 Inflow rate and longitudinal outflow rate through a dried-out cement plug during the dye injection test, specimen CG5309-01. Note that the slow decrease of the longitudinal flow rate still continues after eight months of testing. The applied injection pressure was 1.5 MPa.

O - O : outflow rate
□ - □ : inflow rate

BEST COPY AVAILABLE

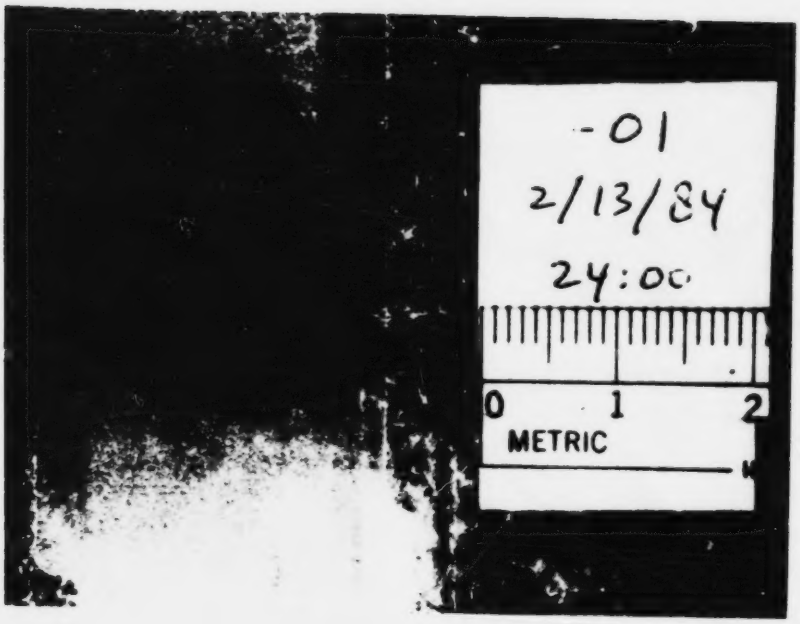

Figure 4.36 Cross-section of a dried-out cement plug in Charcoal granite. Dye traces in the interfacial fissures and in a crack across the body of the plug indicate the preferential flow path. Specimen CG5309-01.

BEST COPY AVAILABLE

CHAPTER FIVE

ANALYSIS AND DISCUSSION OF EXPERIMENTAL RESULTS

5.1 Hydraulic Conductivity Determination

Determining the flow rate during the flow tests is one method of quantifying the sealing performance of the host rock and the cement plug. Flow rate depends on the distance the fluid has to travel in penetrating the seal medium, as well as on the pressure gradient. Since the length of the seals (cement plug, rock bridge) and the injection pressure used during the test are not always the same, hydraulic conductivity is used to quantify and compare the effectiveness of various sealing materials. Hydraulic conductivity, sometimes called the coefficient of permeability or permeability constant (Harr, 1977, p. 93) is independent of distance and has a unit of velocity (L/T). Darcy is another unit of hydraulic conductivity, widely used in the oil industry. One darcy is roughly equal to 10^{-3} cm/s for water at 20°C (Scheidegger, 1963, p. 71, Lambe and Whitman, 1979, p. 287, Freeze and Cherry, 1979, p. 29).

Hydraulic conductivity of the seals can be determined using a solution derived from Darcy's law for one-dimensional flow (Harr, 1962, Freeze and Cherry, 1979). In using Darcy's law, the seals (cement plug, rock bridge) are assumed to be homogeneous porous media. Visual inspection of the wet cement plugs and Charcoal granite specimens suggests that to be the case. These materials are free from dominant macroscopic cracks or joints that may form preferential flow paths. In addition, Darcy's law is valid in these media because of the low velocity of the flow, which assures that the flow is laminar, and the postulated absence of nonhydraulic effects that could complicate flow/pressure relations (Neuzil, 1986). Hydraulic conductivity, K, is a proportionality coefficient that relates the hydraulic gradient, i, and the fluid discharge velocity, v, in the equation:

$$v = Ki \tag{5.1}$$

or

$$v = k\,\gamma/\mu\; dh/dl \tag{5.2}$$

where K is equal to $k\,\gamma/\mu$ and i is equal to dh/dl, the hydraulic head differential with respect to distance. Equations (5.1) and (5.2) show that hydraulic conductivity, K, is a function of both the porous medium and the fluid. It combines the specific or absolute or intrinsic permeability (k) of the porous medium, which has a dimension of area (L^2), and the flow properties of the fluid, i.e. its unit weight (γ) and viscosity (μ).

In terms of quantities obtained directly during a flow test, Darcy's law can be expressed as (Scheidegger, 1963, pp. 69-71, Lambe and Whitman, 1979, p.251):

$$Q/A = K\,(\Delta h/l) \tag{5.3}$$

or

$$K = Ql/(\Delta h)A \tag{5.4}$$

where Q is volumetric flow rate (L^3/T), l is the seal length (L), Δh is the head differential (L), calculated from the injection pressure in the flow tests (1 MPa is equivalent to 10^5 cm of water), and A is the cross-sectional area of the seal (L^2). Equation (5.4) is used to calculate the hydraulic conductivity of the Charcoal granite rock bridge and of the wet cement plugs, based on the experimental results (longitudinal flow rates) given in Chapter 4.

The dried-out cement plugs exhibit preferential flow paths, mainly along the plug/rock interfacial gap (see Chapter 4). A single fissure flow model, rather than Darcy's law for uniform flow through a porous medium, is more appropriate for this condition. The model can be conveniently analyzed by the equivalent parallel plate concept. Laminar flow through individual fissures can be expressed in a form analogous to incompressible viscous flow between smooth parallel plates. Darcy's law can then be applied to determine a coefficient of permeability as a function of an equivalent parallel plate aperture.

An equivalent parallel plate aperture, e, for laminar flow has been computed as (Zeigler, 1976, p. 11; Snow, 1968, p. 79):

$$e = (12\mu q/\gamma i)^{1/3} \tag{5.5}$$

where μ is the dynamic viscosity of the fluid (FT/L^2), q is the volumetric flow rate per unit width of the fissure (L^2/T), γ is the unit weight of the fluid (F/L^3), and i is the hydraulic gradient (L/L).

The hydraulic gradient, i, can be expressed as:

$$i = \Delta P/\gamma l \tag{5.6}$$

where ΔP is the pressure difference between the two ends of the plug (F/L^2) and l is the length of the fissure, i.e. the length of the plug. Since q is the volumetric flow rate, Q, divided by the fissure width, w (which in this case is the circumference of the plug), the equivalent parallel plate aperture or the interfacial gap aperture can be expressed as:

$$e = (12\mu lQ/\Delta Pw)^{1/3} \tag{5.7}$$

which consists of parameters which are known or are measured during the flow tests.

The laminar fissure permeability, K_j, can be computed by:

$$K_j = \gamma e^2/12\mu \qquad (5.8)$$

This expression for K_j replaces K in Darcy's law (equation 5.1) for flow through a single fissure.

The following values are used for the calculation of the interfacial gap aperture, e, and the fissure permeability, K_j (from Blake, 1975, pp. 5.2-5.3):

$$\mu = 1.01 \times 10^{-3} \text{ kg/m-s}$$
$$= 1.01 \times 10^{-2} \text{ poise}$$
$$= 1.01 \times 10^{-7} \text{ N-s/cm}^2$$

$$\rho = 0.9982 \text{ g/cm}^3, \text{ or equivalent to}$$
$$\gamma = 9.79 \times 10^{-3} \text{ N/cm}^3$$

These values are for water at 20°C (68°F), which is slightly below the temperature range measured in the laboratory (Appendix E). The dynamic viscosity and the density of water are assumed to be a good approximation for the values of the water/dye solution used during the last part of the flow testing. During the flow tests, the bottom hole of the specimen is connected to the measuring pipettes, which are at atmospheric pressure. Therefore, the pressure difference ΔP is equal to the gage pressure P. This value, together with the volumetric flow rate, Q, is obtained from experimental data.

Equations (5.7) and (5.8) are used to calculate the interfacial gap aperture and fissure permeability, respectively, of the dried-out cement plug. The calculation assumes that the plug/rock interfacial gap is the sole preferential flow path. This is a good assumption for all specimens with dried-out plugs except one. For specimen CG5309-01, the only specimen which has a crack intersecting its cement plug, this results in an upperbound value of fissure permeability.

It has been shown in Chapter 4 that the flow rate through dried-out cement plugs (and therefore their fissure permeability) decreases with time, especially in the first two months of resaturation. Therefore, a linear relationship between flow velocity, v, and hydraulic gradient, i, (as is the case in laminar flow) is improbable for a series of tests that extends over a long period of time. However, for a shorter period of several flow tests, it can be shown that this relationship is indeed linear. Figure 5.1 shows a plot of volumetric flow rate, Q, vs. pressure difference, ΔP, for specimen CG5309-01, during a ten-day

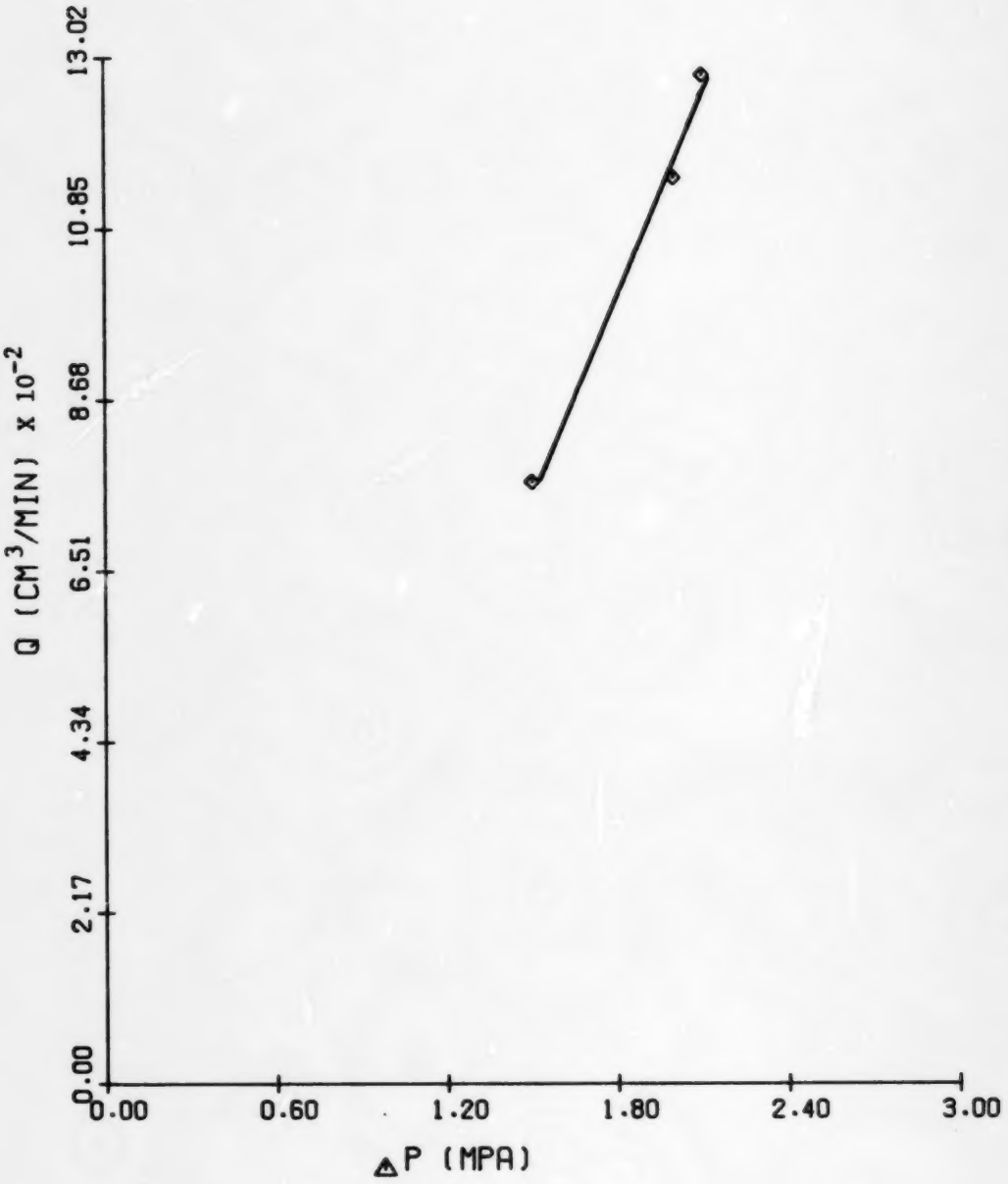

Figure 5.1 Volumetric flow rate, Q, through a dried-out cement plug as a function of pressure difference, ΔP, which is the injection pressure, for specimen CG5309-01. Note the good linearity with $r^2 = 0.99$.

period. This plot exhibits very good linearity with a coefficient of determination, r^2, equal to 0.99. A similar plot is shown in Figure 5.2 for specimen -31V and flow test data obtained on two days. Again the linearity is excellent, with an r^2 value of 1.00. The Q vs. ΔP plot is equivalent to the v vs. i plot, because $v = Q/A$ and $i = \Delta P/\gamma l$ and all the denominators (A, γ, l) are constants.

In the following sections, the hydraulic conductivity results are presented for Charcoal granite, and for wet and dried-out cement plugs. Hydraulic conductivity is plotted for each specimen as a function of time since the first flow testing for that specimen. Hydraulic conductivities of Charcoal granite and wet cement plugs (five specimens) are plotted using the same scale, so they can be compared directly. The hydraulic conductivities of dried-out cement plugs (four specimens) are plotted on a logarithmic scale because they vary by several orders of magnitude.

5.1.1 Hydraulic Conductivity of Charcoal Granite

The hydraulic conductivity of a Charcoal Granite rock bridge (specimen CG5309-04) is given in Figure 5.3. During the nine month testing period, the hydraulic conductivity of Charcoal granite shows a slightly decreasing trend. The values range between 3×10^{-11} and 4×10^{-12} cm/s (3×10^{-8} and 4×10^{-9} darcy). The results indicate a very low permeability intact granite.

5.1.2 Hydraulic Conductivity of Wet Cement Plugs

Figure 5.4 shows the hydraulic conductivity of a wet cement plug (specimen CG5309-06) as a function of time. In eight months of testing, the values vary between 1×10^{-11} and 2×10^{-12} cm/s (1×10^{-8} and 2×10^{-9} darcy), and remain fairly constant with time. The hydraulic conductivity of this plug is slightly lower than that of Charcoal granite, although in the same range.

Figure 5.5 gives the hydraulic conductivity of specimen CG5309-08. During nine months of testing the values fluctuate between 3×10^{-11} and 2×10^{-12} cm/s (3×10^{-8} and 2×10^{-9} darcy). An initial decrease is observed, but in general the values are similar to those of specimen -06.

Figure 5.6 is a plot of hydraulic conductivity versus time for the wet cement seal of specimen CG5309-31V. It shows a decrease in hydraulic conductivity with time. On day 40 the plug length was shortened. When the flow test resumed 20 days later, the hydraulic conductivity jumped up by an order of magnitude, to 3×10^{-8} darcy. As the resaturation process continued, it decreases to a level even lower than the previous values. After more than nine months of testing, the hydraulic conductivity was 4×10^{-10} darcy.

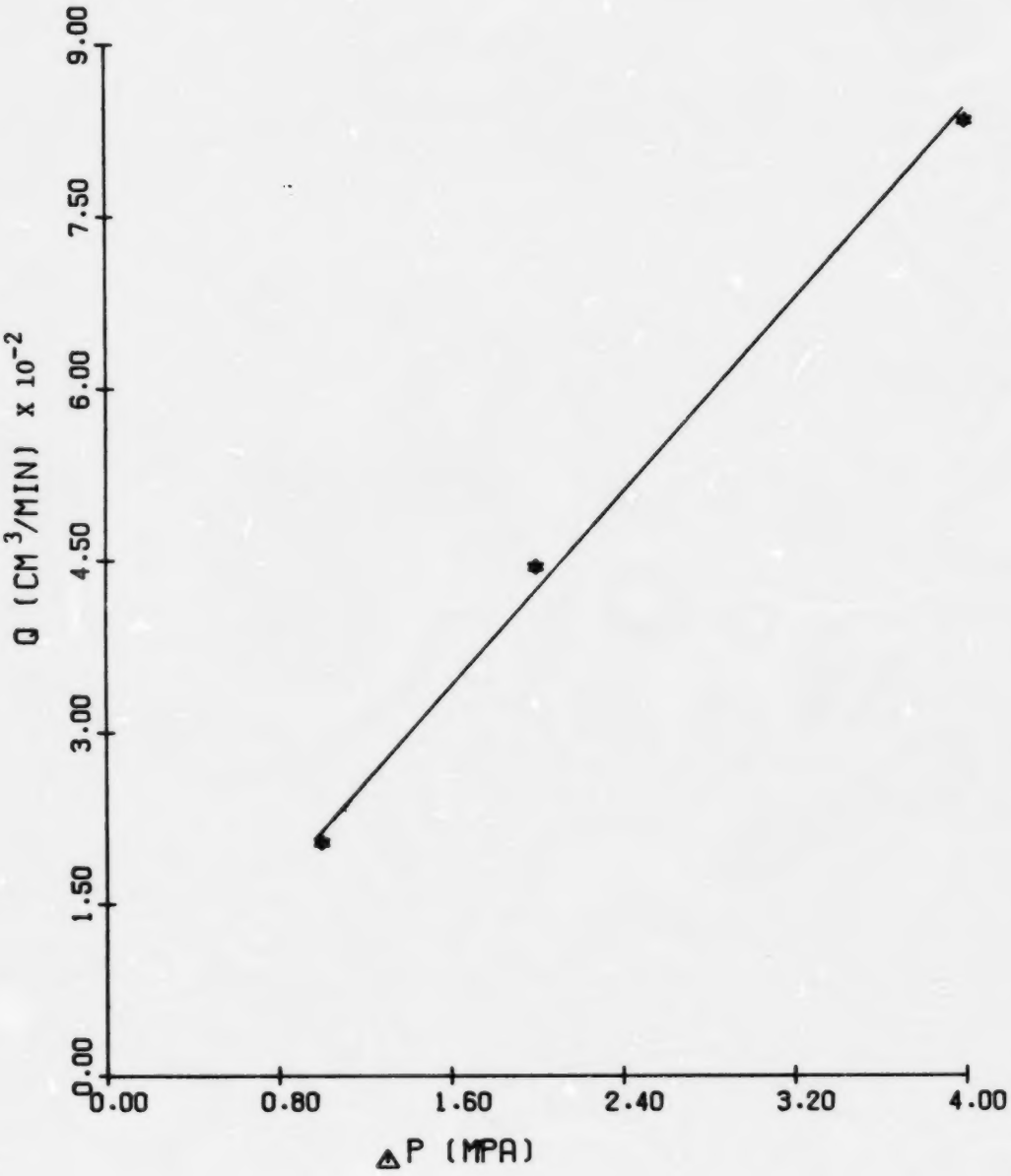

Figure 5.2 Linear relationship of volumetric flow rate, Q, vs. pressure difference, ΔP, for specimen CG5309-31V with oven-dried cement plug. The coefficient of determination $r^2 = 1.00$.

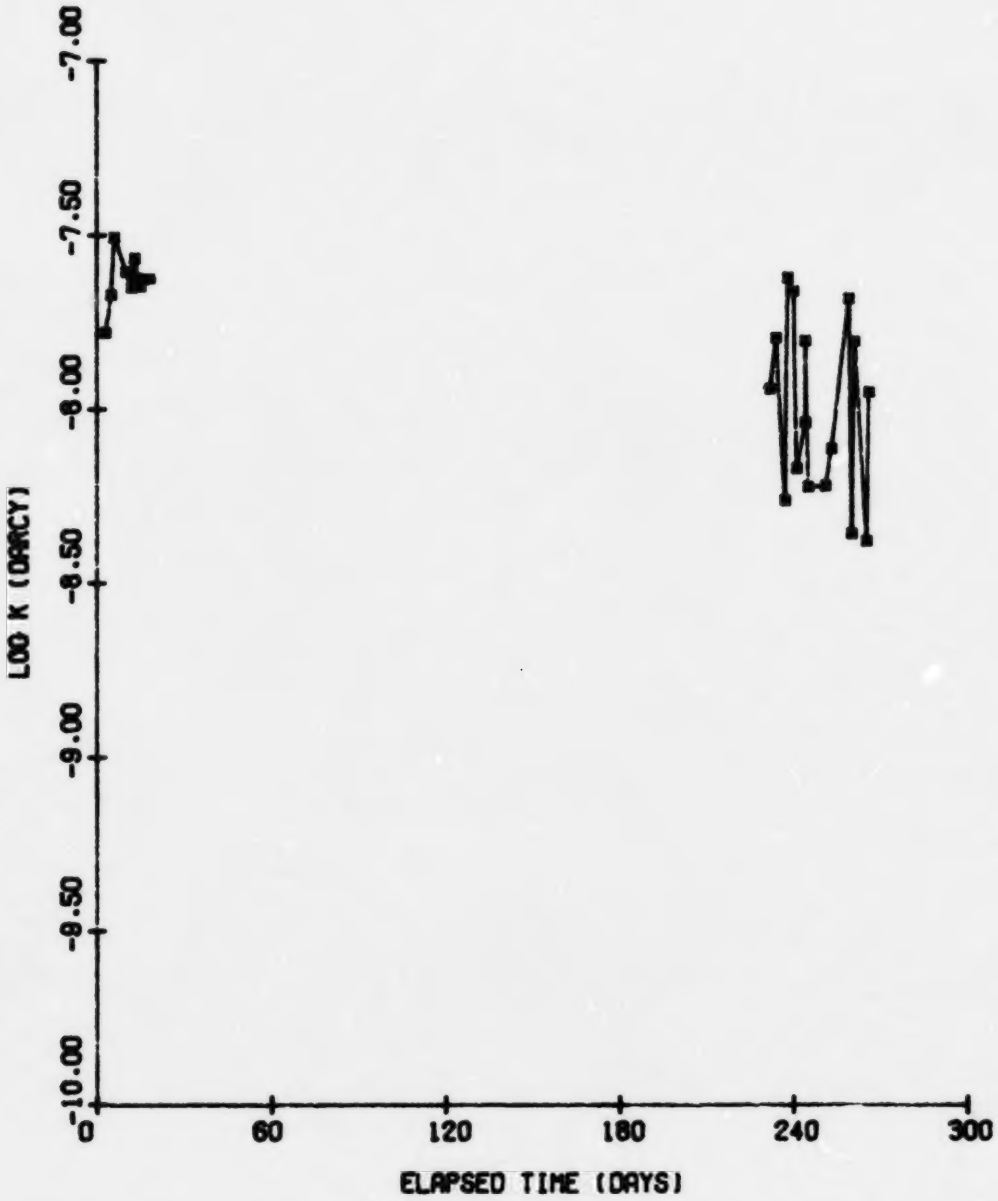

Figure 5.3 Hydraulic conductivity of Charcoal granite rock bridge as a function of time, specimen CG5309-04. Note the low permeability of the rock, in the order of 10^{-8} darcy.

BEST COPY AVAILABLE

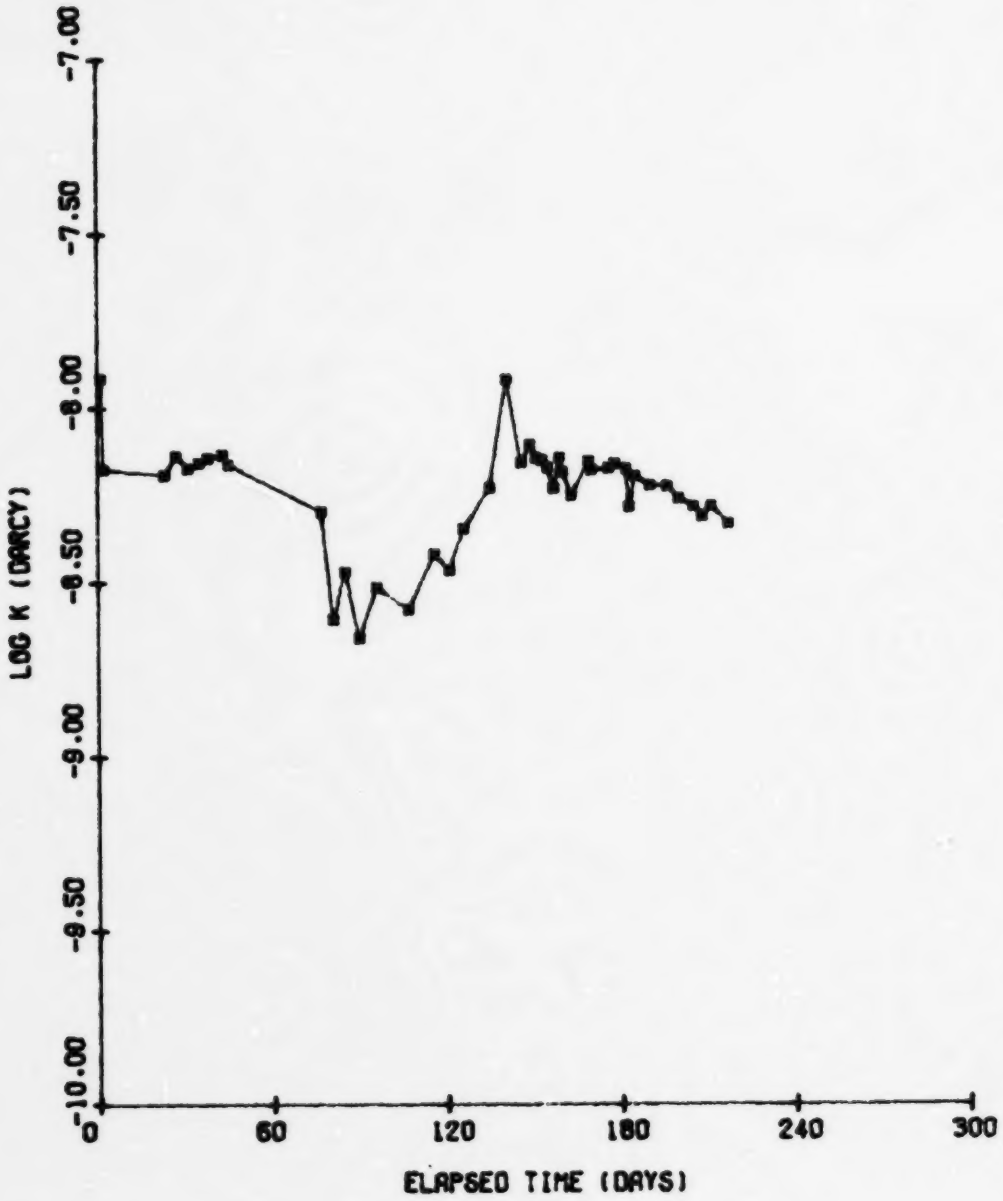

Figure 5.4 Hydraulic conductivity of a wet cement plug in granite as a function of time, specimen CG5309-06. The values are slightly lower than those of Charcoal granite, indicating a good sealing performance.

BEST COPY AVAILABLE

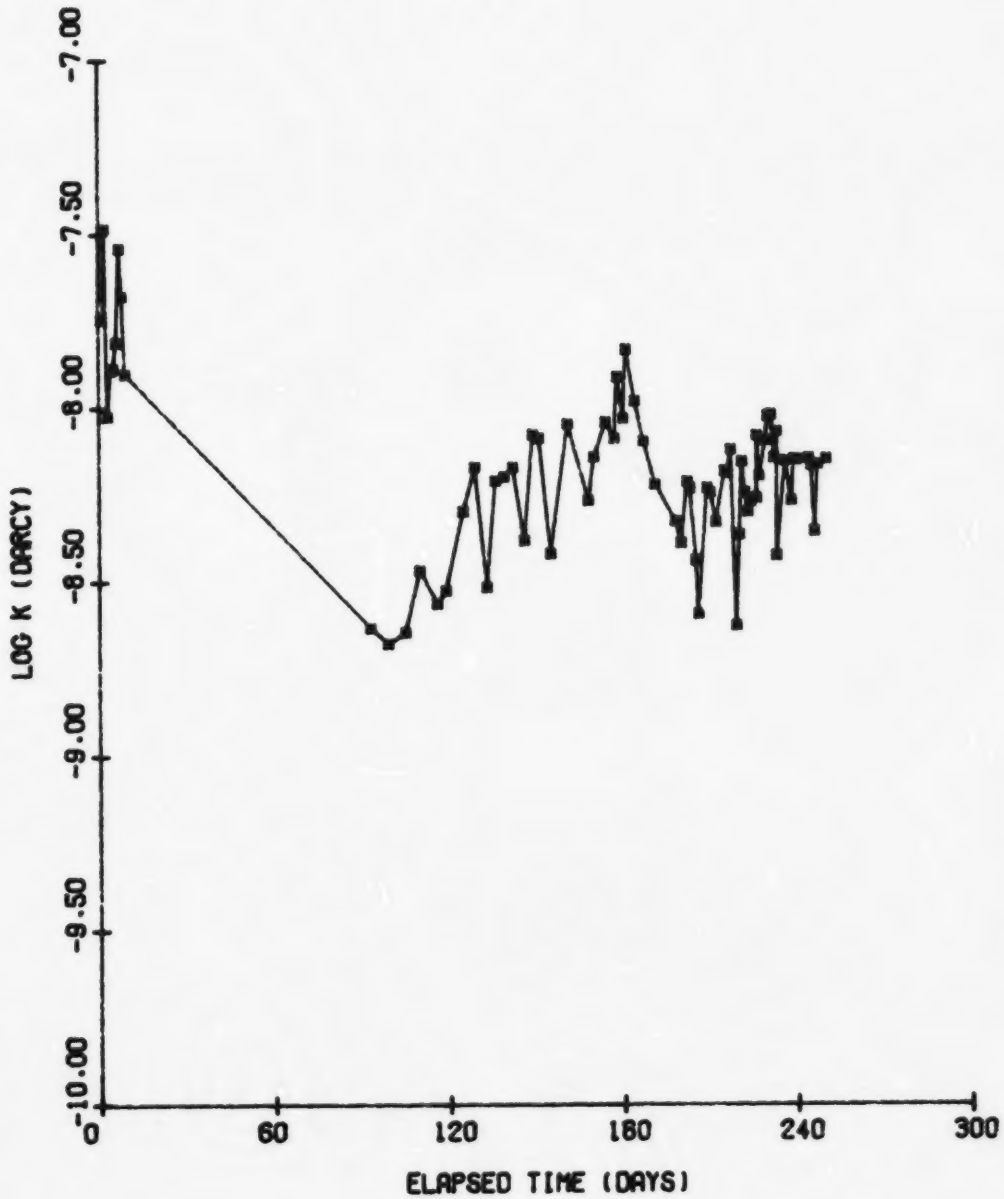

Figure 5.5 Hydraulic conductivity of a wet cement plug in granite as a function of time, specimen CG5309-08. These values are very similar to those for specimen -06

BEST COPY AVAILABLE

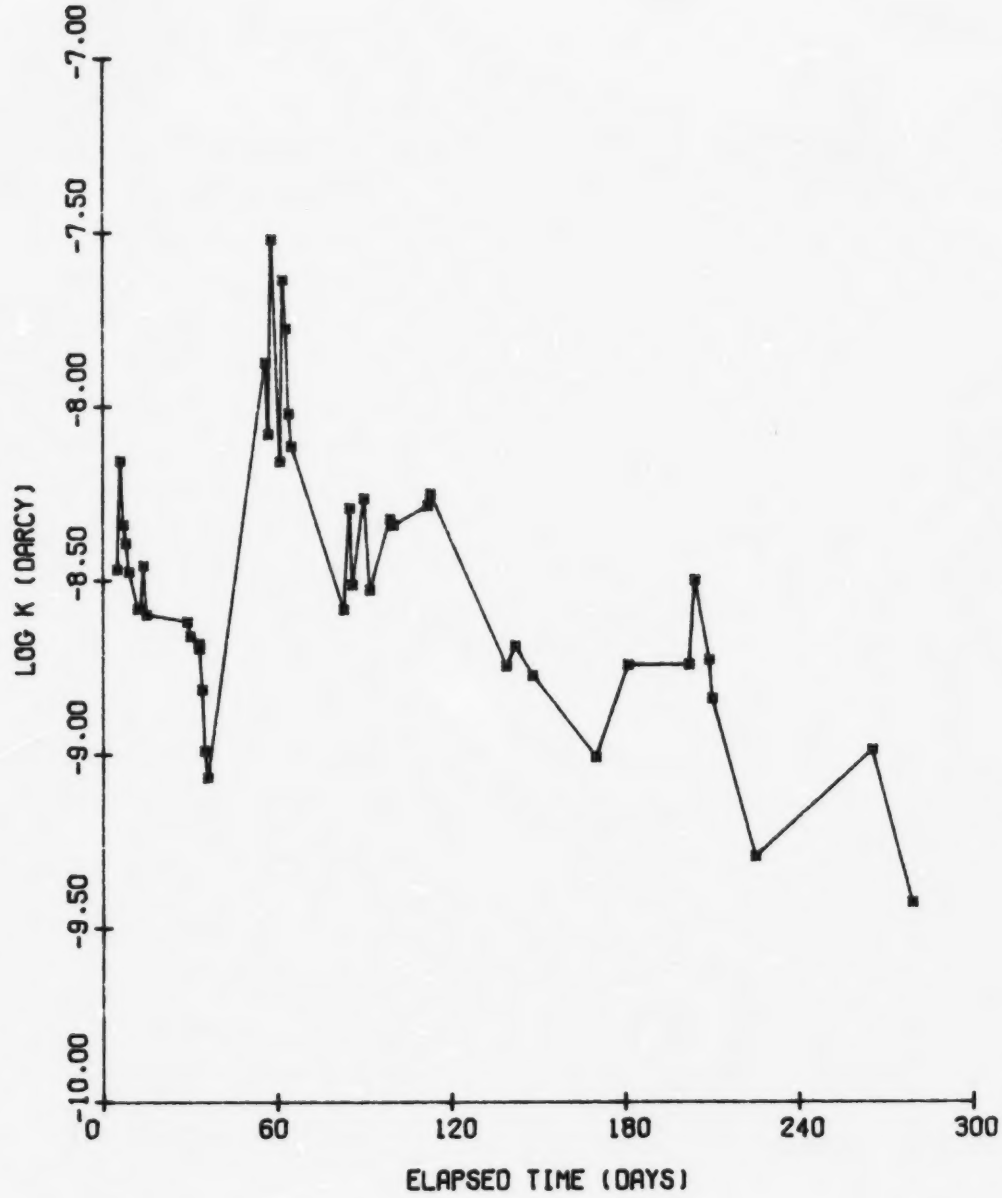

Figure 5.6 Hydraulic conductivity of a wet cement plug in granite as a function of time, specimen CG5309-31V. A decrease in hydraulic conductivity with time is clear. A jump at day 60 occurs when the flow test is restarted after the plug length has been reduced. The final values are an order of magnitude lower than those of samples -06 and -08.

BEST COPY AVAILABLE

Figure 5.7 shows the hydraulic conductivity of the wet cement plug in specimen CG5309-10. In the relatively short testing period (slightly over 40 days) before the specimen failed, the hydraulic conductivity indicates a very low permeability seal, in the same range as that of specimen -31V, between 8×10^{-9} to 5×10^{-10} darcy.

5.1.3 Hydraulic Conductivity of Dried-Out Cement Plugs

Figure 5.8 gives the fissure permeability vs. time for specimen CG5309-01. The cement plug in this specimen was allowed to dry out for seven months prior to flow testing, which results in cement shrinkage and opening up of the plug/rock interface (see Chapter 4). The fissure hydraulic conductivity decreases rapidly during the first two months of testing. It continues to decrease, at a slower rate, until the test is concluded eight months after it began. This decrease of fissure permeability from 2×10^{-2} to 3×10^{-4} cm/s (20 to 0.35 darcy) indicates cement expansion due to resaturation. The interfacial gap aperture decreases from 1.6×10^{-3} cm in the beginning to 2×10^{-4} cm at the conclusion of the test.

Figure 5.9 shows fissure permeability as a function of time for specimen CG5309-28. Its cement plug was left to dry for three months at room temperature before flow testing was initiated. As in specimen -01, an initial rapid decrease of fissure permeability during the first two months is followed by a much slower decrease, which continues until the sixth month, when the test is stopped. During this period, fissure permeability decreased from 1×10^{-3} to 1×10^{-5} cm/s (0.95 to 0.012 darcy). This is an order of magnitude lower than the fissure permeability of specimen -01. However, these values are much higher than the hydraulic conductivity of wet cement plugs, by seven orders of magnitude. The interfacial gap aperture decreased from 3.4×10^{-4} to 4×10^{-5} cm, indicating cement expansion.

Figure 5.9 also shows a fluctuation of fissure permeabilities, especially during the early period of plug resaturation. The upper range values are obtained at high injection pressure (4 MPa), the lower range at lower injection pressure (2 and 1 MPa). Adisoma and Daemen (1984) have calculated the permeability of this specimen using Darcy's law (equation 5.4) and the result is reproduced in Figure 5.10. The values are roughly five orders of magnitude less than the fissure permeability (equation 5.8) given in Figure 5.9. The permeability values in Figure 5.10 are plotted for various injection pressures. Higher injection pressure results in higher permeability, especially during the earlier period of the flow tests when the flow rate is high. Apparently, at the high flow rates encountered in dried-out cement plugs, there is an increasing dependency of permeability on injection pressure. A possible explanation is that the lateral expansion of the rock cylinder is greater than the lateral expansion of the cement plug, especially at higher internal pressures (Appendix G). This causes the interfacial gap to open up more at higher pressures, which results in higher permeabilities. As the flow rate decreases

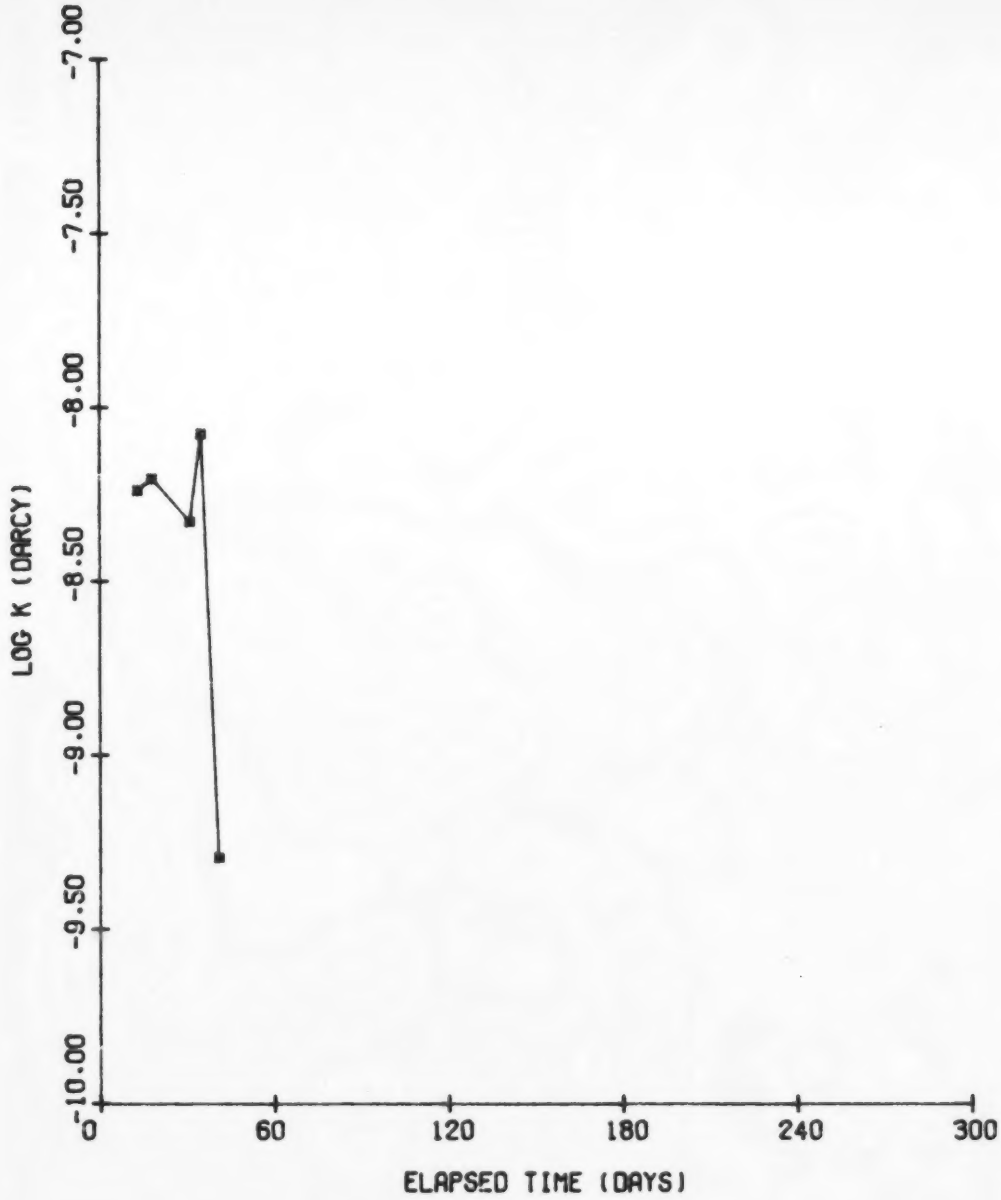

Figure 5.7 Hydraulic conductivity of a wet cement plug in granite as a function of time, specimen CG5309-10. The values indicate a very low permeability seal, in the same range as that of specimen -31V.

BEST COPY AVAILABLE

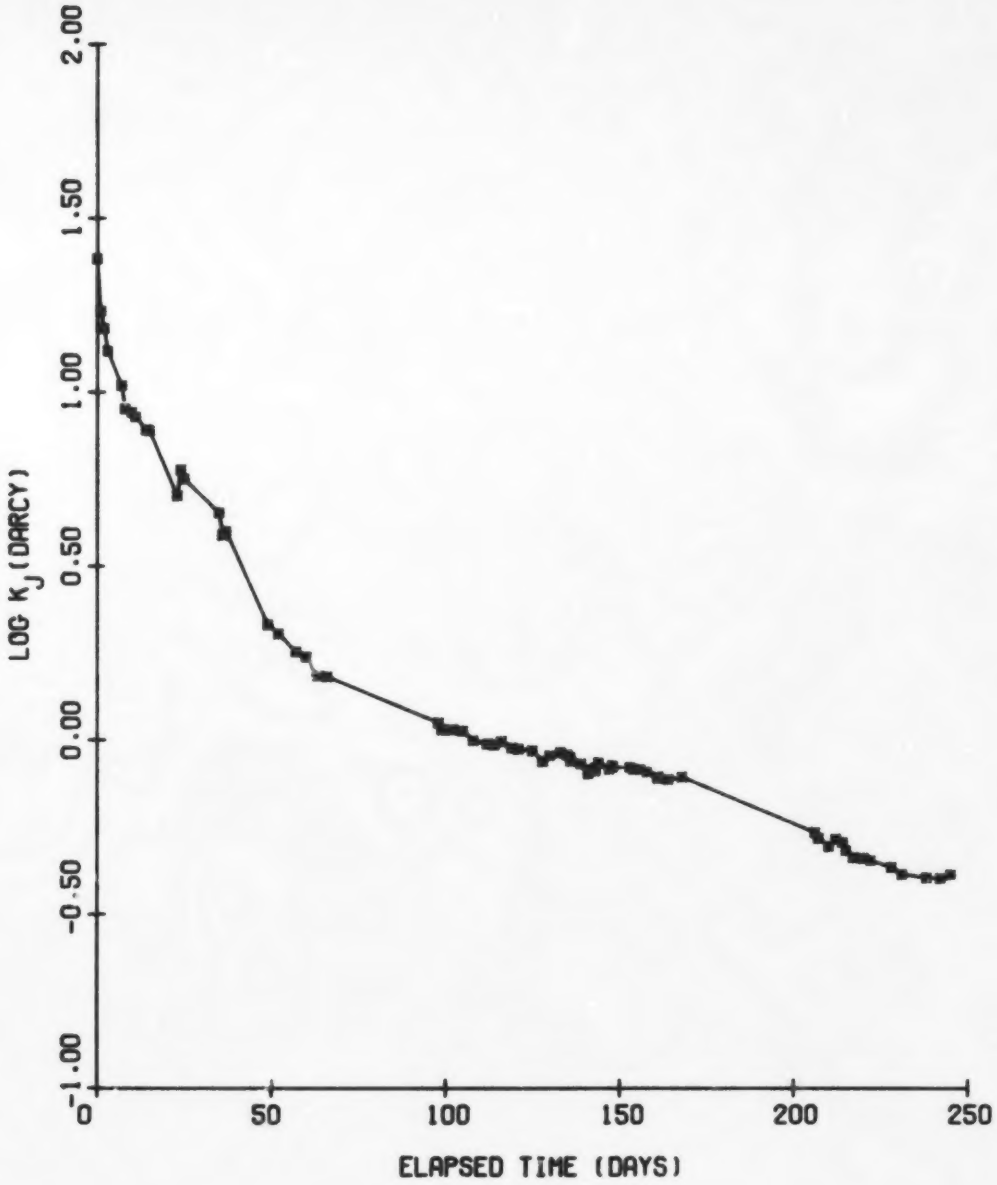

Figure 5.8 Hydraulic conductivity of a dried-out cement plug in granite as a function of time, specimen CG5309-01. Flow occurs through the plug/rock interface and through a crack in the plug body, which explains the high permeability. The seal performance is degraded severely as a result of seven months of drying at room temperature.

BEST COPY AVAILABLE

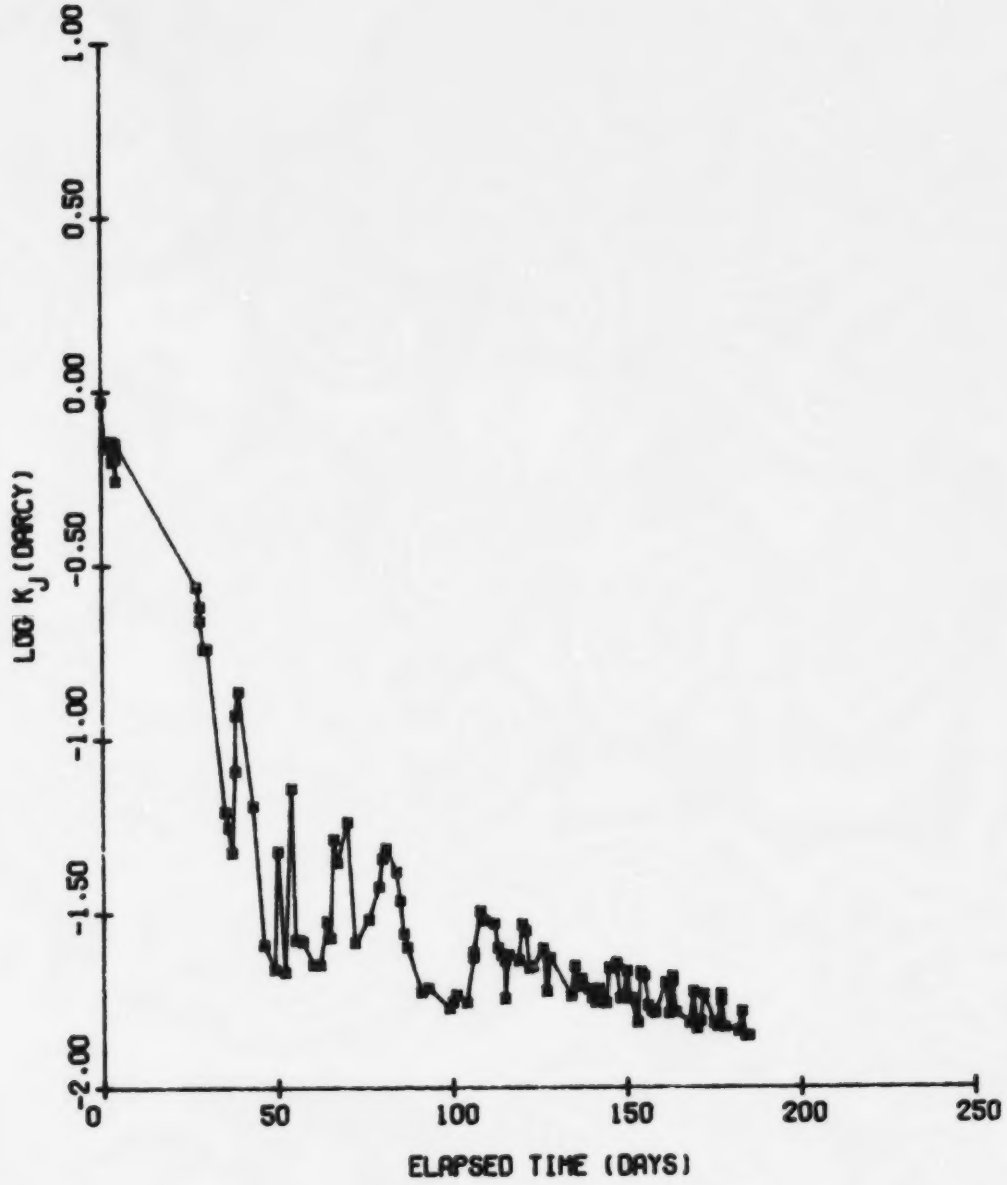

Figure 5.9 Hydraulic conductivity of a dried-out cement plug in granite as a function of time, specimen CG5309-28. The fluctuation in values is due to the dependence of hydraulic conductivity on injection pressure at high flow rates. The permeability decrease with time is very similar to that of specimen -01, but the permeabilities are one to two orders of magnitude lower. The sample was dried for three months, at room temperature.

BEST COPY AVAILABLE

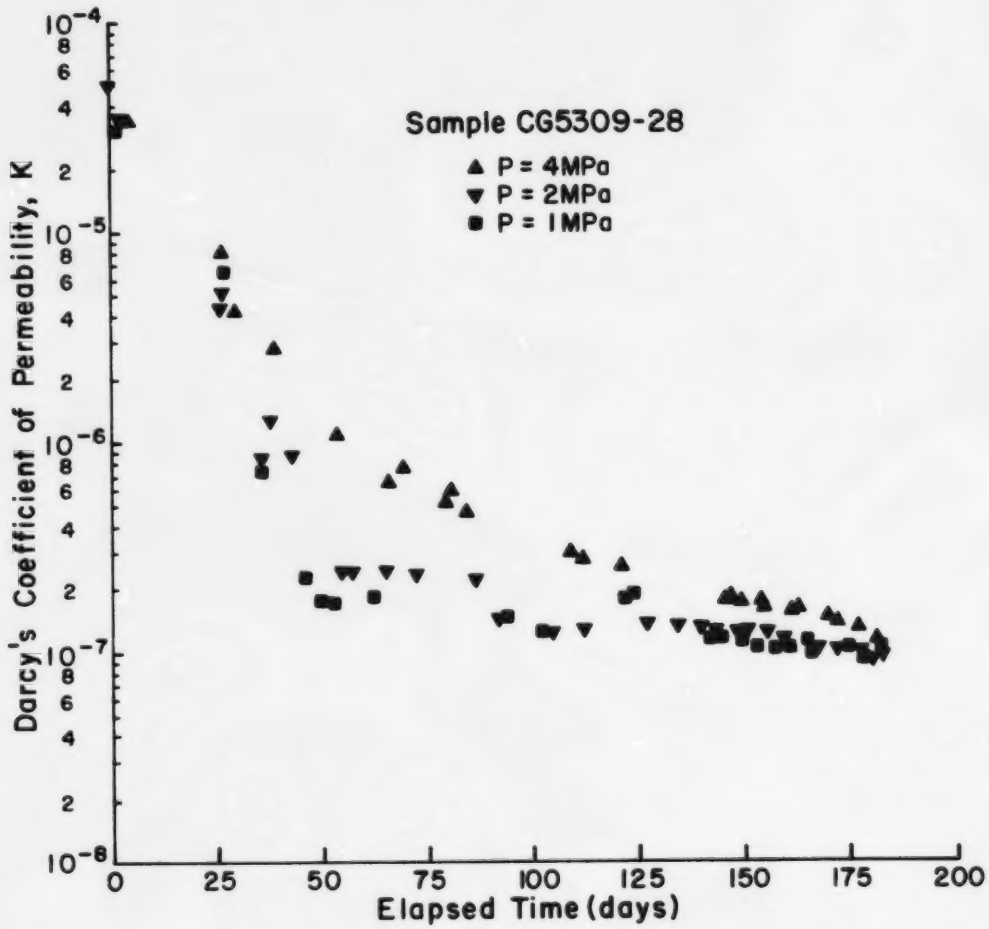

Figure 5.10 Dried-out cement plug permeability calculated using Darcy's law for flow through a porous medium. Higher injection pressure results in higher permeability. This may explain the fluctuation of fissure permeability values in Figure 5.9 (from Adisoma and Daemen, 1984).

BEST COPY AVAILABLE

with time, the permeability becomes less dependent on injection pressure (Figures 5.9 and 5.10).

Figure 5.11 is a plot of fissure permeability vs. time for specimen CG5309-21. The condition of its cement plug is very similar to that of specimen -28. This specimen failed after less than a month of flow testing. The fissure permeability for this specimen is also similar to that of specimen -28. It decreased from 1.5 darcy in the beginning of the test to 0.2 darcy just before the specimen hydraulically fractured 21 days later.

Figure 5.12 shows a fissure permeability vs. time plot of specimen CG5309-31V with an oven-dried (5 days at 90°C) cement plug. During four weeks of flow testing, the fissure permeability decreases from 0.5 to 0.2 darcy, which is in the same range as for specimens -21 and -28. This is nine orders of magnitude higher than the hydraulic conductivity of the plug prior to drying (Figure 5.6). The fissure permeability might have continued to decrease had the flow testing been extended. All indications from specimen -28 and -01 show, however, that the further decrease probably will not be more than an order of magnitude.

5.1.4 Summary of Hydraulic Conductivities

The hydraulic conductivities of Charcoal granite, and of wet and dried-out cement plugs are summarized in Table 5.1. The values for Charcoal granite vary from 30 to 4 nanodarcy. Wet cement plugs are less permeable, with hydraulic conductivity between 30 to 0.4 nanodarcy. Dried-out cement plugs indicate a very high laminar fissure permeability, in the range of 20 to 0.012 darcy.

5.2 Comparison With Other Results

5.2.1 Results in Granite

Brace et al. (1968) describe flow experiments on Westerly granite. Their transient pulse tests show the effect of confining pressure on permeability. As confining pressure increases from 50 to 4000 bars (5 to 400 MPa), permeability decreases from 350 to 4 nanodarcy. These results fall in the same range as the Charcoal granite permeability listed in Table 5.1.

South and Daemen (1986) and Cobb and Daemen (1982) used Charcoal granite in laboratory experiments. South and Daemen performed radial permeameter experiments with cement-plugged Charcoal granite cylinders, as well as cylinders of Oracle granite, Catalina granite, Sentinel Gap basalt, and Topopah Spring tuff. Cobb and Daemen tested rectangular blocks of cement-plugged Charcoal granite specimens in a polyaxial permeameter. Moreover, they all tested the same type of cement used in this study. Both radial and polyaxial permeameter specimens have different loading conditions than specimens in this experiment. Their results indicate, however, that water injection pressure is still the main factor controlling the flow rate.

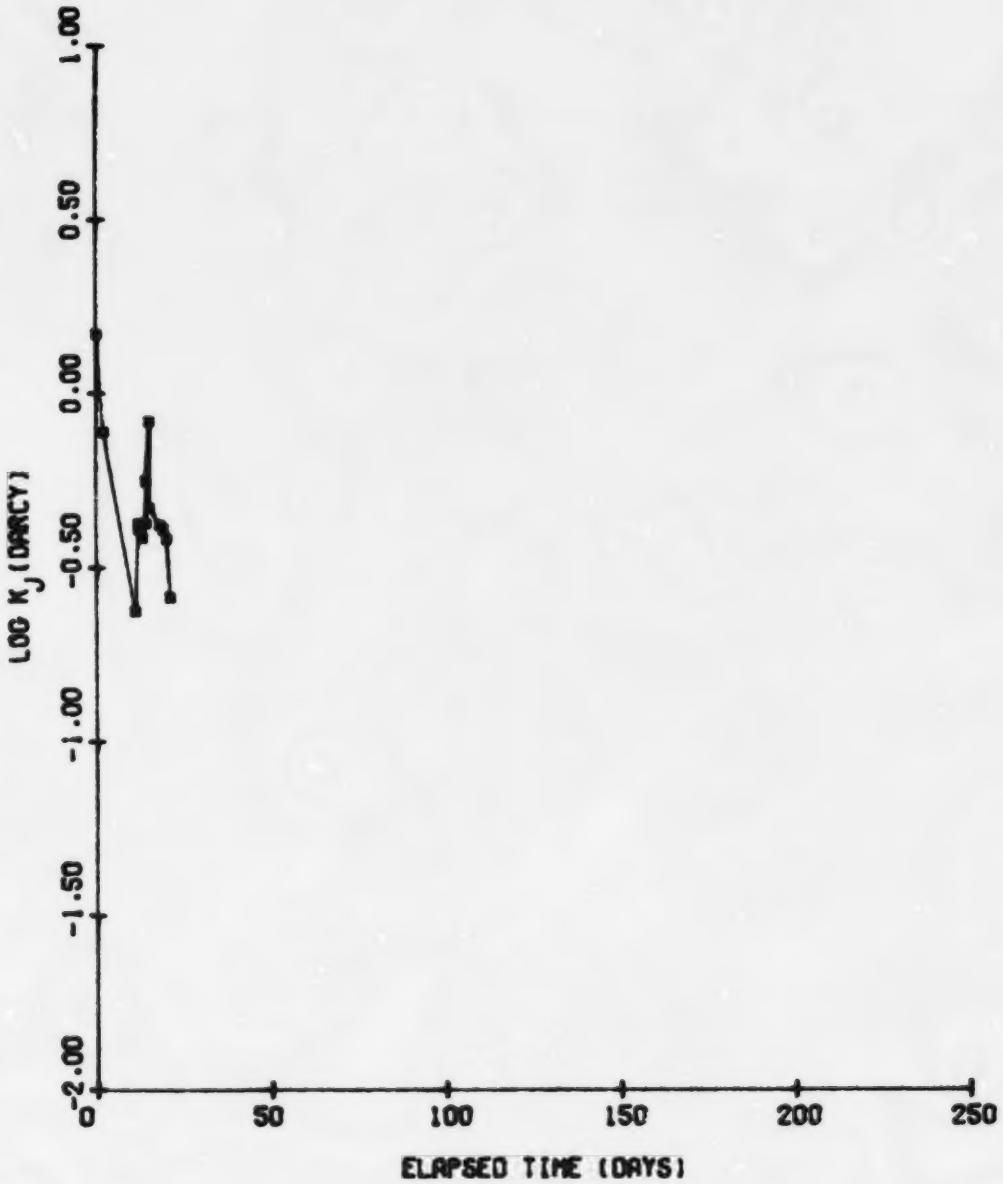

Figure 5.11 Hydraulic conductivity of a dried-out cement plug in granite as a function of time, specimen CG5309-21. The fissure permeability as well as its initial decrease are very similar to the corresponding values of specimen -28. The specimen was dried for three months at room temperature; it failed (hydraulically fractured) during flow testing on day 21.

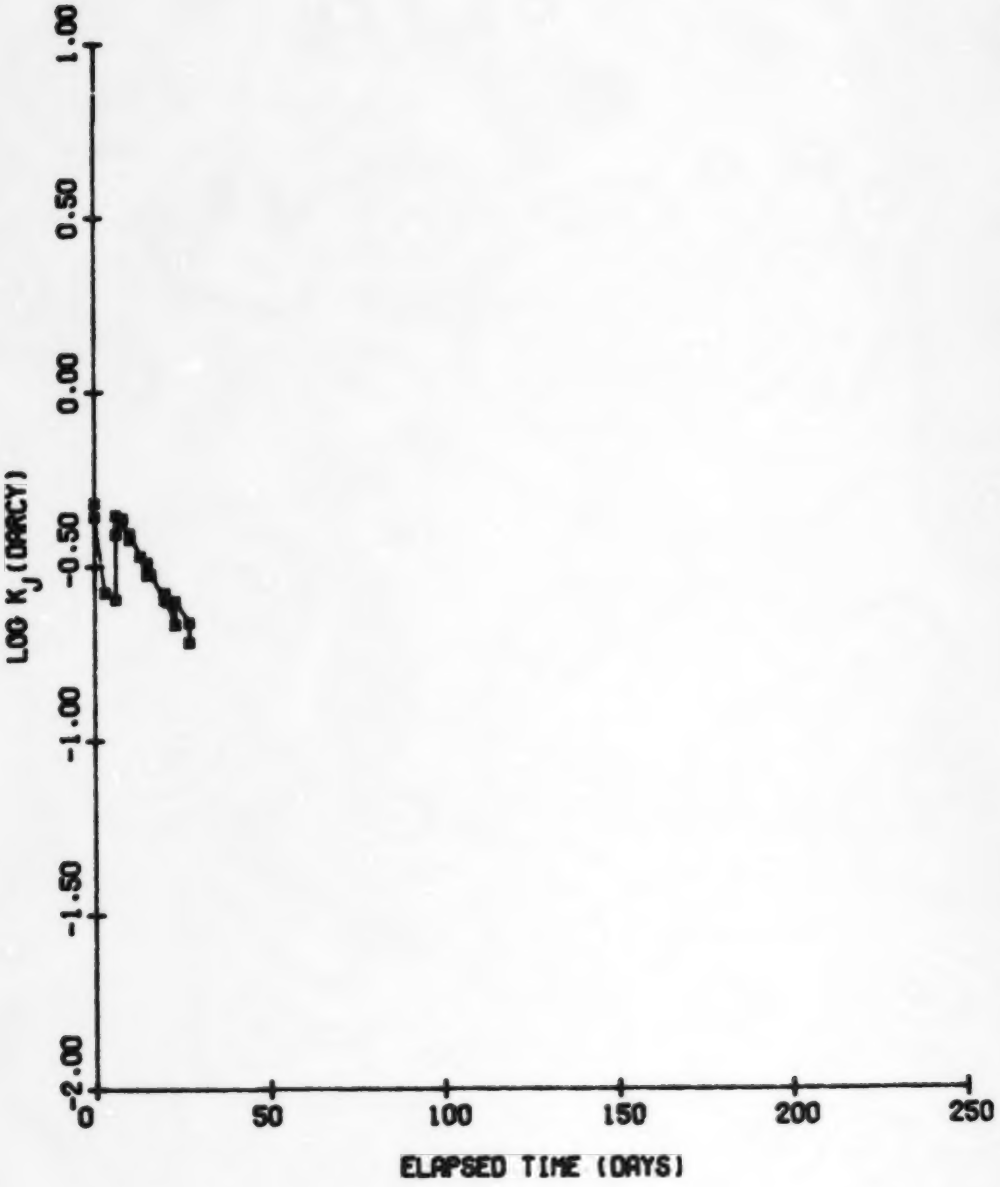

Figure 5.12 Hydraulic conductivity of an oven-dried cement plug in granite as a function of time, specimen CG5309-31V. Short-term drying of cement plugs at higher temperature has the same effect in degrading seal performance as drying for longer times at ambient temperature. Hydraulic conductivity values are similar to those of specimen -28. Drying period was five days at 90°C.

BEST COPY AVAILABLE

Table 5.1 Summary of Hydraulic Conductivities

Specimen #	Type	Hydraulic Conductivity (darcy)	Notes
CG5309-04	Rock bridge	$30x10^{-9}$ to $4x10^{-9}$	Flow testing for 266 days
CG5309-06	Wet cement plug	$10x10^{-9}$ to $2x10^{-9}$	Flow testing for 217 days
CG5309-08	Wet cement plug	$30x10^{-9}$ to $2x10^{-9}$	Flow testing for 250 days
CG5309-31V	Wet cement plug	$30x10^{-9}$ to $0.4x10^{-9}$	Flow testing for 279 days
CG5309-10	Wet cement plug	$8x10^{-9}$ to $0.5x10^{-9}$	Flow testing for 41 days
CG5309-01	Dried-out cement plug	20 to 0.35	Drying: 7 months at room temp. Flow test 245 days
CG5309-28	Dried-out cement plug	0.95 to 0.012	Drying: 3 months at room temp. Flow test 185 days
CG5309-21	Dried-out cement plug	1.5 to 0.2	Drying: 3 months at room temp. Flow test 21 days
CG5309-31V	Oven-dried cement plug	0.5 to 0.2	Drying: 5 days at $90^{o}C$ Flow test 27 days

South and Daemen (1986, p. 11) give a range of 85 to 52 nanodarcy for the permeability of Charcoal granite. They also give the permeability of an intact specimen of Oracle granite as 9 nanodarcy. These values compare favorably with the range of permeabilities obtained here for intact Charcoal granite (Table 5.1). The results for Catalina granite are given as flow rate only (p. 177). A calculation based on this value indicates a permeability of 1.25 microdarcy for Catalina granite. This is roughly twenty times more permeable than intact Charcoal granite, possibly due to microfractures in the Catalina granite. The appearance of slightly higher values from the radial permeameter study is expected, since no separation is made there between the longitudinal flow through the seal (rock bridge) and the peripheral flow through the rock surrounding the seal. The permeabilities in this study (Table 5.1) are based purely on the longitudinal flow through the seal or rock bridge.

Limited experimental data by Cobb and Daemen (1982, pp. 108-109) indicate a permeability range of 7×10^{-11} to 3.7×10^{-12} cm/s (roughly 70 to 3.7 nanodarcy) for Charcoal granite. These values are in agreement with results of specimen CG5309-04 in Table 5.1. The experiments used an outflow collection system that separated the longitudinal and the peripheral flows, similar to the one used here.

5.2.2 Results for Wet Cement Plugs

Measurements by South and Daemen (1986, p. 11) indicate that wet cement seals tested in Charcoal granite are less permeable than the rock. Their results give plug permeabilities in the same range as those of Table 5.1. Results from Catalina granite (p. 177) also show that the flow rate through cement plugs is less than through the rock. Permeability calculations from this outflow rate using equation (5.4) result in values between 1.25 and 0.56 microdarcy for wet cement seals in Catalina granite. The high value (compared to plug permeability in Charcoal granite) is thought to result from the high permeability of the Catalina granite immediately surrounding the cement plug (see previous section). As explained previously, the (low) longitudinal flow through the cement plug and the (much higher) peripheral flow through the Catalina granite are not collected separately.

Cobb and Daemen (1982, pp. 108-109) obtained a range of wet cement plug permeabilities from 6.3×10^{-10} to 1.3×10^{-11} cm/s (630 to 13 nanodarcy). The lower range is in the same order of magnitude as those in Table 5.1. The upper range is an order of magnitude higher.

5.2.3 Results in Dried-Out Cement Plugs

One specimen tested by Cobb and Daemen (1982, p. 109) shows a plug permeability between 5.8×10^{-9} to 1×10^{-9} cm/s or 5.8 to 1 microdarcy, calculated using Darcy's law (equation 5.4). This is two orders of magnitude higher than their previous results. Upon close examination, this particular specimen exhibits a steady decrease of outflow rate with time (Cobb and Daemen, 1982, p. 69). This is typical

of a dried-out cement plug, and indicates that the actual permeability would be much higher if calculated by equation (5.8) for flow along the plug/rock interface.

South and Daemen (1986, pp. 164-167) tested a dried-out cement seal within a Sentinel Gap basalt cylinder. The specimen was oven-dried for 42 days at 54°C. (The initial plug permeability, before drying, was between 60 to 10 nanodarcy). Upon resaturation, plug permeability increases to an initial value of 0.19 millidarcy, and eventually levels off at 2.4 microdarcy. Their calculation is based on Darcy's law for one-dimensional flow through a porous medium (equation 5.4), which may not be correct if preferential flow paths exist. Recalculation for laminar fissure permeability (equation 5.8) gives a value of 2.1 darcy for the first day of the flow test. The permeability decreases rapidly with time and levels off at 0.12 darcy on day 44.

A detailed look at the flow test record for that specimen reveals that resaturation has started 16 days before the specimen is flow tested (South and Daemen, 1986, Table A.4). This suggests a typical phenomenon in a dried-out cement plug: a rapid flow decrease due to the combined effects of resaturation and of cement expansion upon resaturation, and a leveling-off in flow rate (permeability) after about two months. (The fissure permeability stays constant at 0.12 darcy until day 80, when the flow test was stopped). The initial permeability after oven drying (at the beginning of resaturation) is likely to be higher than 2.1 darcy, the permeability at the sixteenth day of resaturation. The permeability of this oven-dried specimen is between those of specimens CG5309-01 and -28 (Table 5.1).

5.2.4 A Comparison with Published Cement and Concrete Permeabilities

A number of results have been reported for cement and concrete permeabilities. It is difficult to make detailed comparisons, because of the numerous variables involved. For example, as pointed out by Pomeroy (1986), "All too often concrete comparisons are based on the result of 28-day tests on continuously wet-cured samples". Pomeroy illustrates the point by quoting results obtained by Lawrence (1984) that show an (oxygen) permeability increase by nearly an order of magnitude for samples cured moist for only 12 hours compared to samples cured moist for 72 hours. Because such variations are not uncommon, permeabilities of cementitious materials preferably should be listed only together with a comprehensive detailed discussion of mix, preparation, curing, aging, and testing conditions. Such a comprehensive survey, although unquestionably of potential value for sealing license application reviews, would be well beyond the scope of this report. The brief overview presented here, therefore, is intended only to provide what may be considered typical order of magnitude values.

Koplik et al. (1979, p. 3-22), in an early report to the U.S. Nuclear Regulatory Commission, quote permeabilities of typical seal materials obtained by Eilers (1973) on the order of 5×10^{-9} to 2×10^{-10} cm/s for small samples aged for three days. They quote results from Eilers (1974) on cement samples cored from the AEC No. 1 Well at Lyons,

Kansas, as giving 7×10^{-9} to 1×10^{-9} cm/s, and results from Rennick et al. (1977) for three cement grouts as being in the range from 4×10^{-9} to 1.4×10^{-10} cm/s, with the lower value determined for an expansive cement.

Coons et al. (1982, p. 23) in a comprehensive evaluation of the applicability of polymer concrete for repository sealing cite a characteristic permeability for cement-based concrete as from less than 0.01 to 1 md (approximately from less than 10^{-8} to 10^{-6} cm/s) from a widely quoted reference by Mather (1967).

Taylor et al. (1980, Section 5.5) performed permeability tests on a series of cement grouts and concretes selected for potential borehole sealing use at BWIP. Results fell in the range from 1×10^{-9} to 10×10^{-9} cm/s. Permeability tests were performed on sanded cement grout and concrete installed in boreholes in basalt, and subjected to fairly complex curing sequences.

Anttonen et al. (1980, p. 3-181) use values of 10^{-8} and 10^{-9} cm/s for the plug permeability in their sensitivity analysis of flow through a seal zone, on the basis that both values fall within the range of permeabilities for concrete.

Gulick et al. (1980b, pp. 23-24, 39-40, 84) report a series of permeability experiments on grouts designed and, for some, installed and tested in evaporite and associated sedimentary formations. This includes tests on cores from plugs installed at great depths, or formed after having been pumped down the hole and recirculated, as well as various curing and aging sequences and durations. Most results of water and brine flow tests are in the range of 1 to 7 microdarcies (10^{-9} to 7×10^{-9} cm/s), with several results falling well below this range, and with a general trend of decreasing hydraulic conductivity with time for most of the grout mixes. Air permeabilities tend to be one to two orders of magnitude higher, and show marked, although erratic, direction variations (horizontal vs. vertical).

Three series of permeability tests on grouts prepared for the Bell Canyon Test (saline environment) are reported by Gulick et al., 1980c. One test measured a freshwater permeability of 10 microdarcies (10^{-8} cm/s) for a specimen cured in water, 190 microdarcies (1.9×10^{-7} cm/s) for a specimen cured in air (Gulick et al., 1980c, p. 43). A second grout showed permeabilities of 0.2 microdarcies (2×10^{-9} cm/s) or less when tested in a steel cylinder, and about 0.2 to 20 microdarcies when tested in anhydrite cylinders, and as a function of curing conditions and time (see also Roy and Burns, 1982). Some samples leaked severely along the interface (pp. 23-24; 54-56). A third series of tests (described more completely in Moore et al., 1979b) yielded permeabilities ranging from 30 millidarcies (3×10^{-5} cm/s) to 0.5 nanodarcy (0.5×10^{-12} cm/s).

Earlier reports by Moore et al. (1979a, p. 50) and McDaniel (1980) stress the dominant influence exerted by various drying procedures on the permeability of cementitious grout, and illustrate this observation with results that differ by three orders of magnitude (gas permeabilities in the 8×10^{-8} to 1.3×10^{-5} darcy range). Preliminary investigations showed excellent reproducibility of gas permeabilities on identically prepared samples, and about two orders of magnitude smaller water permeability for a 78 microdarcy (7.8×10^{-8} cm/s) measurement.

McDaniel (1980) describes permeability tests on various mixtures of three cement types, four fly ashes, sand, salt and water. Cement grouts were cured for 91 days at room temperature, then dried at 100°C. Neat cement paste permeabilities ranged from 2.3×10^{-4} to 8.8×10^{-5} darcy (2.3×10^{-7} to 8.8×10^{-8} cm/s). Nitrogen permeability of mortar (sanded) samples ranged from 4×10^{-6} to 1.6×10^{-4} darcy (4×10^{-9} to 1.6×10^{-7} cm/s). The addition of fly ash reduced the neat cement permeabilities to the 6.8×10^{-5} to 8.5×10^{-6} darcy range, that of the mortars to the 8.5×10^{-6} to 1.3×10^{-4} darcy range. The addition of 10 to 30% salt to the mortars reduced the permeability to the 6.3×10^{-7} to 4.8×10^{-8} darcy (6.3×10^{-10} to 4.8×10^{-11} cm/s) range. Flow tests on fly ash containing mortars installed in 1.59 cm diameter holes in four rock types showed Klinkenberg corrected nitrogen permeabilities from 5.4×10^{-5} to 9.0×10^{-8} darcy, distilled water permeabilities from 3×10^{-5} to less than 10^{-8} darcy. McDaniel (1980, p. 17) points out that drying of plugged rock samples caused interface separation, and extremely high permeability values. Gulick et al. (1980c, pp. 5, 35) also mention drastic flow increases along rock-plug interfaces for some cement grout plugs subjected to drying. Rhoderick and Buck (1981) report clearly visible gap openings between cementitious borehole plugs and the surrounding anhydrite in which they were installed. The swelling cement plugs were installed in anhydrite core constrained in steel pipe. Severe vacuum drying resulted in rapid (overnight) separation between plug and rock.

Lingle et al. (1982, pp. 29-37) and Burns et al. (1982) describe a plug flow test under simulated down-hole conditions on a cement plug in an anhydrite core, by means of dyed water, and observed a preferential flowpath along the plug-rock interface. The gap aperture of about 4 micrometers calculated from the flow rates compares quite closely with similarly calculated apertures for the Bell Canyon test (Christensen and Peterson, 1981; Peterson and Christensen, 1980). These authors develop a comprehensive methodology for the analysis of plug flow tests, an analysis greatly complicated by the simultaneous presence of three parallel flowpaths, i.e. the plug, the plug-rock interface, and the surrounding rock. The latter, again, may have to be treated as several separate flowpaths, e.g. fractures, or a damaged zone, or a zone of changed permeability.

The Bell Canyon test (also Christensen, 1979; Christensen and Hunter, 1979; Christensen, 1980a,b) consisted of an extensive suite of tests performed on a 1.8 m long, 20 cm diameter cement grout plug installed at a depth of 1370 m in an anhydrite bed. Although some ambiguity results from the presence of multiple flowpaths, in all probability the plug hydraulic conductivity was less than fifty microdarcies (5×10^{-8} cm/s), and possibly significantly less.

Buck and Mather (1982) quote from Boa (1978) as a design objective for cement-based grouts for sealing HLW repositories that they should have a permeability not over a few microdarcies (p. 9), and from D'Appolonia Consulting Engineers, Inc. (1978) a "permeability to water of not greater than 0.1 microdarcy when tested at 3 months" (p. 7).

Scheetz et al. (1979) comprehensively characterized an eighteen-year-old cementitious plug recovered from a deep (300 m) borehole section in a salt formation. Gas permeability measurements on cement plug samples gave relatively high values (mostly on the order of millidarcies), but virtually certainly were severely affected by stress-relief during removal from the in-situ emplaced condition and by extensive sample preparation. Samples prepared in the laboratory of materials from similar cement gave permeabilities on the order of 10^{-7} darcy (10^{-10} cm/s). Gas permeabilities from flow tests on cylinders containing sections of the interface between cement and rock resulted in even higher permeabilities than for the plug material itself, again presumably heavily impacted by sample preparation.

White et al. (1979) measured water permeabilities on various cement mixes in the 100 microdarcy to 10 nanodarcy range (10^{-7} to 10^{-11} cm/s). The authors discuss problems associated with water permeability measurements of cement such as changes due to ongoing hydration or leaching effects, as well as comparisons between gas and water measurements.

Wakeley et al. (1981) and Wakeley and Roy (1983) conducted brine flow tests on concretes prepared with various types of aggregate obtained from evaporite formations (results also summarized in Roy and Burns, 1982). Permeabilities ranged from about a microdarcy (10^{-9} cm/s) to less than 10 nanodarcies ($<10^{-11}$ cm/s). They did observe shrinkage and separation between some grouts and restraining cylinder for samples dried (cured) in air, with an implication of the development of a high-permeability flowpath (p. 98).

Roy et al. (1982, p. 102) report permeabilities of much less than 90 nanodarcies (9×10^{-11} cm/s) for a series of cementitious grouts tested after curing for 3 through 365 days while restrained in steel or glass cylinders. The results are based on an upper bound calculation given a no-flow observation. No evidence is presented that either saturation or a steady-state flow condition was established. The test procedure (pp. 23-24) leaves some uncertainty in this regard, although White et al. (1979) stress the reproducibility of their results in the tens of

nanodarcy range. Measurements on larger cylinders, on which flow testing was continued for a significantly longer period of time (14 days), gave results of 60 and 200 nanodarcies (6×10^{-11} cm/s and 2×10^{-10} cm/s). Samples cured without restraint showed considerable variation in hydraulic conductivity, up to nearly 100 microdarcies (10^{-7} cm/s), an observation attributed by the authors to cracks possibly induced by excessive unrestrained expansion. Several observations of such fracturing, especially for relatively large-diameter plugs, have been reported by Akgun and Daemen (1986, Section 2.6).

Kelsall et al. (1982, p. 39) quote results from Gulick et al. (1980a) to support the selection of a cementitious grout for salt repository sealing, in particular on the basis of high strength and hydraulic conductivities as low as 10^{-9} cm/s. They postulate that similar conductivities should be achievable for concretes formulated with locally obtained aggregate.

Burkes and Rhoderick (1983) observed cracking in samples cast from grout used for the Bell Canyon test and stored under brine for up to 3 years. Cracking was attributed to unavoidable small changes in temperature and/or moisture content. The authors do not believe "that similar changes would occur in the actual plugs where temperature and moisture conditions would be more uniform." They also propose that "the addition of some aggregate to future grouts to provide some restraint against such cracking might be a useful precaution." "Examination of three simulated borehole (SBH) samples revealed cracking along the contact of grout to anhydrite in the two samples that had leaked during permeability testing. No such openings were found in the sample that had not been tested. It is thought this cracking was due to such factors as drying, removal of outer restraint, and inadequate thickness of restraining anhydrite or combinations of these factors. Improved methods of fabricating such samples to simulate the actual contact of grout and host rock are still needed."

Buck et al. (1983) report permeabilities for eight different cement grouts, at ages of 7 and 28 days. Most 28-day results fall below 10 nanodarcies (10^{-11} cm/s), all of the 7-day results below 290 nanodarcies (2.9×10^{-10} cm/s), and most well below that. All mixtures were variations of the Bell Canyon test grout, suggesting that considerable flexibility may exist in grout design.

Roy et al. (1983a) detail preliminary results of permeability tests on five broad classes of candidate cementitious materials for salt repository sealing. One salt-containing mixture (p. 23) showed permeabilities of less than 10 nanodarcies (10^{-11} cm/s) for curing times ranging from 3 to 365 days when cured restrained. Unrestrained samples exhibited widely variable permeabilities, from about 100 microdarcies (10^{-7} cm/s) to less than 10 nanodarcies. Extreme variability was observed in the water permeability of two other

salt-containing mixtures, and the authors mention anomalies in curing as well as testing problems (pp. 24-25). "Infiltration of water and migration of salt out of the samples was significant in specimens exposed to curing solutions after only one day hydration ... It is apparent that accurate control of the initial chemical composition of a mixture is necessary to produce the desired properties of a seal material optimized for a specific environment" (p. 38).

Water permeabilities of three fume- and dust-substituted cements range from about 100 microdarcies (10^{-7} cm/s) to less than 10 nanodarcies (10^{-11} cm/s), with one product consistently showing the latter value, for curing times ranging from 7 to 128 days at temperatures from 27 to 90°C. (p. 50) Complex fume- and dust-substituted cements show predominantly permeabilities below 10 nanodarcies, over 180 days curing and at up to 90°C (p. 51 - the higher values listed in the table, except for the 100 nanodarcy measurement, presumably are typographical errors, as suggested by the discussion on p. 48).

Data for two silica sand containing mixtures (p. 67) show permeabilities near or below 10 nanodarcies for one product, and a range from 100 microdarcy (10^{-7} cm/s) to below 10 nanodarcy for a second one. Curing times ranged from 7 to 28 days, temperatures from 26 to 90°C.

Permeability for a salt (NaCl) containing cement grout formulation cured at 60°C in brine is about 100 nanodarcies (10^{-10} cm/s) at 29 and 45 days (p. 91). One similar $CaCl_2$ formulation has permeabilities an order of magnitude smaller, or even less, while a second one showed high flowrates (p. 91). Visual observations (p. 97) suggest that dry curing of this mixture opens up a flowpath between containing ring and plug. Observations on other (probably preliminary) flow tests (p. 90) showed some very high permeabilities.

Permeabilities of concrete composite samples prepared with aggregates from evaporite strata (dolostone and anhydrite) showed permeabilities in the 400 to less than 10 nanodarcy (4×10^{-10} to less than 10^{-11} cm/s) (pp. 102-105), approaching the aggregate permeabilities (p. 12) to within an order of magnitude.

Flow tests on interfaces between a NaCl grout and either dolostone or anhydrite rock samples showed permeabilities on the order of 1 to 0.3 microdarcy (10^{-9} to 3×10^{-10} cm/s) or less than 10 nanodarcy ($<10^{-11}$ cm/s), respectively (p. 106). It is implied that interface tests resulting in rapid flow have not been reported (p. 105), and have been attributed to sample failure, including mortar shrinkage.

One grout type has been tested with respect to the impact of the curing environment on its stability by exposing unrestrained and restrained samples to various environmental conditions. No cracking was observed in restrained samples, nor in unrestrained samples exposed to air or to brine for up to 180 days. Cracking did develop in unrestrained samples in saturated $CaSO_4$, saturated $Ca(OH)_2$, and deionized water (p. 129).

Gureghian et al. (1983) use a hydraulic conductivity of 8.64×10^{-7} m/day (10^{-9} cm/s) for gravel grout in their performance assessment of sealing for a salt repository.

Roy et al. (1983b) summarize water permeability measurements on various slag/cement mixtures for curing times ranging from 7 to 180 days at temperatures ranging from 27 to 250°C. All the results fall in the below 10 nanodarcy ($< 10^{-11}$ cm/s) range, with the exception of one mixture which temporarily showed a two and three order of magnitude higher permeability.

Burnett et al. (1985) describe work on cement paste in support of various concrete design aspects for the Canadian Nuclear Fuel Waste Management Program. They report permeabilities of 1.3×10^{-11} cm/s for sulphate resistant portland cement moist-cured at room temperature, and a reduction by over a factor of two upon the replacement with 35% fly ash, and 10 or 20% silica fume.

Buck (1985a, Table 8) conducted permeability tests on a sanded nonsalt expansive grout designed for salt repository sealing. A simulated borehole test in which the grout was installed and cured against an anhydrite half-cylinder in a cylindrical mold yielded results increasing from about 1 to 100 microdarcies (10^{-9} to 10^{-7} cm/s) over a 63-day aging period. A cylinder of the grout itself showed no flow, i.e. extremely low permeability. This report includes photographs (Figure 4) of a plug-rock interface along which flow channels developed prior to or during testing.

Buck (1985b, Table 9) reported permeability measurements on two candidate concrete mixtures for salt repository sealing. Two nonsalt 6 by 6 in (15 x 15 cm) cylinders did not allow detectable flow, indicating extremely low permeability, while one cylinder leaked. Salt containing concretes gave 0.01 microdarcies (10^{-11} cm/s), and 1.1 microdarcy (1.1×10^{-9} cm/s), and again one cylinder leaked, thus providing no data.

Buck et al. (1985) performed flow tests on sanded and unsanded cement grouts designed for salt repository sealing. One unsanded cylinder gave a 2 microdarcy (2×10^{-9} cm/s) result; leakage interfered with a second measurement. The unsanded sample had a lower permeability, with a flow rate too small to be observed. A flow test on a salt-grout interface resulted in severe interface dissolutioning, presumably due to the fact that the test brine was not truly saturated, or did not remain saturated during pressurization.

Wakeley et al. (1985) and Wakeley and Roy (1985) tested cement-based mixtures proportioned for sealing evaporite and associated rock strata for a potential salt HLW repository. They observed rapid interface separation for unrestrained samples left for only a few days at ambient lab conditions (p. 6), for one mix. Permeabilities for both mixtures

were near or below 10 nanodarcies (10^{-11} cm/s). Interface flow tests between one of the grouts and anhydrite revealed strongly preferential flow along the interface, with sample permeabilities of 10 microdarcies (10^{-8} cm/s) or lower after 28 to 120 days of curing. Flow tests on composites of cementitious grouts with anhydrite or siltstone, cured at high humidity, showed higher permeabilities. "In some cases, flow was consistent at about 10^{-6} darcies for 1 day or more, and then increased sharply for the remainder of the test" (p. 9).

Grutzeck and Roy (1985) tested selected cementitious formulations related to the Bell Canyon Test grouts. One sanded grout containing fly ash and salt gave fairly variable permeabilities, ranging from about 20 microdarcies (2×10^{-8} cm/s) to below 10 nanodarcies (10^{-11} cm/s), with no clear pattern either as a function of time (3 to 400 days) or temperature (38, 60 and 90°C) (pp. 15, 17). A salt-free sanded dense grout including silica flour gave permeabilities consistently below 10 nanodarcies (10^{-11} cm/s) at 38, 60 and 90°C for test periods up to 90 days.

Roy et al. (1985) present a synopsis of the development work that has been performed at The Pennsylvania State University Materials Research Laboratory and at Waterways Experiment Station on cement-based grouts for salt repository sealing. In addition to extensive geochemical discussions and results of a broad range of characterization tests, they include summaries of permeability results presented in many of the WES, SANDIA and ONWI reports that have been summarized very briefly in this section. Kelsall et al. (1985a,b,c, Section 3.1.2.2) briefly summarize the salt repository sealing grout and concrete development work, including the conclusion of an achievable 10^{-9} cm/s hydraulic conductivity.

Wakeley et al. (1986, p. 12) summarize preliminary indications of permeability tests on a salt-free grout designed for sealing a repository in bedded evaporites: "Many such tests were judged to have "failed" as indicated by immediate flow through the specimens at a rate too great to be measured." When flow was measurable, the permeability commonly was in the microdarcy range.

Wakeley and Poole (1986) studied a 36 inch (90 cm) diameter salt-saturated concrete core cast in a steel pipe. Gas permeabilities ranged from 0.4 to 21 millidarcy (4×10^{-7} to 2.1×10^{-5} cm/s). Brine permeabilities ranged from about 2 to 400 millidarcies (2×10^{-6} cm/s to 4×10^{-4} cm/s). These permeabilities are about three orders of magnitude larger than those determined by Buck (1985b) on smaller (6 in - 15 cm) diameter samples of the same and of similar concretes. Strong visual evidence, as well as results from moisture distribution throughout the sample, suggest that a highly preferential flowpath developed along the interface. The calculated permeabilities therefore probably do not represent the permeability of the concrete itself.

Wakeley and Roy (1986, p. 9) give permeabilities in the 10 nanodarcy range and below for three cementitious mixtures designed for a potential Palo Duro Basin salt repository. Measurements of interface flow between anhydrite and one salt-free grout containing fly ash and silica-flour give permeabilities of microdarcies (10^{-9} cm/s) and less for ages from 28 to 120 days. "The interface is documented to be a preferred pathway for water flow." The authors reference Wakeley and Roy (1983), where water permeabilities of anhydrite with a brine-cured salt-containing grout were 80 nanodarcies (8×10^{-11} cm/s) or less. Samples cured in a simulated ground water had permeabilities below 10 nanodarcies. For interface composites cured at high humidity, permeabilities were high. "In some cases, flow was consistent at about 10^{-6} darcy for 1 day or more, and then increased sharply (water flowed freely through the sample)." Microscopic examination revealed anhydrite dissolution along the interface. Interface flow tests between cementitious grouts and steel gave three values below 10 nanodarcy (10^{-11} cm/s), one measurement of 1.4×10^{-4} darcy (1.4×10^{-7} cm/s).

Bush and Piele (1986) conducted a large-scale borehole sealing experiment under simulated in-situ stress (15.9 MPa = 2,300 psi) and temperature (30°C). A 20 cm diameter sanded grout plug containing Class H cement, fly ash, silica flour and other additives was installed in a 39 cm diameter salt core and cured for 28 days. A subsequent 91 hour series of brine flow tests at progressively increasing injection pressures resulted in a series of transient flow measurements. The authors estimate the system permeability to decrease with time to approximately 10^{-6} darcy (10^{-9} cm/s). This test was complemented by extensive post-test analyses, including dye-flow tests. It appears that preferential bypass flowpaths may have developed through the salt around the plug, possibly as a result of expansive stresses generated by the grout and of previously applied external stresses to the hollow salt cylinder. Separate tests on grout cores recovered from the plug yielded 3 results below 10^{-7} darcy (10^{-10} cm/s), the detection capability of the test cell, and one value of 6×10^{-7} darcy. All these are at least four orders of magnitude smaller than the salt permeability data. (The latter obviously is not necessarily representative of the permeability of undisturbed in-situ salt.)

The large-scale borehole sealing test reported by Bush and Piele (1986) was accompanied by an extensive series of parallel and post-test analyses and characterization studies by Scheetz et al. (1986a). Based on a theoretical extrapolation for about twice the test duration, they calculate an equivalent uniform plug permeability of 3.3 microdarcies ($3.3. \times 10^{-9}$ cm/s) (Section 1.3). A measurement on a post-test recovered grout core gave a permeability of less than 10 nanodarcies (10^{-11} cm/s) (Section 2.1.2). Tests on half-cylinder samples of salt and grout, prepared from the mix used for the large plug, resulted in very large flow, primarily through the salt (Section 2.2.1). Permeabilities calculated directly from the brine flow decreased

from 83 microdarcies (8.3×10^{-8} cm/s) at the start of the flow test to 5 microdarcies (5×10^{-9} cm/s) at the end of the test (Section A.5.2). Detailed post-test inspections revealed complicated and extensive salt dissolutioning, confirming the concern that sealing boreholes in salt will depend critically on dissolutioning effects (e.g. Kienzler and Korthaus, 1982). Dye penetration clearly revealed preferential flow along the rock-plug interface, some penetration into the salt, and no penetration into the grout.

Bush and Lingle (1986) performed a full-scale borehole sealing test on an expansive cement grout in an anhydrite core stressed to 4.82 MPa (700 psi) and heated to 30°C. The flow tests conducted after 29 days of curing resulted in immediate large flow. Post-test inspection of the plug revealed numerous vertical channels along the plug-rock interface, obviously forming highly preferential flowpaths. The channels clearly are very similar to those which have been observed in a number of cement plug experiments (e.g. Daemen et al., 1985, Section 2.4.1, Figs. 2.33/35; Daemen et al., 1983, Fig. 3.20), as well as in the failure of a 5 m diameter shaft plug for an oil storage cavern (Sitz, 1981, Fig. 2, quoted by Daemen et al., 1985, Fig. 2.37). As pointed out by Bush and Lingle (1986, Section 9.3), borehole grout placement almost certainly is the cause of the channeling. Sufficient understanding of the causes of the channeling should be developed in order to preclude its development during actual sealing operations.

Permeability tests reported by Bush and Lingle (1986, Table 8-1) gave five results close to one microdarcy (10^{-9} cm/s) for small cylinders of the cement grout used in the large-scale anhydrite plug test.

Scheetz et al. (1986b) analyzed the large-scale anhydrite sealing test reported by Bush and Lingle (1986), and calculated equivalent borehole plug permeabilities close to 1 millidarcy (10^{-6} cm/s) or aperture (rock-plug interface gap) permeabilities of 5 to 8 darcies (5×10^{-3} to 8×10^{-3} cm/s). Separate experiments by Scheetz et al (1986b, p. 24) on the grout indicated considerable bleeding. Scheetz et al. (1986b, p. 51) also discuss several potential causes of the interface channeling in the large-scale anhydrite sealing test, including fluid movement and bubble trains resulting from early outgassing of the cement paste.

Stormont (1986) reports initial results from tests conducted on a series of salt-water based concrete borehole plugs ranging in diameter from 3 ft (91 cm) to 6 in (15 cm). The plugs were emplaced in situ at the Waste Isolation Pilot Plant, near Carlsbad, New Mexico. Gas permeability tests conducted after at least 28 days of curing suggested permeabilities well below one microdarcy (10^{-9} cm/s), except for a plug penetrated by instrumentation cables. Inferred brine seal permeabilities, after 100 days of testing without brine breakthrough, also are considerably less than one microdarcy.

The discussion of cement grout and concrete permeability presented so far has been focused exclusively or predominantly on experimental work carried out in support of various aspects of the U.S. HLW repository sealing efforts. It would seem desirable to broaden this discussion somewhat, by including some results from entirely unrelated permeability studies.

Mott, Hay and Anderson (1984, p. 92) quote from Neville (1983) that dam concrete permeabilities of 10^{-10} cm/s can be obtained, but express clear reservations (on p. 201, also) about the feasibility of achieving such values in practice. (The sources, Neville, 1983, and certainly Corps of Engineers, U.S. Army, 1954, do not claim these values to be in-situ values, contrary to a statement here.) Neville (1983, p. 438) tabulates typical values of permeability of concrete used in dams, taken from Corps of Engineers, U.S. Army (1954), as ranging from 8×10^{-10} cm/s to 35×10^{-10} cm/s. The latter report, including its Revision A, lists permeability results obtained on five samples of each of nine concretes for ages up to five years. Most of the concretes show a fairly systematic decrease in permeability with age, although that trend may be reversing beyond 2 years. The authors draw explicit attention to the considerable variation in results for each type, even after some retesting for cores where results appeared questionable. They postulate (p. 21) that "this variation ... appears to be a characteristic of the permeability of the concrete studied." After 3 months, the permeabilities average 18×10^{-9} cm/s, and range from 6 to 28×10^{-9} cm/s. After 5 years, the average has dropped to 2×10^{-9} cm/s, the range from 3.8 to 6.3×10^{-9} cm/s.

A series of papers by Powers and associates, in particular Powers et al. (1954) and Powers (1958), which have been referenced frequently (e.g. Neville, 1981, Ch. 7; Neville and Brooks, 1987, Ch. 14; Browne and Baker, 1979; Neville, 1971, Ch. 20; Mindess and Young, 1981, Ch. 20; Mehta, 1986, Chs. 2,5; Woods, 1968, Ch. 2; Owens, 1983) have established widely quoted reference numbers for cement paste permeabilities. Typical relations show an approximately exponential increase from about 7×10^{-14} cm/s, the permeability of the cement gel, for a capillary porosity of about 10 per cent, to 10^{-9} cm/s for a capillary porosity of about 35%, the latter range being considered what is normally produced in good quality concrete (Powers, 1958). Mature cement paste permeabilities increased exponentially from about 10^{-12} cm/s for a 0.25 water/cement ratio to 1.3×10^{-10} cm/s for a 0.7 water/cement ratio. Permeability during hydration for a 0.7 water/cement paste dropped from an initial 2×10^{-4} cm/s to 10^{-10} cm/s after 24 days. All these (as indicated, widely quoted) results were obtained from tests on specimens kept wet continuously. Powers et al. (1954) also report results on samples that had been partially dried, for periods of 208, 1040, and 238 days, after wet curing for 141 or 63 days, in a 79% relative humidity environment. These samples showed

permeabilities of 10^{-9} cm/s, a seventy-fold increase over identical control samples that were not allowed to dry.

Neville and Brooks (1987, p. 266) state that a maximum permeability of 1.5×10^{-9} cm/s is often recommended in order to consider concrete as watertight, and is also considered an acceptable limit for some Bureau of Reclamation work (Neville, 1983, p. 439; Mindess and Young, 1981, p. 548).

According to Neville (1983, p. 438; 1971, p. 234) and Neville and Brooks (1987, pp. 266-7), the permeability of concrete can be of the same order of magnitude of that of cement paste, on condition that a low permeability aggregate is used, and that the curing cycle is not interrupted by premature drying. Mehta (1986, p. 113) shows two sets of data (one of which is also given by Taylor, 1977, p. 233) comparing cement pastes (with water/cement ratios from about 0.45 to 1) with concretes containing various aggregate sizes. The concrete permeabilities for one set of data are about one order of magnitude higher, and are about two orders of magnitude higher (10^{-11} cm/s to 10^{-9} cm/s) in the second study. Mehta summarizes the results: "Typically, permeability coefficients for medium-strength concrete (containing 1 1/2 in aggregate, 600 lb/yd^3 cement, and an 0.5 water/cement ratio) and low-strength concrete used in dams (3 to 6 in aggregate, 250 lb/yd^3 cement, and an 0.75 water/cement ratio) are of the order of 10^{-10} and 3×10^{-9} cm/s, respectively." The increased concrete permeability has been attributed to relatively large water voids underneath aggregate (e.g. Taylor, 1977, p. 234) and to microcracking along cement-aggregate interfaces (e.g. Mehta, 1986, pp. 112-113).

The effects of curing and of emplacement on concrete permeability have been stressed repeatedly (e.g. Pomeroy, 1986a,b; Taylor, 1977, pp. 236-239; Mindess and Young, 1981, p. 547; Mehta, 1986, p. 113). Pomeroy (1986b), for example, states that "the W/C ratio is one factor, but compaction and curing are also important and we must take all aspects into account. I would like to see some permeability checks on mature structural concrete, but at present no agreed tests exist." Owens (1985) experimentally demonstrates the influence of the early-age temperature cycle, particularly for concretes made with high-heat portland cement, on concrete permeability. Browne (1986) states that "a concrete surface flooded with water for 7-14 days will provide an extremely impermeable skin reducing penetration considerably, for example by 10,000 times that for concrete cured in air, even when protected by plastic sheets", and discusses the critical importance of compaction. Browne and Baker (1979) illustrate the 10,000 range (10^{-13} cm/s to 10^{-8} cm/s) by means of data from various sources where concretes with water/cement ratios of 0.4 to 0.5 have been tested. They propose compaction and curing as essential factors in determining concrete permeability, and consider a range of in-situ permeabilities for concrete structures from good (10^{-10} cm/s) to lower quality, normal site practice (10^{-8} cm/s), to poor practice (10^{-6} cm/s).

Steam curing is considered by Neville (1971, pp. 234-235; 1983, pp. 438-439) to reduce the permeability, while Neville and Brooks (1987, p. 267) state that the permeability of steam-cured concrete is generally higher than that of moist cured concrete, and that additional fog curing may be required, as seems to be confirmed by the data obtained by Higginson (1961) and cited in Neville (1971, p. 235; 1983, p. 439).

Bleeding and settlement could significantly affect the sealing performance of borehole and shaft plugs. The mechanisms have been discussed at length by Powers (1968, Chs. 11 and 12). Orchard (1979, p. 112) quotes a permeability test procedure developed by Cook (1951) in which concrete specimens were turned on their side for permeability testing, in order to assure that water gain and bleeding channels would be normal to the direction of water flow through the specimen.

Detailed concrete studies have been performed in order to evaluate the performance, e.g. shielding, of nuclear reactor containment vessels. Davis (1972) reports permeabilities of 4.5 to 33.5 x 10^{-12} cm/s (p. 1153; the exponent probably is incomplete on p. 1160) for three high density concretes cured at 20°C for 90 days.

Of particular relevance for seal performance in an unsaturated environment are studies of moisture migration, e.g. as a result of thermal gradients (England and Ross, 1972; Poitevin, 1972; McDonald, 1972; Yuan et al., 1972; Pihlajavaara and Tiusanen, 1972). Kaplan (1972), in a summary review of these papers, notes the emphasis placed on the fact that moisture migration alters the properties of concrete, and that moisture movement studies are essential to an understanding of the properties of concrete at elevated temperatures. England and Ross (1972) report migration tests for concrete samples up to 10 ft (3 m) long with one end heated to up to 150°C. They observed higher than normal water content in zones in between the hot and cool regions, and consider low permeability as one critical parameter, based in part on pore pressure dissipation observations. They consider conventional diffusion theory as invalid, especially in the high-temperature region, where rapid migration is most likely, and propose an alternate analysis method. They conclude that for thick sections such as reactor vessels, drying at less than 100°C should not be significant, because at 100°C it penetrates only 0.3 m after 886 days. Clearly, these effects may be significant over repository time scales, e.g. for shaft and borehole seals, and it may be desirable to establish likely in-situ environments for a repository in an unsaturated environment, and evaluate its impact on cementitious seal drying and shrinkage.

Poitevin (1972) encountered considerable difficulty in truly sealing concrete specimens, and observed relatively fast drying. He found it possible, in most cases, to closely correlate electrical resistivity measurements and moisture content.

McDonald heated one end of a 9 ft (2.7 m) long pie-shaped concrete specimen, with a cross-sectional area increasing from 2 ft x 2 ft (61 x 61 cm) to 2 ft x 2ft 8 in (61 x 81 cm) to a temperature difference of 80°F (44°C). This temperature difference, after about 130 days, did not result in a significant change in moisture content of the block.

Yuan et al. (1972) tested drying of sand-cement mixes with water-cement ratios of 0.40, 0.45, 0.55, and 0.70, after curing in a moist room at 100% relatively humidity for 120 days. The authors concluded that conventional diffusion theory with a constant diffusion coefficient adequately describes the drying of the mortars for the test conditions, i.e. relative humidity from 25 to 75% and temperatures between 40 and 140°F (4.4 and 60°C), on condition that chemical changes, especially carbonation, are prevented.

Pihlajavaara and Tiusanen (1972) present a brief summary of the theory of moisture migration as a result of temperature differences, as well as initial results of experiments on 12 cm long, 1.8 cm diameter cement paste samples with cement-water ratios of 0.30 and 0.45, respectively. The temperature at the two ends of the cylinders was about 23.5 and 48°C, respectively. Changes in moisture content distribution were well established after 20 days, and appeared to be stabilized between 20 and 40 days after starting the tests.

Paul et al (1972) include, as part of a broad description of design, research and construction of a concrete vacuum building, air permeability measurements on concrete. Various sequences of oven drying and water vapor resaturation showed the air permeability to be significantly lower in partially saturated samples than in dry samples.

Neville (1971, pp. 238-240; 1981, pp. 441-443) discusses air and water vapor permeability of concrete. He points out that aggregate grading seems to be particularly important with regard to air permeability. Curing reduces air and water vapor transmission, but drying of concrete of even an advanced age increases the permeability. Water vapor transmission depends markedly on relative humidity on the two sides of the sample. This again may have implications for cement and concrete seals in an unsaturated environment.

Some oil well cement permeability studies are referenced by Smith (1976, pp. 28, 41). Possibly even more so than for concrete, casing cementing seal performance can be dominated by installation problems. "The key to success is proper placement of the cement completely around the casing" (Allen and Roberts, 1982, Vol. 1, p. 99). Examples of typical problems can be found in standard oil and gas drilling and cementing references, e.g. Smith (1976, Ch. 7, especially Sections 7.5 and 7.8) and Allen and Roberts (1982, Vol. 1, Ch. 3; Vol. 2, Ch. 4). Several specific case study examples of problems are referenced by Daemen (1981).

Allen and Roberts (1982, Vol. 1, p. 99) consider an in-place permeability of less than 0.1 md (10^{-7} cm/s) as an acceptable performance level. Smith (1976, p. 28) lists 3-day and 28-day class H cement permeabilities at 320°F (160°C), with results consistently far below 0.1 md, typically 0.001 md (10^{-9} cm/s) or less when substantial fractions (20 to 40%) of silica flour are included, but ranging from 4 to 10 md (4×10^{-6} to $10 \times ^{-6}$ cm/s) when no such admixture is included.

5.2.5 The Effect of Plug vs. Host Rock Mass Permeabilities

Brace (1980) gives a range of in-situ crystalline rock permeabilities, from 0.1 darcy to 1 microdarcy. The high values and wide range are due to the natural fractures in rock masses. South and Daemen (1986, p. 11) indicate the permeability of a fractured specimen of Oracle granite as 60 microdarcy. The hairline fractures are barely visible during unaided eye inspection.

Experimental results on dried-out cement plugs (Table 5.1) indicate that the fissure permeability of the plug/rock interface is in the upper range of the permeability of natural fractures in crystalline rock. It is worth pointing out that the drying conditions in these experiments are severe, either long-term drying (many months) or drying at elevated temperature in the absence of water vapor, and after only a short curing time. It can be inferred that if the drying of cement plugs is not too severe, the interface permeability (after several months of re-wetting) should be in the lower or middle range of the in-situ rock mass permeability. Since a borehole and its immediately surrounding rock comprise only a fraction of the total rock mass, the effect of plug permeability is limited, even if it is higher than the rock mass permeability.

Several parametric studies have been published of the relative importance of flow through rock and seal, usually with emphasis on identifying the potential significance of bypass flow through a modified permeability zone around seals or through the plug-rock interface (e.g. Anttonen et al., 1980, pp. 3-178/183; Chabannes et al., 1980; Hodges et al., 1980; Peterson and Christensen, 1980; Gureghian et al., 1983, Section 5.4; Fernandez et al., 1987, Section 4.1.5; Mott, Hay and Anderson, 1984 (Section 9.4) emphasize the need to include preferential flowpaths in such comparative studies, by illustrating the dominant effect that can be exerted, e.g. by seemingly minor separations between plug and rock). In broad terms these analyses show that differences of one or two orders of magnitude in hydraulic conductivity between the major parts of a seal zone are required in order to have flow through one part truly dominating total flow.

South and Daemen (1986, p. 182) come to the same conclusion after performing a finite element analysis of flow through a cement-plugged rock cylinder. They show that a borehole plug one order of magnitude less permeable than the rock reduces the flow through the plug/rock system by only 6%. A plug permeability two orders of magnitude less than the rock results in only another 1% reduction in flow. Similarly, a plug with a permeability one order of magnitude greater than the rock results in only a one and one-half fold increase in flow rate. If the plug permeability is two orders of magnitude greater than that of the rock, then the flow through the plug and the rock immediately surrounding it increases only six-fold.

5.3 The Effect of Cement Plug Drying on Its Hydraulic Conductivity

The experimental results are summarized in the simplified plot shown in Figure 5.13. This composite plot shows the permeabilities of Charcoal

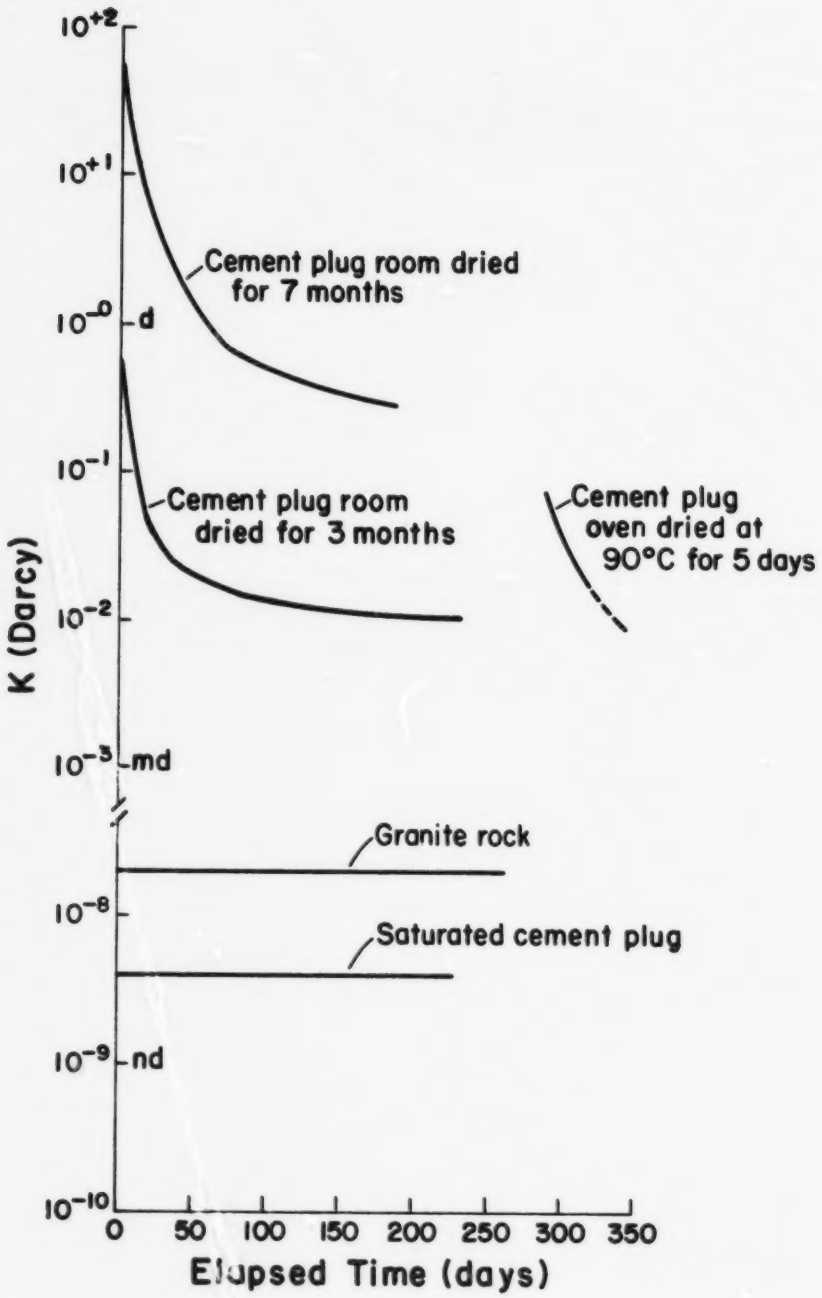

Figure 5.13 Permeabilities of Charcoal granite and of wet and dried-out cement plugs as a function of time. Wet cement plugs are one order of magnitude less permeable than granite. Drying for a long period or at high temperature increases plug permeability by many orders of magnitude and severely degrades plug performance. Performance recovers partially during rewetting.

granite, and of wet and dried-out cement plugs as a function of time. Drying the cement plugs increases their (previously very low) permeability by seven to nine orders of magnitude, depending upon drying period and/or temperature. The very high laminar fissure permeability for dried-out cement plugs is calculated for the plug/rock interfacial gap, which acts as a preferential flow path. The interface opens up as a result of cement plug shrinkage due to drying, verified by the dye injection test (Chapter 4).

Adisoma and Daemen (1984) and South and Daemen (1986) have calculated the dried-out cement plug permeability using Darcy's law, assuming uniform flow. Their calculations give much lower values compared to the fissure permeability in Figure 5.13. This is because the flow is assumed to occur through a larger area, i.e. the entire cross-section of the plug, which is not the case for dried-out plugs. Calculation by Adisoma and Daemen (1984) for these specimens results in two to four orders of magnitude increase relative to the permeability of the wet cement plugs. The calculations are useful to illustrate the effect of drying, similar to comparing flow rates before and after drying.

The dried-out cement plugs all exhibit a similar response when they are resaturated. The flow rates decrease rapidly for the first two months and level off thereafter. An oven-dried cement plug in basalt tested by South and Daemen (1986) exhibits very similar behavior. This indicates some cement expansion upon resaturation, which partially closes the plug/rock interfacial gap. Plug performance is only partially recovered, and hydraulic conductivity is still several orders of magnitude higher than that of the wet cement plugs. The potentially very detrimental consequences of premature cement drying have been observed by others, as documented to some limited extent in Section 5.2.4.

5.4 The Effect of Dynamic Loading on Plug Hydraulic Conductivity

This discussion of the effect of dynamic loading on the hydraulic conductivity applies only for longitudinal flow through the plug. The effect of dynamic loading on the peripheral flow through the surrounding rock is given in Section 4.2. Details of each test are given in that Section. The following summarizes the test conditions:

- Range of acceleration amplitude: 1 to 2 g
- Range of velocity amplitude: 6.4 to 10.4 m/s (21 to 34 ft/s)
- Range of displacement amplitude (stroke length setting): 2.8 to 3.8 cm (1.1 to 1.5 in)
- Range of motion frequency: 2.6 to 3.6 Hz
- Range of dynamic load duration: 20 to 326 seconds
- Range of injection pressure: 1 to 4 MPa

Two specimens with a wet cement plug (CG5309-06 and -31V) were tested in tandem at an acceleration of 1 g. The permeability vs. time plots for these specimens are given in Figures 5.14 and 5.15, with the dynamic loading data superimposed. The result for another specimen (-08) with a wet cement seal is shown in Figure 5.16. This specimen was accelerated to 2 g. Specimen CG5309-28, with a dried-out plug, was

tested at 1 g, specimen -01 at 2 g. Results are given in Figures 5.17 and 5.18, respectively.

The results in Figures 5.14 to 5.18 indicate that hydraulic conductivities of the seal do not change significantly after dynamic loads are applied. Dynamic loads at the above mentioned conditions, considerably more severe than what is likely to be encountered during most earthquake loading, do not change plug permeability by more than the variation without dynamic loading. No preferential flow path develops in wet cement plugs due to the dynamic loads, and their permeability remains lower than that of granite. Even the sealing performance of the dried-out cement seals is not impaired by the dynamic loads. From Section 4.2 it is obvious that the rock immediately surrounding the plug also is still intact after dynamic loads are applied, because the peripheral flow remains constant.

5.5 Transition from Time-dependent to Steady-state Flow

The tests conducted are essentially steady-state flow tests. Transient or time-dependent conditions occur at the beginning of each individual test, when the injection pressure is applied or changed. In one-dimensional transient flow through a porous medium of length l (such as a cement plug or a rock bridge), the hydraulic head, h, is a function of time and position, e.g. distance from one end of the seal. Appendix A gives the governing partial differential equation for transient flow:

$$K/S_s \, \partial^2 h/\partial x^2 = \partial h/\partial t \qquad (5.9)$$

and derivation of its general solution:

$$h(x,t) = x/l \, H_2 + \sum_{n=1}^{\infty} 2/n\pi \, (H_2 - H_1) \cos(n\pi) \sin(n\pi x/l) \exp(-n^2\pi^2 Kt/l^2 S_s) \qquad (5.10)$$

for the initial and boundary conditions:

$$h(x,0) = x/l \, H_1$$

$$h(0,t) = 0 \qquad \text{for all } t \qquad (5.11)$$

$$h(l,t) = H_2 \qquad \text{for } t > 0$$

K is the hydraulic conductivity, S_s is the specific storage, H_1 and H_2 denote the initial and the final head, respectively, x is the length coordinate and t denotes time. Using this general solution, the hydraulic head at any point can be computed for any time. As time increases, the second (time-dependent) term vanishes and the solution approaches the proper steady-state solution.

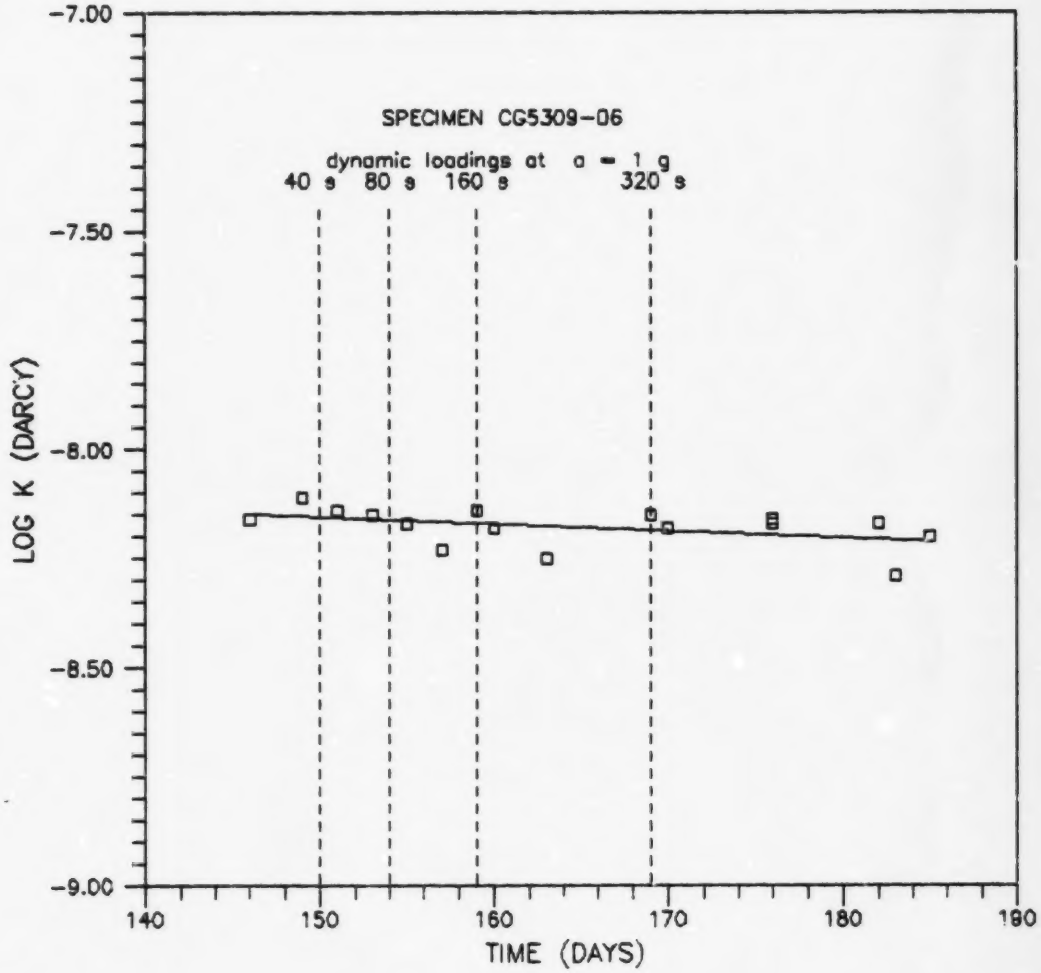

Figure 5.14 The effect of dynamic loading at a = 1 g on the hydraulic conductivity of wet cement plug specimen CG5309-06. No significant change is observed in plug permeability as a result of dynamic loading. Dashed vertical lines indicate the time of dynamic load application, for a duration listed on each line.

BEST COPY AVAILABLE

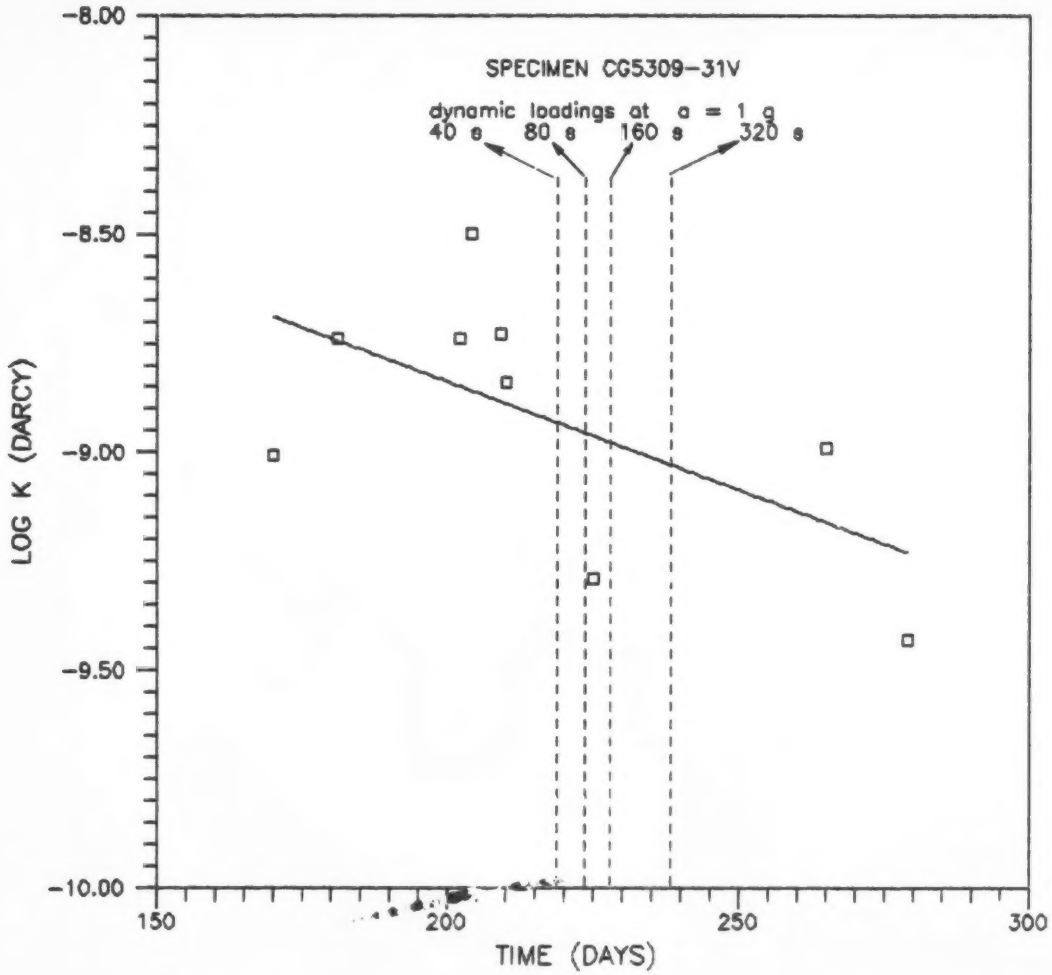

Figure 5.15 The effect of dynamic loading at a = 1 g on the hydraulic conductivity of wet cement plug specimen CG5309-31V. The plug permeability remains low after the application of dynamic loads. Dashed vertical lines indicate the time of dynamic load application, for a duration listed on each line.

BEST COPY AVAILABLE

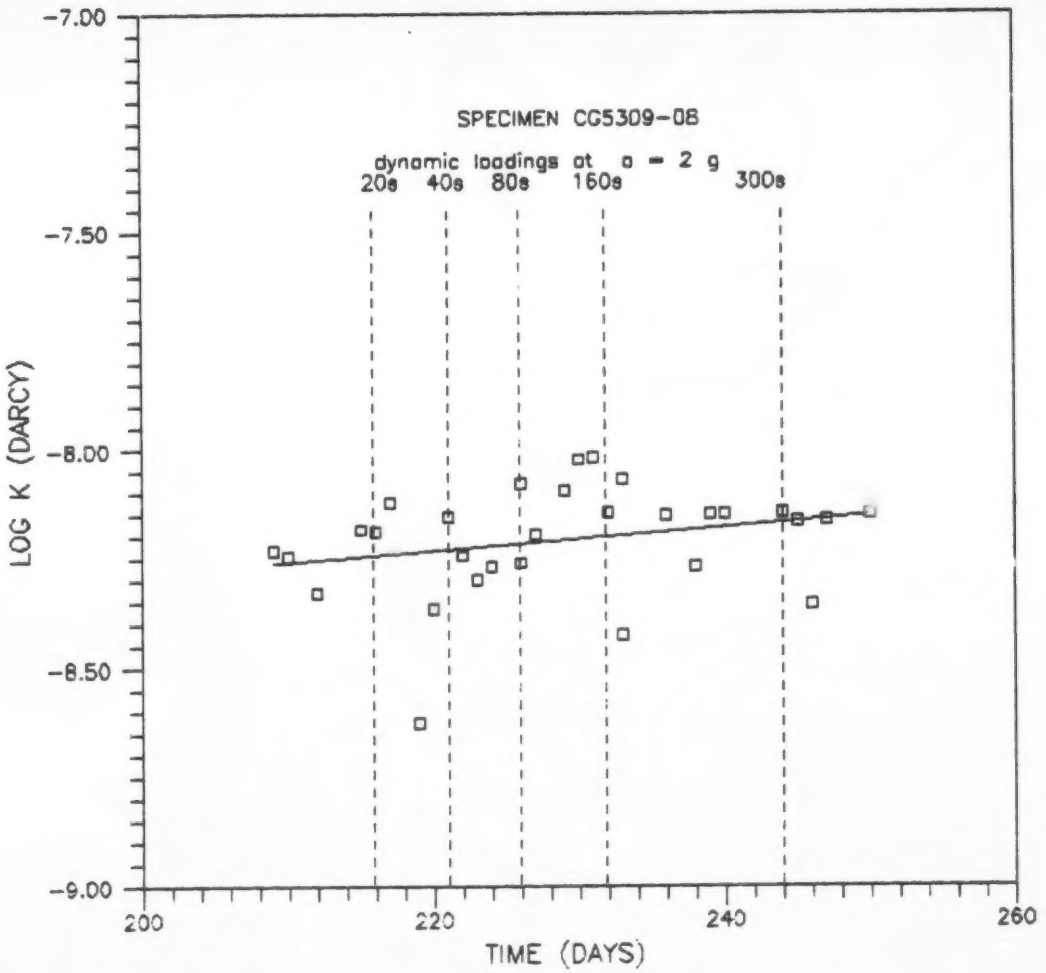

Figure 5.16 The effect of dynamic loading at a = 2 g on the hydraulic conductivity of wet cement plug specimen CG5309-08. The change observed in plug permeability as a result of dynamic loading is less than the permeability variation without dynamic loadings. Dashed vertical lines indicate the time of dynamic load application, for a duration listed on each line.

BEST COPY AVAILABLE

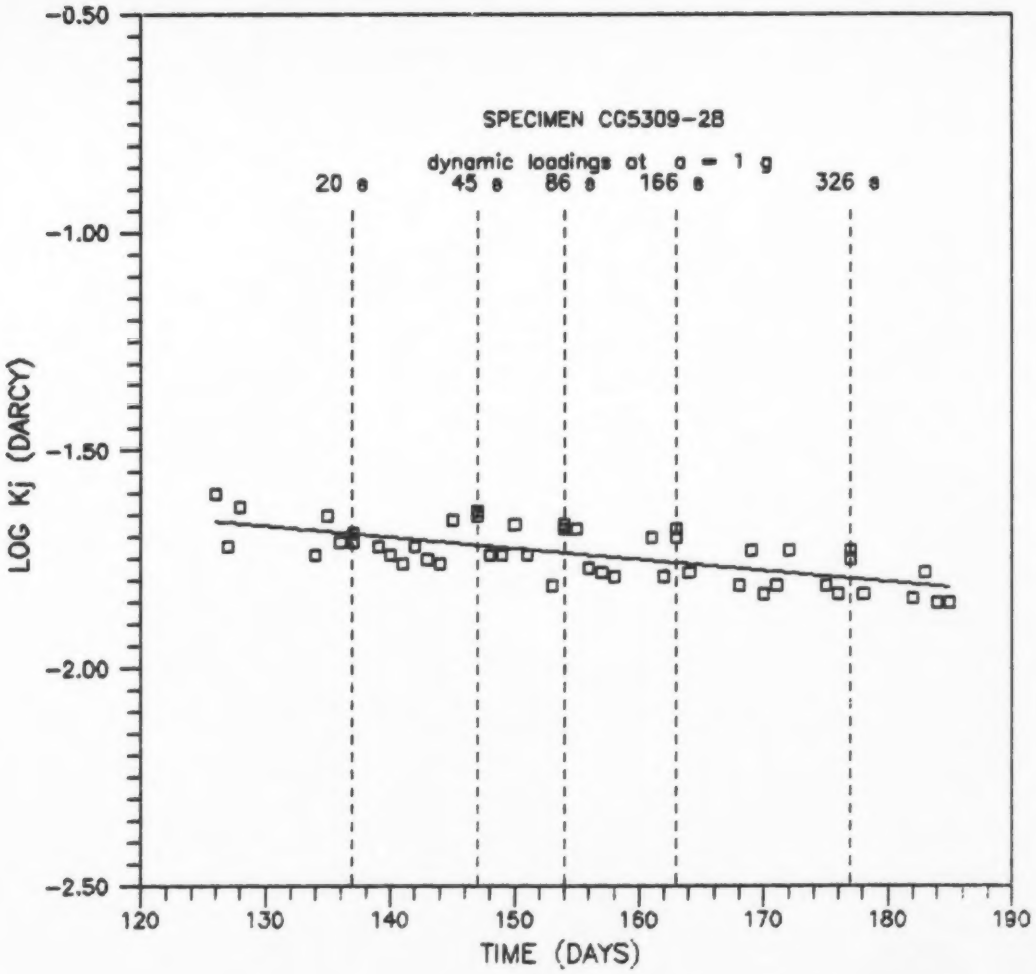

Figure 5.17 The effect of dynamic loading at a = 1 g on the hydraulic conductivity of dried-out cement plug specimen CG5309-28. The fissure permeability remains the same after the application of dynamic loads. Dashed vertical lines indicate the time of dynamic load application, for a duration listed on each line.

BEST COPY AVAILABLE

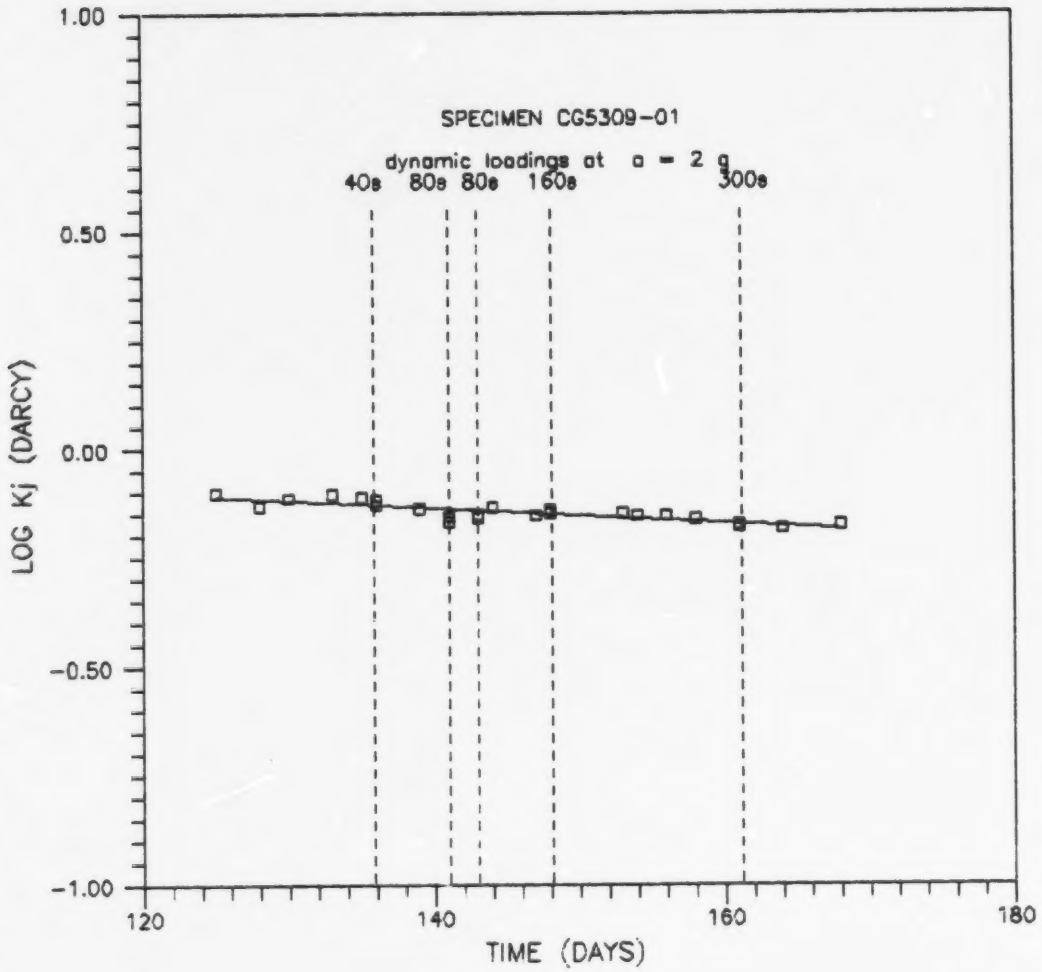

Figure 5.18 The effect of dynamic loading at a = 2 g on the hydraulic conductivity of dried-out cement plug, specimen CG5309-01. No significant change can be observed in the fissure permeability as a result of dynamic loads. Dashed vertical lines indicate the time of dynamic load application, for a duration listed on each line.

BEST COPY AVAILABLE

The hydraulic conductivities of Charcoal granite and of cement plugs obtained are very low (in the order of 10^{-11} to 10^{-12} cm/s). The specific storage, as well as the hydraulic conductivity, can be obtained from transient flow tests (Neuzil et al, 1981). They mention that the transient test is more practical than the steady-state test when the sample permeability is small. The values of specific storage for crystalline rocks are also very small, partly due to their small porosity. Brace et al. (1968) use the assumption of zero specific storage for Westerly granite. This is never strictly valid (Neuzil et al, 1981). It is obvious that as S_s approaches zero, equation (5.10) reduces to a steady flow solution.

As an alternative to the previous analytical solution, a numerical approximation can be used. Desai (1979) has developed a finite element solution for time dependent problems. In this approach, cement seal and rock bridge are discretized into line elements (Figure 5.19). A revised version of computer program DFT/C-1DFE (a one-dimensional finite element program for deformation, flow, temperature and consolidation problems) is used in this analysis. The program is modified for IBM microcomputers. It solves the general equation in (5.9) for the initial and boundary conditions given in (5.11). The output is hydraulic head at the nodal points within the plug at various preset times (Appendix B). The time at which the hydraulic head at each nodal points becomes constant is the transition time from transient to steady flow.

For this analysis, a K value of 1×10^{-11} cm/s (1×10^{-8} darcy) is used for Charcoal granite. For wet cement plugs, the K value used is 3×10^{-12} cm/s (3×10^{-9} darcy). These values are obtained from the flow tests. A specific storage of 1×10^{-11} cm^{-1} is used for all calculations. This value is chosen so that for Charcoal granite, the ratio of K/S_s, the hydraulic diffusivity, equals one cm^2/s. This corresponds to the upper range of the values listed by Neuzil (1986) for Westerly Granite and Creighton Gabbro, and may be high for a curing cement. The specific storage value is rather low, e.g. compared to values calculated from compressibilities (Freeze and Cherry, 1979, eqtn. 2.60). An approximate calculation, assuming a cement compressibility of about 10^{-9} to 10^{-10} m^2/N and a cement porosity between 0.1 and 0.5, suggests a specific storage on the order of 10^{-7} to 10^{-8}/cm. With the cited cement permeability, this would correspond to a hydraulic diffusivity on the order of 10^{-4} to 10^{-5} cm^2/s. The specific storage is within the range of that of a shale, as measured by Neuzil et al. (1981), which has a specific storage of 10^{-6} to 10^{-9} cm^{-1}. Since $S_s = \gamma_w m_v$ and the unit weight of water, γ_w, is 1 g/cm^3, the selected diffusivity is equivalent to a coefficient of volume compressibility,

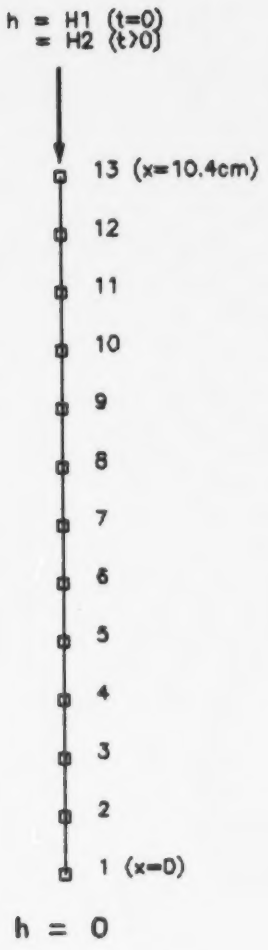

Figure 5.19 Discretization of cement plug into line elements for numerical transient flow analysis, specimen CG5309-31V, l = 10.4 cm.

BEST COPY AVAILABLE

m_v, of 1 x 10^{-11} cm^2/g, which is used as an input for the program. Different values of S_s are used for sensitivity analysis.

Figure 5.20 shows the hydraulic head or pressure in the plug as a function of time, when the injection pressure is increased from 2 to 4 MPa. Pressure is plotted at three different locations within the plug. Figure 5.20a indicates that for a Charcoal granite rock bridge, the transition time is 20 seconds. For a wet cement seal, the transition time is 40 seconds (Figure 5.20b). Since the two are comparable in length (10.2 cm for granite and 10.4 cm for cement) and the specific storage for both is assumed to be the same for these calculations, the longer transition time in cement is attributed to its lower permeability.

Figure 5.21 shows the hydraulic head at each nodal point in the rock bridge and in the cement plug. In Figure 5.21a the injection pressure is increased from 2 to 4 MPa. Hydraulic head at each nodal points in the granite rock bridge is given for the initial condition (t = 0) and for t = 0.5, 1, and 20 seconds when the flow reaches steady-state conditions. In Figure 5.21b the injection pressure in the cement-plugged specimen is increased from 1 to 4 MPa. Hydraulic head at the nodal points within the plug is shown at t = 0, 0.5, 5, and 55 seconds. The latter is the transition time between transient and steady-state flow.

Transition time depends on the plug length and the difference in injection pressure between two successive flow tests ($H_2 - H_1$). Three cement-plugged specimens (CG5309-06, -08, -31V) with plug lengths of 3.1, 5.4, and 10.4 cm, respectively, are studied. The injection pressure varies from 1 to 2 MPa, 2 to 4 MPa, 1 to 4 MPa, and 0 to 4 MPa, resulting in head differences of 1, 2, 3, and 4 MPa at the beginning of each test. Figure 5.22a shows that the transition time strongly depends on plug length. For a given plug length, the head difference affects the transition time only slightly (Figure 5.22b).

The last step in this study is to perform a sensitivity analysis of the transition time by varying the hydraulic diffusivity (K/S_s ratio). This is achieved by varying S_s and keeping K constant, since this is the value obtained from the (steady-state) flow test. Three K/S_s ratios are used, 0.1, 1, and 10 cm^2/s for Charcoal granite, and 0.03, 0.3, and 3 cm^2/s for the cement plug. The sensitivity analysis is carried out at constant plug length and head difference.

Figure 5.23 shows that transition time is inversely proportional to the K/S_s ratio. As the ratio of K/S_s is decreased by an order of magnitude, the transition time is increased by an order of magnitude. Even for fairly extreme assumptions, based on previously cited calculations, i.e. for hydraulic diffusivities of 10^{-4} and 10^{-5} cm^2/s, respectively, the transition times remain at 17 minutes and 2.5 hours,

(a)

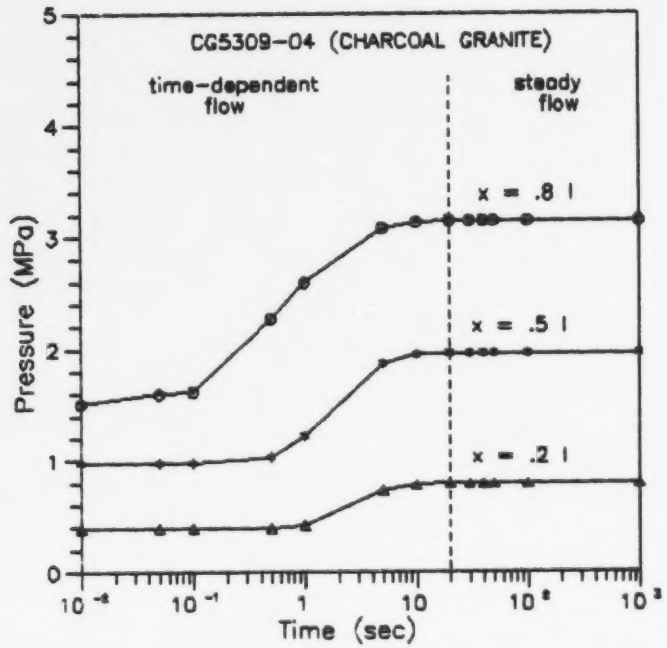

(b)

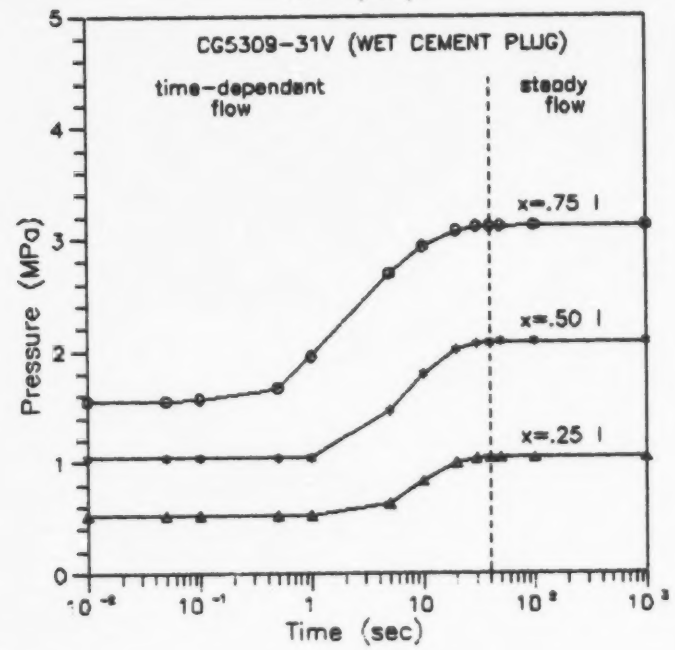

Figure 5.20 Hydraulic head at three locations (x) in a 10.2 cm Charcoal granite rock bridge and in a 10.4 cm wet cement plug as a function of time, when injection pressure is increased from 2 to 4 MPa. (a) Charcoal granite, specimen CG5309-04, transition time 20 s. (b) Cement plug, specimen CG5309-31V, transition time 40 s.

BEST COPY AVAILABLE

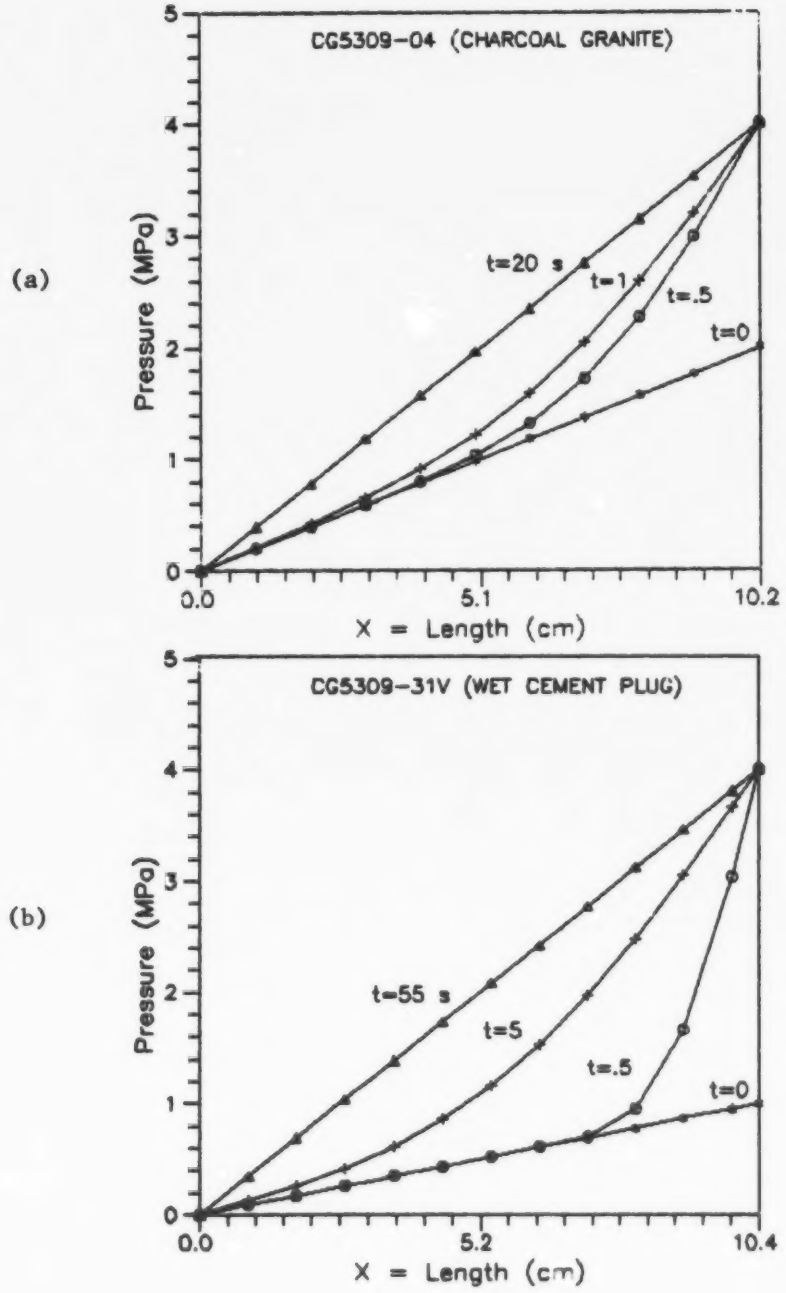

Figure 5.21 Hydraulic head at each nodal point in the Charcoal granite rock bridge and in the wet cement plug for various time steps. (a) Charcoal granite, specimen CG5309-04, injection pressure is increased from 2 to 4 MPa, transition time = 20 s. (b) Cement plug, specimen CG5309-31V, injection pressure is increased from 1 to 4 MPa, transition time = 55 s.

BEST COPY AVAILABLE

(a)

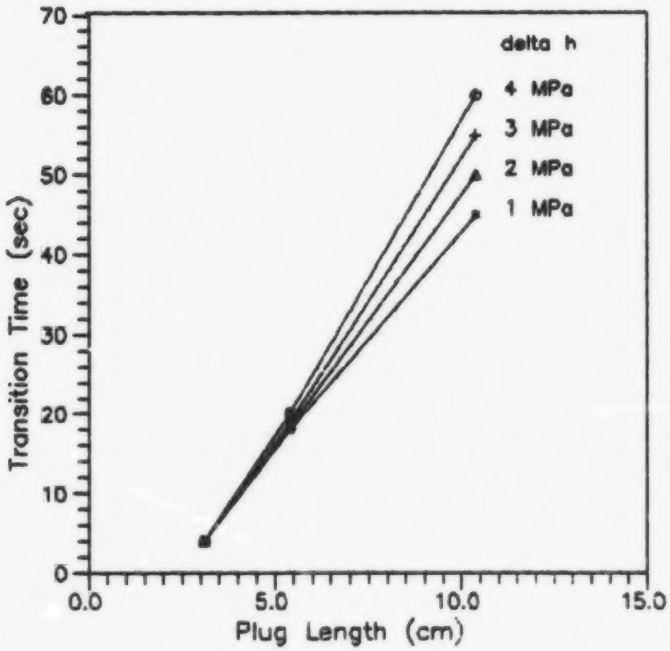

(b)

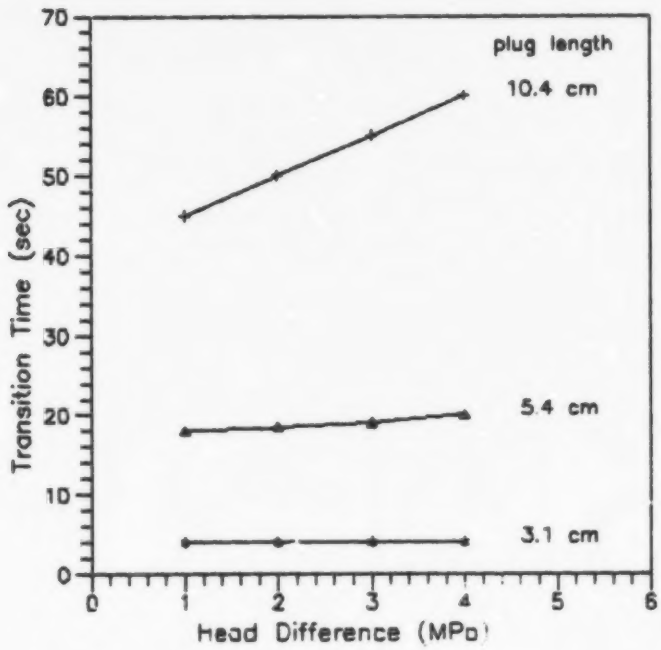

Figure 5.22 Transition time as a function of plug length and head difference ($H_2 - H_1$). (a) Transition time is strongly dependent on the plug length. (b) Transition time is slightly dependent on the head difference.

BEST COPY AVAILABLE

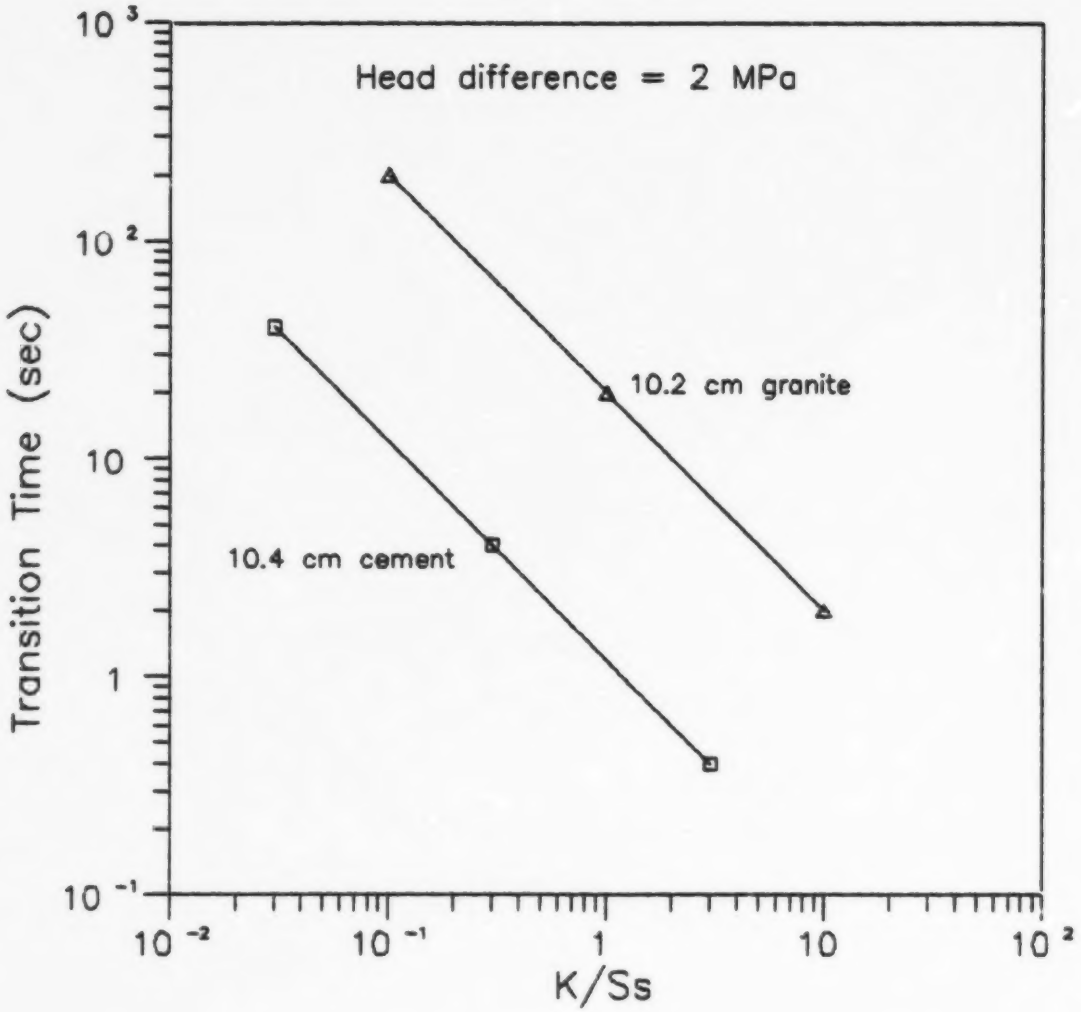

Figure 5.23 Transition time for transient to steady-state flow as a function of K/S_s (hydraulic diffusivity, cm^2/s) ratio. Transition time is inversely proportional to K/S_s.

BEST COPY AVAILABLE

well below the typical 48 hr test duration. The preceding discussion indicates that obtaining the actual value of specific storage, as well as hydraulic conductivity, is critical in determining when the flow reaches steady-state conditions. The severe difficulties that complicate determination of the specific storage are discussed by Neuzil (1986), who also discusses at considerable length the transient flow consequences of low permeability environments, which may very well develop near a repository.

CHAPTER SIX

SUMMARY, CONCLUSIONS, AND RECOMMENDATIONS FOR FURTHER RESEARCH

6.1 Summary

The objective of this research project is to provide an experimental performance assessment of cement borehole plugs subjected to laboratory dynamic loadings. This includes the study of dried plugs, as well as of plugs that have remained wet throughout the testing period.

Review of the literature indicates that deep underground structures in competent rocks are safer than surface structures, and are safer than openings at shallow depth or in fractured rocks, when subjected to earthquakes and large-scale subsurface blasts. It can be expected, therefore, that shaft or borehole seals installed at great (e.g. repository) depth in intimate contact with the surrounding rock walls should show minor, if any, effects from waves impacting on the sealed openings. This is especially true if the seals can be matched mechanically to the surrounding rock mass in order to minimize any impedance differences, and is particularly likely for boreholes, which, in all probability, will be filled over their entire length. The situation is less obvious for shaft plugs, which may be relatively short, i.e. with lengths of the same order of magnitude as the shaft diameter, and certainly much shorter than likely wavelengths.

Steady-state water flow tests have been conducted on cement borehole plugs installed in Charcoal granite cylinders, as well as on the granite rock bridge left in place when axial holes are drilled from both ends of the cylinder. The tests are performed by injecting distilled water into the seal, and measuring the inflows as well as the outflows to obtain the flow rate through the seal. Dynamic loads have been applied to the specimens during ongoing flow tests for various durations and accelerations. Dye markers have been injected during the last stage of the flow tests to identify the flow patterns in wet and in dried cement plugs.

6.2 Conclusions

The flow test results indicate that wet cement seals, i.e. cement borehole plugs that are never allowed to dry, are one order of magnitude less permeable than intact Charcoal granite. Sealing performance can degrade severely when cement seals are allowed to dry. During drying plugs suffer from decoupling along the cement/rock interface, and the permeability increases by several orders of magnitude. Visual inspection after sawing the specimens in half, upon completion of dye injection tests, shows that the flow penetrates the wet plugs uniformly, but occurs nearly exclusively along the plug/rock interface in the dried plugs. The permeability of wet and of dried cement seals does not change significantly after the application of dynamic loads.

The severe seal performance degradation observed when the cement dries out might take place for a seal located above the groundwater table, or in locations sufficiently close to the emplaced waste so that heat drives water away during the initial period following emplacement, or in locations where repository drainage (during construction and operation) results in temporary desaturation. When cement plugs are allowed to dry, they shrink. The subsequent separation along the plug/rock interface becomes a preferential flow path. Upon resaturation, the fissure permeability decreases rapidly, indicating partial closure of the interfacial gap due to cement swelling. This usually continues during the first two months of resaturation, and is followed by a leveling off in fissure permeability. However, this reestablished low permeability still remains several orders of magnitude higher than the permeability of wet cement plugs that are never allowed to dry. The seal performance is not fully recovered.

The extent of seal performance degradation seems related to the length of drying prior to resaturation and to the drying temperature. The longer the cement is allowed to dry and/or the higher the drying temperature is, the more severe the performance degradation. This is due in part to cracking in the cement body itself, which acts as an additional preferential flow path. The presence of a preferential flow path in a dried-out cement seal, as well as the absence thereof in wet cement seals, is confirmed by visual observation during and after dye injection testing.

Dynamic loading was applied during ongoing flow tests using a shaking table. The applied dynamic loads are considerably more severe, in some aspects, than what would be encountered during any likely earthquake or subsurface blast loading. Nevertheless, the effect on seal performance is minimal. Wet cement plug testing indicates that flow rate through the seal (hydraulic conductivity of the seal) does not change significantly after dynamic loads are applied. Permeability change as a result of the dynamic loads is less than permeability variation without dynamic loading. Seal permeability remains lower than the permeability of granite after dynamic loading. Even the fissure permeability of dried cement plugs is not affected by the dynamic loads. The permeability of the dried cement seals remains at the value before dynamic loads are applied. It needs to be pointed out here that the test sequence was such that these plugs already had been subjected to extended water flow testing prior to shaking, i.e. certainly were no longer dry at the time of shaking. Moreover, the dynamic loading (shaking) is applied externally to the plugged rock cylinders, which are accelerated as a unit. These experiments do not induce the potentially most damaging deformations, such as relative longitudinal strain between rock wall and seal, borehole bending, or hole deformations (Fig. 2.1).

The peripheral flow rate through the rock immediately surrounding the seal remains within the original range after dynamic loading tests. This indicates that no new cracks develop in the rock as a result of the applied dynamic loads.

Finite element analysis for one-dimensional flow shows that the transient (time-dependent) conditions at the beginning of each

individual flow test are of short duration relative to the individual test duration. For the short lengths of plugs used, the flow becomes steady in a short time. For all practical purposes, the flow during the tests can be considered as steady-state.

6.3 Suggestions for Future Investigations

The dynamic loading tests performed on the cement-plugged granite cylinders were much more severe in terms of acceleration, velocity amplitude, and duration than what may be realistically experienced. However, size will affect seal performance during an earthquake. In a centrifuge test using models with linear scaling of 1/n, an acceleration scaling factor of n times field acceleration is commonly used (Schofield, 1981, Craig, 1982). For example, an acceleration of 2 g in a model seal 1 inch (2.5 cm) in diameter (as used in these tests) results in identical stresses with that produced by an acceleration of 0.02 g in a prototype seal 100 times in size (about 8.3 ft (2.5 m) in diameter). The Department of Energy has indicated that the typical shaft diameter for a HLW repository is between 21 to 31 ft (U.S. Department of Energy, 1984). Clearly, it would be desirable to perform shaking tests on larger diameter cylinders and seals, and at higher accelerations.

Another factor to be considered in dynamic loading simulations is the duration of the applied load. For models having a linear scaling of 1/n, the time scaling for dynamic displacement which eventually results in increased flow is also 1/n. On the other hand, for diffusion processes or fluid flow the scale factor is $1/n^2$. Hence, the maximum duration for which shaking has been applied here considerably exceeds the likely, even scaled, duration of an actual earthquake. Difficulties arise from the conflicts in selecting the various scaling factors, and a more detailed study along these lines is required. Coates (1981) mentions the problems in trying to fulfill all the similitude requirements (i.e. geometric, kinematic and dynamic similitudes) between the model and the prototype in some cases. Smith (1977) discusses the problems associated with centrifugal modeling in geotechnical engineering, i.e. time scaling and viscous effects in dynamic problems and stress-path considerations.

At the very extreme case, dynamic loading can be considered as impact or transient loading, such as when blasting is carried out adjacent to a plug/rock system. The stresses that might be induced in the plug/rock interface could be simulated by a hammer blow to the sides of a rock specimen containing a borehole seal. In principle, this type of experiment is relatively simple and inexpensive to perform. It would require tight control on impact mass and velocity, and should be accompanied by wave monitoring. Frequencies are likely to be extremely high. The result should give some indication of the upper bound values of stresses in the plug/rock system due to dynamic loads, and how they might affect the permeability. It would be desirable to perform such experiments with controlled hammer (projectile) impacts, such that short wavelength pulses of known magnitude are generated, designed to maximize differential deformation between borehole and plug. Such impacts should be generated both longitudinally and transversely.

The experimental results proclaimed here for dried plugs subjected to shaking have actually been obtained on plugs that had been subjected to renewed waterflow testing for extended periods of time (weeks, as a minimum) prior to shaking. Particularly to represent unsaturated zone conditions, where airflow is likely to be a significant sealing consideration, it would be desirable to complement waterflow testing with airflow testing. This will promote accelerated plug drying, rather than reverse the drying, resaturate, and reverse the shrinkage. A more severe test will result from testing shrunk plugs. Such tests should be performed on plugs subjected to longitudinal and to transverse shaking.

Drying of cement seals has proven to be a critical factor controlling the sealing performance. Every effort should be made to keep cement seals saturated at all times, or certainly for sufficient time to assure complete curing. Allowing cement seals to dry out prematurely will cause cement shrinkage that in turns creates preferential paths for the flow along the plug/rock interfacial separation. Minimizing seal shrinkage by mixing the cement with sand, aggregates or other materials, or by using techniques such as carbonization, is another area in need of further investigation.*

To better understand the time-dependent behavior of cement seals in terms of their permeability, long-term flow testing would be necessary. It is important not only for wet cement seals, but especially for dried-out cement seals to see to what extent the improvement in seal performance will continue with continuous resaturation.

The cement and interface behavior under different moisture conditions are still not fully understood. A more comprehensive test could be devised to measure the expansive stress and stress relief of cement seals at different stages, from pouring, during curing and hardening, at saturated condition, during drying-out and finally at resaturation. It would be desirable to perform such tests at several temperatures, covering the temperature ranges likely to be encountered in the repository environment, as well as over ranges of degrees of saturation of the rock in which the seals are emplaced. The latter types of experiments, preferably, should include testing of seals emplaced in rock with permeabilities and porosities representative for emplacement in unsaturated formations. By controlling the environment in which the blocks are emplaced during curing, a reasonable simulation of unsaturated zone curing and aging should be possible.

All indications are that considerable drying may take place for plugs emplaced in some locations near any repository, as a result of heat generated by the emplaced waste. In all probability such a drying environment will be enhanced significantly for a seal location in an initially unsaturated environment, and where subsequent water infiltration is likely to be very slow. Further deterioration in seal performance probably will result if considerable airflow through the

---

*Personal communications with Erik Nelson (Dowell) and Herbert Brunner (Nukem GmbH), 1984.

plugs takes place. Clearly, this combination of conditions is likely to be encountered at the proposed Yucca Mountain repository site. Such unsaturated, and especially dry conditions assuredly will pose challenging requirements, both for cementitious and for earthen (e.g. bentonitic) seals, with a probable need for particular attention to shrinkage control. Experiments simulating severe, yet not unrealistic, environmental situations that induce such types of performance degradation deserve high priority. They should specifically include such aspects as simulation of curing of cement when emplaced in an unsaturated rock, as well as the effects of drying, airflow, and possibly re-wetting on older hardened cementitious seals.

REFERENCES

Adisoma, G.S. and J.J.K. Daemen, 1984, "Laboratory Assessment of the Effect of Drying on the Performance of Cement Borehole Plugs", Proc. Waste Management '84 Symposium, Vol. 1, R.G. Post (Ed.), Tucson, AZ, March 11-15, pp. 579-583.

Akgun, H. and J.J.K. Daemen, 1986, "Size Influence on the Sealing Performance of Cementitious Borehole Plugs," NUREG/CR-4738, Technical Report, prepared for the Division of Engineering Safety, Office of Nuclear Regulatory Research, U.S. Nuclear Regulatory Commission, by the Department of Mining and Geological Engineering, University of Arizona, Tucson.

Algermissen, S.T., 1980, "Some Aspects of the Seismic Hazards Associated with Radioactive Waste Disposal", Geological Survey Open File Report 80-2017, US Department of the Interior.

Allen, T.J. and A.P. Roberts, 1982, Production Operations - Well Completions, Workover, and Stimulation. Oil and Gas Consultants International, Inc., Tulsa.

American Petroleum Institute, 1977, "Specification RP-10B, Testing Oil Cements and Cement Additives", Twentieth Edition, API, Dallas, TX.

Anttonen, G.J., J.E. O'Rourke, C.L. Taylor, and S.C. McCarel, 1980, "Preconceptual Plug Design," Section 3.7, pp. 3-139/213, Smith et al., 1980.

Applied Technology Council, 1978, "Tentative Provisions for the Development of Seismic Regulations for Buildings", NBS Special Publication 510, National Bureau of Standards, Washington, DC.

Ariman, T. and G.E. Muleski, 1979, "A Review of the Response of Buried Pipelines under Seismic Excitations," pp. 1-29, Lifeline Earthquake Engineering - Buried Pipelines, Seismic Risk, and Instrumentation, PVP-34, T. Ariman, S.C. Liu, and R.E. Nichell (Eds.), The American Society of Mechanical Engineers, New York.

Arnett, R.C., R.G. Baca, J.A. Caggiano, and D.J. Carrell, 1980, "Radionuclide Release Scenario Selection Process for a Possible Basalt Repository," pp. 131-140, Radioactive Release Scenarios for Geologic Repositories, Proceedings of the NEA Workshop, Paris, September 1980. Published by The OECD Nuclear Energy Agency, Paris, 1981.

ASTM C 39-83b, "Standard Test Method for Compressive Strength of Cylindrical Concrete Specimens," Annual Book of ASTM Standards, Vol. 04.02, Concrete and Mineral Aggregates. American Society for Testing and Materials, Philadelphia, PA.

ASTM D 2938-79, "Standard Test Method for Unconfined Compressive Strength of Intact Rock Core Specimens," Annual Book of ASTM Standards, Vol. 04.08, Soil and Rock; Building Stones. American Society for Testing and Materials, Philadelphia, PA.

Atomic Energy of Canada Limited, 1978, Management of Radioactive Fuel Wastes: the Canadian Disposal Program, AECL-6314, J. Boulton (ed.), Atomic Energy of Canada Research Company, Whiteshell Nuclear Research Establishment, Pinawa, Manitoba, Canada, Oct.

Bach, P.S., 1977, "A Summary of Studies on Underground Power Plant Siting", Underground Space, Vol. 2, No. 1, Pergamon Press, New York, NY, pp. 47-51.

Barbreau, A., R. Heremans, and B. Skytte Jensen, 1980, "Radionuclide Migration in Geological Formations," pp. 515-530, Radioactive Waste Management and Disposal, Proceedings of the First European Community Conference, Luxemburg, May 20-23. R. Simon and S. Orlowski, Editors. Harwood Academic Publishers.

Barton, N.R., R. Lien, and J. Lunde, 1974, "Engineering Classification of Rock Massses for the Design of Tunnel Support", Rock Mechanics, Vol. 6, No. 4, pp. 189-236.

Barton, N., A. Makurat, M. Christianson, and S. Bandis, 1987, "Modelling Rock Mass Conductivity Changes in Disturbed Zones," pp. 563-574, Proceedings of the 28th U.S. Symposium on Rock Mechanics, I.W. Farmer et al. (Eds.), Tucson, AZ. A.A. Balkema, Rotterdam.

Bathe, K.-J., 1978, "ADINA - A Finite Element Program for Automatic Dynamic Incremental Nonlinear Analysis", MIT Report 82448-1, December.

Bathe, K.-J., E. L. Wilson, and R. H. Iding, 1974, "NONSAP - A Structural Analysis Program for Static and Dynamic Response of Nonlinear Systems", Report No. UC SESM74-3, Department of Civil Engineering, University of California, Berkeley, CA.

Bauer, A., and P.N. Calder, 1971, "The Influence and Evaluation of Blasting on Stability", Proceedings of the 1st International Conference on Stability in Open Pit Mining, Vancouver, Canada, SME/AIME, New York, NY, pp. 83-95.

Bieniawski, Z.T., 1976, "Rock Mass Classifications in Rock Engineering", Proceedings of the Symposium on Exploration for Rock Engineering", Johannesburg, South Africa, Vol. 1, pp. 97-106.

Blake, L.S. (Ed.), 1975, Civil Engineer's Reference Book, Third Edition, Chapter 5 - Hydraulics, by J. Allen, Butterworths, London, Boston.

Boa, J.A., Jr., 1978, "Borehole Plugging Program (Waste Disposal), Report 1, Initial Investigations and Preliminary Data," Miscellaneous Paper C-78-1, U.S. Army Engineer Waterways Experiment Station, Vicksburg, MS.

Boulton, J. (Ed.), 1978, "Management of Radioactive Fuel Wastes: The Canadian Disposal Program", AECL-6314, Atomic Energy of Canada Limited, Atomic Energy of Canada Research Company, Whiteshell Nuclear Research Establishment, Pinawa, Manitoba.

Brace, W.F., 1980, "Permeability of Crystalline and Argillaceous Rocks", Int. Jour. Rock Mech. Min. Sci. & Geomech. Abstr., Vol. 17, No.5, pp. 241-251.

Brace, W.F., J.B. Walsh, and W.T. Frangos, 1968, "Permeability of Granite Under High Pressure", Jour. Geophysical Research, Vol. 73, No. 6, pp. 2225-2236.

Brebbia, C.A, J.C.F. Telles, and L.C. Wrobel, 1984, Boundary Element Techniques: Theory and Applications in Engineering, Springer-Verlag, Berlin.

Bredehoeft, J.D., A.W. England, D.B. Stewart, N.J. Trask, and I.J. Winograd, 1978, "Geologic Disposal of High-Level Radioactive Wastes - Earth-Science Perspectives," Geological Survey Circular 779, 15 + v pp., U.S. Geological Survey.

Brown, E.T., ed., 1981, Rock Characterization, Testing and Monitoring: ISRM Suggested Methods, Pergamon Press, London, 212 pp.

Browne, R.D., 1986, "Practical Considerations in Producing Durable Concrete," Ch. 4, pp. 97-116, Improvement of Concrete Durability, Proceedings of the Seminar, Institution of Civil Engineers, London, May 1985. Thomas Telford, London.

Browne, R.D. and A.F. Baker, 1979, "The Performance of Structural Concrete in a Marine Environment," Ch. 4, pp. 111-149, Developments in Concrete Technology - 1, F.D. Lydon, ed., Applied Science Publishers, Ltd., London.

Buck, A.D., 1985a, "Development of a Sanded Non-salt Expansive Grout for Repository Sealing Application," Miscellaneous Paper SL-85-6, prepared by Structures Laboratory, Department of the Army, Waterways Experiment Station, Corps of Engineers, Vicksburg, MS, for Department of Energy, Columbus, OH.

Buck, A.D., 1985b, "Development of Two Candidate Concrete Mixtures (Salt, Nonsalt) For Repository Sealing Applications," Miscellaneous Paper SL-85-8, prepared by Structures Laboratory, Department of the Army, Waterways Experiment Station, Corps of Engineers, Vicksburg, MS, for Department of Energy, Columbus, OH.

Buck, A.D., J.A. Boa, Jr., and D.M. Walley, 1985, "Development of a Sanded Expansive Salt Grout for Repository Sealing Application," Miscellaneous Paper SL-85-11, by Department of the Army, Waterways Experiment Station, Corps of Engineers, Vicksburg, MS, for Department of Energy, Columbus, OH.

Buck, A.D. and K. Mather, 1982, "Grout Formulations for Nuclear Waste Isolation," Report No. ONWI-413, Office of Nuclear Waste Isolation, Battelle Memorial Institute, Columbus, OH. Miscellaneous Paper SL-82-6, Structures Laboratory, U.S. Army Engineer Waterways Experiment Station, Vicksburg, MS.

Buck, A.D., J.E. Rhoderick, J.P. Burkes, K. Mather, R.E. Reinhold, and J.A. Boa, Jr., 1983, "Modification of Bell Canyon Test (BCT) 1-FF Grout," Miscellaneous Paper SL-83-18, prepared for Office of Nuclear Waste Isolation, Battelle Memorial Institute, Columbus, OH, and Sandia National Laboratories (Report No. SAND 83-7097), by Structures Laboratory, U.S. Army Engineer Waterways Experiment Station, Vicksburg, MS.

Burkes, J.P. and J.E. Rhoderick, 1983, "Petrographic Examination of Bell Canyon Tests (BCT) 1-FF Field Grouts Over a Three-Year Period," Miscellaneous Paper SL-83-12, Structures Laboratory, U.S. Army Engineer Waterways Experiment Station, Vicksburg, MS, prepared for Office of Nuclear Waste Isolation, Battelle Memorial Institute, Columbus, OH, and Sandia National Laboratories, Albuquerque, NM.

Burkholder, H.C., 1980, "The Development of Release Scenarios for Geologic Nuclear Waste Repositories," pp. 13-26, Radionuclide Release Scenarios for Geologic Repositories, Proceedings of the NEA Workshop, Paris, Sept. 1980. Published by The OECD Nuclear Energy Agency, Paris, 1981.

Burnett, N.C., R.D. Hooton, R.B. Heimann, and M. Onofrei, 1985, "The Development of Durable Cementitious Materials for Use in a Nuclear Fuel Waste Disposal Facility," pp. 461-468, Scientific Basis for Nuclear Waste Management IX, L.O. Werme (Ed.). Symposium held in Stockholm, Sweden, September 1985. Materials Research Society Symposia Proceedings, Vol. 50, Materials Research Society, Philadelphia, PA.

Burns, F.L., R. Lingle, and A. Andrews, 1982, "Cement-Plug Leakage and Drilling Damage Evaluated," pp. 120-129, Oil and Gas Journal, Vol. 80, No. 22, Nov. 22.

Bush, D.D. and R. Lingle, 1986, "A Full-Scale Borehole Sealing Test in Anhydrite Under Simulated Downhole Conditions," BMI/ONWI-581(1), Vol. 1, Technical Report prepared for Office of Nuclear Waste Isolation, Battelle Memorial Institute, Columbus, OH.

Bush, D.D. and S. Piele, 1986, "A Full-Scale Borehole Sealing Test in Salt Under Simulated Downhole Conditions," Volume 1, Technical

Report BMI/ONWI-573(1), prepared by Terra Tek, Inc., for Office of Nuclear Waste Isolation, Battelle Memorial Institute, Columbus, OH.

Carlsson, H.S., 1982, "The Proposed Phase II of the International Stripa Project," pp. 187-196, Geological Disposal of Radioactive Waste - In Situ Experiments in Granite, Proceedings of the Stockholm, Sweden, October 1982 Workshop. Nuclear Energy Agency, OECD, Paris, France, 1983.

Central Electronics Laboratory, 1983, "Sinusoid g-Meter" Manual, University of Arizona Instrument Shop, Tucson, AZ.

Chabannes, C.R., Stephenson, D.E., and R.D. Ellison, 1980, "A Preliminary Evaluation of Various Sealing Configurations," pp. 65-76, Proceedings, Borehole and Shaft Plugging, Workshop, Columbus, OH, May. Published by OECD, Paris.

Christensen, C.L., 1979, "Test Plan - Bell Canyon Test - WIPP Experimental Program - Borehole Plugging," SAND 79-0739, prepared by Sandia National Laboratories, Albuquerque, NM, for U.S. Department of Energy.

Christensen, C.L., 1980a, "Borehole Plugging Program Status Report, October 1, 1978 - September 30, 1979," SAND 79-2141, prepared by Sandia National Laboratories, Albuquerque, NM, for the U.S. Department of Energy.

Christensen, C.L., 1980b, "Sandia Borehole Plugging Program for the Waste Isolation Pilot Plant", Sandia National Laboratories Report No. SAND 80-0390C, paper presented at the Workshop on Borehole and Shaft Plugging, Columbus, OH, May 1980, Proceedings, pp. 225-231. Published by OECD, Paris.

Christensen, C.L. and T.O. Hunter, 1979, "Waste Isolation Pilot Plant (WIPP) Borehole Plugging Program Description," SAND 79-0640, Sandia National Laboratories, Albuquerque, NM.

Christensen, C.L. and E.W. Peterson, 1981, "The Bell Canyon Test Summary Report," SAND 80-1375, prepared by Sandia National Laboratories, Albuquerque, NM, for the U.S. Department of Energy.

Coates, D.F., 1981, Rock Mechanics Principles, Monograph 874, Revised Fourth Edition, CANMET, Energy, Mines and Resources Canada, Ottawa, Appendix F.

Cobb, S.L. and J.J.K. Daemen, 1982, "Polyaxial Testing of Borehole Plug Performance", Topical Report, prepared for U.S. Nuclear Regulatory Commission, SAFER Division, Office of Nuclear Regulatory Research, by the Department of Mining and Geological Engineering, University of Arizona, Tucson, AZ, July, 180 pp.

Committee on Radioactive Waste Management, 1978, "Geological Criteria for Repositories for High-Level Radioactive Wastes", National Research Council/National Academy of Sciences, Washington, DC.

Cook, H.K., 1951, "Permeability Tests of Lean Mass Concrete," Proceedings of the American Society for Testing and Materials, Vol. 51, pp. 1156-65.

Coons, W.E., D. Meyer, and P.C. Kelsall, 1982, "Evaluation of Polymer Concrete for Application to Repository Sealing," OWWI-410, prepared by D'Appolonia Consulting Engineers, Inc., for Office of Nuclear Waste Isolation, Battelle Memorial Institute, Columbus, OH.

Corps of Engineers, U.S. Army, 1954, "Permeability and Triaxial Tests of Lean Mass Concrete," Technical Memorandum No. 6-380, prepared for Office, Chief of Engineers, by Waterways Experiment Station, Vicksburg, MS.

Craig, W.H., 1982, "Conflicts in Dynamic Modeling in Geomechanics", in Design for Dynamic Loading, the Use of Model Analysis, G.S.T. Armer and F.K. Garas (Eds.), Construction Press, London and New York, pp 1-6.

Crouch, S.L., and A.M. Starfield, 1983, Boundary Element Methods in Solid Mechanics, George Allen & Unwin, London.

Daemen, J.J.K., 1981, "Borehole Studies of Rock Engineering Problems in Large-Scale Laboratory Equipment," Geophysical Research Letters, Vol. 8, No. 7, pp. 711-714, July.

Daemen, J.J.K., D.L. South, W.B. Greer, J.C. Stormont, S.A. Dischler, G.S. Adisoma, N.I. Colburn, K. Fuenkajorn, D.E. Miles, B. Kousari, and J. Bertuca, 1983, "Rock Mass Sealing - Annual Report, June 1, 1982 - May 31, 1983," NUREG/CR-3473, prepared for the U.S. Nuclear Regulatory Commission, Division of Radiation Programs and Earth Sciences, by the Department of Mining and Geological Engineering, University of Arizona, Tucson.

Daemen, J.J.K., W.B. Greer, G.S. Adisoma, K. Fuenkajorn, W.D. Sawyer, Jr., A. Yazdandoost, H. Akgun, and B. Kousari, 1985, "Rock Mass Sealing - Annual Report, June 1, 1983 - May 31, 1984," NUREG/CR-4174, prepared for the U.S. Nuclear Regulatory Commission, Division of Radiation Programs and Earth Sciences, by the Department of Mining and Geological Engineering, University of Arizona, Tucson.

Daemen, J.J.K., W.B. Greer, K. Fuenkajorn, H. Akgun, T.S. Avery, J.R. Williams, A.F. Kimbrell, A. Schaffer, and B. Kousari, 1986, "Rock Mass Sealing - Annual Report, June 1, 1984 - May 31, 1985," NUREG/CR-4642, prepared for the U.S. Nuclear Regulatory Commission, Division of Radiation Programs and Earth Sciences, by the Department of Mining and Geological Engineering, University of Arizona, Tucson.

D'Appolonia Consulting Engineers, Inc., 1978, "Development of Plan and Approach for Borehole Plugging Field Testing," ONWI-3, Office of Nuclear Waste Isolation, Battelle Memorial Institute, Columbus, OH.

Datta, S.K., and A.H. Shah, 1982, "Dynamic Response of Buried Pipelines and Tunnels", Earthquake Ground Motion and Its Effects on Structures, AMD - Vol. 53, S. K. Datta (Ed), ASME, New York, NY, pp. 181-197.

Davis, H.S., 1972, "N-Reactor Shielding," Paper SP 34-52, pp. 1109-1161, Vol. II, Concrete for Nuclear Reactors, Special Publication SP-34, American Concrete Institute, Detroit, MI.

Deju, R.A., 1983, "Testimony of Dr. Raul A. Deju, Basalt Waste Isolation Project", before the Subcommittee on Energy Research and Production, Committee on Science and Technology, United States House of Representatives, Washington, DC, March 2, 9:30 am, RHO-BW-SA-293P, Rockwell Hanford Operations, Richland, WA.

Desai, C.S., (Ed.), 1976, Numerical Methods in Geomechanics, Vols. 1-3, ASCE, New York, NY.

Desai, C.S., 1979, Elementary Finite Element Method, Prentice-Hall, Inc., Englewood Cliffs, NJ.

Desai, C.S., and J.F. Abel, 1972, Introduction to the Finite Element Method, Van Nostrand Reinhold Co., New York, NY.

Desai, C.S., and J.T. Christian, (Eds.), 1977, Numerical Methods in Geotechnical Engineering, McGraw-Hill, New York, NY.

DeSalvo, G.J., and J.A. Swanson, 1979, "ANSYS Engineering Analysis System User's Manual", Swanson Analysis Systems, Inc., July.

Dowding, C.H., 1977, "Lifeline Viability of Rock Tunnels - Empirical Correlations and Future Research Needs," pp. 320-336, The current state of knowledge of Lifeline Earthquake Engineering, Proceedings Technical Council on Lifeline Earthquake Engineering Specialty Conference, University of California, Los Angeles, CA, Aug. Published by American Society of Civil Engineers, New York.

Dowding, C.H., 1977, "Seismic Stability of Underground Openings", Proceedings of the Rockstore Conference, Stockholm, Sweden, Vol. 2, pp. 231-238, M. Bergman (Ed.), Pergamon Press, Oxford.

Dowding, C.H., 1978, "Response of Rock Tunnels to Earthquake Shaking," pp. 1347-1351, Vol. III, Proceedings of the ASCE Geotechnical Engineering Division Specialty Conference, Earthquake Engineering and Soil Dynamics, Pasadena, CA, June. Published by American Society of Civil Engineers, New York.

Dowding, C.H., C. Ho, and T.B. Belytschko, 1983, "Earthquake Response of Caverns in Jointed Rock," pp. 142-156, Seismic Design of Embankments and Caverns, T.R. Howard (Ed.), American Society of Civil Engineers, New York.

Dowding, C.H., and A. Rozen, 1978, "Damage to Rock Tunnels from Earthquake Shaking", Journal of the Geotechnical Engineering Division, ASCE, Vol. 104, No. GT2, February, pp. 175-191.

Eberbach Corporation, 1974, "Use and Care of No. 5900 Shaker Power Unit, Reciprocating, Variable Speed, Large Floor Model", Ann Arbor, MI.

Eckel, E.B., 1970, "The March 1964 Alaska Earthquake - Lessons and Conclusions," U.S.G.S. Professional Paper 546, U.S. Geological Survey, Reston, VA.

Eilers, L.H., 1973, "Borehole Sealing - Final Report," ORNL/Sub/15966-73/1, prepared by Dowell, A Division of Dow Chemical Co., for Oak Ridge National Laboratory.

Eilers, L.H., 1974, "Sealing AEC No. 1 Well at Lyons, Kansas," ORNL/Sub/33542-74/1, prepared by Dowell, A Division of Dow Chemical Co., for Oak Ridge National Laboratory.

Einstein, H.H., and C.W. Schwartz, 1979, "Simplified Analysis for Tunnel Supports", Journal of the Geotechnical Engineering Division, ASCE, Vol. 105, No. GT4, April, pp. 499-518.

Einstein, H.H., W. Steiner, and G.B. Baecher, 1979, "Assessment of Empirical Design Methods for Tunnels in Rock". Proceedings of the 1979 Rapid Excavation and Tunneling Conference, Atlanta, GA, Vol. 1, AIME, New York, NY, pp. 683-706.

EMG Accumulators, Inc., 1982, "General Parts Breakdown, Installation and Service Instruction, 'Kwik-Kap Accumulators", a subsidiary of Baxter Technologies, Inc., Port Huron, MI.

England, G.L. and A.D. Ross, 1972, "Shrinkage, Moisture, and Pore Pressures in Heated Concrete," Paper SP 34-42, pp. 883-907, Vol. II, Concrete for Nuclear Reactors, Special Publication SP-34, American Concrete Institute, Detroit, Michigan.

Fernandez, J.A. and M.D. Freshley, 1984, "Repository Sealing Concepts for the Nevada Nuclear Waste Storage Investigations Project," SAND 83-1778. Prepared for the U.S. Department of Energy under Contract DE-AC04-76DP00789 by Sandia National Laboratories, Albuquerque, NM, August.

Fernandez, J.A., P.C. Kelsall, J.B. Case, and D. Meyer, 1987, "Technical Basis for Performance Goals, Design Requirements, and Material Recommendations for the NNWSI Repository Sealing Program," SAND 84-1895, prepared for the U.S. Department of Energy by Sandia National Laboratories, Albuquerque, NM and Livermore, CA.

Freeze, R.A. and J.A. Cherry, 1979, Groundwater, Prentice-Hall, Englewood Cliffs, NJ, 604 pp.

Freshley, M.D., F.H. Dove, and J.A. Fernandez, 1985, "Hydrologic Calculations to Evaluate Backfilling Shafts and Drifts for a Prospective Nuclear Waste Repository in Unsaturated Tuff," Sandia Report SAND 83-2465, prepared by Sandia National Laboratories, Albuquerque, New Mexico, for the U.S. Department of Energy under Contract DE-AC04-76DP00789.

Goto, S. and D.M. Roy, 1981, "The Effect of W/C Ratio and Curing Temperature on the Permeability of Hardened Cement Paste," Cement and Concrete Research, Vol. 11, no. 4, pp. 575-579.

Graham, J.R. and J.E. Backstrom, 1975, "Influence of Hot Saline and Distilled Waters on Concrete," Paper SP 47-15, pp. 325-341, Durability of Concrete, Publication SP-47, American Concrete Institute, Detroit, MI.

Grutzeck, M.W., and D.M. Roy, 1985, "Experimental Characterization and Stability of Salt- and Nonsalt-Containing Grouts and Mortars (BCT-IF- and BCT-IFF-related)," Technical Report BMI/ONWI-568, prepared by Materials Research Laboratory, Pennsylvania State University, for Office of Nuclear Waste Isolation, Battelle Memorial Institute, Columbus, OH.

Gulick, C.W., Jr., J.A. Boa, Jr., and A.D. Buck, 1980a, "Bell Canyon Test (BCT) Cement Grout Development Report," SAND 80-1928, Sandia National Laboratory, Albuquerque, NM.

Gulick, C.W., Jr., J.A. Boa, Jr., D.M. Walley, and A.D. Buck, 1980b, "Borehole Plugging Materials Development Program Report," SAND 79-1514, Sandia National Laboratory, Albuquerque, NM.

Gureghian, A.B., L.A. Scott, and G.E. Raines, 1983, "Performance Assessment of a Shaft Seals System in a HLW Repository in the Gibson Dome Area," ONWI-494, Office of Nuclear Waste Isolation, Battelle Memorial Institute, Columbus, OH.

Harr, M.E., 1962, Groundwater and Seepage, McGraw-Hill, New York, NY, 315 pp.

Harr, M.E., 1977, Mechanics of Particulate Media: A Probabilistic Approach, McGraw-Hill, New York, NY, 543 pp.

Heckman, R.A., and C. Minichino, 1982, Nuclear Waste Management Abstract, IFI/Plenum, New York, NY.

Heineman, R.E., W.A. Carbiener, and S.J. Basham, "The Technical Program for Establishing the Scientific Basis for Geological Disposal," DOE Environmental Control Symposium, Washington, DC, November 28-30.

Hendron, A.J., Jr., and G. Fernandez, 1983, "Dynamic and Static Design Considerations for Underground Chambers," pp. 157-197, Seismic Design of Embankments and Caverns, T.R. Howard (Ed.), American Society of Civil Engineers, New York.

Higginson, E.C., 1961, "Effect of Steam Curing on the Important Properties of Concrete," pp. 281-298, Vol. 58, Journal of the American Concrete Institute, September.

Hildebrand, F.F., 1976, Advanced Calculus for Applications, Second Edition, Prentice-Hall, Englewood Cliffs, NJ, 733 pp.

Hodges, F.N., J.E. O'Rourke, and G.J. Anttonen, 1980, "Sealing a Nuclear Waste Repository in Columbia River Basalt: Preliminary Results," pp. 143-160, Proceedings, Borehole and Shaft Plugging, Workshop, Columbus, OH, May. Published by OECD, Paris.

Hoek, E., and E.T. Brown, 1980, Underground Excavations in Rock, The Institution of Mining and Metallurgy, London.

Hofmann, R., 1976, "STEALTH - A Lagrange Explicit Finite Difference Code for Solids, Structural, and Thermohydraulic Analysis", EPRI NP-176-1, Electric Power Research Institute, Palo Alto, CA, June.

Holmberg, R., 1982, "Charge Calculations for Tunneling", in Underground Mining Methods Handbook, W.A. Hustrulid (Ed.), SME/AIME, New York, NY, pp. 1580-1589.

Holmberg, R., and K. Maki, 1982, "Case Examples of Blasting Damage and Its Influence on Slope Stability", Proceedings of the Third International Conference on Stability in Surface Mining, Vancouver, Canada, C. O. Brawner (Ed.), SME/AIME, New York, NY, pp. 775-778.

Holmberg, R., B. Larsson, and C. Sjoberg, 1984, "Improved Stability through Optimized Rock Blasting", Proceedings of the Tenth Conference on Explosives and Blasting Technique, C. J. Konya (Ed), Society of Explosives Engineers Annual Meeting, Orlando, FL, p. 173.

Holmes, R.S., L.T. Kwan, E.H. Skinner, E.Y. Wong, 1963, "Loading, Response, and Evaluation of Tunnels and Tunnel Liners in Granite," POR-1801, Operation Nougat, Shot Hard Hat, Holmes & Narver, Inc., Los Angeles, CA, April.

Hsieh, P.A., J.V. Tracy, C.E. Neuzil, J.D. Bredehoeft, and S.E. Silliman, 1981, "A Transient Laboratory Method for Determining the Hydraulic Properties of 'Tight' Rocks - I. Theory," Int. Jour. Rock Mech. Min. Sci. and Geomech. Abstr., Vol. 18, pp. 245-252.

Intera Environmental Consultants, Inc., 1981, "Consequence Assessment of Hydrological Communications Through Borehole Plugs," Contractor Report SAND 81-7164, Prepared for Sandia National Laboratories, Albuquerque, NM, November.

Irish, E.R., 1980, "Safety Assessment for the Underground Disposal of Radioactive Wastes - The IAEA Programme," pp. 39-43, Radionuclide Release Scenarios for Geologic Repositories, Proceedings of the NEA Workshop, Paris, September 1980. Published by The OECD Nuclear Energy Agency, Paris, 1981.

Isenberg, J. and C.E. Taylor, 1984, "Performance of Water and Sewer Lifelines in the May 2, 1983 Coalinga, California Earthquake," pp. 176-189, Lifeline Earthquake Engineering: Performance, Design and Construction, J.D. Cooper (Ed.), American Society of Civil Engineers, New York.

Ishii, S., K. Hitotsuya, Y. Izume, K. Soeda, 1982, "Development and Application of Non-Explosive Demolition Agent Used Limestone as Main Material", Onoda Cement Co., Paper presented at the First International SME-AIME Fall Meeting, Honolulu, HI, Sept. 4-9, 1982.

Iwasaki, T., K. Kawashima, and Y. Tajimi, 1981, "Seismic Response of Subsurface Ground with Use of Measured Underground Acceleration," Proc. Int. Conf. on Recent Advances in Geotechnical Earthquake Engineering and Soil Dynamics, Vol. 1, S. Prakash (Ed.), University of Missouri, Rolla, April 26 - May 3, pp. 537-540.

Iwasaki, T., S. Wakabayashi, and E. Tatsuaka, 1977, "Characteristics of Underground Seismic Motions at Four Sites around Tokyo Bay," Wind and Seismic Effects, H.S. Lew (Ed.), U.S. Department of Commerce, May.

Jaeger, J.C., and N.G.W. Cook, 1979, Fundamentals of Rock Mechanics, Third Edition, Chapman and Hall, London.

Kalia, H.N., 1986, "ERG and GRG Review of the Draft of 'Preliminary Test Plan for In Situ Testing From an Exploratory Shaft in Salt - October 1983,'" BMI/ONWI-591, Technical Report, Office of Nuclear Waste Isolation, Battelle Memorial Institute, Columbus, OH, March.

Kaplan, M.F., "Summary: Concrete for the Containment and Shielding of Nuclear Reactors," Paper SP 34-74, pp. 1625-1636, Vol. III, Concrete for Nuclear Reactors, Special Publication SP-34, American Concrete Institute, Detroit, Michigan.

Kelsall, P.C., J.B. Case, D. Meyer, and W.E. Coons, 1982, "Schematic Designs for Penetration Seals for a Reference Repository in Bedded Salt," Report No. ONWI-405, prepared by D'Appolonia Consulting Engineers, Inc., Albuquerque, NM, for Office of Nuclear Waste Isolation, Battelle Memorial Institute, Columbus, OH.

Kienzler, B. and E. Korthaus, 1982, "Untersuchungen zur Ausbildung von Laugezuflusswegen im Steinsalz" (Investigations of the development of brine inflow paths in rock salt), KfK 3411, Kernforschungszentrum Karlsruhe.

Klingsberg, C. and J. Duguid, 1980, "Status of Technology for Isolating High-Level Radioactive Wastes in Geologic Repositories," DOE/TIC 11207 (Draft), U.S. Department of Energy, Office of Waste Isolation, Washington, DC, October.

Kobayashi, S., and N. Nishimura, 1982, "Transient Stress Analysis of Tunnels and Caverns of Arbitrary Shape due to Travelling Waves", in Developments in Boundary Element Methods, Vol. 2, P. K. Banerjee and R. P. Shaw (Eds.), Applied Science Publishers, London, pp. 177-210.

Kocher, D.C., A.L. Sjoreen, and C.S. Bard, 1983, "Uncertainties in Geologic Disposal of High-level Wastes - Groundwater Transport of Radionuclides and Radiological Consequences," NUREG/CR-2506; ONRL-5838; 214 + xiv pp., prepared for the U.S. Nuclear Regulatory Commission by Oak Ridge National Laboratory, Oak Ridge, Tennessee, July.

Koplik, C.M., D.L. Pentz, and R. Talbot, 1979, "Information Base for Waste Repository Design, Vol. 1: Borehole and Shaft Sealing," NUREG/CR-0495, prepared by The Analytic Sciences Corp. for the U.S. Nuclear Regulatory Commission, Washington, DC.

Labreche, D.A., 1983, "Damage Mechanisms in Tunnels Subjected to Explosive Loads," pp. 128-141, Seismic Design of Embankments and Caverns, T.R. Howard (Ed.), American Society of Civil Engineers, New York.

Lambe, T.W. and R.V. Whitman, 1979, Soil Mechanics, S.I. Version, John Wiley & Sons, New York, NY, 553 pp.

Langefors, U., and B. Kihlstrom, 1963, The Modern Technique of Rock Blasting, John Wiley & Sons, New York, NY.

Langefors, U., and B. Kihlstrom, 1978, The Modern Technique of Rock Blasting, Third Edition, John Wiley & Sons, New York, NY.

Leonards, G.A., (Ed.), 1962, Foundation Engineering, McGraw-Hill, New York, NY.

Lingle, R., K.L. Stanford, P.E. Peterson, and S.F. Woodhead, 1982, "Wellbore Damage Zone Experimental Determination," Report No. ONWI-349, Office of Nuclear Waste Isolation, Battelle Memorial Institute, Columbus, OH.

Lorig, L.J., 1985, "A Simple Numerical Representation of Fully Bonded Passive Rock Reinforcement for Hard Rocks," Computers and Geotechnics, Vol. 1, pp. 79-97.

Lorig, L.J. and B.G.H. Brady, 1984, "A Hybrid Computational Scheme for Excavation and Support Design in Jointed Rock Media," Paper 13, pp. 105-112, ISRM Symposium Design and Performance of Underground Excavations, Cambridge, U.K., September, E.T. Brown and J.A. Hudson (Eds.), British Geotechnical Society, London.

Manolis, G.D. and D.E. Beskos, 1981, "Dynamic Analysis of Buried Structures", Proceedings of the International Conference on Recent Advances in Geotechnical Earthquake Engineering and Soil Dynamics, Rolla, MO, Vol. 1, pp. 295-297.

Marechal, J.C., 1972, "Creep of Concrete as a Function of Temperature," Paper Sp 34-30, pp. 547-564, Vol. I, Concrete for Nuclear Reactors, Special Publication SP-34, American Concrete Institute, Detroit, MI.

Marine, I.W., H.R. Pratt, and K.K. Wahi, 1982, "Seismic Effects on Underground Openings," pp. 179-206, The Technology of High-Level Nuclear Waste Disposal, Vol. 2, P.L. Hofmann (Ed.), DOE/TIC-4621(Vol. 2), Technical Information Center, Office of Scientific and Technical Information, U.S. Department of Energy. Available as DE 82009593 from NTIS.

Mather, B., 1967, "Cement Performance in Concrete," Technical Report 6-787, U.S Army Corps of Engineers, Waterways Experiment Station, Vicksburg, MS.

Matheson Catalog, 1981, Matheson Division of Searle Medical Products, USA, Inc.

McDaniel, E.W., 1980, "Cement Technology for Borehole Plugging: An Interim Report on Permeability Measurements of Cementitious Solids," ORNL/TM-7092, Oak Ridge National Laboratory, Oak Ridge, Tennessee.

McDonald, J.E., 1972, "An Experimental Study of Moisture Migration in Concrete," Paper SP-34-45, pp. 957-989, Vol. II, Concrete for Nuclear Reactors, Special Publication SP-34, American Concrete Institute, Detroit, MI.

McGarr, A., 1983, "Estimating Ground Motions for Small Nearby Earthquakes," pp. 113-127, Seismic Design of Embankments and Caverns, T.R. Howard (Ed.), American Society of Civil Engineers, New York.

McGarr, A., R.W.E. Green, and S.M. Spottiswoode, 1981, "Strong Ground Motion of Mine Tremors: Some Implications for Near-Source Ground Motion Paramaters," Bull. Seism. Soc. Am., Vol. 71, pp. 295-319.

Mehta, P.K., 1986, Concrete: Structure, Properties, and Materials, Prentice-Hall, Inc., Englewood Cliffs, NJ.

Merritt, J.L., J.E. Monsees, and A.J. Hendron, Jr., 1985, "Seismic Design of Underground Structures," Ch. 9, pp. 104-131, Vol. 1, Rapid Excavation and Tunneling Conference (RETC), New York, June 1985, C.D. Mann and M.N. Kelley (Eds.), Society of Mining Engineers of AIME, New York.

Miklowitz, J., 1978, The Theory of Elastic Waves and Waveguides, North-Holland Publishing Co., Amsterdam.

Mindess, S. and J.F. Young, 1981, Concrete, Prentice-Hall, Inc., Englewood Cliffs, NJ.

Monsees, J.E. and J.L. Merritt, 1984, "Seismic Design of Underground Structures - Southern California Metro Rail Project," pp. 52-66, Lifeline Earthquake Engineering: Performance, Design and Construction, J.D. Cooper (Ed.), American Society of Civil Engineers, New York.

Moody, J.B., 1982, "Radionuclide Migration/Retardation: Research & Development Technology Status Report", Technical Report, ONWI, Battelle Memorial Institute, Columbus, OH.

Moore, J.G., M.T. Morgan, E.W. McDaniel, H.B. Greene, and G.A. West, 1979a, "Cement Technology for Plugging Boreholes in Radioactive-Waste-Repository Sites: Progress Report for the Period October 1, 1977, to September 30, 1978," ONRL-5524, Oak Ridge National Laboratory, Oak Ridge, TN.

Moore, J.G., M.T. Morgan, E.W. McDaniel, H.B. Greene, and G.A. West, 1979b, "Cement Technology for Plugging Boreholes in Radioactive-Waste-Repository Sites: Progress Report for the Period October 1, 1978, to September 30, 1979," ONRL-5610, Oak Ridge National Laboratory, Oak Ridge, TN.

Mott, Hay and Anderson, 1984, "The Backfilling and Sealing of Radioactive Waste Repositories," Final Report EUR 9115 En, Commission of the European Communities, Luxembourg.

National Research Council, 1983, "A Study of the Isolation System for Geologic Disposal of Radioactive Wastes," Waste Isolation Systems Panel, Board on Radioactive Waste Management, Commission on Physical Sciences, Mathematics, and Resources, National Academy Press, Washington, DC.

Nazarian, H.N., 1973, "Water Well Design for Earthquake-Induced Motions," pp. 377-394, Vol. 99, No. PO2, Journal of the Power Division, Proceedings of the American Society of Civil Engineers.

Neuzil, C.E., 1986, "Groundwater Flow in Low-Permeability Environments," Water Resources Research, Vol. 22, No. 8, pp. 1163-1195, August.

Neuzil, C.E., C. Cooley, S.E. Silliman, J.D. Bredehoeft, and P.A. Hsieh, 1981, "A Transient Laboratory Method for Determining the Hyraulic Properties of 'Tight' Rocks - II. Application," Int. Jour. Rock Mech. Min. Sci. & Geomech. Abstr., Vol. 18, pp. 253-258.

Neville, A.M., 1971, Hardened Concrete: Physical and Mechanical Aspects, ACI Monograph No. 6, American Concrete Institute, Detroit, MI.

Neville, A.M., 1973, Properties of Concrete, Second (metric) Edition, Pitman Publishers, London.

Neville, A.M., 1981, Properties of Concrete, Third Edition, Pitman, London, 779 pp.

Neville, A.M. and J.J. Brooks, 1987, Concrete Technology, Longman Scientific and Technical, Harlow, Essex.

97th Congress, 1983, "Nuclear Waste Policy Act of 1982," Public Law 97-425-Jan-7, 96STAT.2201-2263.

Niwa, Y., S. Kobayashi, and T. Fukui, 1976, "Applications of Integral Equation Method to Some Geomechanical Problems", in Numerical Methods in Geomechanics, C.S. Desai (Ed.), Vol. 1, ASCE, New York, NY, pp. 120-131.

OECD, 1980, Borehole and Shaft Plugging, Proceedings of the Workshop on, organized by the OECD Nuclear Energy Agency and the U.S. Department of Energy, Columbus, OH, Published by The OECD Nuclear Energy Agency, Paris.

OECD, 1984, Geological Disposal of Radioactive Waste, An overview of the current status of understanding and development. An Experts' Report sponsored by the Commission of the European Communities and The OECD Nuclear Energy Agency. Published by Organization for Economic Co-Operation and Development, Paris, February.

Okamoto, S., 1984, Introduction to Earthquake Engineering, Second Edition, University of Tokyo Press, Tokyo.

ONWI - 33(2), 1980, "NWTS Criteria for the Geologic Disposal of Nuclear Wastes: Site Qualification Criteria", Office of Nuclear Waste Isolation, Battelle Memorial Institute, Columbus, OH.

Orchard, D.F., 1979, Concrete Technology, Vol. 2, Practice, Fourth Edition, Applied Publishers Ltd, London.

Oriard, L.L., 1972, "Blasting Effects and Their Control in Open Pit Mining", pp. 197-222, Proceedings of the Second International Conference on Stability in Open Pit Mining, C.O. Brawner and V. Milligan (Eds.), SME/AIME, New York, NY.

Oriard, L.L., 1982a, "Blasting Effects and Their Control", in Underground Mining Methods Handbook, W.A. Hustrulid (Ed.), SME/AIME, New York, NY, pp. 1590-1603.

Oriard, L.L., 1982b, "Influence of Blasting on Slope Stability: State of the Art", Proceedings of the Third International Conference on Stability in Surface Mining, Vancouver, Canada, C.O. Brawner (Ed.), SME/AIME, New York, NY, pp. 43-87.

O'Rourke, M. and L.R.L. Wang, 1978, "Earthquake Response of Buried Pipeline," pp. 720-731, Vol. II, Earthquake Engineering and Soil Dynamics, Proceedings of the ASCE Geotechnical Engineering Division Specialty Conference, Pasadena, CA, June 19-21, American Society of Civil Engineers, New York.

O'Rourke, M.J., S. Sing., and R. Pikul, 1979, "Seismic Behavior of Buried Pipelines," pp. 49-61, Lifeline Earthquake Engineering - Buried Pipelines, Seismic Risk, and Instrumentation, PVP-34, T. Ariman, S.C. Liu, and R.E. Nichell (Eds.), The American Society of Mechanical Engineers, New York.

Owen, G.N., and R.E. Scholl, 1981, "Earthquake Engineering of Large Underground Structures", FHWA/RD-80/195, prepared by URS/John A. Blume & Associates, Engineers, for Federal Highway Administration and National Science Foundation, available through NTIS, Springfield, VA, 287 pp.

Owen, G.N., R.E. Scholl, and T. Brekke, 1979, "Earthquake Engineering of Tunnels", Proceedings of the 1979 Rapid Excavation and Tunneling Conference, Atlanta, GA, Vol. 1, AIME, New York, N.Y., pp. 709-721.

Owen, G.N., P.I. Yanev, and R.E. Scholl, 1980, "Considerations for Developing Seismic Design Criteria for Nuclear Waste Storage Repositories," JAB-00099-128, prepared by URS/John A. Blume & Associates for U.S. Department of Energy Nevada Operations Office under Contract DE-AC08-76DP00099.

Owens, P.L., 1985, "Effect of Temperature Rise and Fall on the Strength and Permeability of Concrete Made With and Without Fly Ash," pp. 134-149, Temperature Effects on Concrete, T.R. Naik (Ed.), STP 858, American Society for Testing and Materials, Philadelphia, PA.

Pao, Y.H., and C.C. Mow, 1973, The Diffraction of Elastic Waves and Dynamic Stress Concentrations, Crane and Russak, New York, NY.

Parker, H., 1968, Simplified Design of Reinforced Concrete, Third Edition, John Wiley & Sons, Inc., New York, NY.

Parrott, L.J. and J.F. Young, 1982, "Shrinkage and Swelling of Two Hydrated Alite Pastes," pp. 35-48, Fundamental Research on Creep and Shrinkage of Concrete, F.H. Wittmann (Ed.), Martinus Nijhoff Publishers, The Hague.

Paul, R.C., D.G. Watt, N.S. Haines, and D.G. Howard, 1972, "Design Features and Concrete Requirements for a Vacuum Building at the Pickering Nuclear Generating Station," Paper SP34-62, pp. 1321-1352, Vol. 3, Concrete for Nuclear Reactors, Special Publication SP-34, American Concrete Institute, Detroit, Michigan.

Pedersen, A. and K.E. Lindstrom-Jensen, 1980, "Selection of Release Scenarios for a Danish Waste Repository in a Salt Dome," pp. 181-196, Radioactive Release Scenarios for Geologic Repositories, Proceedings of the NEA Workshop, Paris, September 1980. Published by The OECD Nuclear Energy Agency, Paris, 1981.

Peterson, E.W. and C.L. Christensen, 1980, "Analysis of Bell Canyon Test Results," SAND 80-7044C, prepared by Sandia National Laboratories, Albuquerque, NM, for the U.S. Department of Energy. Also in Borehole and Shaft Plugging, Proceedings of Workshop, pp. 247-275, Columbus, OH, May 7-9, published by OECD, Paris.

Pigford, T.H., 1983, "The National Research Council Study of the Isolation System for Geologic Disposal of Radioactive Wastes," UCB-NE-4042, LBL-17248, Lawrence Berkeley Laboratory, Berkeley, CA, November.

Pihlajavaara, S.E. and K. Tiusanen, 1972, "A Preliminary Study on Thermal Moisture Transfer in Concrete," Paper SP 34-47, pp. 1019-1033, Vol. II, Concrete for Nuclear Reactors, Special Publication SP-34, American Concrete Institute, Detroit, MI.

Poitevin, P., 1972, "Water Migration in Concrete under a Sustained Temperature Gradient," Paper SP 34-43, pp. 909-929, Vol. II, Concrete for Nuclear Reactors, Special Publication SP-34, American Concrete Institute, Detroit, MI.

Pomeroy, C.D., 1986a, "Requirements for Durable Concrete," Ch. 1, pp. 1-27, Improvement of Concrete Durability, Proceedings of the Seminar, Institution of Civil Engineers, London, May 1985. Thomas Telford, London.

Pomeroy, C.D., 1986b, Contribution to the Discussion, p. 152, Improvement of Concrete Durability, Proceedings of the Seminar, Institution of Civil Engineers, London, May 1985. Thomas Telford, London.

Powers, T.C., 1958, "Structure and Physical Properties of Hardened Portland Cement Paste," Journal of the American Ceramic Society, Vol. 41, No. 1, pp. 1-6, Jan.

Powers, T.C., 1968, The Properties of Fresh Concrete, John Wiley & Sons, Inc., New York.

Powers, T.C., L.E. Copeland, J.C. Hayes, and H.M. Mann, 1954, "Permeability of Portland Cement Paste," J. American Concrete Institute, Vol. 51, No. 11, pp. 285-298, November.

Pratt, H.R., D.E. Stephenson, G. Zandt, M. Bouchon, and W. A. Hustrulid, 1979a, "Earthquake Damage to Underground Facilities", Proceedings of the 1979 Rapid Excavation and Tunneling Conference, Atlanta, GA, Vol. 1, AIME, New York, NY, pp. 19-51.

Pratt, H.R., G. Zandt, and M. Bouchon, 1979b, "Earthquake Related Displacement Fields Near Underground Facilities," DP-1533, UC-70, E.I. du Pont de Nemours & Co., Savannah River Laboratory, Aiken, SC.

Rabcewicz, L.V., 1973, "Principals of Dimensioning the Support System for the New Austrian Tunneling Method", Water Power, Vol. 25, No. 3, March, pp. 88-93.

Rennick, G.E., J. Pasini, C.E. Whieldon, Jr., and D.M. Evans, 1977, "Plugging Techniques that Should Allow Mining Through Wells," Report No. MERC/RI-77/1, U.S. Energy Research and Development Administration, Morgantown Energy Research Center, June.

Rhoderick, J.E. and A.D. Buck, 1981, "Examination of Simulated Borehole Specimens," Report No. ONWI-247, Office of Nuclear Waste Isolation, Battelle Memorial Institute, Columbus, OH. Sandia National Laboratories SAND 81-7109, Albuquerque, NM. Miscellaneous Paper USAE-WES SL-78-1, prepared by Structures Laboratory, U.S. Army Engineer Waterways Experiment Station, Vicksburg, MS.

Ross-Brown, D.M., B.C. Trent, and K.K. Wahi, 1981, "Numerical Simulations of Seismic Loading of Deep Underground Tunnels," Preprint No. 81-408, SME-AIME Fall Meeting, Denver, CO, November 1981.

Roy, D.M., 1981, "Geochemical Factors in Borehole-Shaft Plug Longevity," pp. 338-353, The Technology of High-Level Nuclear Waste Disposal, DOE/TIC-4621 (Vol. 1) (DF 82 009594), Technical Information Center, U.S. Department of Energy.

Roy, D.M. and F.L. Burns, 1982, "Recent Advances in Repository Seal Materials," pp. 631-639, Scientific Basis for Nuclear Waste Management V, W. Lutze (Ed.), Proceedings of the Materials Research Society Fifth International Symposium, June, Berlin, Germany. North Holland, New York.

Roy, D.M., M.W. Grutzeck, and P.H. Licastro, 1979, "Evaluation of Cement Borehole Plug Longevity," ONWI-30, Technical Report, Office of Nuclear Waste Isolation, Battelle.

Roy, D.M., M.W. Grutzeck, K. Mather, and A.D. Buck, 1982, "PSU/WES Interlaboratory Comparative Methodology Study of an Experimental Cementitious Repository Seal Material," Miscellaneous Paper SL-81-2, Structures Laboratory, Waterways Experiment Station, Vicksburg, MS. Also ONWI-324, Office of Nuclear Waste Isolation, Battelle Memorial Institute, Columbus, OH.

Roy, D.M., M.W. Grutzeck, and L.D. Wakeley, 1983a, "Selection and Durability of Seal Materials for a Bedded Salt Repository: Preliminary Studies," ONWI-479, Technical report by Materials Research Laboratory, The Pennsylvania State University, for Office of Nuclear Waste Isolation, Battelle Memorial Institute, Columbus, OH.

Roy, D.M., M.W. Grutzeck, and L.D. Wakeley, 1985, "Salt Repository Seal Materials: A Synopsis of Early Cementitious Materials Development," BMI/ONWI-536, prepared by Materials Research Laboratory, The Pennsylvania State University, for Office of Nuclear Waste Isolation, Battelle Memorial Institute, Columbus, OH.

Roy, D.M., E.L. White, and Z. Nakagawa, 1983b, "Effects of Early Heat of Hydration and Exposure to Elevated Temperatures on Properties of Mortars and Pastes with Slag Cement," pp. 150-167, Temperature Effects on Concrete, T.R. Naik (Ed.), STP 858, American Society for Testing and Materials, Philadelphia, PA.

Ruska Instrument Corporation, 1980, "Positive Displacement Pumps", Catalog No. Pump 80, Houston, TX.

Sabri, S. and J.M. Illston, 1982, "Isothermal Drying Shrinkage and Wetting Swelling of Hardened Cement Paste," pp. 63-72, Fundamental Research on Creep and Shrinkage of Cement, F.H. Wittmann (Ed.), Martinus Nijhoff Publishers, The Hague.

Scheetz, B.E., M.W. Grutzeck, L.D. Wakeley, and D.M. Roy, 1979, "Experimental Studies of Seal Materials for Potential Use in a Los Medanos-Type Bedded Salt Repository," ONWI-325, prepared by the Materials Research Laboratory, The Pennsylvania State University, for Office of Nuclear Waste Isolation, Battelle Memorial Institute, Columbus, OH.

Scheetz, B.E., P.H. Licastro, and D.M. Roy, 1986a, "A Full-Scale Borehole Sealing Test in Salt Under Simulated Downhole Conditions - Volume 2," BMI/ONWI-573(2), prepared by the Materials Research Laboratory, The Pennsylvania State University, for Office of Nuclear Waste Isolation, Battelle Memorial Institute, Columbus, OH.

Scheetz, B.E., P.H. Licastro, and D.M. Roy, 1986b, "A Full-Scale Borehole Sealing Test in Anhydrite Under Simulated Downhole Conditions - Volume 2," BMI/ONWI-581(2), prepared by the Materials Research Laboratory, The Pennsylvania State University, for Office of Nuclear Waste Isolation, Battelle Memorial Institute, Columbus, OH.

Scheidegger, A.E., 1963, The Physics of Flow Through Porous Media, University of Toronto Press, 313 pp.

Schneider, K.J., and A.M. Platt, 1974, "Advanced Waste Management Studies, High-Level Radioactive Waste Disposal Alternatives", BNWL-1900, Battelle Pacific Northwest Laboratory, Richland, WA.

Schofield, A.N., 1981, "Dynamic and Earthquake Geotechnical Centrifuge Modeling", Proc. Int. Conf. on Recent Advances in Geotechnical Earthquake Engineering and Soil Dynamics, Vol. 3, S. Prakash (Ed.), University of Missouri, Rolla, MO, pp. 1081-1100.

Seitz, R.R., B. Sager, and J.D. Davis, 1987, "Numerical Modeling of Radionuclide Transport Through Repository Seals," Waste Management '87, Tucson, Arizona, March 1-5, 1987. Proceedings, Vol. 1, pp. 637-644, R.G. Post (Ed.), Arizona Board of Regents.

Siskind, D.E., M.S. Stagg, J.W. Kopp, and C.H. Dowding, 1980, "Structure Response and Damage Produced by Ground Vibration from Surface Mine Blasting", RI-8507, U.S. Department of the Interior, Bureau of Mines.

Smith, D.K., 1976, Cementing, Society of Petroleum Engineers of AIME, New York.

Smith, I.M., 1977, "Numerical and Physical Modeling", Chapter 17 of Numerical Methods in Geotechnical Engineering, C.S. Desai and J.T. Christian (Eds.), McGraw-Hill, New York, NY, pp. 556-588.

Smith, M.J., G.J. Anttonen, G.S. Barney, W.E. Coons, F.N. Hodges, R.G. Johnston, J.D. Kaser, R.M. Manabe, S.C. McCarel, E.L. Moore, A.F. Noonan, J.E. O'Rourke, W.W. Schulz, C.L. Taylor, B.J. Wood, and M.I. Wood, 1980, "Engineered Barrier Development for a Nuclear Waste Repository in Basalt: An Integration of Current Knowledge," RHO-BWI-ST-7, Rockwell Hanford Operations, Richland, WA.

Snow, D.T., 1968, "Rock Fracture Spacings, Openings, and Porosities", Jour. Soil Mech. and Found. Div. ASCE, Vol. 94, No. SM1, pp. 73-91.

South, D.L., S.L. Cobb, and J.J.K. Daemen, 1981, "Borehole Plug Performance," Waste Mangement '81, American Nuclear Society, Tucson, AZ, Feb. 23-26.

South, D.L. and J.J.K. Daemen, 1986, "Permeameter Studies of Water Flow Through Cement and Clay Borehole Seals in Granite, Basalt and Tuff", NUREG/CR-4748, Technical Report, prepared for the Division of Engineering Safety, Office of Nuclear Regulatory Research, U.S. Nuclear Regulatory Commission, by the Department of Mining and Geological Engineering, University of Arizona, Tucson, AZ, October, 263 pp.

Stevens, P.R., 1977, "A Review of the Effects of Earthquakes on Underground Mines", Open-File Report 77-313, U.S. Department of the Interior, Geological Survey, Reston, VA, April.

Stormont, J.C., 1984, "Plugging and Sealing Program for the Waste Isolation Pilot Plant (WIPP)," SAND 84-1057, prepared for the U.S. Department of Energy by Sandia National Laboratories, Albuquerque, NM.

Stormont, J.C., 1986a, "In Situ Seal Tests at the Waste Isolation Pilot Plant (WIPP)," pp. 167-176, Vol. 2, Proceedings, Waste Management '86, R.G. Post (Ed.), Tucson, AZ, March 2-6.

Stormont, J.C. (Technical Editor), 1986b, "Development and Implementation: Test Series A of the Small-Scale Seal Performance Tests," Sandia Report SAND 85-2602, prepared by Sandia National Laboratories, Albuquerque, NM, for the U.S. Department of Energy.

Sumitomo Cement Co., Ltd., 1983, "Silent Non-Explosive Demolition Agent S-MITE", Sumitomo Corporation, Tokyo, Japan.

Summers, J.B., 1984, "Damage to Irrigation Wells and Other Facilities in the Pleasant Valley Water District Due to the May 2, 1983 Earthquake and Aftershocks," California Department of Conservation, Division of Mines and Geology, Special Publication 66.

Taylor, C.L., G.J. Anttonen, J.E. O'Rourke, and D. Allisot, 1980, "Preliminary Geochemical and Physical Testing of Materials for Plugging of Man-Made Accesses to a Repository in Basalt," RHO-BWI-C-66, Rockwell Hanford Operations, Richland, WA.

Taylor, W.H., 1977, Concrete Technology and Practice, Fourth Edition, McGraw-Hill Book Company, Sydney, Australia.

Terzaghi, K., 1946, "Rock Defects and Loads on Tunnel Supports", in Rock Tunneling with Steel Supports, R.V. Proctor and T.L. White (Eds.), Commercial Sheaving and Stamping Company, Youngstown, OH, revised 1968.

Terzaghi, K., and F.E. Richart, Jr., 1952, "Stresses in Rock About Cavities", Geotechnique, Vol. 3, pp. 57-90.

Timoshenko, S.P. and J.N. Goodier, 1970, Theory of Elasticity, Third Edition, Engineering Societies Monographs, McGraw-Hill Book Co., New York, NY.

URS/John A. Blume & Associates, Engineers, 1986, "Ground Motion Evaluations at Yucca Mountain, Nevada with Applications to Repository Conceptual Design and Siting," SAND 85-7104, Sandia National Laboratories, Albuquerque, NM.

U.S. Department of Energy, 1979, "Management of Commercially Generated Radioactive Wastes", DOE/EIS-0046-D, Vol. 1 of 2, Draft Environmental Impact Statement, Washington, DC.

U.S. Department of Energy, 1982, "NWTS Program Criteria for Mined Geologic Disposal of Nuclear Waste: Repository Performance and Development Criteria", DOE/NWTS-33(3), Office of NWTS Integration, Battelle Memorial Institute, Columbus, OH, Public Draft.

U.S. Department of Energy, 1983, "Summary of the Results of the Evaluation of the WIPP Site and Preliminary Design Validation Program", WIPP-DOE-161, Waste Isolation Pilot Plant, Albuquerque, NM.

U.S. Department of Energy, 1984, "Nuclear Waste Policy Act (Section 112): Draft Environmental Assessment, Yucca Mountain Site, Nevada", DOE/RW-0013, Office of Civilian Radioactive Waste Management, Washington, DC, December.

U.S. Environmental Protection Agency, 1986, "Environmental Standards and Federal Radiation Protection Guidance for Management and Disposal of Spent Nuclear Fuel, High-Level and Transuranic Radioactive Wastes," 40 CFR 191, Federal Register, Final Rule.

U.S. National Committee for Rock Mechanics, 1981, "Rock-Mechanics Research Requirements for Resource Recovery, Construction, and Earthquake-Hazards Reduction", NRC/AMPS/RM-81-1, National Research Council/National Academy of Sciences, Washington, DC.

U.S. Nuclear Regulatory Commission, 1973a, "Regulatory Guide No. 1.60: Design Response Spectra for Nuclear Power Plants," Revision 1, December.

U.S. Nuclear Regulatory Commission, 1973b, "Regulatory Guide No. 1.61: Damping Values for Seismic Analyis for Nuclear Power Plants," October.

U.S. Nuclear Regulatory Commission, 1981, "Disposal of High-Level Radioactive Wastes in Geologic Repositories," Proposed Rule, 10 CFR Part 60, Federal Register, Vol. 46, No. 130, July 8.

U.S. Nuclear Regulatory Commission, 1983a, "Disposal of High-Level Radioactive Wastes in Geologic Repositories," Final Rule 10 CRF 60, Federal Register, Vol. 48, No. 120, June 30.

U.S. Nuclear Regulatory Commission, 1983b, "Staff Analysis of Public Comments on Proposed Rule 10 CFR Part 60, "Disposal of High-Level Radioactive Wastes in Geologic Repositories,"" NUREG-0804, Office of Nuclear Regulatory Research, U.S. NRC, Washington, DC, December.

U.S. Nuclear Regulatory Commission, 1985, "Disposal of High-Level Radioactive Wastes in Geologic Repositories," Final Rule, Unsaturated Zone Amendment, Federal Register, Vol. 50, No. 140, pp. 29641-8, Monday, July 22.

U.S. Nuclear Regulatory Commission, 1986, "Borehole and Shaft Sealing of High-Level Nuclear Waste Repositories," Generic Technical Position, Compiled by Engineering Branch, Division of Waste Management, Washington, DC, February.

U.S. Nuclear Regulatory Commission, 1987, "Disposal of High-Level Radioactive Wastes in Geologic Repositories," 10 CFR, Ch. 1 (1-1-87 Edition), Part 60, Code of Federal Regulations Title 10, Ch. 1, pp. 627-658, U.S. Government Printing Office, Washington, DC.

Voegele, M., C. Fairhurst, and P. Cundall, 1977, "Analysis of Tunnel Support Loads Using a Large Displacement, Distinct Block Model," Storage in Excavated Rock Caverns, Rock Store 77, M. Bergman (Ed.), Proceedings of the First International Symposium, Stockholm, September 1977, Vol. 2, pp. 247-252, Pergamon Press, Oxford, 1978.

Vortman, L.J., 1982, "Ground Motion from Earthquakes and Underground Nuclear Weapons Tests: A Comparison as it Relates to Siting a Nuclear Waste Storage Facility at NTS", SAND81-2214, Sandia National Laboratories, Albuquerque, NM, April.

Vortman, L.J., 1986, "Ground Motion Produced at Yucca Mountain from Pahute Mesa Underground Nuclear Explosions," SAND 85-1605, Sandia National Laboratories, Albuquerque, NM, February.

Vortman, L.J., and J.W. Long, 1982a, "Effects of Repository Depth on Ground Motion - the Pahute Mesa Data", SAND82-0174, prepared by Sandia National Laboratories, Albuquerque, NM, for U.S. Department of Energy, available from NTIS, Springfield, VA.

Vortman, L.J., and J.W. Long, 1982b, "Effects of Ground Motion on Repository Depth - the Yucca Flat Data", SAND82-1647, prepared by Sandia National Laboratories, Albuquerque, NM, for U.S. Department of Energy, available from NTIS, Springfield, VA.

Wahi, K.K. and B.C. Trent, 1982, "Analysis of Seismic Response of Repository Tunnels," Proc. 4th Int. Conf. on Numerical Methods in Geomechanics, Edmonton, Canada, May 31-June 4, pp. 625-634.

Wahi, K.K., B.C. Trent, D.E. Maxwell, R.M. Pyke, C. Young, and D.M. Ross-Brown, 1980, "Numerical Simulations of Earthquake Effects on Tunnels for Generic Nuclear Waste Repositories", DP-1579, prepared for Savannah River Laboratory, E.I. du Pont de Nemours & Co., Aiken, SC, for U.S. Department of Energy, by Science Applications, Inc., Fort Collins, CO.

Wakeley, L.D. and T.S. Poole, 1986, "Posttest Analysis of a Laboratory-Cast Monolith of Salt-Saturated Concrete," Miscellaneous Paper SL-86-13, prepared by Waterways Experiment Station, Corps of Engineers, Vicksburg, MS, for Sandia National Laboratories, Albuquerque, NM.

Wakeley, L.D. and D.M. Roy, 1983, "Experimental Concretes for Sealing Radioactive-Waste Repositories in Evaporite Strata," Cement and Concrete Research, Vol. 13, pp. 97-106.

Wakeley, L.D. and D.M. Roy, 1985, "Cementitious Mixtures for Sealing Evaporative and Clastic Rocks in a Radioactive Waste Repository," Miscellaneous Paper SL-85-16, Structures Laboratory, U.S. Army Engineer Waterways Experiment Station, Vicksburg, MS, prepared for Office of Nuclear Waste Isolation, Battelle Memorial Institute, Columbus, OH, and Sandia National Laboratories, Albuquerque, NM.

Wakeley, L.D. and D.M. Roy, 1986, "Nature of the Interfacial Region Between Cementitious Mixtures and Rocks from the Palo Duro Basin and Other Seal Components," Technical Report BMI/ONWI-580, prepared by Materials Research Laboratory, Pennsylvania State University, for Office of Nuclear Waste Isolation, Battelle Memorial Institute, Columbus, OH.

Wakeley, L.D., D.M. Roy, and M.W. Grutzeck, 1981, "Experimental Studies of Seal Materials for Potential Use in a Los Medanos-Type Bedded Salt Repository," Technical Report No. ONWI-325, prepared by the Materials Research Laboratory, The Pennsylvania State University, for Office of Nuclear Waste Isolation, Battelle Memorial Institute, Columbus, OH.

Wakeley, L.D., D.M. Roy, and M.W. Grutzeck, 1984, "Cementitious Mixtures for Sealing Access Shafts/Boreholes through Evaporite and Clastic Rocks in a Radioactive-Waste Repository," pp. 951-958, Scientific Basis for Nuclear Waste Management VIII, C.M. Jantzen, J.A. Stone, and R.C. Ewing (Eds.), Boston, MA, November 1984 Symposium. Symposia Proceedings Vol. 44, Materials Research Society, Pittsburgh PA, 1985.

Wakeley, L.D., D.M. Walley, and A.D. Buck, 1986, "Development of Freshwater Grout Subsequent to the Bell Canyon Tests (BCT)," Miscellaneous Paper SL-86-2, prepared by Waterways Experiment Station, Corps of Engineers, Vicksburg, MS, for Sandia National Laboratories, Albuquerque, NM.

Wang, L.R.-L., 1979, "Some Aspects of Seismic Resistant Design of Buried Pipelines," pp. 117-131, Lifeline Earthquake Engineering - Buried Pipelines, Seismic Risk, and Instrumentation, PVP-34, T. Ariman, S.C. Liu, and R.E. Nichell (Eds.), The American Society of Mechanical Engineers, New York.

White, E.L., B.E. Scheetz, D.M. Roy, K.G. Zimmerman, and M.W. Grutzeck, 1979, "Permeability Measurements on Cementitious Materials for Nuclear Waste Isolation, pp. 471-478, Scientific Basis for Nuclear Waste Management, Vol. 1, G.J. McCarthy, ed., Proceedings of the Symposium on "Science Underlying Radioactive Waste Management," Materials Research Society Annual Meeting, Boston, Massachusetts, Nov. 28-Dec. 1, 1978, Plenum Press, New York.

Wickham, G.E., H.R. Tiedemann, and E.H. Skinner, 1974, "Ground Support Prediction Model - RSR Concept", Proceedings of the 1974 Rapid Excavation and Tunneling Conference, AIME, New York, NY, pp. 691-707.

Woods, H., 1968, Durability of Concrete Construction, ACI Monograph No. 4, American Concrete Institute, Detroit, MI.

Yanev, P.I. and G.N. Owen, 1978, "Facility Hardening Studies; Design Cost Scoping Studies", JAB-99-123, prepared by URS/John Blume & Associates, Engineers, San Francisco, CA, for the U.S. Department of Energy, Nevada Nuclear Waste Storage Investigations, Las Vegas, NV, 109 pp.

Yuan, R.L., H.K. Hilsdorf, and C.E. Kesler, 1972, "The Effect of Temperature on the Drying of Concrete," Paper SP 34-46, pp. 991-1017, Vol. II, Concrete for Nuclear Reactors, Special Publication SP-34, American Concrete Institute, Detroit, MI.

Zeigler, T.W., 1976, "Determination of Rock Mass Permeability", AD/A-021 192, Technical Report, U.S. Army Engineer Waterways Experiment Station, Vicksburg, MS, 88 pp.

APPENDIX A

ANALYTICAL SOLUTION OF ONE-DIMENSIONAL TRANSIENT FLOW THROUGH POROUS MEDIA

For transient, one-dimensional flow through a homogeneous porous medium (e.g. a cement plug) of length ℓ, the fluid head depends only on the distance x from one end of the plug and the time t. Transient fluid flow, as well as heat flow and consolidation, belong to a class of problems called the initial boundary value problem. The governing partial differential equation is parabolic with the general form (Desai, 1979, p. 108; Hildebrand, 1976, p. 462, 494):

$$\alpha \frac{\partial^2 Q}{\partial x^2} = \frac{\partial Q}{\partial t} \qquad (A.1)$$

Q is the unknown (Head for transient fluid flow, temperature for heat flow, excess pore water pressure for consolidation), α is a material property, x is the position, and t denotes time. The material property α in a fluid flow problem is known as the hydraulic diffusivity, and is equal to K/S_s or $K/\gamma_w m_v$ (Hsieh et al., 1981, p. 246; Desai, 1979, p. 108), where K is the hydraulic conductivity (L/T), S_s is the specific storage (L^{-1}), γ_w is the unit weight of water (F/L^3) and m_v is the coefficient of volume compressibility (L^2/F).

For the transient fluid flow problem, equation (A.1) can be expressed as:

$$\frac{K}{S_s} \frac{\partial^2 h}{\partial x^2} = \frac{\partial h}{\partial t} \qquad (A.2)$$

or

$$\frac{\partial^2 h}{\partial x^2} - \frac{S_s}{K} \frac{\partial h}{\partial t} = 0 \qquad (A.3)$$

In the flow testing experiment, transient flow occurs during the initial period after the injection pressure is applied, increased or decreased. Steady-state conditions exist before the injection pressure is changed from H_1 to H_2. Therefore, the initial condition is a linear function of x:

$$h(x,0) = f(x) = \frac{x}{\ell} H_1 \qquad (A.4)$$

The prescribed boundary conditions are:

$$\begin{aligned} h(0,t) &= 0 \quad \text{for all } t \\ h(\ell,t) &= H_2 \quad \text{for } t > 0 \end{aligned} \qquad (A.5)$$

It is convenient to express the general solution h(x,t) as the sum of:

1) The limiting steady-state distribution (independent of t) after transient effects become negligible.

2) The transient distribution, which must approach zero as t increases indefinitely.

Thus:

$$h(x,t) = h_S(x) + h_T(x,t) \qquad (A.6)$$

where $h_S(x)$ is a linear function of x satisfying the boundary conditions (A.5):

$$h_S(x) = \frac{x}{\ell} H_2 \qquad (A.7)$$

and $h_T(x,t)$ is a particular solution of (A.3) which must vanish as $t \to \infty$, i.e.:

$$h_T(x,\infty) = 0 \qquad (A.8)$$

The sum of h_S and h_T must satisfy the initial condition in (A.4).

Since $h_S(x)$ satisfies the boundary conditions, $h_T(x,t)$ must vanish at x = 0 and x = ℓ for all positive values of t, i.e.:

$$h_T(o,t) = h_T(\ell,t) = 0 \quad (t > 0) \qquad (A.9)$$

Product solutions of the governing partial differential equation in (A.3) satisfying the conditions (A.8) and (A.9) are obtained in the form:

$$h_T(x,t) = a_n \sin\left(\frac{n\pi x}{\ell}\right) e^{-n^2 \pi^2 Kt/\ell^2 S_s} \quad (n = 1,2,3,\ldots) \qquad (A.10)$$

Combining (A.7) and (A.10) gives the general solution:

$$h_T(x,t) = \frac{x}{\ell} H_2 + \sum_{n=1}^{\infty} a_n \sin\left(\frac{n\pi x}{\ell}\right) e^{-n^2 \pi^2 Kt/\ell^2 S_s} \qquad \text{(A.11)}$$

The Fourier coefficients a_n are determined to satisfy the initial condition when t = 0.

$$h(x,t) - h_s(x) = h_T(x,t)$$

or

$$\frac{x}{\ell} H_1 - \frac{x}{\ell} H_2 = \sum_{n=1}^{\infty} a_n \sin\left(\frac{n\pi x}{\ell}\right) \qquad (0 < x < \ell) \qquad \text{(A.12)}$$

and

$$a_n = \frac{2}{\ell} \int_0^{\ell} (H_1 - H_2) \frac{x}{\ell} \sin\left(\frac{n\pi x}{\ell}\right) dx \qquad \text{(A.13)}$$

Rearranging and integrating yields:

$$a_n = \frac{2(H_1 - H_2)}{\ell^2} \int_0^{\ell} x \sin\left(\frac{n\pi x}{\ell}\right) dx$$

$$= \frac{2(H_1 - H_2)}{\ell^2} \left[-\frac{\ell^2}{n\pi} \cos(n\pi) \right]$$

$$a_n = \frac{2}{n\pi} (H_2 - H_1) \cos(n\pi) \qquad \text{(A.14)}$$

Hence, the general solution is

$$h(x,t) = \frac{x}{\ell} H_2 + \sum_{n=1}^{\infty} \frac{2}{n\pi} (H_2 - H_1) \cos(n\pi) \sin\left(\frac{n\pi x}{\ell}\right) e^{-n^2 \pi^2 Kt/\ell^2 S_s} \qquad \text{(A.15)}$$

which can be solved using K and S_s values obtained from the transient flow test.

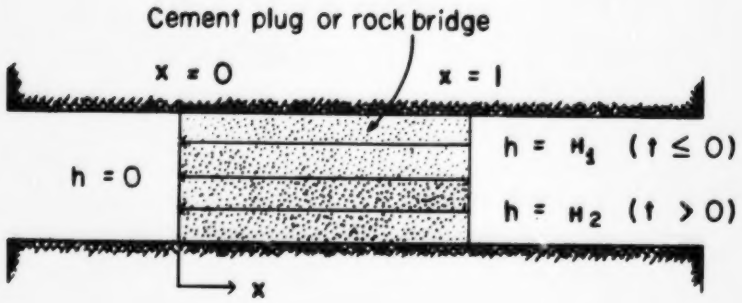

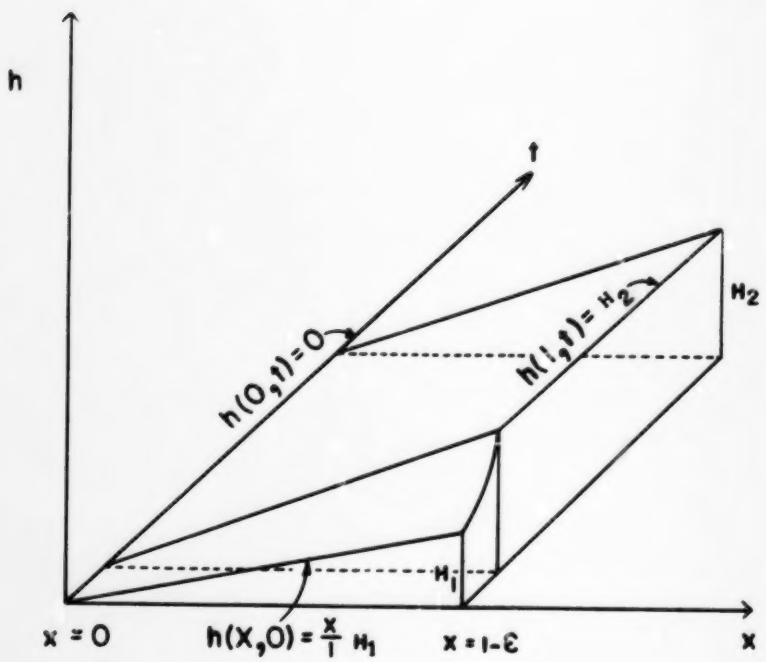

Figure A.1 Schematic diagram of the initial and boundary conditions in the flow testing experiment.

BEST COPY AVAILABLE

APPENDIX B

FINITE ELEMENT SOLUTION OF ONE-DIMENSIONAL FLOW THROUGH A CEMENT PLUG

The analysis presented on the following pages is discussed in Section 5.5 of this report. The analysis has been performed with a slightly modified version of program DFT/C-1DFE (Desai, 1979, Ch. 6).

Material Properties symbols or acronyms:

K = hydraulic conductivity (cm/s)

MV = coefficient of volume compressibility (cm^2/g)

WAT.DENS = unit weight of water (γ_w)

MAT.DENS = material density (ignored in this problem)

** PROBLEM= 19.. SPECIMEN CG5309-31V (10.4 CM CEMENT PLUG): K/Ss=.3
1 TO 4 MPa

INPUT QUANTITIES

INPUT TABLE 1A .. PROBLEM PARAMETERS

NUMBER OF NODE POINTS	...=	13
NUMBER OF MATERIALS	...=	1
NUMBER OF TRACTION CARDS	...=	0
OPTION FOR BODY FORCE =0 OR 1	...=	0
OPTION FOR PROBLEM TYPE	...=	3
SEMI-BAND WIDTH	...=	2
NUMBER OF OUTPUT TIME LEVELS	...=	11

INPUT TABLE 1B...MATERIAL PROPERTIES

MAT	K (CM/S)	MV (CM2/G)	WAT.DENS (G/CM3)	MAT.DENS (G/CM3)
1	.300E-11	.100E-10	.100E+01	.000E+00

INPUT TABLE 2 .. NODAL POINT DATA

NODE	KODE	Y-COORD (CM)	PRESSURE (MPa)
1	1	.000E+00	.000E+00
2	0	.900E+00	.000E+00
3	0	.180E+01	.000E+00
4	0	.270E+01	.000E+00
5	0	.360E+01	.000E+00
6	0	.450E+01	.000E+00
7	0	.540E+01	.000E+00
8	0	.630E+01	.000E+00
9	0	.720E+01	.000E+00
10	0	.810E+01	.000E+00
11	0	.900E+01	.000E+00
12	0	.990E+01	.000E+00
13	1	.104E+02	.400E+01

INPUT TABLE 3 .. ELEMENT DATA

EL. NO	NODE I	NODE J	MTYPE	AREA (CM2)
1	1	2	1	.539E+01
2	2	3	1	.539E+01
3	3	4	1	.539E+01
4	4	5	1	.539E+01
5	5	6	1	.539E+01
6	6	7	1	.539E+01
7	7	8	1	.539E+01
8	8	9	1	.539E+01
9	9	10	1	.539E+01
10	10	11	1	.539E+01
11	11	12	1	.539E+01
12	12	13	1	.539E+01

BEST COPY AVAILABLE

INPUT TABLE 5A .. DATA FOR TIME DEPENDENT PROBLEMS

TIME INCREMENT= .0100 SEC TOTAL TIME= 100.0000 SEC OPTION= 2

INPUT TABLE 5B.. DATA FOR OUTPUT TIME LEVELS

NUMBER	OUTPUT TIME (SEC)
1	.100E-01
2	.500E-01
3	.100E+00
4	.500E+00
5	.100E+01
6	.500E+01
7	.100E+02
8	.500E+02
9	.550E+02
10	.600E+02
11	.100E+03

INPUT TABLE 5C.. INITIAL CONDITIONS

NODE	PRESSURE (MPa)
1	.000E+00
2	.865E-01
3	.173E+00
4	.260E+00
5	.346E+00
6	.433E+00
7	.519E+00
8	.606E+00
9	.692E+00
10	.779E+00
11	.865E+00
12	.952E+00
13	.100E+01

OUTPUT QUANTITIES

OUTPUT TABLE 1 .. TRANSIENT FLOW PROBLEM

ELAPSED TIME = .0100 SEC

NODE	PRESSURE (MPa)
1	.000E+00
2	.865E-01
3	.173E+00
4	.260E+00
5	.346E+00
6	.433E+00
7	.519E+00
8	.605E+00
9	.696E+00
10	.764E+00
11	.934E+00
12	.639E+00
13	.400E+01

ELAPSED TIME = .0500 SEC

NODE	PRESSURE (MPa)
1	.000E+00
2	.865E-01
3	.173E+00
4	.260E+00
5	.346E+00
6	.433E+00
7	.519E+00
8	.606E+00
9	.689E+00
10	.797E+00
11	.769E+00
12	.142E+01
13	.400E+01

BEST COPY AVAILABLE

ELAPSED TIME = .1000 SEC

NODE	PRESSURE (MPa)
1	.000E+00
2	.865E-01
3	.173E+00
4	.260E+00
5	.346E+00
6	.433E+00
7	.519E+00
8	.605E+00
9	.696E+00
10	.774E+00
11	.789E+00
12	.199E+01
13	.400E+01

ELAPSED TIME = .5000 SEC

NODE	PRESSURE (MPa)
1	.000E+00
2	.865E-01
3	.173E+00
4	.260E+00
5	.346E+00
6	.433E+00
7	.519E+00
8	.602E+00
9	.701E+00
10	.954E+00
11	.166E+01
12	.304E+01
13	.400E+01

ELAPSED TIME = 1.0000 SEC

NODE	PRESSURE (MPa)
1	.000E+00
2	.865E-01
3	.173E+00
4	.260E+00
5	.346E+00
6	.432E+00
7	.526E+00
8	.657E+00
9	.899E+00
10	.137E+01
11	.217E+01
12	.330E+01
13	.400E+01

ELAPSED TIME = 5.0000 SEC

NODE	PRESSURE (MPa)
1	.000E+00
2	.125E+00
3	.261E+00
4	.420E+00
5	.614E+00
6	.856E+00
7	.116E+01
8	.153E+01
9	.197E+01
10	.248E+01
11	.305E+01
12	.366E+01
13	.400E+01

ELAPSED TIME = 10.0000 SEC

NODE	PRESSURE (MPa)
1	.000E+00
2	.230E+00
3	.469E+00
4	.723E+00
5	.100E+01
6	.131E+01
7	.164E+01
8	.201E+01
9	.241E+01
10	.283E+01
11	.328E+01
12	.374E+01
13	.400E+01

ELAPSED TIME = 50.0000 SEC

NODE	PRESSURE (MPa)
1	.000E+00
2	.346E+00
3	.692E+00
4	.104E+01
5	.138E+01
6	.173E+01
7	.208E+01
8	.242E+01
9	.277E+01
10	.311E+01
11	.346E+01
12	.381E+01
13	.400E+01

BEST COPY AVAILABLE

ELAPSED TIME = 55.0000 SEC

NODE	PRESSURE (MPa)
1	.000E+00
2	.346E+00
3	.692E+00
4	.104E+01
5	.138E+01
6	.173E+01
7	.208E+01
8	.242E+01
9	.277E+01
10	.312E+01
11	.346E+01
12	.381E+01
13	.400E+01

ELAPSED TIME = 60.0000 SEC

NODE	PRESSURE (MPa)
1	.000E+00
2	.346E+00
3	.692E+00
4	.104E+01
5	.138E+01
6	.173E+01
7	.208E+01
8	.242E+01
9	.277E+01
10	.312E+01
11	.346E+01
12	.381E+01
13	.400E+01

ELAPSED TIME = 100.0000 SEC

NODE	PRESSURE (MPa)
1	.000E+00
2	.346E+00
3	.692E+00
4	.104E+01
5	.138E+01
6	.173E+01
7	.208E+01
8	.242E+01
9	.277E+01
10	.312E+01
11	.346E+01
12	.381E+01
13	.400E+01

** JOB END **

BEST COPY AVAILABLE

APPENDIX C

CEMENT MIXING PROCEDURE, COMPOSITION AND PROPERTIES, AND UNIAXIAL COMPRESSIVE STRENGTH

C.1 Cement Grout Mixing Procedure

Step 1. Weigh out correct amounts of cement and water.

Example:

Ideal Class A Cement	500 g	
10% D53 (expansive agent)	50 g	premixed
1% D65 (dispersant)	5 g	
	555 g	
50% water	250 g	

(All percentages are with respect to the cement component)

Step 2. Pour water into blender (Waring Blendor Model 31 BL 42). Add 3-4 ml D47 (antifoaming agent).

Step 3. Start blender at Speed 2.

Step 4. Add all of the cement within 15 seconds of starting.

Step 5. 15 seconds from time of starting, switch to speed 6 for 35 seconds.

Step 6. Carefully pour desired volume of cement.

Step 7. "Puddle" cement with a glass rod or use an ultrasonic vibrator to remove entrained air.

Step 8. Cure the cement under water.

C.2 Cement Composition and Properties

System 1

Composition: Ideal Class A (Tijeras Canyon)
10% D53
1% D65
50% H_2O

Slurry density: 15.7 lb/gal

Thickening time @ BHCT = 110°F: 30Bc - 200 min
100Bc - 247 min

Compressive strength @ BHST = 110°F: 3800 psi @ 14 days curing

API free water: 0.0 cc

Percent expansion: 1 day - 0.12
BHST = 110°F 3 days - 0.14
7 days - 0.18
14 days - 0.18

BHCT = Bottom hole circulating temperature

Bc = Bearden units of slurry consistency

D53 = Expansive agent

D65 = Dispersant

BHST = Bottom hole static temperature

(Materials and properties courtesy of Dowell, Tulsa, Oklahoma)

C.3 Uniaxial Compressive Strength Testing of Cement

System 1 cement was poured in galvanized steel pipes with nominal inside diameters of 15, 27, 51, 79 and 102 mm (0.5, 1, 2, 3 and 4 inches) and cured under water for two weeks.

A problem was encountered in removing the cement cylinders from the pipes due to the cement expansion. After heating for two weeks at 93°C (200°F) in an oven, some of the cement cylinders could be removed. However, three of the five cylinders that were recovered had a length to diameter ratio less than two.

Specimen ends were cut using a Highland Park and a Covington rock saw. End surfaces were ground smooth and parallel using a Kent KGS-250 AH automatic grinder.

Uniaxial compressive tests were carried out on the 15, 27, 51 and 79 mm diameter cylinders using a Soiltest VersaTester 60,000 lbs capacity loading frame. The 102 mm diameter specimen was tested on a 500,000 lbs SBEL CT500 machine. A nominal loading rate of 30 psi/s (0.21 MPa/s) was used throughout. The uniaxial compressive strength was normalized to an equivalent length to diameter ratio of one using the expression (Jaeger and Cook, 1979, p. 144):

$$\sigma_{c1} = \frac{\sigma_{cf}}{(.778 + .222\ D/L)} \qquad (C.1)$$

where σ_{c1} is the adjusted uniaxial compressive strength for L/D = 1. σ_{cf} is the observed uniaxial compressive strength, D is specimen diameter and L is specimen length. This is a variation of ASTM D2938, which normalizes to L/D = 2 for rock core tests, as does the ASTM C39 standard for testing concrete cylinders:

$$\sigma_{c2} = \sigma_{cf}/(0.88 + 0.24\ D/L) \quad \text{for } L/D < 1.8 \qquad (C.2)$$

The test results are summarized in Table C.1. Total time lapse between pouring and testing was 33 days.

Table C.1 Uniaxial Compressive Strengths of Cement Cylinders

Sample Number	D (mm)	L (mm)	L/D	Unit Weight (g/cm^3)	σ_{cf} (MPa)	σ_{c1} (MPa)	σ_{c2} (MPa)
C1	102	191	1.9	1.71	51.85	57.94	
C2	79	89	1.1	1.64	37.86	38.63	34.47
C3	51	129	2.5	1.68	30.97	35.72	
C4	27	55	2.0	1.65	31.92	35.91	
C5	15	21	1.4	1.76	39.41	42.08	37.48
Average:				1.69			
Standard Deviation:				0.05			

D = diameter
L = length
σ_{cf} = calculated (observed) strength
σ_{c1} = strength adjusted for L/D = 1 (Equation C.1)
σ_{c2} = strength adjusted for L/D = 2 (Equation C.2)

APPENDIX D

LIST OF TEST EQUIPMENT

Table D.1 Equipment List

Item	Description	Manufacturer	Quantity
Flow Test Components:			
Pressure intensifier	Pressure ratio 36:1 Capacity 32 cm^3	University Instrument Shop	2
Hydraulic accumulator	Bladder type, #3301-012.200 Capacity 1 pint (473 cm^3)	EMG	3
Water pump	a) Positive displacement, #2240, cap. 500 cm^3 b) " " , cap. 1000 cm^3	Ruska Univ. Inst. Shop	1 1
Pressure gage	a) Range 0-4 MPa (0-600 psi) b) Range 0-7 MPa (0-1000 psi)	Pacific Scientific PPI	2 3
Displacement dial gage	Range 10.000", resolution 0.001"	Starret	1
Flowmeter	a) Model 610, range 0.002 to 1.0 cm^3/min Capacity 250 psi (max) b) Model 10, range 0.002 to 1.1 cm^3/min Shielded, cap. 600 psi (max)	Matheson Gilmont	1 3
Compression packer	All stainless steel construction with natural rubber sleeve. O.D. = 0.98" Length of end plates & rubber sleeve = 4.0"	Baski Water Instr.	1
Nitrogen gas tank & pressure regulator	Cap. 220 ft^3 Single-stage regulating valve		3 3

201

Table D.1 Equipment List--Continued

Item	Description	Manufacturer	Quantity
Measuring pipettes	a) Cap. 1 ml w/ 0.01 ml gradation		12
	b) Cap. 5 ml w/ 0.1 ml gradation		2
	c) Cap. 10 ml w/ 0.1 ml gradation		2
	d) Cap. 24 ml w/ 0.1 ml gradation		2
Transparent plastic tubing	3/18" O.D.	Tygon	5 m
Catheter	0.65 mm x 61.0 cm	Bard Biomedical	5
Syringe	6 cc, 20 cc, 60 cc	Bard Biomedical	5
Rubber stopper	1.25" O.D.		20
316 stainless steel tubing	1/8" O.D., 0.035 " wall thickness	Wisco	15 m
Copper tubing	1/4" O.D.		10 m
Quick connect	a) body: st. steel SS-QM2-B-200	Swagelok	6
	b) stem: st. steel SS-QM2-S-200		6
Needle valve	a) brass	Hoke	2
	b) st. steel, w/ mount		5
Connector	a) male, 8CM12-316SS, 1/2" O.D. - 3/4" pipe	Hoke	8
	b) female, 2CF4-316SS, 1/8 " O.D. - 1/2" pipe		8
Plug	2P-316SS, 1/8" O.D. - 7/16" Hex. size	Hoke	5
Tube cross	2C-316SS, 1/8" O.D. - 7/16" Hex. size	Hoke	5

202

Table D.1 Equipment List- Continued

Item	Description	Manufacturer	Quantity
Tee, all tube	4M brass, 1/4" O.D.	Hoke	3
Reducer	4R8-316SS, 1/4" O.D. - 1/2" O.D.	Hoke	8
Reducing union	4RU2-316SS, 1/4" O.D. - 1/8" O.D.	Hoke	13
Bulkhead union	2BU-316SS, 1/8" O.D.	Hoke	5
Flow Test Accessories:			
Scotchweld Structural Adhesive	Epoxy 2216A (gray) and 2216B (white)	3M	2 cans
Gasket sealant	Non-hardening type	Permatex	1 tube
Silicon lubricant	High-vacuum grease	Dow Corning	1 tube
Dye marker	Red and yellow green, water-soluble liquid concentrate	Formulab	
Dual Thermometer-Hygrometer	Model No. 3310-40, measuring temperature and relative humidity	Cole-Parmer	1
Temperature recorder	Continuous 1-week recording	Dickson	1
Dynamic Loading Test Components:			
Shaking table & power unit	Model 5900, variable speed, large, reciprocating	Eberbach	1
Platform		Eberbach	1

203

Table D.1 Equipment List--Continued

Item	Description	Manufacturer	Quantity
Utility carrier		Eberbach	1
Crosswise bar clamp		Eberbach	2
Specimen holder	Aluminum seat & top clamp and a set of 4 steel cables and turnbuckles	University Instrument Shop	2 sets
Sinusoid g-meter	Range 0 to 5 g, 0 to 5 Hz	Univ. Inst. Shop	1
Slotted optical limit switch	MCT 8, with infrared emitter & sensor	Monsanto	1
Infrared light breaker	Styrene		1

204

APPENDIX E

TEMPERATURE, RELATIVE HUMIDITY, EVAPORATION RECORDS

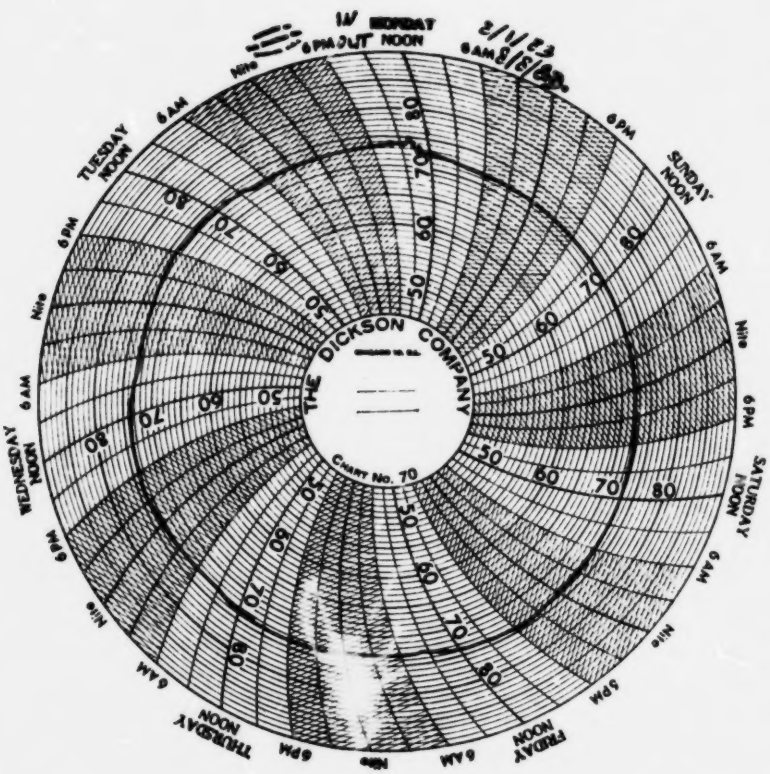

Figure E.1 An example of weekly temperature reading recorded by a Dickson continuous temperature recorder.

BEST COPY AVAILABLE

Table E.1 Evaporation Record, 3/15-6/27/83. Water Level in Pipette (cm^3).

Date	24 cm^3 Pipette	10 cm^3 Pipette	5 cm^3 Pipette	2 cm^3 Pipette
3/15/83	16.60			
3/16	16.58			
3/17	16.55			
3/21	16.46			
3/22	16.45			
3/23	16.42			
3/24	16.39			
3/25	16.37			
3/26	16.33			
3/27	16.31			
3/28	16.30			
3/29	16.27			
3/30	16.25			
3/31	16.22			
4/1	16.20			
4/2	16.19			
4/3	16.17			
4/4	16.12			
4/5	16.10			
4/6	16.08			
4/7	16.05			
4/8	16.02			
4/9	16.00			
4/10	15.98			
4/11	15.97			
4/12	15.95			
4/13	15.92			
4/14	15.90			
4/15	15.89			
4/16	15.86			
4/17	15.83			
4/18	15.80			
4/19	15.79			
4/20	15.77			
4/21	15.75			
4/22	15.72			
4/23	15.70			
4/24	15.68			
4/25	15.66			
4/26	15.62			
4/27	15.60			
4/29	15.57		4.80	1.971
4/30	15.54		4.79	1.960

Table E.1 Evaporation Record, 3/15-6/27/83. Water Level in Pipette (cm^3).--Continued

Date	24 cm^3 Pipette	10 cm^3 Pipette	5 cm^3 Pipette	2 cm^3 Pipette
5/1	15.50		4.77	1.945
5/2	15.48		4.75	1.800
5/3	15.46		4.72	1.781
5/4	15.40		4.70	1.770
5/5	15.39		4.68	1.760
5/6	15.38		4.67	1.750
5/7	15.35		4.64	1.740
5/8	15.31		4.61	1.727
5/9	15.30		4.60	1.721
5/10	15.28		4.58	1.711
5/11	15.26		4.57	1.700
5/12	15.23		4.56	1.691
5/13	15.21		4.54	1.682
5/14	15.19		4.52	1.671
5/15	15.17		4.50	1.662
5/16	15.14		4.48	1.655
5/17	15.11		4.47	1.650
5/18	15.10		4.45	1.640
5/19	15.09		4.44	1.630
5/20	15.03		4.41	1.621
5/21	15.00		4.40	1.611
5/22	14.98		4.38	1.602
5/23	14.97		4.37	1.600
5/24	14.95		4.37	1.593
5/25	14.93		4.35	1.587
5/26	14.91		4.33	1.580
5/27	14.89		4.31	1.571
5/28	14.88		4.30	1.566
5/29	14.86		4.29	1.561
5/30	14.83		4.29	1.559
5/31	14.82		4.28	1.551
6/1	14.81		4.27	1.549
6/2	14.80		4.27	1.540
6/3	14.80		4.25	1.533
6/6	14.72		4.21	1.519
6/7	14.71		4.20	1.510
6/8	14.70		4.19	1.502
6/9	14.69		4.17	1.496
6/10	14.69		4.17	1.491
6/13	14.61		4.13	1.472
6/14	14.60		4.11	1.470
6/15	14.59		4.10	1.461
6/16	14.59		4.09	1.459

Table E.1 Evaporation Record, 3/15-6/27/83. Water Level in Pipette (cm^3).--Continued

Date	24 cm^3 Pipette	10 cm^3 Pipette	5 cm^3 Pipette	2 cm^3 Pipette
6/17	14.56	9.50	4.08	1.451
6/20	14.50	9.41	4.05	1.437
6/21	14.48	9.39	4.03	1.429
6/22	14.48	9.39	4.02	1.423
6/23	14.43	9.34	4.01	1.420
6/24	14.42	9.31	4.00	1.413
6/26	14.39	9.27	3.98	1.400
6/27	14.39	9.24	3.97	1.397

BLANK PAGE

Table E.2 Temperature, Humidity, and Evaporation Records, 6/28-8/13/83.

Date	Water Level in Pipette (cm^3)				Temperature (^oF)		Humidity (%)	
	24 cm^3	10 cm^3	5 cm^3	2 cm^3	Morning	Evening	Morning	Evening
6/28/83	14.38	9.23	3.97	1.390	70	70	40	37
6/29	14.34	9.21	3.96	1.385	69	70	37	36
6/30	14.31	9.19	3.94	1.380	70	70	37	35
7/1	14.31	9.19	3.93	1.374	70	70	41	36
7/2	14.28	9.13	3.92	1.372	-	70	-	37
7/3	14.26	9.10	3.90	1.361	-	69	-	36
7/4	14.25	9.10	3.90	1.360	69	69	40	41
7/5	14.24	9.09	3.89	1.352	70	-	41	-
7/6	14.22	9.07	3.88	1.350	72	71	51	49
7/7	14.21	9.05	3.87	1.344	72	71	55	56
7/8	14.20	9.02	3.87	1.341	71	71	64	65
7/9	14.19	9.00	3.86	1.338	71	71	61	60
7/10	14.18	8.99	3.85	1.335	70	70	61	61
7/11	14.18	8.99	3.85	1.331	71	71	62	59
7/12	14.16	8.98	3.83	1.330	72	71	59	59
7/13	14.15	8.97	3.83	1.323	72	71	59	56
7/14	14.14	8.97	3.82	1.321	71	72	59	58
7/15	14.13	8.92	3.81	1.319	72	72	39	58
7/16	14.11	8.90	3.80	1.313	70	69	59	49
7/17	14.10	8.90	3.80	1.310	69	68	49	46
7/18	14.09	8.89	3.79	1.308	72	70	53	57
7/19	14.09	8.88	3.78	1.301	71	72	55	48
7/20	14.08	8.84	3.78	1.299	72	73	60	60
7/21	14.05	8.82	3.77	1.294	73	-	61	-
7/22	14.04	8.81	3.77	1.291	73	-	63	-
7/25	14.01	8.80	3.75	1.282	71	-	64	-
7/26	14.00	8.79	3.74	1.281	72	72	61	60
7/27	14.00	8.78	3.73	1.279	72	72	62	60
7/28	14.00	8.75	3.73	1.272	72	72	60	60

209

Table E.2 Temperature, Humidity, and Evaporation Records, 6/28-8/13/83.--Continued

Date	Water Level in Pipette (cm^3)				Temperature (^oF)		Humidity (%)	
	24 cm^3	10 cm^3	5 cm^3	2 cm^3	Morning	Evening	Morning	Evening
7/29	13.99	8.72	3.72	1.271	71	-	61	-
8/1	13.98	8.70	3.71	1.261	70	71	64	63
8/2	13.95	8.70	3.70	1.260	72	72	64	62
8/3	13.92	8.69	3.70	1.259	71	71	64	62
8/4	13.91	8.69	3.69	1.254	71	70	63	62
8/5	13.91	8.66	3.68	1.251	72	70	63	62
8/6	13.90	8.65	3.68	1.248	70	69	63	63
8/7	13.88	8.63	3.67	1.243	-	69	-	65
8/8	13.88	8.61	3.67	1.241	70	71	64	62
8/9	13.86	8.60	3.66	1.239	72	71	64	63
8/10	13.86	8.60	3.66	1.239	74	-	70	-
8/11	13.85	8.60	3.66	1.239	71	71	64	64
8/12	13.85	8.60	3.66	1.238	71	-	64	-
8/13	13.82	8.57	3.63	1.229	70	-	64	-

210

Table E.3 Temperature, Humidity and Evaporation Records, 10/17/83-4/3/84.

Date	Water Level (cm^3) 1 cm^3 pipette	Temperature (^oF) Morning	Evening	Humidity (%) Morning	Evening
10/17/83	0.919	74	72	50	54.5
10/18	0.910	73	73	53.5	53.1
10/19	0.906	74	74	56.5	52
10/20	0.899	74	74	54	51
10/21	0.891	74	-	51.7	-
10/23	-	71	72	52.5	55
10/24	0.874	72	74	54	51.5
10/25	0.866	74	73	50	49
10/26	0.861	73	73	49	49.5
10/27	0.854	73	73	50	50
10/28	0.849	74	74	53	52
10/29	0.843	73	72	52	54
10/30	0.836	72	73	53.5	54
10/31	0.832	73	74	54	55
11/1	0.827	72	73	54	52.5
11/2	0.822	73	72	52	53
11/3	0.816	73	73	53	55
11/4	0.812	73	73	55	54
11/5	0.806	73	-	53.5	-
11/6	0.802	-	72	-	54
11/7	0.799	72	75	52.9	53
11/8	0.792	75	-	51.2	-
11/9	0.789	74	73	46	52
11/10	0.781	74	74	46.5	45.5
11/11	0.775	73	73	45.5	47.5
11/12	-	-	-	-	-
11/13	0.764	72	-	50	-
11/14	0.761	72	74	49.5	46.5
11/15	0.754	73	73	45.3	43
11/16	0.749	74	-	43	-
11/17	0.743	74	74	44.5	43
11/18	0.738	74	74	45	44.5
11/19	0.732	73	74	37.5	38
11/20	0.727	73	-	38	-
11/21	0.720	74	-	44.5	-
11/22	0.716	73	74	40.5	40
11/23	0.710	73	73	40	38
11/24	0.704	-	72	-	38
11/25	0.700	72	74	39	41
11/26	0.692	72	-	38.5	-
11/27	0.686	71	-	37.5	-
11/28	0.682	73	73	37.3	37.5
11/29	0.678	78	74	38	38

Table E.3 Temperature, Humidity and Evaporation Records, 10/17/83-4/3/84.--Continued

Date	Water Level (cm^3) 1 cm^3 pipette	Temperature (^oF) Morning	Evening	Humidity (%) Morning	Evening
11/30	0.671	73	74	38.9	40
12/1	0.668	75	75	44.9	44.5
12/2	0.662	75	75	48.5	48
12/3	0.657	74	74	46	46
12/4	0.651	74	74	48	45
12/5	0.649	74	75	43.9	40
12/6	0.644	74	75	39.2	40
12/7	0.640	74	75	39.2	39.5
12/8	0.633	74	74	39.5	40
12/9	0.628	75	-	39.5	-
12/12	0.613	73	74.3	40.4	39.5
12/13	0.608	74	74.5	39.1	38
12/14	0.603	74	74.3	38	37.8
12/15	0.598	-	74	-	39.6
12/16	0.591	-	74.3	-	40.5
12/19	0.580	73	74	41	41
12/20	0.576	74	-	40	-
12/21	0.571	74	74.5	41.8	40
12/22	0.566	74	-	41.2	-
12/23	0.560	75	75	39	40
12/26	0.546	74	74.5	48.5	50
12/27	0.542	72	75.5	48.2	45.5
12/28	0.540	75	75	45.8	41.5
12/29	0.535	74	-	39	-
12/30	0.530	74	74	37	38
12/31	0.528	74	73.5	37.4	38
1/2/84	0.518	73	-	42	-
1/3	0.513	73	74	40.1	40.5
1/4	0.510	74	75	40.5	41.5
1/5	0.505	74	-	42.8	-
1/6	0.501	75	74.5	44.8	47.5
1/7	0.499	75	74	48.1	47
1/8	0.491	-	74	-	46
1/9	0.488	74.5	75	46	46.5
1/10	0.700	74.5	-	41	-
1/11	0.697	74	74.5	38	38.5
1/12	0.691	74	74	39	37.5
1/13	0.688	74	74	38.2	38
1/15	0.679	-	73	-	40
1/16	0.674	73	-	40	-
1/17	0.670	75	-	41	-
1/18	0.667	74	74	36.5	37
1/19	0.662	73	73	37	37

Table E.3 Temperature, Humidity and Evaporation Records, 10/17/83-4/3/84.--Continued

Date	Water Level (cm^3) 1 cm^3 pipette	Temperature (^oF) Morning	Evening	Humidity (%) Morning	Evening
1/20	0.659	73	74	36.5	36
1/21	0.654	72	72.5	34.5	35
1/23	0.647	72	73	35.5	35.5
1/24	0.641	73	74	36	36
1/25	0.638	74	74.5	36	36
1/26	0.632	74	74.5	36	36
1/27	0.628	74	74	36.5	36
1/28	0.624	72.5	72.5	36.5	37
1/30	0.617	72	73	36	36
1/31	0.612	72.5	74	36.5	37
2/1	0.609	74	-	37	-
2/2	0.605	74	74.5	38.5	39
2/3	0.601	73.5	-	39	-
2/5	0.592	-	72	-	36.5
2/6	0.589	73	73	37	37
2/7	0.583	74	74.5	38	37.5
2/8	0.580	74	75	37.5	37.5
2/9	0.577	73.5	-	35.5	-
2/10	0.573	73.5	73	35.5	35
2/11	0.568	73	73.5	35	33.5
2/12	0.563	72.5	72.5	33.5	33.5
2/13	0.560	72.5	73	34	34
2/14	0.557	73	74	34	34
2/15	0.550	73	-	33	-
2/16	0.548	73	-	33.5	-
2/17	0.541	74	74.5	34.4	33.5
2/18	0.538	72.5	72.5	33	33
2/19	0.532	-	72	-	34
2/20	0.530	72	73	34	34
2/21	0.526	73	-	34	-
2/22	0.521	74	75	33	34
2/23	0.519	75	76	33	33.5
2/24	0.512	-	76	-	33
2/25	0.509	-	75	-	33.5
2/26	0.504	-	74	-	33
2/27	0.500	74	75	32.5	32.5
2/28	0.497	73	73	32	32
2/29	0.492	72	73	32.1	33
3/1	0.489	72	-	33.5	-
3/2	0.484	74	72	35	34
3/3	0.480	71	-	34	-
3/4	0.477	-	69.5	-	31
3/5	0.473	71	-	32	-

Table E.3 Temperature, Humidity and Evaporation Records, 10/17/83-4/3/84.--Continued

Date	Water Level (cm^3) 1 cm^3 pipette	Temperature (^oF) Morning	Temperature (^oF) Evening	Humidity (%) Morning	Humidity (%) Evening
3/6	0.470	73.5	74.5	33	33
3/7	0.465	-	75	-	32.5
3/8	0.460	75	76	33	32.5
3/9	0.458	71	76.5	33.5	33
3/12	0.445	75	-	33.5	-
3/13	0.441	74	-	35	-
3/14	0.438	74	-	35	-
3/17	0.425	-	73	-	35
3/18	0.421	-	72.5	-	33
3/19	0.419	72.5	73	33.5	33.5
3/20	0.415	73.5	73.5	34	33.5
3/21	0.411	73.5	74	34	33.5
3/22	0.408	74	-	35	-
3/23	0.403	73.5	-	32.5	-
3/24	0.400	73	-	32	-
3/26	0.391	-	73	-	34
3/27	0.388	73	-	35	-
3/28	0.385	73.5	-	33	-
3/29	0.380	-	73	-	32
3/30	0.378	73	-	32.5	-
3/31	0.373	73	-	33	-
4/1	0.369	-	72	-	32
4/2	0.366	73	-	34	-
4/3	0.362	-	73.5	-	33

APPENDIX F

FLOW TEST RESULTS AND LABORATORY NOTES

Table F.1 Test Results for Specimen CG5309-04 (Rock Bridge)

Date	Injection Pressure (MPa)		Flow Rate (cm^3/min)	r^2	Test Duration (min)	Number of Data
3/31-4/1[a,b]	1.5	L	-	-	1460	31
		R	-	-		31
4/2-4/4[b,c]	1.6	L	7.42×10^{-5}	0.77	1585	10
		R	7.70×10^{-5}	0.98		17
4/5[b,c,e]	2.6	L	1.61×10^{-4}	0.58	1331	18
		R	1.61×10^{-4}	0.96		18
4/5-5/7[b,c]	2.2	L	1.13×10^{-4}	0.82	1820	19
		R	1.99×10^{-4}	0.99		19
4/8-4/12[b,d]	1.3	L	8.76×10^{-5}	0.39	2712	13
		R	9.38×10^{-5}	0.98		20
4/12-4/13[b,e]	3.0	L	2.04×10^{-4}	0.97	470	13
		R	1.95×10^{-4}	1.00		18
4/13-4/14[b,d,e]	3.5	L	1.37×10^{-4}	0.93	375	11
		R	2.76×10^{-4}	0.99		17
4/14[b,e]	4.0	L	2.21×10^{-4}	1.00	450	19
		R	2.76×10^{-4}	0.99		19
4/15	3.2	L	1.45×10^{-4}	0.92	445	18
		R	2.10×10^{-4}	0.98		19
4/18	2.5	L	1.51×10^{-4}	0.93	720	26
		R	1.72×10^{-4}	0.98		26
11/23[f]	1	L	4.07×10^{-5}	0.92	291	5
		R	3.67×10^{-5}	0.97	291	5
		F	4.20×10^{-2}		484	7
11/24-11/26	1	L	4.55×10^{-5}	0.81	140	
		R	5.14×10^{-5}	0.98	223	4
		F	4.20×10^{-2}		2669	14
11/30-12/1	1.1	L	4.49×10^{-5}	0.92	391	
		R	7.72×10^{-5}	0.97	424	8
		F	1.81×10^{-1}		2069	20

Table F.1 Test Results for Specimen CG5309-04 (Rock Bridge)--Continued

Date	Injection Pressure (MPa)		Flow Rate (cm^3/min)	r^2	Test Duration (min)	Number of Data
12/7-12/9	1.1	L	2.04×10^{-5}	0.99	199	
		R	no flow		1732	11
		F	3.10×10^{-1}		1732	11
12/19-12/20[g]	1	L	6.18×10^{-5}	0.92	649	
		R	6.68×10^{-5}	0.94	649	11
		F	1.14×10^{-1}		1711	14
11/27-11/28	2	L	no flow		1578	14
		R	3.51×10^{-5}	0.89	1289	11
		F	1.79×10^{-1}		1578	14
12/1-12/2	2.1	L	no flow		2281	10
		R	4.55×10^{-5}	0.81	284	4
		F	3.00×10^{-1}		2281	10
12/4-12/5	2	L	no flow		782	
		R	5.89×10^{-5}	0.90	173	4
		F	3.98×10^{-1}		782	11
12/6	2.1	L	4.34×10^{-5}	0.96	192	4
		R	4.04×10^{-5}	0.85	269	6
		F	4.70×10^{-1}		658	12
12/21[h]	2.1	L	no flow		1444	8
		R	2.96×10^{-5}	0.96	391	4
		F	> 1.00		1444	8
12/26	2	L	5.42×10^{-5}	1.00	387	4
		R	2.68×10^{-5}	0.95	515	6
		F	3.02×10^{-1}		719	6
12/28[i]	2.1	L	no flow		666	10
		R	no flow		666	10
		F	> 1.00		666	10
11/29[j]	4	L	no flow		435	9
		R	3.07×10^{-4}	1.00	435	9
		F	3.40×10^{-1}		435	9
12/5	4	L	9.21×10^{-5}	0.68	75	3
		R	2.02×10^{-4}	0.99	510	10
		F	4.60×10^{-1}		510	10

Table F.1 Test Results for Specimen CG5309-04 (Rock Bridge)--Continued

Date	Injection Pressure (MPa)		Flow Rate (cm^3/min)	r^2	Test Duration (min)	Number of Data
12/12	3.5	L	no flow		563	6
		R	6.77×10^{-5}	0.82	490	3
		F	4.60×10^{-1}		563	6
12/14	4	L	no flow		437	7
		R	9.91×10^{-5}	0.90	243	4
		F	4.60×10^{-1}		437	7
12/22[k]	4	L	1.50×10^{-5}	1.00	265	3
		R	2.01×10^{-4}	1.00	337	4
		F	> 1.00		389	5
12/27[k]	4	L	4.97×10^{-5}	0.99	293	4
		R	1.44×10^{-4}	0.92	473	7
		F	> 1.00		473	7
12/30[l]	4					

r^2 = coefficient of determination
L = peripheral flow rate through the rock
R = longitudinal flow rate through the rock bridge (one-dimensional flow)
F = inflow rate observed in the flowmeter

NOTES:

(a) Flow tests start on 110 mm rock bridge. No outflow recorded, saturation process.
(b) Slight seepage (leakage) in the epoxy bond.
(c) Air bubbles in the outflow lines.
(d) Test done intermittently within the time period.
(e) Seepage from the rock specimen.
(f) Cut rock bridge length to 101.6 mm and restart flow testing.
(g) Clean oil from flowmeter.
(h) Flowmeter float covered with oil.
(i) Leakage in flowmeter; float covered with oil.
(j) Large seepage through rock cylinder.
(k) Large seepage and leakage.
(l) Epoxy bond failed; steel connector popped out from sample.

Table F.2 Test Results for Specimen CG5309-08 (Wet Cement Seal)

Date	Injection Pressure (MPa)		Flow Rate (cm^3/min)	r^2	Test Duration (min)	Number of Data
7/6[a]	1	L	9.59×10^{-5}	0.87	240	7
		R	no flow	-	390	9
		D	2.77×10^{-3}	0.85	390	7
		F	6.80×10^{-3}	-	390	9
7/6-7/7	1	L	1.51×10^{-4}	0.91	360	7
		R	1.11×10^{-4}	0.93	360	7
		D	8.01×10^{-3}	0.99	1085	15
		F	1.48×10^{-2}	-	1085	15
7/11-7/12	1	L	1.56×10^{-4}	1.00	375	7
		R	7.99×10^{-5}	0.96	375	7
		F	1.80×10^{-2}	-	1360	15
7/15-7/16[b]	1	L	1.43×10^{-4}	0.99	450	11
		R	7.73×10^{-5}	0.89	195	5
7/7-7/8	2	L	2.01×10^{-4}	0.98	467	9
		R	4.04×10^{-4} [c]	0.99	467	9
		D	1.70×10^{-2}	1.00	1435	18
7/12-7/13[d]	2	L	1.42×10^{-4}	0.98	435	6
		R	1.90×10^{-4}	0.96	435	5
7/13-7/14[e]	2	L	1.40×10^{-4}	0.98	633	13
		R	3.55×10^{-4} [f]	0.99	633	13
7/9-7/10[g]	4	L	no flow	-	255	6
		R	2.34×10^{-4}	0.97	255	6
7/10-7/11g	4	L	no flow	-	660	17
		R	3.16×10^{-4} [h]	0.98	450	10
7/14[i]	4	L	1.34×10^{-4} [j]	0.99	526	13
		R	4.21×10^{-4}	0.92	616	16
7/17[k]						
10/18-10/21/83	3.8	L	2.69 E-04	0.96	656	12
		R	5.29 E-05	0.98	3390	34
		F	1.70 E-01 [l]		3540	39

Table F.2 Test Results for Specimen CG5309-08 (Wet Cement Seal)--Continued

Date	Injection Pressure (MPa)		Flow Rate (cm^3/min)	r^2	Test Duration (min)	Number of Data
11/7-11/10	3.8	L	1.86 E-04	0.87	1377	20
		R	1.18 E-04	0.99	4950	38
		F	2.70 E-01		4985	40
11/19	4	L	6.97 E-05	0.98	115	3
		R	1.52 E-04	1.00	452	7
		F	9.90 E-02		452	7
11/21-11/23	3.8	L	2.28 E-04	0.90	557	11
		R	1.48 E-04	1.00	2992	14
		F	4.70 E-01		2992	14
10/5-10/8	2	L	2.31 E-04	0.97	915	11
		R	2.87 E-05	1.00	906	10
		F	4.50 E-02		4048	26
10/13-10/14	2	L	1.85 E-04	0.96	835	11
		R	2.59 E-05	0.98	835	11
		F	5.00 E-01		1795	13
10/21-10/27	1.9	L	2.30 E-04	0.97	1590	20
		R	3.99 E-05	0.98	8600	48
		F	2.00 E-01		8600	48
10/28-11/1[n]	2	L	3.16 E-04	0.98	390	10
		R	3.37 E-05	0.96	5294	29
		F	3.00 E-02		5657	32
11/10-11/14	1.8	L	2.24 E-04	0.94	1136	15
		R	7.46 E-05	0.99	6400	28
		F	8.50 E-01		6400	28
11/23-11/28	2	L	1.81 E-04	0.98	2603	19
		R	8.29 E-05	1.00	7450	33
		F	3.30 E-01		7450	33
10/3-10/5	1	L	1.71 E-04	0.99	345	7
		R	no flow		2490	19
		F	2.50 E-02		2490	19
10/9-10/12	1	L	1.53E-04	0.95	1123	13
		R	no flow		4156	27
		F	7.00 E-02		4156	27

Table F.2 Test Results for Specimen CG5309-08 (Wet Cement Seal)--Continued

Date	Injection Pressure (MPa)		Flow Rate (cm^3/min)	r^2	Test Duration (min)	Number of Data
11/1-11/4	1	L	1.20 E-04	0.92	872	9
		R	1.84 E-05	0.95	935	8
		F	4.00 E-02		4076	29
11/14-11/19	1	L	2.75 E-04	0.93	1534	23
		R	1.88 E-05	0.93	4836	27
		F	6.60 E-02		6796	33
11/28-12/1	1	L	3.68 E-04	0.97	612	14
		R	2.56 E-05	0.91	2631	19
		F	2.00 E-01		3677	23
12/1-12/3[g]	3.6	L	1.26×10^{-4}	0.89	1061	14
		R	1.86×10^{-4}	0.99	3208	18
		F	4.20×10^{-1}		3208	18
12/13-12/15	3.7	L	1.36×10^{-4}	0.95	1237	13
		R	2.05×10^{-4}	1.00	3013	19
		F	4.00×10^{-1} 1		1345	13
12/29-12/31	3.8	L	1.67×10^{-4}	0.91	846	7
		R	1.91×10^{-4}	0.99	2561	11
1/8-1/10/84[g]	3.9	L	1.93×10^{-4}	0.82	353	9
		R	1.93×10^{-4}	1.00	2530	22
1/24[g]	4	L	1.74×10^{-4}	0.94	226	7
		R	1.51×10^{-4}	0.99	783	14
		D	6.42×10^{-2}		797	15
2/1	4.1	L	1.68×10^{-4}	0.98	348	5
		R	1.44×10^{-4}		348	5
		D	6.40×10^{-2}	1.00	348	5
2/6	4	L	1.83×10^{-4}	0.85	498	8
		R	1.62×10^{-4}	0.99	498	8
		D	5.99×10^{-2}	1.00	417	7
2/7	4	L	3.47×10^{-4}	0.94	258	8
		R	1.60×10^{-4}	0.98	235	7
		D	5.96×10^{-2}	1.00	268	9
2/7[o]						

Table F.2 Test Results for Specimen CG5309-08 (Wet Cement Seal)--Continued

Date	Injection Pressure (MPa)		Flow Rate (cm^3/min)	r^2	Test Duration (min)	Number of Data
2/7	4	L	1.50×10^{-4}	0.84	70	3
		R	1.87×10^{-4}	0.99	274	7
		D	6.04×10^{-2}	1.00	201	6
2/13	4	L	3.51×10^{-4}	0.95	402	8
		R	1.73×10^{-4}	0.98	376	7
		D	5.91×10^{-2}	1.00	402	8
2/13[p]						
2/13	4	L	no flow		85	4
		R	1.41×10^{-4}	1.00	85	4
		D	6.10×10^{-2}	1.00	85	4
2/14	4	L	3.44×10^{-5}	0.88	56	5
		R	1.24×10^{-4}	0.97	269	7
		D	6.06×10^{-2}	1.00	269	7
2/20	4	L	1.25×10^{-4}	0.96	513	11
		R	1.99×10^{-4}	0.99	513	11
		D	5.83×10^{-2}	1.00	513	11
2/24	4	L	2.41×10^{-4}	0.89	418	9
		R	2.11×10^{-4}	0.99	418	9
		D	6.12×10^{-2}	1.00	429	10
		F	1.66×10^{-1}		429	10
3/1	4	L	2.18×10^{-4}	0.99	349	6
		R	1.76×10^{-4}	0.98	384	8
		D	6.24×10^{-2}	1.00	384	8
		F	3.00×10^{-1}		384	8
3/6	4	L	1.40×10^{-4}	0.97	143	7
		R	1.77×10^{-4}	0.97	240	9
		D	6.40×10^{-2}	1.00	240	9
		F	1.50×10^{-1}		240	9
3/6[q]						
3/6-3/7	4	L	1.60×10^{-4}	0.99	280	7
		R	1.69×10^{-4}	1.00	644	15
		D	6.62×10^{-2}	1.00	440	12
		F	2.00×10^{-1}		644	15

Table F.2 Test Results for Specimen CG5309-08 (Wet Cement Seal)--Continued

Date	Injection Pressure (MPa)		Flow Rate (cm^3/min)	r^2	Test Duration (min)	Number of Data
3/12	4	L	3.52×10^{-4}	0.99	280	8
		R	1.76×10^{-4}	0.97	280	8
		D	6.48×10^{-2}	1.00	280	8
		F	2.68×10^{-1}		280	8
12/3-12/5	2	L	9.13×10^{-5}	0.92	1828	13
		R	1.01×10^{-4}	0.96	3013	21
		F	3.51×10^{-1}		3013	21
12/22-12/23[r]	2	L	1.89×10^{-4}	0.97	311	4
		R	8.89×10^{-5}	1.00	1893	8
		F	2.98×10^{-1}		1893	8
12/26-12/28	2	L	1.69×10^{-4}	0.98	1417	14
		R	1.12×10^{-4}	0.99	3038	25
		F	2.29×10^{-1}		2207	18
12/31	2.2	L	2.28×10^{-4}	0.96	544	6
		R	1.66×10^{-4}	0.98	544	6
1/2	2	L	3.02×10^{-4}	0.91	291	9
		R	1.15×10^{-4}	0.99	1311	11
1/4-1/7	2	L	2.89×10^{-4}	0.93	1677	23
		R	1.29×10^{-4}	1.00	4364	30
1/12-1/13	1.9	L	1.07×10^{-4}	0.87	1094	9
		R	7.05×10^{-5}	1.00	2180	15
1/20	2.1	L	no flow		263	5
		R	6.11×10^{-5}	0.92	263	5
		D	2.95×10^{-2}	0.99	263	5
1/21-1/22	2.1	L	no flow		741	5
		R	5.30×10^{-5}	1.00	339	3
		D	2.80×10^{-2}	1.00	741	5
1/25	2.1	L	3.25×10^{-4}	0.98	399	7
		R	7.60×10^{-5}	1.00	799	8
		D	2.93×10^{-2}	1.00	828	10

Table F.2 Test Results for Specimen CG5309-08 (Wet Cement Seal)--Continued

Date	Injection Pressure (MPa)		Flow Rate (cm^3/min)	r^2	Test Duration (min)	Number of Data
1/26-1/27	2	L	2.41×10^{-4}	0.92	332	5
		R	4.50×10^{-5}	0.99	1178	9
		D	2.88×10^{-2}	1.00	910	8
1/30-1/31	2	L	2.42×10^{-4}	0.88	566	8
		R	7.24×10^{-5}	1.00	865	10
		D	2.78×10^{-2}	1.00	1060	12
2/2-2/3	2.1	L	2.55×10^{-4}	0.98	499	6
		R	6.08×10^{-5}	0.99	1151	12
		D	2.84×10^{-2}	1.00	984	11
2/11	2	L	1.70×10^{-4}	0.96	223	4
		R	5.33×10^{-5}	0.98	379	6
		D	2.54×10^{-2}	1.00	563	7
2/15	2	L	2.60×10^{-4}	0.99	370	8
		R	6.64×10^{-5}	0.99	370	8
		D	2.59×10^{-2}	1.00	370	8
2/17	2	L	2.39×10^{-4}	0.92	131	4
		R	6.78×10^{-5}	0.97	214	6
		D	2.71×10^{-2}	1.00	250	7
$2/17^s$						
2/17	2.1	L	1.81×10^{-4}	0.96	216	5
		R	8.25×10^{-5}	0.95	538	7
		D	2.78×10^{-2}	1.00	538	7
2/21	2	L	4.38×10^{-4}	0.95	380	7
		R	1.17×10^{-4}	0.99	355	6
		D	2.56×10^{-2}	1.00	380	7
2/22	2	L	2.65×10^{-4}	0.92	508	8
		R	1.18×10^{-4}	0.99	508	8
		D	2.44×10^{-2}	0.95	508	8
2/27	2	L	1.16×10^{-4}	0.66	558	8
		R	8.70×10^{-5}	1.00	687	9
		D	2.67×10^{-2}	1.00	687	9
		F	1.66×10^{-1}		687	8

Table F.2 Test Results for Specimen CG5309-08 (Wet Cement Seal)--Continued

Date	Injection Pressure (MPa)		Flow Rate (cm^3/min)	r^2	Test Duration (min)	Number of Data
3/2	2	L	4.77×10^{-4}	0.97	263	7
		R	8.75×10^{-5}	0.96	697	7
		D	2.77×10^{-2}	1.00	707	8
		F	2.40×10^{-1}		707	8
3/9	2	L	3.93×10^{-4}	0.81	466	5
		R	8.49×10^{-5}	0.99	722	7
		D	2.78×10^{-2}	1.00	785	8
		F	2.46×10^{-1}		785	8
12/6-12/9	1	L	1.49×10^{-4}	0.96	2129	19
		R	2.35×10^{-5}	0.93	4820	28
		F	5.00×10^{-2}		5252	31
12/19-12/22	1	L	2.87×10^{-4}	0.95	1151	18
		R	3.33×10^{-5}	0.96	2258	20
		F	2.30×10^{-2}		4374	25
1/3	1.1	L	3.56×10^{-4}	0.93	538	8
		R	9.97×10^{-5}	0.97	627	11
1/27-1/28	1	L	2.68×10^{-4}	0.95	376	6
		R	1.58×10^{-5}	0.95	604	8
		D	1.50×10^{-2}	1.00	2054	10
2/9-2/10	1	L	3.29×10^{-4}	0.97	482	10
		R	1.46×10^{-5}	0.92	568	10
		D	1.37×10^{-2}	1.00	2209	14
2/16-2/17	1	L	4.76×10^{-4}	0.97	487	10
		R	5.14×10^{-5}	0.96	413	9
		D	1.37×10^{-2}	1.00	1436	12
2/23	1	L	2.11×10^{-4}	0.91	180	4
		R	4.43×10^{-5}	0.80	325	7
		D	1.37×10^{-2}	1.00	325	7
2/23[t]						
2/23-2/24	1	L	3.38×10^{-4}	1.00	63	3
		R	2.32×10^{-5}	0.98	817	6
		D	1.43×10^{-2}	1.00	1105	7

Table F.2 Test Results for Specimen CG5309-08 (Wet Cement Seal)--Continued

Date	Injection Pressure (MPa)		Flow Rate (cm^3/min)	r^2	Test Duration (min)	Number of Data
2/28-2/29	1	L	2.99×10^{-4}	0.97	980	6
		R	3.34×10^{-5}	0.96	2174	10
		D	1.37×10^{-2}	1.00	1978	9
		F	1.73×10^{-1}		2174	10
3/7-3/8	1	L	2.05×10^{-4}	0.89	821	11
		R	2.73×10^{-5}	0.90	1849	13
		D	1.37×10^{-2}	1.00	1849	13
		F	1.88×10^{-1}		1849	13

r^2 = coefficient of determination
L = peripheral outflow rate through the rock around the plug
R = longitudinal outflow rate through the cement plug (one-dimensional flow)
D = inflow rate calculated from pressure intensifier piston displacement
F = inflow rate observed in the flowmeter

NOTES:

(a) Start flow tests and begin sample saturation. Valve in the water inflow line was found almost totally closed at the end of this test.
(b) Test duration is 2257 min, no flow during part of it.
(c) Flow rate = 1.44×10^{-4} cm^3/min with $r^2 = 0.75$ at 18 data, 1435 min.
(d) Leakage observed in the epoxy bond; total test duration is 1385 min.
(e) Leakage observed in the epoxy bond at two spots.
(f) Flow rate = 1.03×10^{-4} cm^3/min with $r^2 = 0.31$ at 18 data, 1485 min.
(g) Heavy seepage through the top half of the cylinder.
(h) Flow rate = 1.50×10^{-4} cm^3/min with $r^2 = 0.55$ at 17 data, 660 min.
(i) Heavy seepage and leakage in the epoxy bond.
(j) Flow rate = 3.51×10^{-5} cm^3/min with $r^2 = 0.15$ at 16 data, 616 min.
(k) Epoxy bond had to be replaced due to excessive leakage.
(l) Inflow rate on the high side, flowmeter float is covered by oil coming out of the pressure gage.
(m) Inflow rate on the high side, leakage in flowmeter connection.
(n) Clean oil from flowmeter tube and float.
(o) Dynamic loading at P = 4 MPa, acceleration = 2g, duration = 20 sec.
(p) Dynamic loading at P = 4 MPa, acceleration = 2g, duration = 40 sec.
(q) Dynamic loading at P = 4 MPa, acceleration = 2g, duration = 300 sec.
(r) Some minor seepage.
(s) Dynamic loading at P = 2 MPa, acceleration = 2g, duration = 80 sec.
(t) Dynamic loading at P = 1 MPa, acceleration = 2g, duration = 160 sec.

Table F.3 Test Results for Specimen CG5309-06 (Wet Cement Seal)

Date	Injection Pressure (MPa)		Flow Rate (cm^3/min)	r^2	Test Duration (min)	Number of Data
6/29-6/29/83[a]	1	L	no flow	-	1012	14
		R	no flow	-	1012	14
		D	9.46×10^{-3}	0.98	509	5
6/29-6/30	1.1	L	1.37×10^{-4}	0.94	665	13
		R	1.52×10^{-4}	0.85	1480	18
		D	9.94×10^{-3}	1.00	1480	18
7/1[b]						
7/18-7/19	1	L	no flow	-	1290	9
		R	no flow	-	1290	9
		F	4.50×10^{-3}	-	1290	9
7/19-7/21	1	L	4.38×10^{-5} [c]	0.92	416	8
		R	no flow	-	2805	25
		F	4.50×10^{-3}	-	2805	25
7/26-7/28	1	L	4.34×10^{-5}	0.92	278	8
		R	no flow	-	2791	39
8/1	1	L	5.97×10^{-5} [d]	0.97	482	11
		R	no flow	-	707	14
8/8-8/9	1	L	8.26×10^{-5}	0.99	500	8
		R	no flow	-	1890	15
6/30-7/1[e]	2	L	5.33×10^{-5}	0.93	575	13
		R	1.52×10^{-4}	0.99	1433	21
		D	9.94×10^{-3}	1.00	1323	20
7/21-7/22[f]	2	L	2.49×10^{-5}	0.84	435	8
		R	1.46×10^{-4}	0.99	435	8
7/28	2	L	3.33×10^{-5}	0.86	438	8
		R	no flow	-	1436	19
8/2-8/3[f]	2	L	7.35×10^{-5}	0.97	505	9
		R	1.58×10^{-4}	0.98	650	12
8/9-8/11[f]	2	L	5.71×10^{-5}	0.78	464	8
		R	1.67×10^{-4}	0.83	170	4

Table F.3 Test Results for Specimen CG5309-06 (Wet Cement Seal)--Continued

Date	Injection Pressure (MPa)		Flow Rate (cm^3/min)	r^2	Test Duration (min)	Number of Data
7/25	4	L	2.19×10^{-5}	0.86	470	14
		R	3.31×10^{-4}	0.98	470	14
7/29	4	L	3.94×10^{-5}	0.73	458	16
		R	3.06×10^{-4}	0.95	458	16
8/4-8/6[g]	4	L	5.83×10^{-5}	0.96	476	12
		R	3.27×10^{-4}	1.00	3125	31
8/11-8/12[g]	4	L	7.58×10^{-5}	0.97	447	14
		R	3.13×10^{-4}	0.99	1350	18
9/12-9/14/83	4	L	1.07×10^{-4}	0.99	881	10
		R	2.29×10^{-4}	0.99	2841	20
		D	2.57×10^{-3}	1.00	2543	19
		F	5.50×10^{-3}		2841	20
9/19-9/23	4	L	5.32×10^{-5}	0.94	1146	13
		R	1.54×10^{-4}	0.99	4831	29
		D	1.83×10^{-3}	1.00	5347	32
		F	1.80×10^{-3}		5347	32
10/1-10/4	4	L	3.03×10^{-5}	0.87	441	13
		R	1.39×10^{-4}	0.95	4021	40
		D	1.65×10^{-3}	1.00	5395	41
10/12-10/14	4	L	4.49×10^{-5}	0.96	673	12
		R	1.20×10^{-4}	0.95	2851	30
		D	1.42×10^{-3}	1.00	5565	38
		F	3.60×10^{-3}		5565	38
10/20-10/24	4	L	7.62×10^{-5}	0.96	802	16
		R	1.73×10^{-4}	0.98	3643	34
		D	1.27×10^{-3}	1.00	6032	42
10/28-11/5	4	L	7.28×10^{-5}	0.95	982	17
		R	2.04×10^{-4}	0.98	7339	51
		D	1.17×10^{-3}	1.00	10617	64
11/23-11/25	4	L	no flow		2783	10
		R	3.56×10^{-4}	0.98	1811	9
11/25[h]						

Table F.3 Test Results for Specimen CG5309-06 (Wet Cement Seal)--Continued

Date	Injection Pressure (MPa)		Flow Rate (cm^3/min)	r^2	Test Duration (min)	Number of Data
11/25-11/28	4	L	no flow		4602	23
		R	3.27×10^{-4}	1.00	2805	22
9/9-9/12	2	L	5.76×10^{-5}	0.98	499	8
		R	no flow		4054	18
		D	1.17×10^{-3}	0.99	4054	18
		F	7.60×10^{-3}		4054	18
9/16-9/19	2	L	6.84×10^{-5}	0.95	1082	13
		R	5.62×10^{-5}	0.94	172	3
		D	9.63×10^{-4}	1.00	4871	25
9/23-9/28	2	L	8.18×10^{-5}	0.99	885	7
		R	4.98×10^{-5}	0.97	480	3
		D	7.82×10^{-4}	0.99	6930	31
		F	1.40×10^{-3}		1059	7
10/4-10/8	2	L	4.36×10^{-5}	0.86	863	7
		R	no flow		6557	31
		D	5.27×10^{-4}	0.94	6557	30
10/14-10/18	2	L	4.44×10^{-5}	0.85	650	10
		R	no flow		5210	25
		D	6.15×10^{-4}	1.00	5210	25
		F	1.80×10^{-2}		5210	23
10/26-10/28	2	L	3.87×10^{-5}	0.89	883	13
		R	7.76×10^{-5}	0.92	730	10
		D	5.90×10^{-4}	1.00	3517	25
11/6-11/14	2	L	5.78×10^{-5}	0.91	1964	30
		R	1.34×10^{-4}	0.96	2353	37
		D	5.58×10^{-4}	0.99	10983	59
11/18-11/23	2	L	no flow		7112	24
		R	1.58×10^{-4}	1.00	5907	23
11/28-11/29	2.1	L	no flow		1170	8
		R	1.69×10^{-4}	1.00	1170	8
11/29[1]						
11/29-12/1	2.1	L	no flow		2492	16
		R	1.61×10^{-4}	1.00	2492	16

Table F.3 Test Results for Specimen CG5309-06 (Wet Cement Seal)--Continued

Date	Injection Pressure (MPa)		Flow Rate (cm^3/min)	r^2	Test Duration (min)	Number of Data
9/15-9/16	1	L	no flow		1376	13
		R	no flow		1376	13
		D	5.02×10^{-4}	0.94	1226	10
9/28-9/30	1	L	7.35×10^{-5}	1.00	245	3
		R	no flow		2951	19
		D	8.95×10^{-5}	0.97	2951	19
10/8-10/11	1	L	2.08×10^{-5}	0.88	557	6
		R	no flow		3789	17
		D	3.47×10^{-4}	0.99	1693	14
10/18-10/20	1	L	8.52×10^{-5}	0.99	453	8
		R	no flow		2692	25
		D	3.12×10^{-4}	0.99	2247	18
11/15-11/17	1	L	7.65×10^{-5}	0.94	1181	16
		R	1.37×10^{-4}	0.96	824	12
		D	3.66×10^{-4}	0.93	3160	23
12/1-12/3/83[j]	1.1	L	no flow		3204	18
		R	7.34×10^{-5}	1.00	3204	18
12/6-12/9	1.1	L	no flow		5258	31
		R	7.00×10^{-5}	1.00	5258	31
12/19-12/22	1.1	L	no flow		4304	23
		R	8.37×10^{-5}	0.96	4304	23
1/5-1/9/84	1.1	L	no flow		5289	29
		R	6.48×10^{-5}	0.99	5289	29
1/27-1/30[k]	1.1	L	no flow		4245	13
		R	6.53×10^{-5}	0.99	2869	12
		F	2.80×10^{-2}		1818	9
12/4	2.2	L	no flow		324	6
		R	1.80×10^{-4}	0.99	324	6
12/4[l]						
12/4-12/5	2.2	L	no flow		1331	12
		R	1.64×10^{-4}	1.00	1331	12

Table F.3 Test Results for Specimen CG5309-06 (Wet Cement Seal)--Continued

Date	Injection Pressure (MPa)		Flow Rate (cm^3/min)	r^2	Test Duration (min)	Number of Data
12/22-12/23[m]	2	L	no flow		2256	12
		R	1.57×10^{-4}	0.80	2256	12
12/26-12/28	2	L	no flow		3469	26
		R	1.52×10^{-4}	0.95	3032	24
1/2-1/5/84	2.1	L	no flow		4290	33
		R	1.43×10^{-4}	1.00	4290	33
1/12-1/16	2	L	no flow		6159	25
		R	1.25×10^{-4}	1.00	6159	25
1/19-1/24	2	L	no flow		6652	36
		R	1.11×10^{-4}	1.00	6652	36
		F	2.70×10^{-2}		6652	36
1/30-2/1[n]	2.1	L	1.48×10^{-5}	0.99	390	5
		R	1.11×10^{-4}	0.91	3140	29
		F	1.01×10^{-1}		3140	29
12/13-12/14/83	4	L	no flow		1521	14
		R	3.19×10^{-4}	1.00	1521	14
12/14[o]						
12/14-12/15	4	L	no flow		2151	6
		R	3.01×10^{-4}	0.97	2151	6
12/29-12/31	4	L	no flow		3119	17
		R	2.89×10^{-4}	1.00	3119	17
1/9-1/10/84	4	L	no flow		1558	15
		R	2.71×10^{-4}	1.00	1558	15
1/24-1/26[p]	4	L	2.34×10^{-5}	0.95	1274	14
		R	2.38×10^{-4}	1.00	3061	26
		F	6.30×10^{-2}		3061	26
2/7[q]						

r^2 = coefficient of determination
L = peripheral outflow rate through the rock around the cement plug

Table F.3 Test Results for Specimen CG5309-06 (Wet Cement Seal)--Continued

R = longitudinal outflow rate through the cement plug (one-dimensional flow)
F = inflow rate observed in the flowmeter
D = inflow rate calculated from piston displacement of the pressure intensifier

NOTES:

(a) Start flow tests and begin saturation.
(b) Epoxy bond failed at 4 MPa injection pressure.
(c) Flow rate = 6.25×10^{-5} cm^3/min with $r^2 = 0.98$ at 4 data, 120 min on 7/19.
(d) Flow rate = 3.35×10^{-5} cm^3/min with $r^2 = 0.63$ at 14 data, 707 min.
(e) Epoxy bond leaks in two spots.
(f) Test duration is longer; no flow is recorded during part of it.
(g) Sample sides only slightly damp; seepage was unusually low for P = 4 MPa.
(h) Dynamic loading at P = 4 MPa, acceleration = 1.0 g, duration = 40 sec.
(i) Dynamic loading at P = 2 MPa, acceleration = 1.0 g, duration = 80 sec.
(j) Flow test is conducted using hydraulic accumulator.
(k) Flow test is conducted using pressure intensifier.
(l) Dynamic loading at P = 2 MPa, acceleration = 1 g, and duration = 160 sec.
(m) Start dye injection test using Formulabs' red dye marker.
(n) 2/1/84: the end of the testing program.
(o) Dynamic loading at P = 4 MPa, acceleration = 1 g, and duration = 320 sec.
(p) Red dye seeping out in radial direction from sample sides.
(q) 2/7/84: cut the sample in half lengthwise using a large oil-cooled saw.

Table F.4 Test Results for Specimen CG5309-31V (Wet Cement Seal)

Date	Injection Pressure (MPa)		Flow Rate (cm^3/min)	r^2	Test Duration (min)	Number of Data
4/20[a]	1.5	L	no flow	-	1290	11
		R	no flow	-	1290	11
4/21	1.5	L	no flow	-	450	9
		R	no flow	-	450	9
4/22	2	L	no flow	-	370	5
		R	no flow		370	5
4/25	2	L	no flow	-	600	10
		R	2.05×10^{-5}	0.91	600	10
4/26	2	L	1.43×10^{-4}	0.98	650	9
		R	4.21×10^{-5}	0.70	650	9
4/27-4/28	2.5	L	1.88×10^{-4}	0.97	955	12
		R	3.45×10^{-5}	0.92	955	12
4/28[b]	3	L	1.75×10^{-4}	0.88	588	14
		R	3.67×10^{-5}	0.88	588	14
5/4	3	L	1.58×10^{-4}	0.96	321	12
		R	3.16×10^{-5}	0.97	321	12
4/29[b]	3.5	L	1.42×10^{-4}	0.79	470	12
		R	3.54×10^{-5}	0.87	470	12
5/3	3.5	L	1.68×10^{-4}	0.91	390	12
		R	2.79×10^{-5}	0.90	445	13
5/2[b]	4	L	2.45×10^{-4}	0.93	360	12
		R	3.17×10^{-5}	0.91	504	16
5/5[c]	2.5	L	9.83×10^{-5}	1.00	93	3
		R	1.90×10^{-5}	0.74	333	7
5/16	2.5	L	no flow	-	429	7
		R	no flow	-	429	7
5/17-5/18	2.5	L	1.80×10^{-4}	0.79	904	12
		R	no flow	-	904	12
5/18-5/19	2	L	1.41×10^{-4}	0.93	1400	14
		R	no flow	-	1400	14

Table F.4 Test Results for Specimen CG5309-31V (Wet Cement Seal)--Continued

Date	Injection Pressure (MPa)		Flow Rate (cm^3/min)	r^2	Test Duration (min)	Number of Data
5/19-5/20	1.5	L	1.14×10^{-4}	0.82	1424	13
		R	1.09×10^{-5}	0.86	1424	13
5/20	3	L	3.10×10^{-4}	0.91	420	8
		R	1.98×10^{-5}	0.82	420	8
5/23	3	L	2.04×10^{-4}	0.99	255	8
		R	1.82×10^{-5}	0.67	255	8
5/23	3.5	L	2.44×10^{-4}	0.99	607	8
		R	2.20×10^{-5}	0.45	607	8
5/24	3.5	L	1.10×10^{-4}	0.85	908	12
		R	1.62×10^{-5}	0.63	908	12
5/26	3.5	L	1.14×10^{-4}	0.98	240	5
		R	9.08×10^{-6}	0.71	495	10
5/25	4	L	1.71×10^{-4}	0.99	437	8
		R	1.24×10^{-5}	0.61	617	11
5/27[c]	3.5		-	-	90	2
6/13[d]	1	L	no flow	-	317	5
		R	no flow	-	317	5
6/14	1	L	3.78×10^{-5}	0.94	440	8
		R	no flow	-	440	8
6/15	1	L	5.02×10^{-5}	0.61	620	8
		R	9.99×10^{-5}	0.97	620	8
6/16	1	L	no flow	-	1137	7
		R	6.20×10^{-5}	0.68	1137	7
		D	6.89×10^{-3}	0.90	1392	7
6/17	1	L	no flow	-	420	6
		R	2.25×10^{-4}	0.99	420	6
		D	9.23×10^{-3}	0.76	420	5
7/15	1	L	1.48×10^{-4}	0.97	290	7
		R	2.29×10^{-5}	0.87	245	6

Table F.4 Test Results for Specimen CG5309-31V (Wet Cement Seal)--Continued

Date	Injection Pressure (MPa)		Flow Rate (cm^3/min)	r^2	Test Duration (min)	Number of Data
7/22	1	L	1.64×10^{-4}	0.98	410	8
		R	no flow	-	410	8
7/25	1	L	1.60×10^{-4}	0.99	475	10
		R	no flow	-	475	10
7/26	1	L	1.68×10^{-4}	0.99	498	15
		R	no flow	-	702	19
8/1	1.2	L	2.00×10^{-4}	0.98	561	13
		R	no flow	-	1415	16
8/5-8/6	1.1	L	1.65×10^{-4}	0.93	238	5
		R	no flow	-	1896	13
8/8-8/9	1.1	L	1.50×10^{-4}	0.91	508	9
		R	no flow	-	1896	16
6/20	1.5	L	no flow	-	640	8
		R	7.75×10^{-5}	0.85	390	8
		D	1.19×10^{-2}	1.00	390	5
6/21	1.5	L	no flow	-	505	8
		R	2.58×10^{-4}	0.99	505	8
		D	1.19×10^{-2}	1.00	505	8
6/22	2	L	no flow	-	639	10
		R	2.50×10^{-4}	0.98	639	10
		D	1.62×10^{-2}	1.00	1252	8
7/14-7/15[e]	2	L	1.80×10^{-4}	0.99	466	7
		R	7.59×10^{-5}	0.97	466	7
7/18-7/19	2	L	1.89×10^{-4}	0.83	438	7
		R	no flow	-	1370	10
7/19-7/20[e]	2	L	1.55×10^{-4}	0.97	526	9
		R	8.09×10^{-5}	0.99	526	9
7/27	2	L	1.19×10^{-4}	0.99	395	8
		R	no flow	-	816	19

Table F.4 Test Results for Specimen CG5309-31V (Wet Cement Seal)--Continued

Date	Injection Pressure (MPa)		Flow Rate (cm^3/min)	r^2	Test Duration (min)	Number of Data
7/28-7/29[e]	2	L	1.49×10^{-4}	0.98	380	8
		R	7.07×10^{-5}	0.99	380	8
8/2-8/3	1.9	L	1.50×10^{-4}	1.00	285	5
		R	no flow	-	1249	10
8/9-8/11[e]	2	L	1.18×10^{-4}	0.97	464	8
		R	7.73×10^{-5}	0.99	464	8
6/23	2.5	L	no flow	-	918	11
		R	1.78×10^{-4}	0.87	918	11
		D	2.07×10^{-2}	1.00	1030	8
7/11-7/12	2.3	L	1.13×10^{-4}	0.97	372	5
		R	no flow		865	9
6/24	3	L	no flow	-	550	11
		R	1.72×10^{-4}	0.75	385	7
		D	2.63×10^{-2}	0.98	165	5
6/26	3.5	L	no flow	-	511	11
		R	no flow	-	511	11
		D	9.65×10^{-2}	0.94	449	9
6/27[c]	3.5	-		-	-	-
7/12-7/14[e]	3.5	L	1.64×10^{-4}	0.96	635	13
		R	6.80×10^{-5}	0.84	575	12
7/21	4	L	1.14×10^{-4}	0.97	574	16
		R	8.86×10^{-5}	0.96	902	22
7/29	4	L	1.20×10^{-4}	0.98	452	16
		R	1.36×10^{-4}	0.99	452	16
8/4-8/5	4	L	1.04×10^{-4}	0.95	606	15
		R	no flow	-	1665	23
8/11[e]	4	L	1.78×10^{-4}	0.99	402	13
		R	1.67×10^{-4} [f]	1.00	402	13

Table F.4 Test Results for Specimen CG5309-31V (Wet Cement Seal)--Continued

Date	Injection Pressure (MPa)		Flow Rate (cm^3/min)	r^2	Test Duration (min)	Number of Data
9/9/83	4	L	no flow		1675	18
		R	6.12×10^{-5}	0.98	32	3
		F	6.96×10^{-2}		1675	18
9/15-9/16[g]	4	L	3.06×10^{-5}	0.60	243	4
		R	5.03×10^{-5}	0.80	243	4
		F	1.15×10^{-1}		1851	20
9/21-9/22	4	L	no flow		1971	10
		R	no flow		1971	10
		F	9.70×10^{-2}		1971	10
9/28-9/29	4	L	8.10×10^{-6}	1.00	247	3
		R	no flow		1133	14
		F	1.49×10^{-1}		1133	14
10/5	4	L	1.67×10^{-5}	0.80	252	7
		R	no flow		858	17
		F	6.18×10^{-1}		858	17
10/6-10/8	4	L	3.95×10^{-5}	0.98	472	4
		R	2.93×10^{-5}	1.00	2639	15
		F	1.88×10^{-1}		2639	15
10/16-10/17	4	L	3.20×10^{-5}	0.98	358	4
		R	no flow		358	4
		F	1.60×10^{-1}		1998	19
10/18	4	L	5.05×10^{-5}	0.97	224	6
		R	5.39×10^{-5}	0.97	224	6
		F	1.65×10^{-1}		1245	11
11/15	4	L	4.16×10^{-5}	0.96	361	5
		R	5.59×10^{-5}	0.73	625	6
		F	1.35×10^{-1}			
11/16-11/17[h]	4	L	4.20×10^{-5}	0.98	489	7
		R	4.32×10^{-5}	0.86	1993	15
		F	3.40×10^{-2}		2087	16
11/23-11/25	4	L	no flow		2777	9
		R	no flow		2777	9
		D	8.89×10^{-3}	1.00	2777	9

Table F.4 Test Results for Specimen CG5309-31V (Wet Cement Seal)--Continued

Date	Injection Pressure (MPa)		Flow Rate (cm^3/min)	r^2	Test Duration (min)	Number of Data
11/25[i]						
11/25-11/27	4	L	no flow		3361	13
		R	no flow		3361	13
		D	9.30×10^{-3}	1.00	3361	13
9/3-9/5[g]	2	L	no flow		2543	11
		R	no flow		2543	11
		F	4.50×10^{-1}		2543	11
9/6	2.2	L	2.45×10^{-5}	0.93	215	4
		R	2.94×10^{-5}	0.92	278	4
		F	1.51×10^{-1}		967	12
9/7-9/8	2	L	no flow		1844	11
		R	no flow		1844	11
		F	1.48×10^{-1}		1844	11
9/12-9/14	2	L	no flow		3616	18
		R	no flow		3616	18
		F	5.17×10^{-2}		3616	18
9/19-9/21	2	L	1.24×10^{-5}	0.88	229	3
		R	no flow		2942	24
		F	6.80×10^{-2}		2942	24
9/23-9/26	2	L	3.89×10^{-5}	1.00	546	4
		R	no flow		4805	21
		F	1.39×10^{-1}		4805	21
9/29-10/2	2	L	5.60×10^{-5}	0.96	320	6
		R	no flow		4140	23
		F	9.20×10^{-2}		4140	23
10/9-10/12	2	L	4.05×10^{-5}	0.98	140	3
		R	no flow		3720	23
		F	1.61×10^{-1}		3720	23
11/8-11/9	2.1	L	no flow		1956	17
		R	2.84×10^{-5}	0.91	204	3
		F	2.20×10^{-2}		1956	17

Table F.4 Test Results for Specimen CG5309-31V (Wet Cement Seal)--Continued

Date	Injection Pressure (MPa)		Flow Rate (cm^3/min)	r^2	Test Duration (min)	Number of Data
11/10-11/11	2.1	L	no flow		2199	15
		R	4.97×10^{-5}	0.96	165	4
		F	2.35×10^{-2}		2199	15
11/19-11/23	2	L	no flow		5643	21
		R	no flow		5643	21
		D	3.41×10^{-3}	0.97	5634	21
11/28-11/29	2	L	no flow		1807	18
		R	no flow		1807	18
		D	4.23×10^{-3}	0.99	1807	18
11/29[j]						
11/29-12/1	2	L	2.30×10^{-5}	1.00	131	3
		R	no flow		2472	16
		D	4.84×10^{-3}	1.00	2472	16
9/26-9/28	1.1	L	no flow		2105	12
		R	no flow		2105	12
		F	1.06×10^{-1}		2105	12
10/2-10/4	1	L	1.49×10^{-5}	0.79	455	3
		R	no flow		3001	25
		F	8.50×10^{-2}		3001	25
10/12-10/15	1	L	no flow		4970	23
		R	no flow		4970	23
		F	9.00×10^{-2}		4970	23
11/7	1	L	no flow		833	13
		R	no flow		833	13
		F	9.00×10^{-3}		833	13
12/1-12/3/83	4	L	2.24×10^{-5}	0.97	820	12
		R	1.52×10^{-5}	0.99	193	3
		D	9.81×10^{-3}	1.00	2960	18
12/3-12/4	4	L	2.15×10^{-5}	0.98	232	5
		R	no flow		1560	8
		D	9.40×10^{-3}	1.00	1560	8
12/4[k]						

Table F.4 Test Results for Specimen CG5309-31V (Wet Cement Seal)--Continued

Date	Injection Pressure (MPa)		Flow Rate (cm^3/min)	r^2	Test Duration (min)	Number of Data
12/4-12/5	4	L	3.68×10^{-5}	0.93	357	6
		R	no flow		1461	14
		D	9.90×10^{-3}	1.00	1461	14
12/12-12/14	4	L	2.71×10^{-5}	0.92	2062	13
		R	no flow		3309	23
		D	1.01×10^{-2}	1.00	3309	23
12/14[1]						
12/14-12/15	4	L	2.92×10^{-5}	0.98	553	3
		R	no flow		1471	5
		D	1.02×10^{-2}	1.00	1471	5
12/29-12/31	4	L	4.59×10^{-5}	0.95	3088	15
		R	no flow		3126	16
		D	6.46×10^{-3}	1.00	3126	16
1/9-1/12/84	4	L	2.86×10^{-5}	0.96	3608	23
		R	3.08×10^{-5}	0.82	448	8
		D	6.72×10^{-3}	1.00	4588	28
1/24-1/26	4	L	7.24×10^{-5}	0.97	3095	27
		R	1.12×10^{-5}	0.86	2421	23
12/6-12/9	2.1	L	no flow		5265	31
		R	no flow		5265	31
		D	4.95×10^{-3}	1.00	5265	31
12/20-12/23	2	L	1.18×10^{-5}	0.75	379	6
		R	no flow		4273	20
		D	5.28×10^{-3}	1.00	4273	20
12/23-12/26[m,n]	2	L	1.79×10^{-5}	0.67	1866	17
		R	no flow		7659	32
		D	3.77×10^{-3}	1.00	7659	32
1/2-1/9[o,p]	2.1	L	3.60×10^{-5}	0.97	3957	48
		R	no flow		10256	63
		D	3.15×10^{-3}	1.00	10256	62
1/19-1/24	2	L	3.26×10^{-5}	0.94	5095	28
		R	no flow		6650	36

Table F.4 Test Results for Specimen CG5309-31V (Wet Cement Seal)--Continued

Date	Injection Pressure (MPa)		Flow Rate (cm^3/min)	r^2	Test Duration (min)	Number of Data
12/19-12/20	1	L	no flow		1484	9
		R	no flow		1484	9
		D	2.69×10^{-3}	1.00	1383	7
1/26-1/31[g]						g

r^2 = coefficient of determination
L = peripheral outflow rate through the rock around the cement seal
R = longitudinal outflow rate through the cement plug (one-dimensional flow)
D = inflow rate calculated from pressure intensifier's piston displacement
F = inflow rate measured in the flowmeter

NOTES:

(a) Start flow tests on a 104 mm long plug; saturation begins.
(b) Leakage in the epoxy bond.
(c) Epoxy bond failed. New epoxy put in place after the test.
(d) Cement plug shortened from 104 mm to 42 mm to induce higher flow rate.
(e) Test duration is longer; no flow is recorded in part of it.
(f) Flow rate = 1.22×10^{-4} cm^3/min with r^2 = 0.91 at 16 data, 719 min.
(g) Small leakage in the flowmeter connection.
(h) Replace flowmeter top to reduce leakage.
(i) Dynamic loading at P = 4 MPa, acceleration = 1.0 g, duration = 40 sec.
(j) Dynamic test at P = 2 MPa, acceleration a = 1.0 g, duration t = 80 sec.
(k) Dynamic loading at P = 4 MPa, acceleration = 1 g, duration = 160 sec.
(l) Dynamic loading at P = 4 MPa, acceleration = 1 g, duration = 320 sec.
(m) 12/23/83: start dye injection test using Formulabs' yellow liquid concentrate dye marker.
(n) 12/26/83: dye seepage from the top and sides of the sample.
(o) 1/8/84: yellow dye color is noticed in L-outflow tube.
(p) 1/3/84: yellow dye color is noticed in R-outflow tube.
(q) Sample oven-dried at 90°C (195°F) for five days.

Table F.5 Test Results for Specimen CG5309-10 (Wet Cement Seal)

Date	Injection Pressure (MPa)		Flow Rate (cm^3/min)	r^2	Test Duration (min)	Number of Data
10/3-10/5/83[a]	1.1	L	no flow		2312	23
		R	no flow		2312	23
		F	1.05×10^{-2}		2312	23
12/1-12/3[b]	1.1	L	no flow		2834	14
		R	no flow		2834	14
		F	no reading		2834	14
10/5-10/6	2.1	L	no flow		893	6
		R	no flow		893	6
		F	6.00×10^{-3}		893	6
10/6-10/14	2	L	no flow		10986	52
		R	no flow		10986	52
		F	1.10×10^{-2}		10986	52
10/24-10/30	2.1	L	no flow		7627	21
		R	no flow		7627	21
		F	2.30×10^{-3}		7627	21
11/6-11/9[b]	2	L	5.72×10^{-5}	1.00	263	7
		R	9.50×10^{-5}	0.90	415	8
		F	no reading		3561	32
11/17-11/23[b]	2	L	no flow		8863	32
		R	no flow		8863	32
		F	no reading		8863	32
12/3-12/5[b]	2.1	L	no flow		3017	21
		R	no flow		3017	21
		F	no reading		3017	21
10/14-10/18	3	L	6.30×10^{-5}	0.91	104	3
		R	9.78×10^{-5}	0.97	5473	27
		F	1.20×10^{-2}		6109	33
10/18-10/24	4	L	3.54×10^{-5}	0.94	837	16
		R	1.41×10^{-4}	0.94	4005	61
		F	1.23×10^{-2}		8872	76
10/30-11/6	4	L	1.53×10^{-5}	0.94	1394	18
		R	1.06×10^{-4}	0.90	4337	43
		F	1.90×10^{-2}		11353	58

Table F.5 Test Results for Specimen CG5309-10 (Wet Cement Seal)--Continued

Date	Injection Pressure (MPa)		Flow Rate (cm^3/min)	r^2	Test Duration (min)	Number of Data
11/9-11/17	4	L	no flow		10218	54
		R	1.15×10^{-4}		1020	17
		F	2.75×10^{-3}		10218	54
11/23-11/28[c]	3.9	L	no flow		7293	32
		R	no flow		7293	32
		F	4.70×10^{-3}		7293	32
12/6-12/7[d]	3.9	L	no flow		1470	12
		R	no flow		1470	12
		F	4.30×10^{-2}		1470	12
12/9[e]						

r^2 = coefficient of determination
L = outflow rate through the rock around the plug (peripheral)
R = outflow rate through the plug and plug-rock interface (longitudinal - one dimensional)
F = inflow rate measured in the flowmeter

NOTES:

(a) Start flow testing; a mechanical packer is used in the top hole.
(b) Inflow rate too low to be observed in the flowmeter.
(c) Inflow rate increased during the last eight hours of the test due to slight displacement of the packer.
(d) Packer would not hold in place; the rubber sleeve failed causing high inflow rate. Rubber sleeve replaced after the test.
(e) Sample fractured in tension, possibly due to the combination of overpressure and overtightening the packer nut.

Table F.6 Test Results for Specimen CG5309-28 (Dried-Out Cement Seal)

Date	Injection Pressure (MPa)	Flow Rate (cm^3/min)		r^2	Test Duration (min)	Number of Data
2/7/83[a]	1.5	L	-		63	
		R	2.57×10^{-1}	1.00		9
2/8	0.4	L	-		372	
		R	4.60×10^{-2}	1.00		7
2/9	0.8	L	-		90	
		R	8.71×10^{-2}	1.00		10
2/10	0.5	L	-		210	
		R	4.72×10^{-2}	1.00		10
2/10[b]	2.2	L	3.28×10^{-4}	0.24	70	14
		R	2.54×10^{-1}	1.00		14
2/11	0.3	L	-		135	
		R	2.89×10^{-2}	1.00		8
2/11	0.2	L	-		315	
		R	1.55×10^{-2}	1.00		11
2/11[b,d]	3.5	L	-		45	
		R	3.98×10^{-1}	1.00		9
3/6[d]	3.0	L	3.92×10^{-4}	0.92	90	13
		R	8.20×10^{-2}	1.00		13
3/6-3/7	330	-	-		1.0	
		R	2.24×10^{-2}	1.00		14
3/7[d]	2.5	L	2.16×10^{-4}	0.95	165	19
		R	4.85×10^{-2}	1.00		19
3/8	1.5	L	1.03×10^{-4}	0.92	287	21
		R	2.21×10^{-2}	1.00		21
3/9[d]	4.0	L	3.34×10^{-4}	0.90	165	17
		R	5.90×10^{-2}	1.00		17
3/10[e]	-	-	-	-	-	-
3/14-3/15[d]	1.7	L	1.53×10^{-4}	0.89	730	22
		R	4.96×10^{-3}	1.00		22

Table F.6 Test Results for Specimen CG5309-28 (Dried-Out Cement Seal)--Continued

Date	Injection Pressure (MPa)	Flow Rate (cm^3/min)		r^2	Test Duration (min)	Number of Data
3/15[c]	1.3	L	8.17×10^{-5}	0.97	925	16
		R	3.25×10^{-3}	0.99		16
		F	1.70×10^{-2}			
3/16-3/17	0.5	L	-		1475	
		R	9.71×10^{-4}	0.99		18
		F	1.10×10^{-2}			
3/17[c]	2.1	L	2.11×10^{-4}	0.94	150	16
		R	9.15×10^{-3}	1.00		16
3/17[d]	3.6	L	2.29×10^{-4}	0.93	95	10
		R	2.74×10^{-2}	1.00		10
3/18[d]	4.5	L	4.75×10^{-4}	0.98	229	19
		R	4.32×10^{-2}	1.00		19
3/22-3/23[d]	2.5	L	2.21×10^{-4}	0.85	1005	16
		R	7.71×10^{-3}	0.99		31
3/24-3/26[c,f]	1.0	L	4.78×10^{-5}	0.75	2710	8
		R	7.77×10^{-4}	0.98		23
		F	1.30×10^{-2}			
3/28-3/29[c]	1.4	L	8.56×10^{-5}	0.81	1488	19
		R	8.54×10^{-4}	0.98		19
		F	1.70×10^{-2}			
3/29-3/30[d]	2.9	L	2.88×10^{-5}	0.57	789	7
		R	5.70×10^{-3}	1.00		24
3/31-4/1[c]	0.7	L	-	-	2120	-
		R	4.15×10^{-4}	0.99		31
4/2[b,d]	3.8	L	8.73×10^{-5}	0.66	145	13
		R	1.40×10^{-2}	1.00		13
4/3-4/4[d]	1.7	L	-		925	
		R	1.39×10^{-3}	1.00		20
4/4-4/5[d]	2.0	L	3.91×10^{-5}	0.50	1680	30
		R	1.64×10^{-3}	1.00		30

Table F.6 Test Results for Specimen CG5309-28 (Dried-Out Cement Seal)--Continued

Date	Injection Pressure (MPa)		Flow Rate (cm^3/min)	r^2	Test Duration (min)	Number of Data
4/5-4/6 [b]	1.2	L	2.02×10^{-5}	0.60	680	15
		R	9.65×10^{-4}	0.99		18
		F	1.50×10^{-2}			
4/7-4/9	0.4	L	-		3311	
		R	2.56×10^{-4}	0.99	0.99	20
		F	1.05×10^{-2}			
4/10-4/11	0.9	L	1.02×10^{-4}	0.64	1225	12
		R	5.73×10^{-4}	0.99		12
		F	1.50×10^{-2}			
4/12-4/13 [d]	2.6	L	4.76×10^{-5}	0.67	517	20
		R	2.56×10^{-3}	1.00		20
4/13-4/14	1.5	L	1.44×10^{-4}	0.66	1350	24
		R	1.25×10^{-3}	1.00		26
		F	1.70×10^{-2}			
4/14[d]	3.5	L	1.44×10^{-4}	0.96	450	20
		R	7.79×10^{-3}	1.00		20
4/15[b]	3.0	L	7.69×10^{-5}	0.96	435	18
		R	5.27×10^{-3}	1.00		18
4/18[g]	4.0	L	9.94×10^{-5}	0.96	660	28
		R	1.05×10^{-2}	1.00		28
4/20-4/21[f]	2.1	L	-		620	
		R	1.67×10^{-3}	1.00		19
4/22-4/26[f]	2.5	L	1.21×10^{-4}	0.99	1450	18
		R	2.50×10^{-3}	1.00		21
4/27	2.9	L	1.62×10^{-4}	0.98	375	7
		R	4.01×10^{-3}	1.00		9
4/28[d]	3.5	L	2.14×10^{-4}	0.96	587	13
		R	6.41×10^{-3}	0.98		13
4/29[d]	4.0	L	2.40×10^{-4}	0.99	410	10
		R	8.13×10^{-3}	1.00		11
5/2[d]	3.5	L	2.00×10^{-4}	0.95	524	13
		R	5.62×10^{-3}	1.00		17

Table F.6 Test Results for Specimen CG5309-28 (Dried-Out Cement Seal)--Continued

Date	Injection Pressure (MPa)		Flow Rate (cm^3/min)	r^2	Test Duration (min)	Number of Data
5/3	3.0	L	1.94×10^{-4}	0.96	545	15
		R	3.63×10^{-3}	1.00		15
5/4	2.5	L	1.80×10^{-4}	0.99	563	16
		R	2.18×10^{-3}	0.99		16
5/5	2.0	L	1.20×10^{-4}	0.96	605	10
		R	1.52×10^{-3}	1.00		12
5/9-5/10	1.6	L	2.19×10^{-4}	1.00	1520	14
		R	7.78×10^{-4}	1.00		22
5/10-5/12[b]	1.1	L	4.50×10^{-5}	0.90	2550	20
		R	5.57×10^{-4}	1.00		23
5/16-5/18	0.7	L	4.81×10^{-5}	0.81	2105	12
		R	2.90×10^{-4}	1.00		19
5/18-5/19	0.5	L	8.42×10^{-5}	0.97	1400	9
		R	2.20×10^{-4}	0.99		14
5/19-5/20	1.4	L	1.94×10^{-4}	0.91	951	12
		R	6.62×10^{-4}	1.00		12
5/20-5/23[f]	2.0	L	3.05×10^{-4}	1.00	1165	17
		R	8.77×10^{-4}	1.00		20
5/27/83	4	L	2.38×10^{-4}	0.99	535	7
5/27-5/28		R	3.97×10^{-3}	1.00	769	11
5/30	4	L	2.13×10^{-4}	0.85	464	21
		R	3.84×10^{-3}	1.00	464	21
6/8	4	L	2.13×10^{-4}	0.99	555	22
		R	3.57×10^{-3}	1.00	555	22
6/24[h]	4	L	1.07×10^{-4}	0.73	100	6
7/2-7/3		R	2.47×10^{-3}	1.00	544	13
7/4	4	L	1.12×10^{-4}	0.75	235	14
		R	2.60×10^{-3}	1.00	235	14
7/4[i]						

Table F.6 Test Results for Specimen CG5309-28 (Dried-Out Cement Seal)--Continued

Date	Injection Pressure (MPa)		Flow Rate (cm^3/min)	r^2	Test Duration (min)	Number of Data
7/4	4	L	1.26×10^{-4}	0.94	107	6
		R	2.54×10^{-3}	1.00	220	10
7/7	4	L	8.29×10^{-5}	0.95	630	17
		R	2.40×10^{-3}	1.00	630	17
7/11	4	L	1.50×10^{-4}	0.98	480	17
		R	2.37×10^{-3}	1.00	480	17
		D	5.24×10^{-2}	1.00	460	16
7/11[j]						
7/11	4	L	1.04×10^{-4}	0.61	93	6
		R	2.31×10^{-3}	1.00	93	6
		D	5.20×10^{-2}	1.00	93	6
7/12	4	L	1.50×10^{-4}	0.96	432	12
		R	2.28×10^{-3}	1.00	432	12
		D	5.15×10^{-2}	1.00	270	10
7/18[k]	4	L	1.52×10^{-4}	0.95	460	10
		R	2.13×10^{-3}	1.00	460	10
		D	5.51×10^{-2}	1.00	405	9
7/20	4	L	1.96×10^{-4}	0.97	438	17
		R	2.15×10^{-3}	1.00	438	17
		D	5.25×10^{-2}	1.00	408	15
7/20[l]						
7/20	4	L	3.29×10^{-4}	0.96	133	10
		R	2.27×10^{-3}	1.00	133	10
		D	5.42×10^{-2}	1.00	133	10
7/26[k]	4	L	2.30×10^{-4}	0.97	612	18
		R	1.95×10^{-3}	1.00	612	18
		D	5.44×10^{-2}	1.00	570	17
7/29	4	L	1.83×10^{-4}	0.93	600	19
		R	1.90×10^{-3}	1.00	600	19
		D	5.20×10^{-2}	1.00	490	17

Table F.6 Test Results for Specimen CG5309-28 (Dried-Out Cement Seal)--Continued

Date	Injection Pressure (MPa)		Flow Rate (cm^3/min)	r^2	Test Duration (min)	Number of Data
8/3	4	L	2.67×10^{-4}	0.98	239	11
		R	1.90×10^{-3}	1.00	239	11
		D	5.22×10^{-2}	1.00	211	10
8/3[m]						
8/3	4	L	1.53×10^{-4}	0.90	380	12
		R	1.78×10^{-3}	1.00	380	12
		D	5.21×10^{-2}	1.00	380	12
8/9	4	L	9.71×10^{-5}	0.98	489	12
		R	1.60×10^{-3}	1.00	489	12
		D	5.16×10^{-2}	1.00	429	11
5/26	3.5	L	2.46×10^{-4}	0.99	495	10
		R	3.26×10^{-3}	1.00	495	10
6/7	3.5	L	2.96×10^{-4}	0.97	545	10
		R	2.86×10^{-3}	1.00	545	10
5/24	3	L	2.46×10^{-4}	0.99	618	11
		R	2.06×10^{-3}	1.00	618	11
6/3	3	L	1.36×10^{-4}	0.86	360	6
		R	2.11×10^{-3}	1.00	397	7
6/6	3	L	1.55×10^{-4}	0.86	794	11
		R	2.00×10^{-3}	1.00	794	12
6/23	3	L	9.39×10^{-5}	0.88	825	9
		R	1.56×10^{-3}	1.00	825	9
6/24	3	L	1.53×10^{-4}	0.98	432	10
		R	1.55×10^{-3}	1.00	432	10
6/24[h]						
6/24	3	L	1.13×10^{-4}	0.57	205	6
		R	1.67×10^{-3}	0.99	205	6
6/26	3	L	no flow	-	715	11
		R	1.50×10^{-3}	1.00	715	11

Table F.6 Test Results for Specimen CG5309-28 (Dried-Out Cement Seal)--Continued

Date	Injection Pressure (MPa)		Flow Rate (cm^3/min)	r^2	Test Duration (min)	Number of Data
6/29-6/30	3	L	no flow	-	660	11
		R	1.51×10^{-3}	1.00	660	11
5/24	2.5	L	2.42×10^{-4}	0.81	909	12
		R	1.44×10^{-3}	1.00	909	12
6/2	2.5	L	1.56×10^{-4}	0.89	725	10
		R	1.33×10^{-3}	1.00	725	10
6/15	2.5	L	2.33×10^{-4}	0.88	620	8
		R	1.37×10^{-3}	1.00	1040	10
6/22	2.5	L	1.34×10^{-4}	0.99	638	10
		R	1.26×10^{-3}	1.00	638	10
6/2-6/2	2	L	1.10×10^{-4}	0.99	230	6
		R	9.10×10^{-4}	1.00	1298	14
6/14	2	L	1.58×10^{-4}	0.67	685	8
6/14-6/15	2	R	9.80×10^{-4}	0.99	1375	9
6/20	2	L	no flow	-	390	6
		R	7.93×10^{-4}	1.00	390	6
6/21	2	L	1.13×10^{-4}	0.98	495	8
		R	9.37×10^{-4}	1.00	495	8
6/24[h]						
6/27	2	L	9.16×10^{-5}	0.86	695	12
		R	9.21×10^{-4}	1.00	695	12
6/30	2	L	4.16×10^{-5}	0.97	387	11
		R	8.86×10^{-4}	1.00	770	17
7/4[i]						
7/5	2	L	1.03×10^{-4}	0.96	460	12
		R	9.13×10^{-4}	1.00	725	16
7/8	2	L	7.15×10^{-5}	0.73	580	12
		R	9.14×10^{-4}	1.00	580	12

Table F.6 Test Results for Specimen CG5309-28 (Dried-Out Cement Seal)--Continued

Date	Injection Pressure (MPa)		Flow Rate (cm^3/min)	r^2	Test Duration (min)	Number of Data
7/11[j]						
7/13	2	L	7.26×10^{-5}	0.97	703	15
		R	8.50×10^{-4}	0.99	995	18
		D	2.31×10^{-2}	1.00	900	16
7/15	2	L	1.25×10^{-4}	0.94	456	10
		R	7.89×10^{-4}	1.00	456	10
		D	2.78×10^{-2}	0.93	286	7
7/20[l]						
7/25	2	L	1.08×10^{-4}	0.95	480	10
		R	7.17×10^{-4}	1.00	480	10
		D	2.18×10^{-2}	1.00	378	8
7/28	2	L	8.60×10^{-5}	0.83	970	18
		R	7.28×10^{-4}	1.00	970	18
		D	2.30×10^{-2}	1.00	790	14
8/2-8/3	2	L	1.32×10^{-4}	0.94	528	7
		R	6.90×10^{-4}	1.00	1470	14
		D	2.30×10^{-2}	1.00	1248	11
8/3[m]						
8/8	2	L	1.01×10^{-4}	0.78	906	13
		R	6.59×10^{-4}	1.00	906	13
		D	2.28×10^{-2}	0.99	906	13
8/11-8/12	2	L	1.06×10^{-4}	0.45	1348	18
		R	6.28×10^{-4}	1.00	1348	18
		D	2.32×10^{-2}	1.00	1187	14
5/31	1.5	L	3.56×10^{-5}	0.91	510	10
		R	7.55×10^{-4}	1.00	510	10
6/1	1.5	L	7.88×10^{-5}	0.82	260	6
		R	7.03×10^{-4}	1.00	260	6
6/13-6/14	1.5	L	1.30×10^{-4}	0.83	641	10
		R	7.52×10^{-4}	1.00	1505	14

Table F.6 Test Results for Specimen CG5309-28 (Dried-Out Cement Seal)--Continued

Date	Injection Pressure (MPa)		Flow Rate (cm^3/min)	r^2	Test Duration (min)	Number of Data
6/9	1	L	no flow	-	558	6
		R	6.17×10^{-4}	1.00	558	6
6/10	1	L	1.58×10^{-4}	0.97	550	9
		R	6.28×10^{-4}	1.00	550	9
6/24[h]						
6/28-6/29	1	L	5.52×10^{-5}	0.97	445	8
		R	4.40×10^{-4}	1.0	1995	23
7/2-7/2	1	L	1.96×10^{-5}	0.88	532	10
		R	4.37×10^{-4}	1.00	1811	15
7/4[i]						
7/6-7/7	1	L	1.34×10^{-4}	0.99	310	9
		R	4.60×10^{-4}	0.99	1250	20
7/9-7/11	1	L	no flow	-	2220	21
		R	3.60×10^{-4}	1.00	2220	21
		D	1.18×10^{-2}	1.00	1860	18
		F	1.90×10^{-2}	-	1860	18
7/11[j]						
7/14-7/15	1	L	9.56×10^{-5}	0.89	499	9
		R	4.03×10^{-4}	1.00	1379	17
		D	1.16×10^{-2}	1.00	1379	17
		F	1.60×10^{-2}	-	1379	17
7/19-7/20[1]	1	L	1.03×10^{-4}	0.98	585	10
		R	3.94×10^{-4}	0.98	1405	14
		D	1.12×10^{-2}	1.00	1071	9
7/21-7/22	1	L	9.36×10^{-5}	0.98	583	17
		R	3.99×10^{-4}	0.99	1900	30
		D	1.13×10^{-2}	1.00	1620	21
		F	1.60×10^{-2}	-	1900	21
7/26-7/28	1	L	7.03×10^{-5}	0.95	490	9
		R	3.38×10^{-4}	1.00	2193	24
		D	1.25×10^{-2}	1.00	1423	21

Table F.6 Test Results for Specimen CG5309-28 (Dried-Out Cement Seal)--Continued

Date	Injection Pressure (MPa)		Flow Rate (cm^3/min)	r^2	Test Duration (min)	Number of Data
8/1-8/2	1	L	1.37×10^{-4}	0.98	535	13
		R	3.58×10^{-4}	0.99	1428	17
		D	1.12×10^{-2}	1.00	1158	11
8/3[m]						
8/4-8/5	1	L	8.31×10^{-5}	0.98	596	10
		R	3.42×10^{-4}	1.00	2357	24
		D	1.12×10^{-2}	1.00	2094	22
		F	1.80×10^{-2}	-	2357	25
8/10	1	L	1.11×10^{-4}	0.96	480	9
		R	3.14×10^{-4}	0.98	1558	14
		D	1.09×10^{-2}	1.00	1223	8

r^2 = coefficient of determination
L = outflow rate through the rock surrounding the plug (pheripheral flow)
R = outflow rate through the plug and plug-rock interface (one-dimensional longitudinal flow)
F = inflow rate observed in the flowmeter
D = inflow rate calculated from piston displacement of the pressure intensifier.

NOTES:

(a) Start flow tests and resaturation on cement plug that was dried (stored) for 3 months at room temperature.
(b) Air bubbles in the outflow lines.
(c) Slight seepage from the sides of the rock specimen.
(d) Seepage from the sides and top of the rock specimen.
(e) Water leakage in the pressure intensifier, O-ring failure.
(f) Test is done intermittently within the period of time indicated.
(g) Vacuum pump oil was used in pipettes to prevent evaporation.
(h) Dynamic test at 3 MPa, with acceleration a = 1.0 g and time t = 20 sec.
(i) Dynamic test at 4 MPa, a = 1.0 g, t = 25 sec.
(j) Dynamic test at 4 MPa, a = 1.0 g, t = 41 sec.
(k) Water loss; cap was opened unintentionally.

Table F.6 Test Results for Specimen CG5309-28 (Dried-Out Cement Seal)--Continued

NOTES--Continued

(l) Dynamic test at 4 MPa, a = 1.0 g, t = 80 sec.
(m) Dynamic test at 4 MPa, a = 1.0 g, t = 160 sec.
(n) Flow rate = 1.18×10^{-4} cm^3/min with $r^2 = 0.99$ at 9 data points, 501 min on 8/5.

Table F.7 Test Results for Specimen CG5309-01 (Dried-Out Cement Seal)

Date	Injection Pressure (MPa)		Flow Rate (cm^3/min)	r^2	Test Duration (min)	Number of Data
5/30/83[a]	1.5	R	2.85×10^{1}	1.00	0.83	11
5/31	1.5	R	1.69×10^{1}	1.00	1.33	17
6/1	1.5	R	1.42×10^{1}	1.00	1.67	21
6/2	1.5	R	1.13×10^{1}	1.00	1.83	23
6/6	1.5	R	8.00×10^{0}	1.00	2.67	14
6/7	1.5	R	6.34×10^{0}	1.00	3.33	21
6/9	1.5	R	6.10×10^{0}	1.00	3.67	12
6/10	1.5	R	5.84×10^{0}	1.00	3.67	12
6/13	1.5	R	5.13×10^{0}	1.00	4.67	15
6/14	1.5	R	5.08×10^{0}	1.00	4.67	15
6/17[b]	1.5	R	1.03×10^{-2}	0.99	112	13
6/17[c]	1.5	R	1.76×10^{0}	0.98	11	7
6/20[b]	1.5	R	3.83×10^{-1}	0.99	10	19
6/21[b]	1.5	R	7.58×10^{-2}	0.99	131	14
6/21[c]	1.5	R	2.49×10^{0}	0.99	3.83	6
6/22	1.5	R	2.65×10^{0}	1.00	4	8
6/22[b]	1.5	R	$3.9i \times 10^{-2}$	0.99	136	20
6/22[c]	1.5	R	5.05×10^{-1}	0.96	13	9
6/23	1.5	R	3.43×10^{0}	0.99	6.67	15
6/24	1.5	R	3.12×10^{0}	1.00	7.5	16
7/4	1.5	R	2.23×10^{0}	1.00	10.5	22
		R	2.25×10^{0}	1.00	9.5	20

Table F.7 Test Results for Specimen CG5309-01 (Dried-Out Cement Seal)--Continued

Date	Injection Pressure (MPa)		Flow Rate (cm^3/min)	r^2	Test Duration (min)	Number of Data
7/5	1.5	R	1.78×10^{0}	1.00	11	23
		D	1.82×10^{0}	1.00	10	18
7/6	1.5	R	1.86×10^{0}	1.00	11	23
		D	1.93×10^{0}	1.00	10	19
7/18	1.5	R	7.27×10^{-1}	1.00	13	27
7/21	1.5	R	6.64×10^{-1}	1.00	14	29
7/26	1.5	R	5.55×10^{-1}	1.00	15	31
7/29	1.5	R	5.27×10^{-1}	1.00	12	25
8/1	1.5	R	4.37×10^{-1}	1.00	12	25
8/4	1.5	R	4.33×10^{-1}	1.00	12	25
7/8	0.9	R	1.12×10^{0}	1.00	21	22
7/10	1.2	R	6.95×10^{-1}	1.00	15	16
9/5/83	1.5	R	2.73×10^{-1}	1.00	18	19
9/6	1.3	R	2.54×10^{-1}	0.98	18	19
9/9	1.5	R	2.54×10^{-1}	1.00	17	18
9/12	1.5	R	2.51×10^{-1}	1.00	17	18
9/15	1.5	R	2.28×10^{-1}	1.00	20	21
		F	3.20×10^{-1} [d]		13	14
9/19	1.5	R	2.20×10^{-1}	1.00	23	16
		F	3.00×10^{-1}		23	16
9/21	1.5	R	2.18×10^{-1}	1.00	20	21
		F	3.20×10^{-1}		20	21
9/23	1.5	R	2.26×10^{-1}	1.00	13	21
		F	3.20×10^{-1}		13	21

Table F.7 Test Results for Specimen CG5309-01 (Dried-Out Cement Seal)--- Continued

Date	Injection Pressure (MPa)		Flow Rate (cm^3/min)	r^2	Test Duration (min)	Number of Data
9/26	1.5	R	2.12×10^{-1}	1.00	19	20
		F	3.30×10^{-1}		19	20
9/28	1.5	R	2.10×10^{-1}	1.00	16	17
		F	3.05×10^{-1}		15	16
10/2	1.5	R	2.06×10^{-1}	1.00	24	16
		F	2.70×10^{-1}		24	16
10/5	1.5	R	1.85×10^{-1}	1.00	26	16
		F	2.60×10^{-1}		26	16
10/7	1.5	R	1.97×10^{-1}	1.00	20	21
		F	2.85×10^{-1}		19	20
10/10	1.5	R	2.03×10^{-1}	1.00	15	16
		F	2.90×10^{-1}		14	15
10/12	1.5	R	1.98×10^{-1}	1.00	20	21
		F	3.05×10^{-1}		19	20
10/13[e]	1.5	R	1.94×10^{-1}	1.00	11	12
		F	2.85×10^{-1}		11	12
10/13						
10/13	1.5	R	1.86×10^{-1}	1.00	14	15
		F	2.90×10^{-1}		14	15
10/16	1.5	R	1.81×10^{-1}	1.00	29	11
		F	2.85×10^{-1}		29	11
10/18[f]	1.5	R	1.70×10^{-1}	1.00	10	11
		F	3.15×10^{-1}		10	11
10/18						
10/18	1.5	R	1.64×10^{-1}	1.00	18	15
		F	3.15×10^{-1}		18	15
10/20	1.5	R	1.73×10^{-1}	1.00	20	21
		F	2.85×10^{-1}		19	20

Table F.7 Test Results for Specimen CG5309-01 (Dried-Out Cement Seal)--Continued

Date	Injection Pressure (MPa)		Flow Rate (cm^3/min)	r^2	Test Duration (min)	Number of Data
10/20[g]						
10/20	1.5	R	1.69×10^{-1}	1.00	29	17
		F	2.25×10^{-1}		29	17
10/21	1.5	R	1.83×10^{-1}	1.00	28	15
		F	4.95×10^{-1}		28	15
10/24	1.5	R	1.72×10^{-1}	1.00	20	21
		F	2.90×10^{-1}		19	20
10/25	1.5	R	1.78×10^{-1}	1.00	18	19
		F	3.30×10^{-1}		17	18
10/25[h]						
10/25	1.5	R	1.75×10^{-1}	1.00	20	21
		F	2.90×10^{-1}		19	20
10/30	1.5	R	1.75×10^{-1}	1.00	28	18
		F	4.35×10^{-1}		28	18
10/31	1.5	R	1.72×10^{-1}	1.00	20	21
		F	3.40×10^{-1}		19	20
11/2	1.5	R	1.72×10^{-1}	1.00	20	21
		F	2.80×10^{-1}		19	20
11/4	1.5	R	1.67×10^{-1}	1.00	20	21
		F	2.55×10^{-1}		19	20
11/7	1.5	R	1.59×10^{-1}	0.99	12	11
		F	2.20×10^{-1}		12	11
11/7[i]						
11/7	1.5	R	1.57×10^{-1}	1.00	14	15
		F	3.00×10^{-1}		14	15
11/10	1.5	R	1.55×10^{-1}	1.00	20	19
		F	2.80×10^{-1}		19	18

Table F.7 Test Results for Specimen CG5309-01 (Dried-Out Cement Seal)--Continued

Date	Injection Pressure (MPa)		Flow Rate (cm^3/min)	r^2	Test Duration (min)	Number of Data
11/14	1.5	R	1.59×10^{-1}	1.00	31	20
		F	3.50×10^{-1}		31	20
12/22[j]	2.1	R	1.28×10^{-1}	1.00[k]	20	16
		F	7.00×10^{-2}		20	16
12/23	2.0	R	1.15×10^{-1}	1.00	45	17
		F	1.00×10^{-1}		45	17
12/26	2.0	R	1.06×10^{-1}	1.00	19	18
		F	7.40×10^{-2}		19	12
12/28	1.1	R	6.28×10^{-2}	1.00	30	15
		F	5.00×10^{-2}		28	14
12/30	1.1	R	6.09×10^{-2}	1.00	19	13
		F	5.00×10^{-2}		19	13
12/31	1.5	R	7.64×10^{-2}	1.00	22	15
		F	5.60×10^{-2}		22	14
1/2/84	1.5	R	7.12×10^{-2}	1.00	20	21
		F	5.00×10^{-2}		19	20
1/5	1.5	R	7.07×10^{-2}	1.00	22	15
		F	5.20×10^{-2}		21	14
1/7	1.5	R	6.91×10^{-2}	1.00	28	16
		F	5.00×10^{-2}		27	15
1/13	1.5	R	6.44×10^{-2}	1.00	38	17
		F	1.29×10^{-1}		38	17
1/16	1.5	R	6.01×10^{-2}	1.00	32	17
		F	8.50×10^{-2}		32	17
1/23	1.5	R	5.80×10^{-2}	1.00	20	21
		F	1.05×10^{-1}		19	20
1/27	1.5	R	5.75×10^{-2}	1.00	27	15
		F	5.00×10^{-2}		26	14

Table F.7 Test Results for Specimen CG5309-01 (Dried-Out Cement Seal)--Continued

Date	Injection Pressure (MPa)	Flow Rate (cm^3/min)		r^2	Test Duration (min)	Number of Data
1/30[1]	1.5	R	5.99×10^{-2}	0.99	20	19c
		F	9.18×10^{-2}		19	18

r^2 = coefficient of determination
R = outflow rate through the plug-rock interface (longitudinal - one dimensional)
F = inflow rate measured in the flowmeter
D = inflow rate calculated from piston displacement of the pressure intensifier

NOTES:

(a) Start flow tests and resaturation of the cement plug that was dried at room temperaure for 7 months.
(b) Flow rate inconsistenly low; interface clogging suspected.
(c) Flow rate increased drastically after the valve was closed and opened several times.
(d) Begin observing inflow rate using Matheson No. 610 flowmeter.
(e) Dynamic test at 1.5 MPa, acceleration a = 2.0 g, for 40 seconds.
(f) Dynamic test at 1.5 MPa, acceleration a = 2.0 g, for 80 seconds.
(g) Dynamic test at 1.5 MPa, acceleration a = 2.0 g, for 80 seconds.
(h) Dynamic test at 1.5 MPa, acceleration a = 2.0 g, for 160 seconds
(i) Dynamic test at 1.5 MPa, acceleration a = 2.0 g, for 300 seconds.
(j) Start dye injection testing using Formulabs' red liquid concentrate dye marker.
(k) Begin observing inflow rate using Gilmont No. 10 flowmeter.
(l) End of testing; cut the sample in half lengthwise (2/7/84).

Table F.8 Test Results for Specimen CG5309-21 (Dried-Out Cement Seal)

Date	Injection Pressure (MPa)	Flow Rate (cm^3/min)	r^2	Test Duration (min)	Number of Data
2/11/83[d]	1.8	L -		25	
		R 6.36×10^{-1}	1.00		6
2/13[b]	.3	L -		30	
		R 4.01×10^{-2}	.97		3
2/22	0.2	L -		625	
		R 4.50×10^{-3}	.97		13
2/22-2/23	0.5	L -		643	
		R 2.69×10^{-2}	1.00		6
2/23	0.6	L -		435	
		R 3.06×10^{-2}	1.00		13
2/24	1.0	L 1.34×10^{-4}	.71	379	12
		R 4.65×10^{-2}	.99		12
2/25	1.4	L -		170	
		R 7.54×10^{-2}	1.00		10
2/25[c]	2.8	L 1.48×10^{-3}	.95	99	14
		R 2.30×10^{-1}	1.00		14
2/26[d,e]	4.2	L 3.50×10^{-3}	0.99	33	15
		R 6.22×10^{-1}	1.00		15
2/26	0.8	L 2.15×10^{-4}	0.88	307	11
		R 5.05×10^{-2}	1.00		11
3/1[e]	0.8	L -		325	
		R 4.25×10^{-2}	1.00		21
3/2-3/3	0.5	L 1.08×10^{-4}	0.64	690	17
		R 2.54×10^{-2}	1.00		17
3/3-3/4	0.4	L 3.28×10^{-5}	0.35	680	21
		R 1.85×10^{-2}	1.00		21
3/4[d,e,f]	6.1	L 4.25×10^{-3}	0.87	13	13
		R 1.57×10^{0}	1.00		13

Table F.8 Test Results for Specimen CG5309-21 (Dried-Out Cement Seal)--Continued

Date	Injection Pressure (MPa)	Flow Rate (cm^3/min)	r^2	Test Duration (min)	Number of Data
3/4[g]	7.0	-			

r^2 = coefficient of determination
L = peripheral flow through the rock surrounding the plug
R = longitudinal flow through the plug and plug-rock interface

NOTES: (a) Start flow tests and resaturation of the cement plug that was room dried at room temperature for 3 months.
(b) Leakage in the pressure intensifier due to O-ring failure.
(c) Slight seepage from the sides of the specimen.
(d) Seepage from the sides and top of specimen.
(e) Air bubbles noticed in the outflow lines.
(f) Leakage noticed and corrected in the inflow line.
(g) Rock specimen failed in tension.

Table F.9 Test Results for Specimen CG5309-31V (Oven-Dried Cement Plug)

Date	Injection Pressure (MPa)		Flow Rate (cm^3/min)	r^2	Test Duration (min)	Number of Data
2/1/84[a]						
2/7[b]	2	R	1.08×10^{-1}	0.99	50	7
		F	1.05×10^{-1}		50	7
	1.1	R	5.20×10^{-2}	1.00	99	7
		F	3.60×10^{-2}		99	7
2/10	4	R	8.92×10^{-2}	0.98	21	12
		F	1.00×10^{-1}		21	12
2/13	4	R	8.33×10^{-2}	0.98	42	13
		F	8.80×10^{-2}		42	13
	2	R	7.96×10^{-2}	1.00	59	14
		F	5.10×10^{-2}		59	14
	1	R	4.82×10^{-2}	1.00	78	9
		F	3.60×10^{-2}		78	9
2/14	1	R	4.38×10^{-2}	1.00	103	11
		F	4.20×10^{-2}		103	11
2/15	2	R	9.32×10^{-2}	1.00	49	13
		F	7.20×10^{-2}		49	13
2/17	4	R	1.51×10^{-1}	1.00	20	11
		F	1.80×10^{-1}		20	11
2/17	2	R	8.01×10^{-2}	1.00	43	12
		F	5.40×10^{-2}		43	12
2/20	1	R	3.21×10^{-2}	1.00	90	9
		F	3.40×10^{-2}		90	9
2/22	4	R	1.06×10^{-1}	1.00	39	13
		F	1.45×10^{-1}		39	13
	2	R	6.01×10^{-2}	1.00	55	12
		F	4.80×10^{-2}		55	12
2/23	1	R	2.67×10^{-2}	1.00	58	13
		F	2.70×10^{-2}		58	13

Table F.9 Test Results for Specimen CG5309-31V (Oven-Dried Cement Plug) --Continued

Date	Injection Pressure (MPa)		Flow Rate (cm^3/min)	r^2	Test Duration (min)	Number of Data
2/27	4	R	8.33×10^{-2}	1.00	30	11
		F	1.37×10^{-1}		30	11
	2	R	4.44×10^{-2}	1.00	41	12
		F	5.80×10^{-2}		41	12
2/28	1	R	2.04×10^{-2}	1.00	119	12
		F	3.00×10^{-2}		119	12
3/2	4	R	6.49×10^{-2}	1.00	54	10
		F	1.45×10^{-1}		54	10
	2	R	4.09×10^{-2}	1.00	70	11
		F	5.50×10^{-2}		70	11
3/6	1	R	1.36×10^{-2}	1.00	372	10
		F	4.20×10^{-2}		372	10
3/6[c]	3.6	R	5.95×10^{-2}		42	2
		F	1.00×10^{-1}		42	2

r^2 = coefficient of determination
R = longitudinal flow rate through the plug-rock interface (one-dimensional flow)
F = inflow rate observed in the flowmeter

NOTES:

(a) Start resaturation, but epoxy bond would not hold pressure; cracking due to 5 days of oven drying at 90°C caused excessive leakage in the epoxy bond.
(b) Add yellow dye in the top hole; it was seeping immediately into the R-outflow pipette. Mechanical packer was used instead of stainless steel-epoxy combination.
(c) Hydraulic accumulator failed to maintain pressure, bladder was punctured.

APPENDIX G

ROCK CYLINDER AND BOREHOLE PLUG DEFORMATION DURING BOREHOLE PRESSURIZATION

Flow tests on cylindrical Charcoal granite specimens can be represented mechanically as a hollow cylinder system with internal pressure p_1 and external pressure p_2. If the internal (hole) radius is R_1 and external (cylinder) radius is R_2, then the outward displacement of the specimen at any distance r from the center is given by:

$$\mu = \frac{(p_2 R_2^2 - p_1 R_1^2)r}{2(\lambda + G)(R_2^2 - R_1^2)} + \frac{(p_2 - p_1)R_1^2 R_2^2}{2G(R_2^2 - R_1^2)r}$$

where λ and G are Lame's constants (Jaeger and Cook, 1979, Section 5.11). In this case, $p_2 = 0$, and one is interested in the increase in the internal diameter, i.e. the displacement μ_{R1} at $r = R_1$. Therefore,

$$\mu_{R1} = -\frac{p_1 R_1}{2G}$$

or

$$\mu_{R1} = -p_1 R_1 \frac{1 + \nu_R}{E_R}$$

where ν_{R1} and E_R are Poisson's ratio and Young's modulus of the rock, respectively.

The lateral expansion of a cement plug (cylinder) with a radius R_1, under an axial stress p_1 can be calculated from its Young's modulus, E_c, and Poisson's ratio, ν_c. Assuming no lateral confinement from the rock cylinders:

$$\Delta_{R1} = \varepsilon_{lat} \cdot R_1$$

$$= \nu_c \cdot \varepsilon_{ax} \cdot R_1$$

$$= \nu_c \cdot \frac{p_1}{E_c} \cdot R_1$$

where ϵ_{lat} and ϵ_{ax} are the lateral and axial strains of the cement plug due to the axial stress p_1

Using E_R = 56,530 MPa, ν_R = 0.19 for Charcoal granite, and E_c = 7,627 MPa, ν_c = 0.14 for cement (see Section 3.2), the calculated outward displacements for specimen 5309-28 are given in the following table:

Specimen	R_1 (mm)	p_1 (MPa)	μ_{R1} - rock (mm)	Δ_{R1} - cement (mm)	$\mu_{R1} - \Delta_{R1}$ (mm)
5309-28 (dried-out cement plug)	12.9	1	2.72×10^{-4}	2.37×10^{-4}	0.35×10^{-4}
		2	5.43×10^{-4}	4.74×10^{-4}	0.69×10^{-4}
		4	10.86×10^{-4}	9.47×10^{-4}	1.39×10^{-4}

As the injection pressure (p_1) increases, $\mu_{R1} - \Delta_{R1}$ increases, resulting in a wider interfacial gap and increased flow rate.

It needs to be recognized that the calculation involves several simplifying assumptions. It assumes an infinite cylinder, pressurized over its entire length. In fact, a finite cylinder is pressurized over only part of its length (about one third). Thus, the calculation overestimates the outward radial displacement of the cylinder, certainly along the plugged length. The calculation assumes a uniform stress distribution throughout the plug, whereas in fact stress transfer occurs from the plug to the rock cylinder, and, for example, the lower end of the plug is free of stress. Hence, the calculation tends to overestimate the transverse plug expansion due to an applied axial stress on top of the plug.

NRC FORM 335 (6 87) U.S. NUCLEAR REGULATORY COMMISSION

BIBLIOGRAPHIC DATA SHEET

1 REPORT NUMBER (Assigned by TIDC add Vol No if any)
NUREG/CR-5129

2 Leave blank

3 TITLE AND SUBTITLE
Experimental Assessment of the Influence of Dynamic Loading on the Permeability of Wet and of Dried Cement Borehole Seals

4 RECIPIENT'S ACCESSION NUMBER

5 DATE REPORT COMPLETED
MONTH February YEAR 1988

6 AUTHOR(S)
G. Adisoma and J.J.K. Daemen

7 DATE REPORT ISSUED
MONTH April YEAR 1988

8 PERFORMING ORGANIZATION NAME AND MAILING ADDRESS (Include Zip Code)
Department of Mining and Geological Engineering
University of Arizona
Tucson, AZ 85721

9 PROJECT TASK/WORK UNIT NUMBER

10 FIN NUMBER
NRC-04-78-271
FIN B6627

11 SPONSORING ORGANIZATION NAME AND MAILING ADDRESS (Include Zip Code)
Division of Engineering
Office of Nuclear Regulatory Research
U.S. Nuclear Regulatory Commission
Washington, DC 20555

12a TYPE OF REPORT
Technical

12b PERIOD COVERED (Inclusive dates)
1985-1986

13 SUPPLEMENTARY NOTES

14 ABSTRACT (200 words or less)

An experimental sealing performance assessment of cement borehole plugs that have been subjected to dynamic loading is provided. This includes a study of plugs that have dried, as well as of plugs that have remained wet throughout the testing period.

An introductory literature review indicates that deep underground structures in competent rock are safer than surface structures, openings at shallow depth, and openings in fractured rocks, when subjected to earthquakes and subsurface blasts.

Cement plugs are installed in 2.5 cm diameter coaxial holes in 15 cm diameter granite cylinders. Water is injected under pressure on top of the plugs and is collected below the plugs. Hydraulic conductivities are calculated. Once a long-term steady-state flow trend has been established, the samples are subjected to dynamic loading on a shaking table. Shaking is performed at accelerations up to 2 g and for up to 300 seconds.

Wet cement seals are less permeable than intact Charcoal granite. Sealing performance can degrade severely when cement seals are allowed to dry. Dye injection shows very limited and uniform penetration into wet plugs, but strongly preferential flow along the plug/rock interface of dried plugs. The permeability of wet and of rewetted previously dried cement seals does not change significantly after the application of dynamic loads.

Sealing in an unsaturated environment may affect the drying (curing, aging) conditions of cementitious seals, as well as the structure of earthen seals. An unsaturated environment will need to be integrated realistically into sealing performance tests and analyses.

15a KEY WORDS AND DOCUMENT ANALYSIS

15b DESCRIPTORS

Borehole sealing
Shaft sealing
Cement permeability
Cement drying
Hydraulic conductivity
Repository sealing
Repository closure
Permeability
Cement shrinkage
Granite
Seal permeability
Plug permeability
Rock permeability
Flow testing

16 AVAILABILITY STATEMENT
Unlimited

17 SECURITY CLASSIFICATION (This report) **Unclassified**

18 NUMBER OF PAGES

19 SECURITY CLASSIFICATION (This page) **Unclassified**

20 PRICE
$

*U.S. GOVERNMENT PRINTING OFFICE:1988-202-292:80050

UNITED STATES
NUCLEAR REGULATORY COMMISSION
WASHINGTON, D.C. 20555

OFFICIAL BUSINESS
PENALTY FOR PRIVATE USE, $300

SPECIAL FOURTH CLASS RATE
POSTAGE & FEES PAID
USNRC
PERMIT No. G-67